The University Of Sheffield.

Malectin-like receptor-like kinases mediate pollen tube reception in *Arabidopsis thaliana*

By:

Sergio Galindo-Trigo

A thesis submitted in partial fulfilment of the requirements for the degree of Doctor of Philosophy

The University of Sheffield
Faculty of Science
Department of Animal and Plant Sciences

November 2018

Acknowledgements

I would like to thank my supervisors and the Department of Animal and Plant Sciences for giving me the opportunity to embark on this PhD project and join the rich plant science community in the University of Sheffield. My main supervisor Lisa M Smith has provided a dedicated and personal supervision, ensured a flexible working environment and constantly contributed to my project with interesting ideas, for all of which I am very grateful. A big thank you goes to my second supervisor Julie E Gray for her interest in my work, insightful and thought-provoking lab meeting discussions and contagious positivity.

I am very grateful for all the help and support my project has received from Jurriaan Ton, Andrew Fleming and their lab groups. David Pardo and Ana López have been incredibly helpful and offered lots of Spanish support throughout these four years, *gracias*! Thanks to Naomi, Tom, Sarah, Ellie, Alice, Matt, Marion, Shauni, Hannah, and everyone else in D59 for being a very welcoming bunch, for all the help, the after work fun, and most importantly, for all the cake.

Part of this thesis was carried out in collaboration with Noel Blanco-Touriñán, Thomas A DeFalco and Cyril Zipfel, who I would like to thank for all of their work, insightful ideas and proactivity. Thank you Noel for always being a great support and a better friend after all these years since our MSc (great) times in Valencia.

My time in the Department would not have been the same without everyone I have met and the friends I made. A huge thanks to Sarah Sommer for being a great friend, for all the coffee and biscuits, and for the international understanding in this rainy country. I do not forget all the help and advice received from Bobby Caine, specially during the first and most challenging months of my time in Sheffield, thank you!

Finally, on a personal level I have to acknowledge the people I have been lucky enough to meet in Sheffield and have kept me sane during the most challenging times, have celebrated the success, and have been a part of my family while I have been here. I would also like to thank my first mentor, Mónica Balsera, for introducing me to scientific research and motivating me to pursue a career in science. Lastly, I thank the part of my family that has always encouraged my education, valued my achievements and accompanied me every step of the way; *A mi madre, mi hermano y a mi tia Jeroni, muchas gracias por inculcar en mi el interés por la ciencia y por vuestro apoyo en mis decisiones personales y profesionales. Esta tesis os la dedico a vosotros*.

Publications and collaborators

Research presented in Chapter 4 of this thesis will be submitted for publication under the title: "*CrRLK1L receptor-like kinases HERK1 and ANJEA are female determinants of pollen tube reception*". This work was carried out in collaboration with Noel Blanco Touriñán (IBMCP, Universidad Politécnica de Valencia, Spain), Thomas A DeFalco (The Sainsbury Laboratory, Norwich, UK; current address: University of Zurich, Switzerland), and Cyril Zipfel (The Sainsbury Laboratory, Norwich, UK; current address: University of Zurich, Switzerland), who performed the protein-protein interaction assays described in Chapter 4.

A literature review covering the functional conservation of CrRLK1L proteins in plants was prepared during the first stages of my PhD and was subsequently extended and reformatted for publication as a Minireview in Frontiers in Plant Science:

> **Galindo-Trigo S, Gray JE and Smith LM (2016)** Conserved Roles of CrRLK1L Receptor-Like Kinases in Cell Expansion and Reproduction from Algae to Angiosperms. *Front. Plant Sci.* 7:1269. doi: 10.3389/fpls.2016.01269

Additionally, I have contributed to the final stages of development of a research project led by my supervisor Lisa M Smith addressing the characterisation of a malectin domain-containing kinesin in Arabidopsis. This work has also been submitted for publication and is presently under peer review with the title: "*A malectin domain kinesin functions in pollen and seed development in Arabidopsis*".

Abstract

Development of plant organs requires constant monitoring of endogenous and environmental cues for which plant cells have evolved a wide array of sensors. Among them, the receptor-like kinase (RLK) family is of particular relevance for plants due to its remarkable expansion during plant evolution. RLKs sense exogenous and endogenous signals, controlling a myriad of processes such as responses to hormones and pathogens. The *Catharanthus roseus* RLK 1-like (CrRLK1L) group of RLKs is known to control immunity and developmental processes like reproduction and cell expansion, and have been postulated to act as signalling hubs in which several cellular pathways converge. This is best exemplified by its most studied member, FERONIA (FER), a receptor of rapid alkalinisation factor (RALF) peptides and cell wall components, and a mediator of receptor complex assembly during pathogen perception.

In this project the Arabidopsis CrRLK1L receptor family was examined with the goal of identifying novel functions in plant development for uncharacterised or already characterised members. A CrRLK1L T-DNA mutant set was obtained and several higher order mutants generated to reveal defects masked by functional redundancy between related CrRLK1Ls. Initial screens identified roles for HERCULES RECEPTOR KINASE 1 (HERK1), HERK2 and THESEUS1 (THE1) in abscisic acid signalling during germination and a role during reproduction for HERK1 and its uncharacterised homolog ANJEA (ANJ). Further experiments confirmed the involvement of HERK1 and ANJ in controlling pollen tube reception in the ovule. HERK1 and ANJ were found to localise in the filiform apparatus of the synergid cells, to influence the relocalisation of NORTIA after pollen tube arrival and to physically associate with LORELEI. Additionally, the Arabidopsis RALF family was probed to identify regulators of reproduction, yielding the identification of peptides RALFL4 and RALFL19 as determinants of pollen tube growth stability.

Table of contents

List of figures

List of tables

Abbreviations

ABA, Abscisic acid

ABI2, ABSCISIC ACID INSENSITIVE 2

AHA2, PROTON ATPASE 2

amiRNA, Artificial microRNA

ANJ, ANJEA

ANX1, ANXUR1

ANX2, ANXUR2

BiFC, Bimolecular fluorescence complementation

BUPS1, BUDDHA'S PAPER SEAL 1

BUPS2, BUDDHA'S PAPER SEAL 2

CoIP, Co-immunoprecipitation

Col-0, Columbia-0 accession of *Arabidopsis thaliana*

CrRLK1L, *Catharanthus roseus* RLK 1-like

CVY1, CURVY1

DIC, Differential interference contrast microscopy

DNA, Deoxyribonucleic acid

ERU, ERULUS

FA, Filiform apparatus

FER, FERONIA

FLS2, FLAGELLIN SENSING 2

GFP, GREEN FLUORESCENT PROTEIN

GPCR, G-protein coupled receptor

GPI, Glycosylphosphatidylinositol

GUS, β-glucuronidase

H_2DCF-DA, Dichlorofluorescein diacetate

HERK1, HERCULES RECEPTOR KINASE 1

HERK2, HERCULES RECEPTOR KINASE 2

HK, Histidine kinase

KD, Kinase-dead

LatB, Latrunculin-b

LB, Lysogeny broth medium

LRE, LORELEI

LRR, Leucine-rich repeat

LRX, LEUCINE-RICH REPEAT EXTENSIN

MDS1, MEDOS1

MDS2, MEDOS2

MDS3, MEDOS3

MDS4, MEDOS4

MRI, MARIS

MS, Murashige & Skoog medium

NAA, 1-naphtaleneacetic acid

NASC, Nottingham Arabidopsis Stock Centre

NTA, NORTIA

PCR, Polymerase chain reaction

RALF, Rapid alkalinisation factor

RLCK, Receptor-like cytoplasmic kinase

RLK, Receptor-like kinase

RNA, Ribonucleic acid

ROP, RHO OF PLANTS

ROPGEF, ROP GUANINE EXCHANGE FACTOR

ROS, Reactive oxygen species

RT-PCR, Reverse transcription PCR

SERK, SOMATIC EMBRYOGENIC RECEPTOR KINASE

T-DNA, Transfer-DNA

THE1, THESEUS1

WT, Wild-type

Y2H, Yeast two hybrid

Chapter 1

Introduction

1.1 Signalling at the surface of plant cells

From the simplest bacteria to the most complex eukaryote, the cells of every organism sense their environment to adjust their metabolism accordingly and ensure an efficient adaptation. The sessile lifestyle of plants entails a greater dependence on their capacity to modulate cell physiology upon changing conditions in their environment. Plants adjust their physiology constantly upon changes in light intensity, temperature, mechanical forces, water and nutrient availability, presence of pathogens and even neighbouring plants. These inputs are constantly being registered at the cell surface by receptors that specifically detect changes in the surroundings of the cell so they can be integrated and translated into adequate cellular responses. The plasma membrane therefore constitutes a communication platform that not only allows the reception of extracellular inputs but also constitutes the site of emission of signals that trigger modification of the local biochemistry and cell-to-cell communication to coordinate distal parts of a plant's organ. Because plant cells are encapsulated in cell walls that impede cell migration and lock cells in a specific position of the plant, intercellular communication is as relevant for the adaption to a changing environment as it is crucial to coordinate the development of the multicellular structure of plant organs.

Receptors are generally membrane proteins (integral or peripheral) that specifically bind to molecular signatures or alter their biochemical properties upon certain stimuli to trigger an intracellular cascade of events leading to a cellular response. Diversity in receptor structure entails a multitude of signalling recognition and transmission mechanisms that generally involves structural rearrangements of the receptor, exchange of interaction partners, post-translational modifications of the receptor or its interactors, or a combination of these steps. Some of the best characterised and most common cell surface receptor systems are the histidine kinases (HKs), G-protein coupled receptors (GPCRs) and receptor-like kinases (RLKs). The following sections provide a brief overview of HK and G-protein signalling to then focus on the RLK of plants, core topic of this dissertation.

1.1.1 Histidine kinases

HKs are part of the two component system (TCS) receptor module that comprises HKs and response regulators (RRs; [1]). The TCS is the main receptor system in bacteria and while it has not been found in animals, it is well conserved in the plant lineage [2]. HKs are membrane proteins that autophosphorylate a conserved histidine upon ligand binding to then trigger phosphorylation of the RRs. In plants, the phosphorylation of the RRs is mediated by a third component, the histidine-containing phosphotransfer protein (HpT; [3]). HKs are known to regulate a variety of responses including responses to hormones, osmotic stress, cold, drought and pathogens [3]. The best characterised plant HKs are the ethylene and cytokinin receptor systems [4-5]. The majority of these HKs present transmembrane regions within a highly variable N-terminus through which they are thought to recognise the signal, followed by a conserved C-terminal kinase domain. HKs have been found to work as dimers and to trigger reciprocal phosphorylations that lead to the activation of the downstream RRs (Figure 1.1A). Exceptions lacking the N-terminal transmembrane domains have also been reported for some plant HKs although their role as cytoplasmic receptors or co-receptors to membrane attached HKs awaits clarification [3].

1.1.2 G-protein coupled receptors

G-protein signalling is commonly described as the best characterised pathway due to the intensive research in animal cells in the last decades [6]. Core signalling elements involve heterotrimeric G-protein subunits Gα, Gβ and Gγ and a GPCR. Heterotrimeric G-protein subunits are membrane anchored proteins while GPCRs are 7-pass transmembrane proteins. Classically, the GPCR receives the signal, undergoes a conformational change in the transmembrane spans and subsequently impacts the activity of intracellularly bound G-proteins. In the resting state, G-proteins form a Gαβγ heterotrimer that interacts with the intracellular side of the GPCR. Upon GPCR activation, the Gα subunit guanine nucleotide exchange activity is switched on, a GDP molecule is then exchanged for GTP, rendering the Gα subunit active and promoting the dissociation of the trimer of G-subunits and activating downstream signalling [7]. While this is true for animal cells, plant cell heterotrimeric G-protein signalling mechanistics are still under debate [8-10]. On one hand, while 7-pass transmembrane proteins are present in the plant genome there is little evidence to support their role as regulators of the G-protein guanine nucleotide exchange activity [9]. Additionally, biochemical properties of the Gα proteins in plants seem to differ from the animal ones as plant Gα do not require a GPCR to exchange GDP for GTP, meaning that either the

pathway is constitutively on, or that there is a molecular brake that is deactivated to activate the signalling pathway [11]. Plant G-protein signalling has been linked to sugar sensing through the REGULATOR OF G-PROTEIN SIGNALLING 1 (RGS1) protein, believed to suppress Gα GTP hydrolysis until glucose is sensed [12-13]. However, sugar sensing does not directly explain all the phenotypes observed in mutants of the different G subunits, raising the question of whether, in plants, this signalling pathway has been relegated to sugar sensing only [8-9]. Whereas some authors believe this is the case and the control of sugar levels in plants would impact other signalling pathways to maintain balanced plant growth [8], others disagree and hypothesise the G-protein pathway must be directly involved in each of the processes for which a mutant G-protein phenotype has been reported [9]. In support of the latter, detected interactions between G-subunits and several RLKs like FLAGELLIN SENSING 2 (FLS2), FERONIA (FER) and BRASSINOSTEROID INSENSITIVE 1 (BRI1) could explain G-protein involvement in immunity, stomatal responses and development [14-16]. In the light of this evidence some authors have proposed a completely different scenario from the canonical (animal) G-protein signalling in which plant heterotrimeric G-proteins would be mainly regulated via RLK-mediated phosphorylation and not by guanine-nucleotide exchange (Figure 1.1B; [9, 11]). Future research will aid clarifying the degree of conservation of this signalling pathway between animal and plant cells.

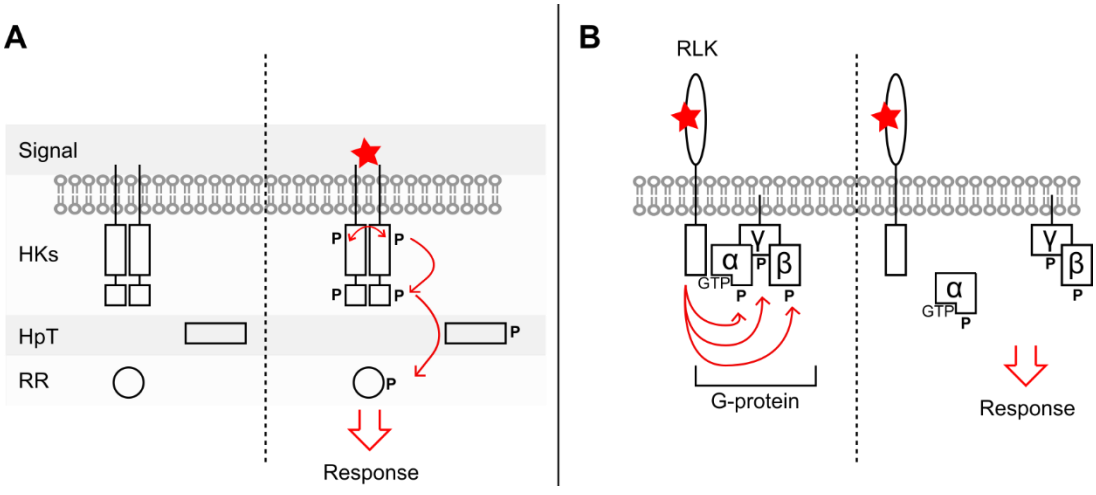

Figure 1.1 Models of histidine kinase (HK) and G-protein signalling in plants. A, simplified diagram of histidine kinase signal transduction involves transphosphorylation of the HKs and phosphorylation of the response regulator (RR) via histidine-containing phosphotransfer protein (HpT; [3]). **B**, simplified diagram of the latest proposed mechanism of G-protein signalling in plants involving receptor-like kinases (RLKs) as G-protein coupled receptor that interacts with and phosphorylates the G-protein subunits (Gα, Gβ and Gγ) to render them active and trigger downstream cascades. Red star represents a specific extracellular signal [9].

1.1.3 Receptor-like kinases

The RLKs constitute the largest receptor family in plants, accounting for more than 600 members in Arabidopsis [17]. Typical RLK domain organisation comprises an N-terminal signal peptide, an extracellular domain that confers signal perception specificity, a transmembrane span and an intracellular serine/threonine kinase domain; RLKs lacking an extracellular domain are also found and generally referred to as receptor-like cytoplasmic kinases (RLCKs; [17-18]). RLKs usually localise to the plasma membrane of the cell as transmembrane proteins, exposing their ectodomains to the apoplast and their kinase domain to the cytoplasm. Remarkable diversity in plant RLKs ectodomains explains their involvement in a wide range of cellular processes including sensing of endogenous peptidic and non-peptidic hormones, pathogen-associated molecular patterns and cell wall integrity, among others [18].

1.1.3.1 RLK family expansion and diversity

Phylogenetic analysis of kinases in multiple species revealed the plant RLK family is monophyletic with respect to their kinase domain and shares a common ancestor with animal Pelle receptors, giving these receptor kinases a deeply rooted function in the regulation of eukaryotic cells [17, 19]. Receptor kinases are over-represented in the land plant genome in comparison with animals and earlier divergent plants like algae and, given that the relative representation of RLKs is conserved across multiple lineages of land plants, it is likely that this receptor family expanded before the divergence of the land plants [17, 19]. The RLKs are therefore believed to represent a key tool in the adaptation to land and in the development of complex three-dimensional multicellular structures that comprise the body plan of land plants [17, 20].

Plant RLKs are commonly classified according to their extracellular domain into a total of 23 subfamilies, including cytoplasmic and membrane-attached RLCKs (Figure 1.2; [17]). Phylogenetic reconstruction of Arabidopsis RLKs evolutionary history using the kinase domain sequences revealed a total of 44 subfamilies in which related extracellular domains cluster together, indicating that the 23 RLK subfamilies emerged early in the evolution of this receptor family by domain shuffling and have expanded in number later on by multiple gene duplication events [17]. Interestingly, comparison of RLKs from Arabidopsis and rice demonstrated that RLKs families involved in development have remained stationary in comparison to those involved in defence since the divergence of eudicots and monocots, exemplifying the evolutionary pressure imposed by pathogens on certain RLK subfamilies to expand and diversify [21]. The

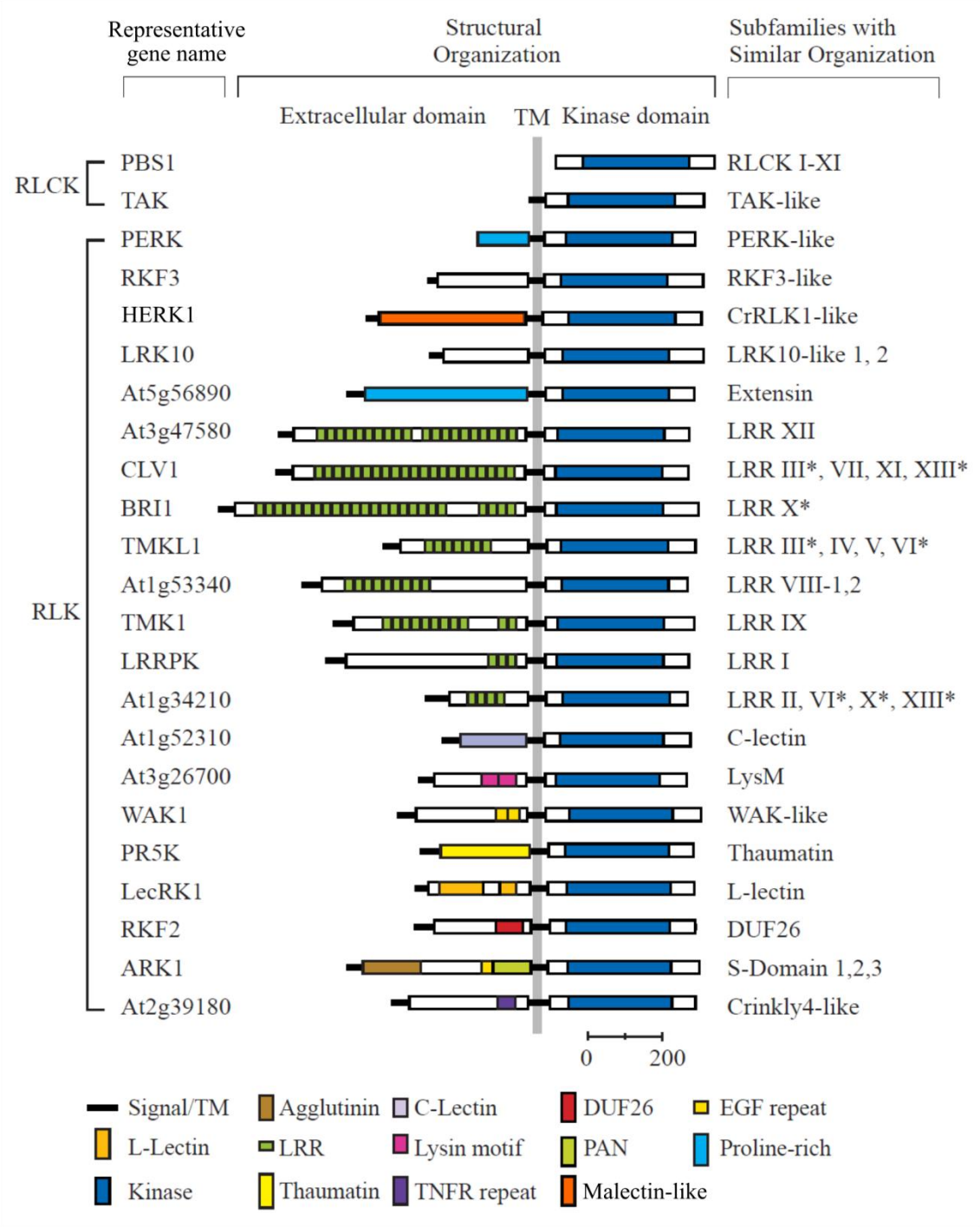

Figure 1.2 Domain organisation of the 23 distinct subfamilies of RLKs and RLCKs of plants adapted from Shiu and colleagues 2001 [17]. TM, transmembrane; C-lectin, C-type lectin; DUF, domain of unknown function; EGF, epidermal growth factor; L-lectin, legume lectin; LRR, leucine-rich repeat; PAN, plasminogen/apple/nematode domain; TNFR, tumour necrosis factor receptor.

extracellular domain of eight of the 23 subfamilies contain multiple leucine-rich repeats (LRRs), generally thought to mediate protein-protein interactions (Figure 1.2; [22]). LRR RLKs constitute a third of Arabidopsis RLKs and members of this family include

plant development regulators like BRASSINOSTEROID INSENSITIVE 1 (BRI1; brassinolide recognition; [23-24]), CLAVATA1 (CLV1; CLV3 peptide recognition; [25]) and HAESA (HAE; IDA peptide recognition; [26]); as well as very well characterised immunity regulators like FLS2 (flagellin recognition; [27]) and EF-TU RECEPTOR (EFR; recognition of EF-Tu; [28]). Other well characterised RLK subfamilies include the wall-associated kinase (WAK) and *Catharanthus roseus* RLK1-like (CrRLK1L) subfamilies which bind cell wall components like pectin through their extracellular domains, as well as small secreted peptides in the case of CrRLK1Ls [29-33]. Lysine motif (LysM) RLKs specifically recognise N-acetyl glucosamine (NAG)-containing carbohydrates present in pathogenic and symbiotic bacteria, as well as in chitin [34-36]. Lectin-containing RLKs (LecRKs) recognise specific sugar moieties present in cell walls of pathogens and nematodes and have been linked to defence against pathogens [37-38].

1.1.3.2 Ligand sensing mechanisms from structural evidence

Structural information about the three-dimensional organisation of RLK-ligand complexes obtained through X-ray crystallography in recent years has advanced our understanding in the molecular mechanisms underlying the signal recognition by plant RLKs. To date, structural evidence has been obtained for members of the LRR RLK, LysM RLK and LecRK families of receptors [39-40].

LRR RLKs like FLS2 and HAE, among others, bind small peptides in an extended conformation along several of their LRRs through multiple hydrophilic and hydrophobic interactions between the RLK and the peptide's backbone and post-translational modifications [26-27, 39-41]. Several LRR RLK-ligand structures combined with targeted mutagenesis have highlighted the importance for ligand perception of the peptide C-terminal residues as well as its post-translational modifications [26-27, 39, 41]. LRRs can be interrupted by non-LRR tracts of amino acids, known as island domains, that protrude from the typical LRR horseshoe arrangement to create a cleft for ligand binding [39-40, 42]. This is the case for LRR RLKs BRI1 and PHYTOSULFOKINE RECEPTOR (PSKR), receptors of brassinosteroids and phytosulfokine, respectively, in which direct binding of the ligand at the interface between LRRs and island domain protrusions triggers a conformational change in the island domain [24, 39, 43].

Ectodomains of LysM RLKs like CHITIN ELICITOR RECEPTOR KINASE 1 (CERK1) contain three LysM motifs that fold tightly against one another and are responsible for

binding chitin [34, 36]. Ligand binding occurs through the second LysM domain without remarkable conformational changes [34]. Exposure to long chains of chitin is expected to promote oligomerisation of LysM RLKs by binding to the building block of chitin, NAG, at different positions along the chitin molecule, as reported for bacterial LysM-containing proteins [34, 44].

The receptor complex of the Brassica self-incompatibility S-LOCUS RECEPTOR KINASE (SRK) and S-LOCUS CYSTEINE-RICH PROTEIN (SCR) is the only solved structure of a cysteine-rich peptide-receptor complex in plants [40, 45-46]. Interestingly, binding of SCR to the LecRLK SRK induced dimerisation with another SCR-SRK complex, forming a tetramer that is stabilised by contacts between both receptors and peptidic ligands [40, 45]. Crystal structures of the extracellular domains of CrRLK1L members of Arabidopsis ANX1 and ANX2 have also been solved in which tandem domains with structural similarity to the malectin protein (termed the malectin-like domain) appear to stack against each other forming a cleft proposed to mediate protein-ligand interactions [47-49]. Based on the predicted structural similarity to the animal malectin protein, the CrRLK1L malectin-like extracellular domain was regarded as a putative carbohydrate binding domain [50-51]. While biochemical analysis has demonstrated the CrRLK1L extracellular domains can bind pectin [30-31], structural analysis revealed that the residues involved in carbohydrate coordination of the malectin protein are absent in the CrRLK1L malectin-like domain [47-48], suggesting the carbohydrate binding mechanism is not conserved between these structurally-related proteins. However, structural information of CrRLK1L-ligand complexes remains elusive and therefore the description of the molecular mechanism of CrRLK1L ligand recognition awaits further investigation. Furthermore, studying the mechanistics of plant malectin domain-mediated functions will help us understand RLKs beyond the CrRLK1L family, as malectin domains can be found in the ectodomains of LRR-RLKs like OUTGROWTH-ASSOCIATED PROTEIN KINASE (OAK; [52]) or INCREASED OOMYCETE SUSCEPTIBILITY 1 (IOS1; [53]), either located in an N-terminal position followed by LRRs, or between LRRs and upstream to the transmembrane region [49].

1.1.3.3 Signal transduction mechanisms

Classically, RLK downstream signalling activation follows a three step mechanism: first, extracellular recognition of the ligand takes place, inducing changes in the RLK conformation and kinase domain autophosphorylation; secondly, RLK homo- or hetero-dimerisation occurs, rendering their respective intracellular kinase domains in close proximity; and finally, transphosphorylation of the kinase domains elicits interaction with

downstream signalling elements and consequent activation of the signalling cascade. In animals many RLK signalling cascades involve the activation of a monomeric ras-like G-protein (see [18, 39, 54] for reviews).

While LysM RLKs can form homodimers upon chitin binding, LRR RLKs like BRI1, PSRK, FLS2 or HAE are known to recruit members of the SOMATIC EMBRYOGENIC RECEPTOR KINASE (SERK) family of LRR RLKs to form heterodimers [24, 26, 55-56]. Interestingly, SERK proteins are able to establish specific interactions with ligand-bound ectodomains of several of the abovementioned LRR RLKs, suggesting this family of small LRR RLKs is versatile in forming co-receptors to these ligand-bound receptors [39]. In some cases, ligand binding induces small conformational changes in the topology of the RLK ectodomain that reconstruct the interaction surface between ligand-bound receptor and SERK co-receptor [24, 55]. In cases where ligand perception does not trigger substantial structural rearrangements in the receptor [26, 56], direct contact of the SERK co-receptor with both the ligand and receptor stabilises the complex formation. All reports of LRR RLK-SERK complex structure indicate that the C-termini of each interactor appear in close proximity, suggesting their respective intracellular kinase domains should be capable of establishing physical interactions required for transphosphorylation [39].

Notably, up to 20% of Arabidopsis RLKs lack one or more of the signatures known to be essential for kinase activity while conserving the overall kinase domain structure and are therefore considered kinase-defective, kinase-dead or pseudokinase RLKs [57]. These kinase-defective RLKs are thought to function as i) mediators of receptor complex assembly, or as ii) negative regulators of RLK signalling by acting as dummy substrates for active RLKs, competing with functional RLK co-receptors and thus damping the intensity of the signal [39, 57]. Although our understanding of the mechanistics of the regulation imposed by pseudokinases is still superficial, high representation within the plant RLK family suggests they likely execute core functions in RLK signalling.

1.2 Functions of the *Catharanthus roseus* RLK 1-like family

The CrRLK1L family owes its name to the first member, CrRLK1, identified in *Catharanthus roseus* cell cultures as a novel type of RLK given the lack of similarity of its extracellular region to any known protein at the time [58]. Members of the CrRLK1L family present an N-terminal signal peptide, a plant-specific malectin-like domain, comprising a tandem array of two regions with structural similarity to the animal

malectin protein [47-49], a transmembrane region and an intracellular kinase domain. This group of RLKs has drawn the attention of the scientific community in the last decade since the characterisation of Arabidopsis CrRLK1Ls FER and THESEUS1 (THE1) as determinants of fertility and cell wall integrity, respectively [59-61]. We now know the CrRLK1Ls are receptors of small cysteine-rich peptides of the RAPID ALKALINISATION FACTOR (RALF) family and are capable of binding cell wall components like pectin, although a mechanistic explanation awaits structural information about CrRLK1L-ligand complexes [31-33, 62-64]. The following sections of this introductory chapter summarise the multitude of functions performed by CrRLK1Ls during development and immunity in Arabidopsis (see Figure 1.3 for a summary of CrRLK1L interactors).

1.2.1 Reproduction

Six CrRLK1Ls have been reported to influence reproduction in Arabidopsis, FER, ANXUR1 (ANX1), ANX2, BUDDHA'S PAPER SEAL 1 (BUPS1), BUPS2 and ERULUS (ERU). ANX1/2, BUPS1/2 and ERU control reproduction from the paternal side by ensuring proper pollen tube growth [65-67]. Pollen tubes grow by tip growth exclusively and therefore the description of this signalling pathway has been included in the tip growth section (section 1.2.2). FER was the first CrRLK1L to be identified in the reproductive context as *fer* mutants displayed a reduced seed set caused by impaired pollen tube reception in the ovule [59]. FER was found to execute maternal control of fertilisation by regulating the reception of the pollen tube in the female gametophyte from the synergid cells [60]. Although the exact mechanism through which FER regulates the reception of pollen tubes is still unknown, reactive oxygen species (ROS) production and Ca^{2+} oscillations during pollen tube reception are known to be important for fertility and defective in *fer* mutants [68-69]. FER forms a receptor complex with LORELEI (LRE), a glycosylphosphatidylinositol (GPI)-anchored protein at the synergid cells although the nature of the signals perceived by this complex is still up for debate [70-71]. NORTIA (NTA), a MILDEW-LOCUS O (MLO) protein, is another synergid cell determinant of pollen tube reception that controls Ca^{2+} oscillations and relocates within the synergid cell upon pollen tube arrival in a FER-dependent manner [69, 72]. A more detailed description of the control of pollen tube reception by CrRLK1Ls can be found in the fourth chapter of this dissertation.

1.2.2 Tip growth

Tip growth is a specialised type of cell expansion that determines the growth of certain

plant structures such as root hairs, trichomes and pollen tubes by localising the cell wall remodelling machineries to a specific pole of the cell [73]. CrRLK1Ls are heavily involved in the control of tip growth as FER is required for root hair and trichome tip growth, ERU is necessary for root hair and pollen tube growth, and ANX1/2 and BUPS1/2 ensure pollen tube tip growth stability.

Root hairs in *fer* and *eru* mutants fail to elongate and sometimes burst [74-76]. FER and ERU localise at the plasma membrane and accumulate at the tip of growing root hairs [74, 77]. FER is required for maintenance of NADPH oxidase-mediated ROS production at the tip of root hairs [74]. The kinase domain of FER interacts with and phosphorylates RHO OF PLANTS GUANINE NUCLEOTIDE EXCHANGE FACTOR (ROPGEF) which in turn promotes the activation of ROP proteins, monomeric G-proteins thought to directly trigger NADPH oxidase activity [74]. LRE-LIKE GPI-ANCHORED PROTEIN 1 (LLG1) interacts with the FER ectodomain and ensures proper delivery of FER to the plasma membrane [70]. Additionally, plasma membrane localised RLCK MARIS (MRI) is a downstream element of FER signalling in root hairs although the exact mechanism of action remains speculative [78]. ERU is important for maintenance of cytoplasmic Ca^{2+} gradients and cell wall remodelling at the tip of root hairs as *eru* mutants present altered pectin dynamics caused by increased pectin methylesterase inhibitor activity [75, 77]. Additionally, FER and PROTON ATPASE 2 (AHA2) are differentially phosphorylated in *eru* mutants indicating that FER signalling and the control of apoplastic pH executed by AHA2 are also interconnected with ERU's control of root hair tip growth [77].

Two pairs of redundant CrRLK1Ls have been demonstrated to control pollen tube tip growth. Both *anx1 anx2* and *bups1 bups2* mutants display aberrant pollen tube growth and premature pollen tube burst *in vitro* and *in vivo* [62, 65-66]. ANX1, ANX2, BUPS1 and BUPS2 localise at the plasma membrane of pollen tubes and form heterocomplexes to mediate the perception of autocrine RALF signals, RALFL4 and RALFL19, to maintain pollen tube growth stability [62]. ANX1/2 downstream signalling controls deposition of cell wall materials and activation of NADPH oxidases to maintain tip-focused gradients of ROS [78-79]. Furthermore, MRI also constitutes a downstream signalling element in this RALFL4/19-ANX1/2-BUPS1/2 signalling pathway [80].

Finally, FER and CURVY1 (CVY1) are necessary for correct trichome branch growth, as collapsed and distorted trichomes are abundant in *fer* and *cvy* loss-of-function mutants [68, 81]. Whether similar pathways to those controlling root hair and pollen tube tip growth take place in trichomes is still unclear and requires further investigation.

1.2.3 Cell wall integrity control

As introduced in the previous section, CrRLK1L proteins are tightly associated with cell wall integrity and remodelling in tip growing structures; however, this association persists beyond that specific type of cell expansion. THE1 was the first CrRLK1L linked to cell wall integrity as *the1* mutants were identified through a suppressors screen of a cellulose synthase mutation [61]. THE1 signalling is responsible for the production of ROS and the accumulation of lignin upon cell wall damage as demonstrated using loss-of-function and over-expresser *THE1* mutants [61, 82]. Very recently, THE1 has been reported to influence root elongation and lateral root initiation in cooperation with RALF34. THE1 is a pH-dependent receptor for RALFL34 and the control of lateral root initiation is hypothesised to involve the surveillance of cell wall integrity at root initiation sites [63].

FER influences cell expansion in multiple contexts, including roots, hypocotyls, petioles and pavement cell interdigitations. On one hand, FER perceives RALF1 in the root to modulate cell expansion by triggering an intracellular cascade that involves interaction with RLCK RESISTANCE TO PSEUDOMONAS SYRINGAE PV MACULICOLA 1 (RPM1)-INTERACTING PROTEIN KINASE (RIPK) and subsequent phosphorylation of the AHA2 proton pump, thus modulating the apoplastic pH which in turn modifies the rigidity of the cell wall [32, 83]. On the other hand, FER is also able to bind pectin's building block polygalacturonic acid, one of the major components of the cell wall [64]. Upon saline stress-induced cell wall loosening, FER-mediated pectin sensing primes the cell to withstand the recovery phase [64]. Additionally, FER pectin sensing has been demonstrated to trigger ROPGEF-ROP downstream signalling to mediate pavement cell lobing [31]. Furthermore, ectodomains of ANX1, ANX2, BUPS1 and BUPS2 are also capable of binding pectin *in vitro*, suggesting a generalised role of the CrRLK1L family in sensing cell wall disruptions [64].

Homeostasis in the absorption and accumulation of metal ions like nickel (Ni), copper (Cu) and lead (Pb) is crucial for proper plant growth. Plants sensitive to these metals have developed strategies to minimise the cellular toxicity they impose by, for instance, retaining these cations in the cell wall [84]. Modification of cell wall polymers like pectin by pectin methylesterases can increase the abundance of negatively charged groups that normally coordinate Ca^{2+} ions [85]. Ni, Cu or Pb can also be coordinated by the exposed carboxyl groups within the cell wall and therefore reduce their cellular toxicity [84]. Several members of the Arabidopsis CrRLK1L family have been reported to modulate the tolerance to metal ions in root and hypocotyl growth in seedlings,

including FER, HERCULES RECEPTOR KINASE 1 (HERK1), HERK2, THE1, as well as the recently characterised MEDOS1 (MDS1), MDS2, MDS3 and MDS4 [86-87]. Although the molecular basis of these responses in CrRLK1L mutants is still unclear, cell wall integrity surveillance by direct sensing of pectin upon exposure to metal ions is a likely explanation [87].

1.2.4 Immunity

Plant immunity relies heavily on plasma membrane RLKs, with several LRR RLKs including FLS2, EFR and the SERK protein BRI1-ASSOCIATED RECEPTOR KINASE 1 (BAK1) being key to pathogen sensing (see [88] for review). CrRLK1Ls FER, ANX1 and ANX2 are also involved in modulating responses to pathogens. The first evidence of the involvement of FER in immunity showed that *fer* mutants present enhanced resistance to powdery mildew infection in rosette leaves [69]. More recently, FER has been characterised to regulate RLK complex formation during bacterial pathogen perception [33]. Briefly, pathogen detection prompts the formation of FLS2/BAK1 or EFR/BAK1 complexes, necessary to trigger immune signalling [88]. In the absence of FER, the formation of these complexes is weaker, impairing the immune signalling and increasing susceptibility to bacterial pathogens [33]. Furthermore and in a negative feedback loop, the RALFL23 propeptide is proteolytically processed upon pathogen recognition and exported to the apoplast where it binds FER, in turn impairing FER's capacity to facilitate immune receptor complex formation [33]. Finally, FER chaperone LLG1 interacts with FLS2/BAK1 complexes to modulate plant immunity, and BAK1 has been shown to mediate RALF1 sensing in the context of root growth, depicting a tight relationship between signalling pathways of development and immunity [89-90].

FER’s most closely related CrRLK1Ls, ANX1 and ANX2, were also found to affect plant immunity through direct interaction with FLS2/BAK1 protein complexes [91]. In contrast to FER, ANX1 and ANX2 impose a negative control of plant immunity by impeding the association of FLS2 and BAK1 and therefore hindering pathogen recognition [91]. Whether RALF peptides also influence ANX1/2 control of plant immunity remains to be investigated. Notably, certain pathogenic fungi produce RALF peptides that have been demonstrated to be determinants of pathogenicity and to signal through FER, possibly mimicking RALFL23 endogenous negative regulation of immunity to promote fungal infection [92].

1.2.5 Cross-talk with other hormonal signalling pathways

Several connections have been established between CrRLK1Ls and well characterised hormonal signals such as auxins, ethylene and abscisic acid (ABA). Auxins promote root elongation inhibition and root hair growth via ROP and NADPH oxidase-dependent mechanisms [93]. *fer* and *eru* mutants are partially insensitive to exogenous auxins in this context, and given FER involvement in ROP signalling and NADPH oxidase activation to sustain root hair growth as well as ERU functions in root hair development [74-75], it is plausible that these CrRLK1Ls are downstream effectors of this auxin regulated process. Additional evidence for the involvement of these two CrRLK1Ls in auxin signalling was provided by the identification of *ERU* as a direct transcriptional target of AUXIN RESPONSE FACTOR 7 (ARF7) and ARF19 [77], and the control of pavement cell lobe formation by FER-mediated activation of ROP signalling [31] - another auxin-dependent process [93].

fer mutants present premature senescence of leaves and short hypocotyls, suggestive of ethylene hypersensitivity [94-95]. In support of this hypothesis, the FER kinase domain was found to interact with and phosphorylate S-ADENOSYLMETHIONINE SYNTHETHASE 1 (SAM1) and SAM2, two enzymes directly involved in the synthesis of ethylene [94, 96]. SAM1 and SAM2 proteins are more abundant in *fer* plants, which were also found to contain higher levels of ethylene, suggesting FER executes a negative regulation of ethylene biosynthesis via SAM1 and SAM2, thus explaining the ethylene-hypersensitive-like phenotypes of *fer* mutants [94].

Two reports have depicted an intricate interconnection between CrRLK1L and ABA signalling. First, FER was described as a negative regulator of ABA signalling as: i) *fer* mutants are hypersensitive to exogenous ABA, ii) FER downstream interactors ROPGEF and ROP were shown to directly enhance PROTEIN PHOSPHATASE 2C (PP2C) ABSCISIC ACID-INSENSITIVE 2 (ABI2) activity, a core negative regulator of ABA signalling, and iii) *ropgef* and *rop* mutants are also hypersensitive to ABA [97]. Second, this linear model was expanded to a bidirectional regulation in which FER activity is positively regulated by ABA in a feedback loop that ensures a balanced response [98]. In brief, RALF1 activates FER activity to enhance ABI2 phosphatase activity via ROPGEF and ROP factors, dampening ABA signalling. Conversely, ABI2 and related phosphatases inactivate RALF1-FER signalling by interacting with and dephosphorylating FER. Given that ABA signalling renders ABI2 phosphatase inactive, the current model supports that ABA affects RALF1-FER signalling positively via ABI2 inactivation. This model is further supported by the hypersensitivity to ABA displayed

by *ralf1* mutant lines [98].

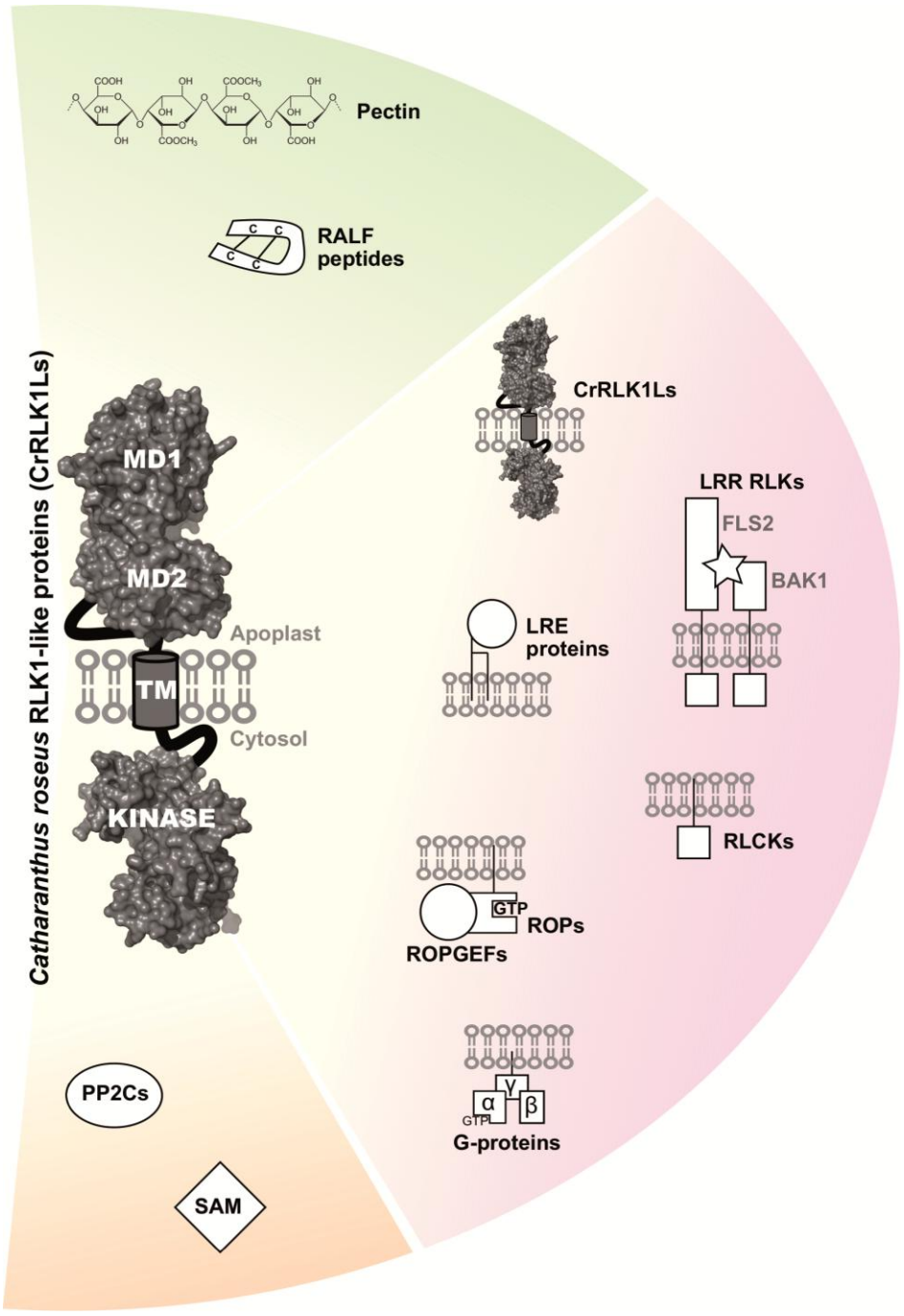

Figure 1.3 Interactors of the CrRLK1L family in Arabidopsis. Graphic summary of the Arabidopsis CrRLK1L interactome [14, 31-33, 62-64, 68, 70, 74, 83, 91, 97-98]. CrRLK1L representation contains modelled malectin-like and kinase domains of ANJ (At5g59700) based on ANX1 malectin-like structure (PDB 5y96; [47, 94]) and Pto kinase (PDB 2qkw; [99]); homology searches and models generated with SWISS-MODEL (https://swissmodel.expasy.org/interactive), graphic representation generated in Pymol (Molecular Graphics System, Version 2.0 Schrödinger, LLC.). Extracellular, plasma membrane-located and cytosolic interactors in green, purple and orange, respectively. MD1, N-terminal malectin domain; MD2, C-terminal malectin domain; TM, transmembrane domain.

1.3 Rationale, objectives and hypotheses

Clearly, research in recent years has portrayed the CrRLK1L family as a core component of plant development and defence mechanisms. Its best characterised member, FER, is regarded as a versatile signalling hub at which a multitude of endogenous and exogenous inputs converge to trigger multiple intracellular cascades that ensure a balanced response. Recent work has evidenced that FER is not unique within the CrRLK1L family as multiple other members have been assigned versatile functions in controlling diverse developmental processes and influencing plant immunity (i.e. ANX1/2 control of reproduction and immunity or THE1 involvement in cell expansion and lateral root initiation). To date and including the results enclosed within this dissertation, *At2g23200* and *At5g24010* are the only Arabidopsis CrRLK1Ls that remain completely uncharacterised. It is nevertheless noteworthy that despite exhaustive research in recent years, many questions require further investigation to obtain a clearer picture of the CrRLK1L molecular mechanism of action. For instance, it remains to be clarified whether homo- or heterodimers of CrRLK1Ls are formed in the resting state or upon ligand sensing and whether CrRLK1Ls with apparent opposed functions are in competition for ligands and co-receptors to modulate signalling. It is also necessary to shed light on the structural basis of ligand perception, receptor complex formation and signal transduction by the CrRLK1Ls and answer questions like: Which ectodomain regions are involved in the binding of cell wall polymers and RALF peptides and how are cell wall disturbances sensed? Do LORELEI proteins have a co-receptor role in the perception of apoplastic signals or do they only serve as chaperones? Does the downstream signalling network described for FER constitute a common pathway for other CrRLK1Ls? What are the molecular determinants of specificity in signalling for different CrRLK1Ls and what can we learn from them to engineer desirable traits into plants of agricultural importance?

Our understanding about the CrRLK1L functions has increased greatly since the onset of this PhD project when only eight of the 17 Arabidopsis CrRLK1L had been partially characterised. RALF1-FER was the only reported ligand-receptor example and much of what we now know about downstream signalling, crosstalk with immunity and other hormonal pathways was still undiscovered. To unravel new regulatory roles of CrRLK1Ls in Arabidopsis a set of mutants was obtained and screened for defects in a variety of developmental processes in which certain CrRLK1Ls play a role. Double and triple mutants were also generated to uncover mutant phenotypes masked by functional redundancy between related members of this receptor family. Preliminary

phenotyping of these lines yielded the identification of previously uncharacterised mutant phenotypes during germination in response to exogenous ABA and in reproduction. Multiple approaches were undertaken to characterise HERK1 and ANJEA (At5g59700; ANJ) as regulators of reproduction, including the use of mutants, genetic reporter lines, histochemical assays, as well as biochemical methods to locate these two redundant CrRLK1Ls within the signalling pathway that controls pollen tube reception. Finally, given the tight relationship between RALF peptides and CrRLK1Ls, the RALF family of peptides was probed in search for putative regulators of reproduction, allowing the identification of a redundant pair of peptides, RALFL4 and RALFL19, as pollen tube growth determinants.

In summary, the main objectives pursued during the development of the present thesis were i) to identify new functions in plant development among characterised and uncharacterised CrRLK1Ls to shed light on the versatility of this family of receptors in the control of development (see Chapter 3); ii) to characterise the nature of the reproductive defect identified in plants lacking functional HERK1 and ANJ to further our understanding of the control of reproduction executed by CrRLK1Ls (see Chapter 4); and iii) to find regulators of reproduction among the RALF peptide family aiming to identify putative ligands for HERK1, ANJ or FER during pollen tube reception (see Chapter 5). These objectives were built around the following hypotheses: first, functional redundancy between members of the CrRLK1L family was expected given the lack of evident developmental defects in multiple single mutants of closely related homologs. Second, preliminary phenotyping of *herk1 anj* mutants suggested a hypothetical scenario in which these two CrRLK1Ls would execute similar functions as those reported for FER or ANX1 and ANX2 in controlling pollen tube reception or pollen tube growth, respectively. Finally, it was hypothesised that RALF peptides could constitute the signal sensed by these CrRLK1Ls based on the similarity of the phenotypes observed in *fer* and *herk1 anj* mutants in the reception of pollen tubes and the growing evidence of CrRLK1Ls as RALF peptide receptors.

Chapter 2

Materials and methods

2.1 Biological materials

2.1.1 Plant materials and growth

Arabidopsis thaliana Columbia-0 (Col-0) accession was routinely used as a control in all experiments. A list of confirmed *A. thaliana* lines used in this dissertation is included in Annexe Table 1. For most experiments, *A. thaliana* plants were germinated directly on soil. Seeds were stratified at 4°C in a 0.1% agarose solution (w/v) for three or four days, sown onto soil containing a 4:1 mix of M3 Levington compost:sand and transferred to a controlled environment growth chamber (Conviron) with 22ºC continuous temperature, 16 hours per day of ~120 $\mu mols^{-1}m^{-2}$ light and 60% humidity. Seeds were kept under high humidity conditions until the cotyledons were fully expanded, then were gradually adapted to standard humidity (60%) over two days. Basta-resistant transformants were selected on soil during germination by soaking the soil mixture with a 1:1000 (v/v) Whippet solution (150 g/L glufosinate ammonium; AgChem Access Ltd). For seed harvest, inflorescences with mature siliques were placed in glassine bags and allowed to mature for a further week to minimise seed loss by silique dehiscence. Inflorescences were then detached from the plant and kept in glassine bags for two weeks to allow seed maturation and dehydration before seed collection and separation from plant debris. Seeds were stored in microcentrifuge tubes at room temperature in a dry environment.

Germination and growth of *A. thaliana* seedlings *in vitro* was used to select transformants and in phenotyping experiments. Seeds were vapour-phase sterilised with chlorine gas by exposing them to the fumes produced by the combination of 50 mL of bleach with 1.5 mL of concentrated HCl in a closed container for four hours [100]. Sterile seeds were sown onto half-strength Murashige & Skoog medium plus supplements (MS; [101]), pH 5.7 (adjusted with KOH), 0.8% agar (w/v), stratified at 4°C for four days and then incubated in a growth cabinet (Snijders Scientific) at 22ºC continuous temperature and 16 hours per day of ~90 $\mu mols^{-1}m^{-2}$ light. To select transgenic plants in the T1 generation, 100 µL of dry, sterile seed were sown onto half strength MS supplemented with antibiotics in 12x12 cm petri dishes, sowing multiple plates per construct. Kanamycin and hygromycin-B at 50 and 25 µg/mL, respectively,

were added when the media cooled down after autoclaving. In phenotyping experiments, sterile seeds were resuspended in 0.01% agarose solution (w/v) and pipetted onto the growth medium with wide-bored pipette tips. All supplements were added after autoclaving to avoid loss of bioactivity except for NaCl which was added prior to autoclaving for convenience. After sowing, plates were kept open in the laminar flow cabinet for an additional 20 minutes before sealing with micropore tape to allow excess resuspension solution to dry and thus avoid seed slippage. After stratification, plates were placed horizontally or vertically in the growth cabinet depending on the purpose of the experiment. In vertical growth experiments, growth medium was prepared with 1% agar (w/v) to minimise root penetration in the growth medium. When required, selected seedlings were transferred from the germination plates to freshly prepared control or test plates with the aid of sterile forceps.

2.1.2 Crosses and isolation of double homozygous T-DNA insertion lines

Homozygous individuals from two T-DNA insertion lines were grown on soil under standard conditions until their first inflorescences developed. For the female parent, one to four flower buds were selected according to their maturation stage (preferentially buds in which sepals are very close to forming an opening around the stigma; avoiding the first few buds in the inflorescence; stage 12 as per [102]), and emasculated. The rest of the buds in the selected inflorescences were removed to avoid cross-pollination. On the same or the following day, pollinations were performed by covering the mature stigmas with pollen from freshly dehisced anthers of the corresponding male parent [103]. Seeds from cross-pollinated siliques were collected and kept in the same conditions as seed stocks. Typically, a set of 5-10 F1 plants from the cross pollination was grown until maturity. The F2 generation of seed, in which both T-DNA insertion alleles are segregating, was collected and 20-50 F2 plants were genotyped for the corresponding genes. When no double homozygous plants were found in the F2 generation, one or more plants homozygous for one insertion and hemizygous for the insertion in the second gene were selected, and the following generations were genotyped for the segregating gene. Double homozygous plants for the insertions found were allowed to set seeds and the homozygosity state was double-checked in three to five plants from the following generation. See section 2.2.1 for plant genotyping procedures and Annexe Table 2 for the list of oligonucleotides used for genotyping.

2.1.3 Live ovule dissection and pollen tube growth *in vitro*

Flowers of the desired stage were detached from the inflorescence, placed on double-

sided adhesive tape (3M) and manipulated with Inox No. 5 forceps under a dissection microscope. First, sepals, petals and stamens were removed from the flower, leaving the pistil and pedicel. Pistils were laid on tape so one replum faced upwards. With a 30-gauge needle, incisions were made along the pistil between the replum and both ovary valves. Valves were opened and pressed against the adhesive surface, exposing the inside of the ovary. The ovary was immediately covered with 20-30 µL of a buffered solution (half-strength MS, 5% sucrose, pH 5.7 adjusted with KOH) to minimise dehydration. Another 20-30 µL of buffer were deposited on a clean 18x18 mm coverslip. Incisions at the junction of the replum and style and pedicel were made, the upper half of the ovary was carefully separated from the bottom half with No. 5 forceps and it was immediately transferred to the buffer on the coverslip. The bottom half of the ovary was separated from the valves by carefully pressing along both sides of the bottom replum with No. 5 forceps, gently detaching it from the adhesive surface and immediately transferring it to the coverslip. A microscope slide was placed over the coverslip allowing the ovary-containing buffer droplet to touch the slide, letting the surface tension adhere the coverslip to the slide. Excess buffer was removed by placing filter paper between the slide and coverslip and ovules were immediately observed by widefield or confocal microscopy.

Pollen germination *in vitro* was carried out as per Boavida and colleagues [104]. Flowers from the main inflorescences of young flowering plants were selected by visually inspecting for freshly dehisced anthers shedding pollen. Pollen germination medium contained 10% sucrose, 0.01% boric acid, 1 mM $MgSO_4$, 5 mM $CaCl_2$, 5 mM KCl and 1.5% agarose at pH 7.5 (adjusted with KOH). Medium without agarose was prepared and autoclaved; small aliquots of medium were mixed with the corresponding amount of agarose in microcentrifuge tubes in a water bath at 80°C until fully dissolved. 300 µL of the germination medium were quickly pipetted to a warm microscope slide creating a thin and flat pad. The slides were kept in a high humidity chamber for a few minutes for the medium to set and to avoid dehydration. Pollen grains were deposited onto the germination medium pad by gently rubbing the flowers on the agarose pad under a dissection microscope. Pollen-containing slides were returned to the high humidity conditions and kept at 22°C for three to six hours. Slides were covered with a coverslip and immediately visualised under a widefield microscope.

2.1.4 Bacterial materials, growth and transformation

Escherichia coli strain DH5α (*fhuA2 lacΔU169 phoA glnV44 Φ80' lacZΔM15 gyrA96 recA1 relA1 endA1 thi-1 hsdR17*) was used routinely for all cloning purposes and

plasmid DNA replication. *E. coli* was grown at 37°C on LB medium (10 g/L NaCl, 5 g/L yeast extract and 10 g/L tryptone), supplemented with 15 g/L agar for solid medium [105]. *Agrobacterium tumefaciens* strains ASE (kanamycin, tetracycline and chloramphenicol resistant), and GV3101(pMP90) (rifampicin and gentamycin resistant) were routinely used for plant transient and stable transformations. A modified LB medium with lower salt content was used for *Agrobacterium* growth (5 g/L NaCl; [100]).

2.1.5 Floral dip method for transformation of *A. thaliana*

The floral dip method was used to generate stable transgenic lines of *A. thaliana* [106-107]. For each transformation event, a set of nine to 18 healthy, adult plants early in their flowering stage were used. *Agrobacterium* carrying the desired transformation construct were grown in 250 mL of low-salt LB with the appropriate antibiotics overnight, pelleted at 3000g for 15 minutes and resuspended in a 5% sucrose solution. Immediately before dipping the plants, 0.025% of Silwet-L77 (v/v) was added to the bacterial solution. Inflorescences were dipped in the solution for two minutes, excess bacterial solution was removed by gently laying the inflorescence material on paper and then kept under high humidity and low light intensity conditions overnight. Seeds were harvested and transformants recovered from the T1 generation as per section 2.1.1. Five or more T1 transformants were obtained for each genetic construct and plant genotype.

2.2 Molecular biology procedures

2.2.1 Plant genotyping

Genotyping of plants was routinely carried out by PCR using "quick and dirty" genomic DNA preparations as template. Briefly, this fast DNA extraction procedure involved the immersion of a small developing leaf in extraction buffer (200 mM Tris-HCl at pH 7.5, 250 mM NaCl, 25 mM EDTA and 0.5% SDS); homogenisation of the sample with a micropestle in a microcentrifuge tube; removal of insoluble materials by centrifugation (five minutes at full speed in a microcentrifuge); addition of one volume of isopropanol followed by five minutes of incubation at room temperature; recovery of DNA by centrifugation (five minutes at full speed in a microcentrifuge); wash of DNA pellets with 75% ethanol solution and resuspension in water after air drying the DNA pellet for 30 minutes (adapted from [108]). Generally, 1 µL of genomic DNA solution was used in 10 µL PCR reactions containing 1 µL of 10x reaction buffer, 1 µL of 2 mM dNTPs, 0.3 µL of 10 µM primer A, 0.3 µL of 10 µM primer B and 1 µL of Taq DNA polymerase.

Standard thermocycling parameters involved an initial denaturation step of 5 minutes at 94°C followed by 35 cycles of 30 seconds at 94°C (denaturation), 30 seconds at 58°C (annealing) and one minute at 72°C (extension); and a final extension step of 5 minutes at 72°C. Annealing temperatures and extension times were optimised when required. PCR products were subsequently analysed by electrophoresis on 1% agarose gels and product sizes were inferred by comparison with commercial DNA ladders (i.e. Bioline's Hyperladder 1kb). Consult Annexe Table 2 for the list of primers used.

2.2.2 Plant gene expression analysis

RNA from 100 mg of floral tissues from several plants per line was extracted using E.Z.N.A. plant RNA extraction kit (OmegaBio-Tek). RNA quality was assessed by electrophoresis on 1% agarose gels and concentrations estimated by NanoDrop (Thermofisher Scientific, NanoDrop 8000). RNA concentrations were normalised between samples, DNaseI-treated and transcribed into first strand cDNA with random hexamers using the RevertAid cDNA synthesis kit (Thermofisher Scientific). RT-PCRs were carried out with genotyping PCR conditions and 45 seconds of extension time. Primers used for RT-PCR can be found in the Annexe Table 2.

2.2.3 Cloning

2.2.3.1 PCR amplification of inserts

Several genetic constructs were generated in this PhD project for multiple purposes including the generation of transgenic reporter lines, transient expression assays and testing of protein-protein interactions (Table 2.1). All constructs were generated by classical cloning or Gateway technology (Thermofisher Scientific; sections 2.2.3.2 and 2.2.3.4, respectively). Plasmid DNA or genomic DNA from *A. thaliana* plants was used as template for the amplification of insert sequences with HF Phusion DNA polymerase (New England Biolabs; NEB) or KOD Hotstart DNA polymerase (Merck) following the manufacturer's instructions for PCR conditions and between 30-35 cycles of denaturation, annealing and extension. Phusion DNA polymerase was commonly used for all cloning applications requiring a proof-reading DNA polymerase except for overlapping PCRs, in which KOD DNA polymerase proved more successful. Primers were designed in Primer3web (http://primer3.ut.ee/) with melting temperatures of 55-65°C. Annealing temperatures were calculated from the Primer3web report for KOD polymerase reactions and using NEB's Tm calculator for Phusion DNA polymerase reactions (https://tmcalculator.neb.com/#!/main). When genomic DNA was used as

template, primer sequences were checked for possible additional binding sites in the *A. thaliana* genome by searching against the genomic sequences in Phytozome (https://phytozome.jgi.doe.gov/pz/portal.html#!search). Modifications of the primer's 5' terminus included TOPO overhang sequence 5'-CACC-3' (Thermofisher Scientific), restriction enzyme cutting sites and additional nucleotides depending on the restriction enzyme's cleavage activity near the end of DNA fragments (https://www.neb.com/tools-and-resources/usage-guidelines/cleavage-close-to-the-end-of-dna-fragments).

Table 2.1 List of genetic constructs generated in the present study. Also listed are the corresponding set of primers used to amplify their respective DNA inserts and purpose. See Annexe Table 2 for the complete set of primers and corresponding sequences.

Plasmid	Primers	Purpose
pFER::FER-GFP pFK224	MPK096, MPK097, MPK100, MPK101	Complementation, reporter
pANJ::ANJ-GFP pFK224	MPK110,MPK113	Complementation, reporter
pHERK1::HERK1 pFK224	MPK098,MPK099, MPK102, MPK103	Complementation
pANJ::ANJ-KD-GFP pFK224	MPK112,MPK113, CLN086, CLN087	Complementation, reporter
pHERK1::HERK1-KD pFK224	MPK102, MPK103, CLN088, CLN089	Complementation
pANJ::GUS pGWB433	CLN080, CLN081	Reporter
pHERK1::GUS pGWB433	CLN078, CLN079	Reporter
pRALFL4::RALFL4-GFP pFK224	CLN091, CLN094	Complementation, reporter
pRALFL19::RALFL19-GFP pFK224	CLN097, CLN100	Complementation, reporter
pRALFL4::GUS pGWB433	CLN090, CLN092	Reporter
pRALFL19::GUS pGWB433	CLN096, CLN098	Reporter
pLAT52::amiRALF8/9/15 pLMS167	OTH039-OTH042	Knock-down
pLAT52::amiRALF4/19 pLMS167	OTH035-OTH038	Knock-down
pLAT52::amiRALF11/12/13 pLMS167	OTH031-OTH034	Knock-down
pNTA::amiRALF14 pLMS167	OTH047-OTH050	Knock-down
pNTA::amiRALF18 pLMS167	OTH043-OTH046	Knock-down
pFK224GFP	CLN035, CLN036	Modified backbone
pLAT52 pLMS167	CLN054, CLN055	Modified backbone

pNTA pLMS167	CLN044, CLN051	Modified backbone
p35S::FER-nYFP pEarleygate201	CLN049, CLN050	BiFC
p35S::FER-cYFP pEarleygate202	CLN049, CLN050	BiFC
p35S::ANJ-nYFP pEarleygate201	CLN047, CLN048	BiFC
p35S::ANJ-cYFP pEarleygate202	CLN047, CLN048	BiFC
p35S::HERK1-nYFP pEarleygate201	CLN045, CLN046	BiFC
p35S::HERK1-cYFP pEarleygate202	CLN045, CLN046	BiFC
ANJexJM-AD pGADT7AD	MPK148, MPK160	Y2H
ANJexJM-BD pGBKT7	MPK148, MPK160	Y2H
HERK1exJM-AD pGADT7AD	MPK144, MPK159	Y2H
HERK1exJM-BD pGBKT7	MPK144, MPK159	Y2H
LRE(23-138)-AD pGADT7AD	CLN056, CLN057	Y2H
LRE(23-138)-BD pGBKT7	CLN056, CLN057	Y2H
p35S::FER-GFP pGWB405	CLN049, CLN050	CoIP
p35S::FER-MYC pGWB420	CLN049, CLN050	CoIP
p35S::ANJ-GFP pGWB405	CLN047, CLN048	CoIP
p35S::ANJ-MYC pGWB420	CLN047, CLN048	CoIP
p35S::HERK1-GFP pGWB405	CLN045, CLN046	CoIP
p35S::HERK1-MYC pGWB420	CLN045, CLN046	CoIP
p35S::HA-LRE::rbcS pMLBart	GEN011, CLN073, CLN102, CLN103	CoIP

Overlapping PCRs were required for the generation of artificial microRNA (amiRNA; [109]) and site-directed mutagenesis constructs. In brief, overlapping PCRs allowed the concatenation of several DNA fragments in a two-step PCR protocol. The first step involved the amplification of each fragment separately using primers with an additional 15-20 nucleotides on the primer's 5' terminus complementary to the next concatemer's 3' terminus. PCR products from each amplicon obtained in the first step were diluted 20-50 times and used as DNA template in overlapping PCR. In the overlapping PCR, concatemers will present 35-40 complementary nucleotides at their contiguous ends, the 3' termini of which will act as primers for the DNA polymerase to extend the amplicons into longer DNA molecules containing all fragments. An additional pair of

primers complementary to the 5' and 3' ends of the final molecule were added to the overlapping PCR mix to amplify the full-length DNA fragment. Generation of PCR products of the expected size was verified by DNA electrophoretic analysis on 1% agarose gels and subsequently isolated from unspecific products by DNA gel extraction (see section 2.2.3.2). Site-directed mutagenesis was performed to generate the kinase-dead constructs of HERK1 and ANJ (*pANJ::ANJ-KD-GFP* and *pHERK1::HERK1-KD*) with slight modifications of the methodology explained above for overlapping PCRs as per [110].

2.2.3.2 Classical cloning

Restriction digests and ligations were used to produce complementation and GFP reporter lines, knock-down amiRNA lines, as well as yeast two hybrid (Y2H) and *p35S::HA-LRE::rbcS* co-immunoprecipitation (CoIP) constructs (Table 2.1). These cloning events required the amplification of insert sequences with proof-reading DNA polymerases followed by PCR product clean-up. PCR clean-up commercial kits QIAquick PCR Purification Kit (Qiagen) and Monarch PCR Cleanup Kit (NEB) were used to purify the PCR product following the manufacturer's indications. Alternatively, phenol:chloroform extractions followed by DNA precipitation were used to purify DNA from PCR reactions or restriction digests. Briefly, one volume of phenol:chloroform:isoamyl alcohol (25:24:1) was added to the DNA sample and vortexed vigorously until both phases created an even emulsion. Once two phases separated again, samples were centrifuged for five minutes at high speed and the aqueous (upper) phase carefully pipetted to a fresh microcentrifuge tube. DNA was precipitated by adding one tenth of the sample's volume of sodium acetate 3 M pH 5.0 and 2.8 volumes of ethanol, mixing well and incubating at -20°C overnight or at -80°C for one hour. Samples were centrifuged for 30 minutes at 4°C and maximum speed in a pre-cooled benchtop microcentrifuge and DNA pellets washed with 75% ethanol then resuspended in water.

Restriction digests of 1 µg of clean insert and backbone DNA were set up in 30-50 µL reactions and incubated at 37°C overnight unless stated otherwise in the manufacturer's instructions (i.e. due to star activity or different temperature requirements). Restriction products were separated on 1% agarose gels and bands of the expected size extracted with QIAquick Gel Extraction Kit (Qiagen) or Monarch DNA Gel Extraction Kit (NEB) following their instruction manuals and eluted in water.

When cloning involved a unique restriction site and blunt-end ligations, the backbone

DNA ends were dephosphorylated to minimise religation and insert DNA ends phosphorylated to promote insert-backbone ligation. Dephosphorylations were carried out by adding 1 µL of FastAP Thermosensitive Alkaline Phosphatase (Thermofisher Scientific) to the restriction digest reaction and by setting up an additional dephosphorylation step with FastAP prior to ligation. FastAP was heat-inactivated prior to ligations by incubating the sample at 75°C for five minutes. T4 Polynucleotide Kinase (T4 PNK; Thermofisher Scientific) was used to phosphorylate the 5' ends of the insert DNA molecules prior to ligations following the manufacturer's instructions.

Ligations were carried out in 10-20 µL reactions with T4 DNA ligase (Thermofisher Scientific) including up to 100 ng of total DNA as estimated in agarose gel electrophoresis in a 3:1 (insert:backbone) or higher ratio. Ligations were incubated at room temperature for one hour in cohesive-end ligations with inserts of up to 2 kb, or overnight in all other cases. Ligations were transformed into *E. coli* DH5α cells and colonies screened for the presence of the desired insert:backbone combination by colony PCRs using insert and backbone-specific primers (sections 2.2.4 and 2.2.5). Plasmids from colonies presenting the construct of interest were sequenced to double-check the colony PCR results and ensure they contained the expected nucleotide sequence.

2.2.3.3 Backbone modifications

Generation of the complementation and amiRNA constructs required an additional step of modification of the plasmid backbones *pFK224* and *pLMS167* prior to cloning of their respective inserts. *pFK224* is a pGreen IIS-based plasmid designed for Gateway-mediated recombination of *promoter::coding sequence* inserts to generate a *promoter::coding sequence-GFP* final expression cassette. As classical cloning was the strategy chosen for the generation of these constructs, the *pFK224* required the removal of the Gateway recombination cassette prior to the ligation of the insert of interest. *pFK224* was digested with BsrGI (Thermofisher scientific) which removed the recombination cassette and GFP coding sequence. The resulting backbone was religated and constituted *pFK224noGFP*, used to generate *pHERK1::HERK1pFK224* (Table 2.1). The GFP gene was re-introduced into the BsrGI-digested *pFK224* via BsrGI by amplifying the GFP coding sequence from the original *pFK224* using a reverse primer that included a synonymous two nucleotide change that disrupted an additional BsrGI site in amino acids 236-238 of GFP. The resulting GFP-containing *pFK224* lacking the LR recombination cassette was named *pFK224GFP* and was used to generate the reporter constructs *pFER::FER-GFP*, *pANJ::ANJ-GFP*,

pRALFL4::RALFL4-GFP and *pRALFL19::RALFL19-GFP* (Table 2.1). All of these inserts were cloned into *pFK224noGFP* or *pFK224GFP* via KpnI/BamHI digests, except for *pFER::FER-GFP* and *pHERK1::HERK1* which were cloned via three-way ligations with the following restriction site combinations: KpnI-*promoter*-NotI-*coding sequence*-BamHI.

amiRNA constructs required the generation of the backbones *pLAT52pLMS167* and *pNTApLMS167*. *p35S* and LR recombination cassette were removed from *pLMS167* by restriction digests with BamHI or KpnI/BsrGI to be replaced with *pNTA* and *pLAT52* promoters, respectively. *pNTA* was PCR amplified from a *pNTA>>TdTomato* construct (kindly provided by M. Bayer; Max Planck Institute for developmental biology, Tübingen, Germany; unpublished); *pLAT52* was amplified from genomic DNA of the SAIL T-DNA line *lre-7* which contains a *pLAT52*-driven GUS reporter cassette [111]. *pNTA* and *pLAT52* were cloned into the pre-digested *pLMS167* via KpnI/BsrGI or BamHI, respectively, producing the final backbones *pNTApLMS167* and *pLAT52pLMS167*. Overlapping PCR products of amiRNAs *amiRALF8/9/15*, *amiRALF4/19* and *amiRALF11/12/13* were cloned into *pLAT52pLMS167* via BsrGI digests; amiRNAs *amiRALF14* and *amiRALF18* were cloned into *pNTApLMS167* via NotI digests.

2.2.3.4 Complementation and Y2H constructs

To test genetic complementation of the *herk1 anj* reproductive defect and observe the cellular localisation of HERK1 and ANJ the genomic regions spanning 2 kb upstream of the ATG start codon and the full-length coding sequences of *HERK1* and *ANJ* were cloned using the restriction enzymes KpnI and BamHI into a *pGREENIIS*-based binary vector containing a C-terminal GFP. Whereas the *pANJ::ANJ-GFP* construct was easily obtained, no *pHERK1::HERK1-GFP* clones could be identified in multiple rounds of cloning aiming to optimise the ligation efficiency. A different strategy to generate the GFP-tagged clone of *HERK1* was pursued in which a GFP-less version of the backbone was generated first, *pHERK1::HERK1* was then cloned via KpnI/BamHI to subsequently reintegrate the C-terminal GFP via BsrGI digests and ligation. A *pHERK1::HERK1* construct was obtained with this approach however no clones were recovered with an in-frame C-terminal GFP. Several clones were found to contain a GFP fragment but, unfortunately, in all cases the GFP had been cloned in the opposite orientation when 50% of clones with either orientation would be expected, suggesting the *pHERK1::HERK1-GFP* construct may induce bacterial toxicity. Furthermore, previous studies using GFP-tagged versions of HERK1 to study its cellular localisation

did not use its native promoter and instead used *pBRI::HERK1-GFP* [112], suggesting similar difficulties may have been encountered.

The extracellular juxtamembrane regions of HERK1 and ANJ (HERK1exJM, ANJexJM, respectively; as per [70]) corresponding to the 81 amino acids N-terminal of the transmembrane domain were cloned into Y2H vectors *pGADT7* and *pGBKT7* via SmaI restriction digests. Similarly, the coding sequence of the amino acids 23-138 of LRE was cloned into the Y2H vectors to avoid the signal peptide and GPI anchor target sequences of LRE (LRE(23-138); as per [70]). The resulting constructs presented the fragments of the proteins of interest in frame with their respective activation and DNA-binding domains (AD and BD, respectively).

2.2.3.5 Gateway cloning

Gateway cloning technology was used to produce GUS reporter constructs, bimolecular fluorescence complementation (BiFC) and CoIP constructs (Table 2.1). First, promoter or coding sequences were amplified from *A. thaliana* genomic DNA with proof-reading DNA polymerases using a 5'-modified forward primer containing the sequence 5'-CACC-3'. The resulting PCR products were incorporated into pENTR/D-TOPO entry vectors following indications in the instructions manual (Thermofisher Scientific). pENTR/D-TOPO reactions were transformed into *E. coli* cells, colonies screened by colony PCR and inserts confirmed by sequencing of the recombination cassette. Sequence-verified entry clones were used in LR recombination reactions to transfer the corresponding promoter or coding sequence to the destination vector using LR Recombinase II (Thermofisher Scientific). LR reactions were set up according to the manufacturer's indications and DNA concentrations were estimated by DNA electrophoresis on 1% agarose gels of linearised entry and destination vectors. When entry and destination vectors encoded the same bacterial antibiotic resistance gene, prior to LR recombination, entry clones were digested with EcoNI which linearises the entry vector by cleaving outside of the recombination cassette. LR reactions were transformed into *E. coli* cells, colonies screened by colony PCR and inserts confirmed by sequencing of the expression cassette.

Coding sequences of *HERK1*, *ANJ* and *FER* excluding the stop codon were cloned into *pENTR/D-TOPO* entry vectors and were subsequently transferred via LR recombination to the destination vectors *pEarleygate201* and *pEarleygate202* (*p35S*-driven expression and C-terminal nYFP or cYFP, respectively; [113]) to test direct interaction between these receptors *in planta*.

To test co-immunoprecipitation of HERK1, ANJ and LRE, over-expression constructs *p35S::HERK1-GFP, p35S::HERK1-MYC*, *p35S::ANJ-GFP* and *p35S::ANJ-MYC* were generated by cloning the *HERK1* and *ANJ* coding sequences without stop codons into *pENTR/D-TOPO* entry vectors and subsequent LR recombination into destination vectors *pGWB405* and *pGWB420* (MYC tag and GFP tag, respectively; [114]). Additionally, a *p35S::HA-LRE* expression cassette in a *pSK* backbone (kindly provided by C. Li; [70]) was transferred to an *Agrobacterium*-compatible backbone *pMLBart*.

2.2.4 Bacterial transformation

Heat-shock was used routinely to transform *E. coli* [105]. Briefly, heat-shock competent cells stored at -80°C were placed on ice until the majority of the solution had defrosted; DNA sample of up to 10% of the cells volume was added to the competent cells and incubated on ice for an additional 30 minutes; cells were then heat-shocked by incubating the aliquot at 42°C for one minute and returning it to ice for two minutes. 800 µL of SOC medium (0.5% yeast extract, 2% typtone, 10 mM NaCl, 2.5 mM KCl, 10 mM $MgCl_2$, 10 mM $MgSO_4$ and 20 mM glucose) at room temperature was used to dilute the heat-shocked cells. Cells were allowed to recover for 45 mibnutes to one hour at 37°C with gentle shaking (150 rpm) and then plated on solid LB medium supplemented with the corresponding antibiotics (100 mg/mL ampicillin, 50 mg/mL kanamycin or 50 mg/mL spectinomycin). Plates were incubated at 37°C overnight and colonies analysed on the following day (see section 2.2.5).

Plasmid DNA was transformed into *Agrobacterium* competent cells by the freeze-thaw method or electroporation [115-116]. For freeze-thaw transformation, an aliquot was thawed on ice and DNA sample of up to 10% of the volume was added and mixed. Cells with DNA were incubated on ice for 20 minutes then transferred to liquid nitrogen for one minute and thawed in a 37°C water bath for four minutes. 500 µL of low-salt LB at room temperature were added to the sample and cells were allowed to recover at 28°C with gentle shaking for two hours then plated on solid low-salt LB supplemented with antibiotics (50 mg/mL kanamycin, 100 mg/mL spectinomycin, 50 mg/mL gentamycin, 25 mg/mL chloramphenicol, 50 mg/mL rifampicin and/or 5 mg/mL tetracycline). Colonies were recovered on plates after 48-72 hours of growth at 28°C. Electrotransformation of *Agrobacterium* competent cells was carried out by thawing an aliquot on ice, adding 1 µL of DNA and incubating on ice for five minutes, transferring the cells to a pre-chilled electroporation cuvette avoiding formation of air bubbles, applying an electric pulse (Capacity: 25 µF, Voltage: 2.5k V, Resistance: 200 O, Duration: 5 milliseconds), transferring to a fresh microcentrifuge tube and immediately

adding 500 µL of room temperature low-salt LB. Cells were allowed to recover at 28°C with gentle shaking for four hours and subsequently plated on solid low-salt LB supplemented with antibiotics. Plates were incubated at 28°C for two or three days and colonies were subsequently probed for presence of the plasmid DNA of interest (see section 2.2.5).

2.2.5 Bacterial genotyping

Bacterial colonies were screened for presence of the desired genetic construct by genotyping PCRs. *E. coli* colonies were directly genotyped by transferring a very small amount of the colony to a 10 µL PCR reaction and mixing well. PCR reaction preparation and thermocycling conditions were as per section 2.2.1. Primers specific to each construct and yielding PCR products of less than 1.5 kb were preferred. *Agrobacterium* colony PCRs were also performed as explained above, however inconsistent results were often encountered due to lower plasmid copy-number or inhibition of the PCR reaction. An alternative method to screen for the presence of the desired plasmid was therefore set up in which several individual colonies were grown overnight in liquid, low-salt LB with the corresponding antibiotics, cells from 1 mL of the overnight culture were pelleted, washed with water twice and resuspended in 50-100 µL of water. This cell suspension was used in standard genotyping PCR reactions by adding 1-2 µL to a 10 µL PCR reaction. PCR reaction preparation and thermocycling conditions were as per section 2.2.1 with 40 cycles of denaturation, annealing and extension. Primers specific to each construct and yielding PCR products of less than 1.5 kb were also preferred. *E. coli* or *Agrobacterium* colonies harbouring the plasmid of interest were grown overnight in liquid medium with antibiotics and preserved at -80°C in 20% glycerol stocks (v/v).

2.3 Protein-protein interaction procedures

2.3.1 Yeast two hybrid

Yeast two hybrid (Y2H) assays presented in this dissertation were suggested and designed by the author but performed by Noel Blanco Touriñán (IBMCP, Valencia, Spain). Direct interaction assays in yeast were carried out following the Clontech small-scale LiAc yeast transformation procedure. Yeast strain Y187 was transformed with pGADT7 constructs and yeast strain Y2HGold with pGBKT7 constructs (including empty vectors as controls). Yeast diploid cells carrying both plasmids were obtained by mating and interaction tests were surveyed on selective media lacking leucine,

tryptophan and histidine.

2.3.2 Co-immunoprecipitation

Co-immunoprecipitation (CoIP) assays included in this thesis were carried out as part of a collaborative experiment with Thomas A. DeFalco (The Sainsbury Laboratory, Norwich, UK; current address: University of Zurich, Switzerland). *A. tumefaciens* strain GV3101(pMP90) carrying constructs of interest were infiltrated into *Nicotiana benthamiana* leaves. Leaves were co-infiltrated with *A. tumefaciens* carrying a P19 silencing suppressor. 2 days after infiltration leaves were harvested and frozen in liquid nitrogen before extraction in buffer (20 mM MES pH 6.3, 100 mM NaCl, 10% glycerol, 2 mM EDTA, 5 mM DTT, supplemented with 1% IGEPAL and protease inhibitors). Immunoprecipitations were carried out in the same buffer with 0.5% IGEPAL for four hours at 4ºC with GFP-trap (Chromotek) or Anti-HA Affinity Matrix (Roche) resin. Beads were washed with the same buffer and bound proteins were eluted by addition of SDS loading dye and heating to 90ºC for 10 min. Proteins were separated by SDS-PAGE and detected via Western blot following blocking (in TBS-0.1% Tween-20 with 5% non-fat milk powder) with the following antibody dilutions: α-GFP-HRP (B-2, Santa Cruz), 1:5000; α-HA-HRP (3F10, Roche), 1:3000.

2.3.3 Bimolecular fluorescence complementation

Bimolecular fluorescence complementation (BiFC) was assayed by *Agrobacterium*-mediated transient expression of nYFP and cYFP tagged constructs in *N. benthamiana* leaves [117]. *N. benthamiana* plants were grown on soil under our standard conditions (see section 2.1.1) after germination on wet filter paper at room temperature and low light conditions in the laboratory. *N. benthamiana* plants with four to six true leaves were the preferred growth stage for BiFC assays. *Agrobacterium* lines carrying the desired constructs were grown in liquid, low-salt LB, cells pelleted by centrifugation, resuspended to an OD_{600} of 0.4 in a buffer containing 10 mM $MgCl_2$, 10 mM MES-KOH pH 5.6, 100 µM acetosyringone and incubated at room temperature for two to three hours on a rocking table. All constructs were co-infiltrated with *Agrobacterium* carrying a P19 RNA silencing suppressor construct in a volumetric ratio of 1:1:0.1 (nYFP:cYFP:P19; [118]). *N. benthamiana* leaves were infiltrated with the *Agrobacterium* mixture on the abaxial side until infiltrated areas of 3-4 cm^2 were obtained. *N. benthamiana* plants were kept in high humidity conditions for an hour prior to infiltration to promote stomatal opening to facilitate infiltration. Infiltrated areas were screened for YFP fluorescence reconstitution two or three days after infiltration by

epifluorescence microscopy with water-mounting on microscope slides.

2.4 Histochemistry procedures

Imaging of all samples generated through the histochemistry procedures summarised below was carried out in the following systems: a stereomicroscope Leica M165 FC with LASX software; widefield microscopes Olympus BX51 epifluorescence microscope equipped with CoolLED fluorescence system and Cell B software, and Leica DM6 B epifluorescence microscope equipped with a CoolLED pE-2 fluorescence system and LASX software; and inverted confocal microscope Nikon A1 equipped with 405 nm, 457-514nm argon laser, 561nm sapphire laser and 642nm diode laser and NIS Elements software.

2.4.1 Aniline blue staining of pollen tubes

Flowers of the desired stage were detached from the inflorescence and placed on double-sided sticky tape (3M). Sepals, petals and stamens were removed from the flower and the carpels with pedicel were transferred to the fixing solution (3:1 ethanol:acetic acid). After an overnight incubation the fixing solution was exchanged for the softening solution (8 M NaOH) and incubated overnight at room temperature. Softening solution was subsequently removed and specimens were washed with water four times with 10 minutes incubation between each washing step. Specimens were transferred to the staining solution (0.1% (w/v) aniline blue (Fisons Scientific) in 0.1 M K_2PO_4-KOH buffer, pH 11) and incubated in the dark at room temperature for at least three hours (adapted from [119]). Carpels were mounted in 50% glycerol and imaged with an epifluorescence microscope using a 400 nm LED light source and a filter set with 340-380 nm excitation, emission filter of 425 nm (long pass) and 400 nm dichroic mirror. Confocal images were acquired using 403.5 nm laser line, 30.7 µm pinhole size and filter set with 405 nm dichroic mirror and 525/50 nm emission filter cube. When individual ovules were screened for pollen tube reception defects the samples were subjected to a "pistil squash", in which the coverslip was gently pressed against the sample therefore compressing the specimen, disrupting the ovary valve’s integrity and allowing inspection of individual ovules.

2.4.2 SR2200 staining of callose

Quick callose staining of live samples was carried out by exposing live dissected ovules to a 1000x dilution of SR2200 (Renaissance Chemicals Ltd) in half-strength MS,

5% (w/v) sucrose, pH 5.7. Samples were mounted on microscope slides directly in the staining solution and after 5-10 minutes of incubation strong fluorescence could be observed in callose-containing, medium-exposed cellular structures like pollen tubes and the filiform apparatus of the synergid cells. Microscopy imaging parameters were used as in aniline blue-stained samples (section 2.4.1).

2.4.3 H_2DCF-DA staining of reactive oxygen species

Staining of ROS in live ovules was carried out as per [68]. Briefly, ovules were dissected as per section 2.1.3, using the ROS staining buffer to cover the dissected ovary during manipulation (25 µM H_2DCF-DA (Thermo Scientific), 50 mM KCl, 10 mM MES buffer pH 6.15). Dissected ovules were incubated in the staining buffer for 15 minutes and subsequently washed in excess wash buffer (50 mM KCl, 10 mM MES buffer pH 6.15) three times. Washes were performed on a clean coverslip by carefully removing the solution with filter paper without touching the specimen and submerging it in excess wash buffer for three minutes. Washed ovules were mounted in wash buffer and immediately imaged with an epifuorescence microscope using a 470 nm LED light source and a filter set with 470/40 nm excitation filter, 460/50 nm emission filter and 495 nm dichroic mirror. Strong H_2DCF-DA fluorescence was normally observed along the replum and transmitting tract of the ovule, probably due to wound-induced ROS production during the dissection process.

2.4.4 Christensen's method for confocal imaging of female gametophytes

Observation of the female gametophyte structure was performed as per [120]. Christensen's protocol relies on autofluorescence of cell walls and nuclei achieved after cross-linking, fixation and clearing of the ovules. Briefly, ovules from unpollinated carpels were dissected as per section 2.1.3 and immediately transferred to a 4% (v/v) solution of glutaraldehyde, 12.5 mM sodium cacodylate buffer pH 6.9 and incubated at room temperature for two hours following an initial 30 minutes of vacuum infiltration. Specimens were dehydrated in an ethanol wash series (20%-100%, 20% intervals, 30 minutes each) and cleared in a benzyl benzoate:benzyl alcohol 2:1 mixture for 2 hours. Samples were mounted on immersion oil and coverslips sealed to the microscope slides with nail varnish. Female gametophyte structure was visualised in an inverted confocal microscope Nikon A1 with 35.8 µm pinhole size, 642.4 nm laser line and filter set of 640 nm dichroic mirror and 595/50 nm emission filter cube.

2.4.5 GUS staining

Promoter::GUS transcriptional reporter lines were subjected to GUS staining assays in which β-glucuronidase activity *in planta* is studied. Plant organs or small seedlings were collected and immersed in ice-cold 90% acetone for 30 minutes. Acetone was removed and specimens washed in excess wash buffer (50 mM $NaPO_4$ buffer pH 7.2) for 30 minutes. Samples were then transferred to GUS staining buffer (2 mM X-Gluc (Melford Laboratories Ltd), 50 mM $NaPO_4$ buffer pH 7.2, 2 mM potassium ferrocyanide, 2 mM potassium ferricyanide and 0.2% (v/v) Triton-X), vacuum-infiltrated for 30 minutes and incubated at 37°C for several hours or overnight. Samples were cleared in 75% ethanol and imaged under a widefield microscope or stereomicroscope [121]. At least four independent lines were analysed per construct to infer gene expression patterns.

2.4.6 Propidium iodide staining of root cell walls

Visualisation of root cell walls was carried out by submerging *in vitro* vertically-grown seedling roots in 50 µL of 10 µg/mL propidium iodide on a microscope slide, covering the root system with a coverslip and incubating at room temperature for two to three minutes. Roots were subsequently washed three times with water (100 µL of water in each washing step) by carefully pipetting 100 µL of water on one side of the coverslip and removing the excess mounting solution with filter paper on the opposite side of the coverslip. Roots were immediately imaged in an epifluorescence microscope with an LED excitation line of 535 nm and a 500-550 nm emission filter.

2.4.7 Clearing of leaves for differential interference contrast microscopy

Observation of leaf pavement cells and trichome morphology required clearing and fixing the leaves prior to analysis in widefield system using differential interference contrast microscopy (DIC) microscopy. Leaves were first fixed overnight in Carnoy fixative solution (7:1 ethanol:acetic acid). Leaves were then rehydrated by wash series with solutions containing decreasing proportions of ethanol (100-0% ethanol; 20% steps; 30 minutes incubation at room temperature for each step). Samples were bleached overnight in a 5% sodium hypochlorite solution at room temperature or until completely transparent. Bleaching solution was subsequently replaced with 90% ethanol for long-term storage.

2.5 Quantification, statistical analyses and figure production

ImageJ (https://imagej.net) and Fiji software were used for quantification of root, petiole and leaf lengths and seed sizes. Leica LASX software was used to obtain quantitative information about fluorescence intensity profiles in synergid cells. Quantitative data were collected, organised and analysed in Microsoft Excel or OriginPro 2018b (OriginLab) files. Statistical significance between averages in seed set, root, and petiole length were assessed with Student's *t* tests. When more than four comparisons were required, one-way ANOVA was performed using Origin Pro 2018b, followed by Tukey's honest significant difference test if differences were detected. χ-square tests were used to compare distributions obtained in seed germination experiments, pollen tube overgrowth assays and ROS measurements in ovules, using the distribution obtained in wild-type plants as the expected distribution. In distributions in which categories presented 0 individuals, Fisher's exact tests were used to identify statistically significant differences. In all tests, * $p<0.05$, ** $p<0.01$, and *** $p<0.001$. Sample size *n* is indicated in the graphs or figure legends. Graphs were produced in Microsoft Excel or OriginPro 2018b and figures built and integrated with Inkscape (https://inkscape.org/en/). In boxplot graphs, the mean was represented by a square; the median was shown as a horizontal line; the interquartile range (IQR) as a coloured box; and data points outside of the 1.5xIQR range (represented by whiskers) were considered outliers and shown as black diamonds.

Chapter 3

Identifying new functions for CrRLK1L receptors in Arabidopsis

3.1 Introduction

The *Catharanthus roseus* receptor-like kinase 1-like (CrRLK1L) proteins are one of the plant RLK subfamilies that have drawn most attention in recent years. The founding member, CrRLK1, was identified in 1996 in Madagascar periwinkle (*Catharanthus roseus*) cell cultures as a member of a novel class of RLKs containing an extracellular domain lacking homology to any identified proteins [58]. Since then, the majority of the research on CrRLK1Ls has been carried out on the *Arabidopsis thaliana* CrRLK1L family. Identification of functions for Arabidopsis CrRLK1Ls FERONIA (FER) and THESEUS1 (THE1) positioned this subfamily of RLKs as putative reproduction and cell wall integrity regulators in plants [59, 61].

3.1.1 CrRLK1L domain organisation

CrRLK1L receptors share a domain organisation comprising (amino-to-carboxyl terminus orientation) a signal peptide, a malectin-like domain, a hydrophobic transmembrane stretch and a kinase domain (Figure 3.1A; [50]). The signal peptide is predicted to send these receptors to the plasma membrane of the cell, where they mature as a single transmembrane span protein, with an extracellular malectin-like domain and a cytoplasmic kinase domain [50]. The malectin-like ectodomain contains two regions in tandem with predicted structural similarity to the carbohydrate-binding malectin protein characterised in animal cells [49]. Therefore, these RLKs have been considered putative sensors of cell wall integrity through direct interaction with cell wall carbohydrates [122]. Evidence for direct interaction between the CrRLK1L ectodomain and carbohydrates remained elusive until recently, when the capacity of FER ectodomain to bind polygalacturonic acid (the building block of pectin) was demonstrated [30-31]. However, lack of residues required for di-glucose binding by the

animal malectin protein in plant malectin-like domains suggests that while carbohydrate binding is conserved across kingdoms, the CrRLK1L-pectin interaction may have a different structural basis [47-48].

Multiple studies support a further role for the CrRLK1L proteins as receptors of small secreted cysteine-rich peptides belonging to the rapid-alkalinisation factor (RALF) family, regulating a variety of processes including cell expansion, response to pathogens and maintenance of pollen tube growth [32-33, 62]. Capable of sensing a variety of cues, the CrRLK1Ls constitute signalling hubs that allow the plant cell to respond and adapt correctly to changes in its surroundings.

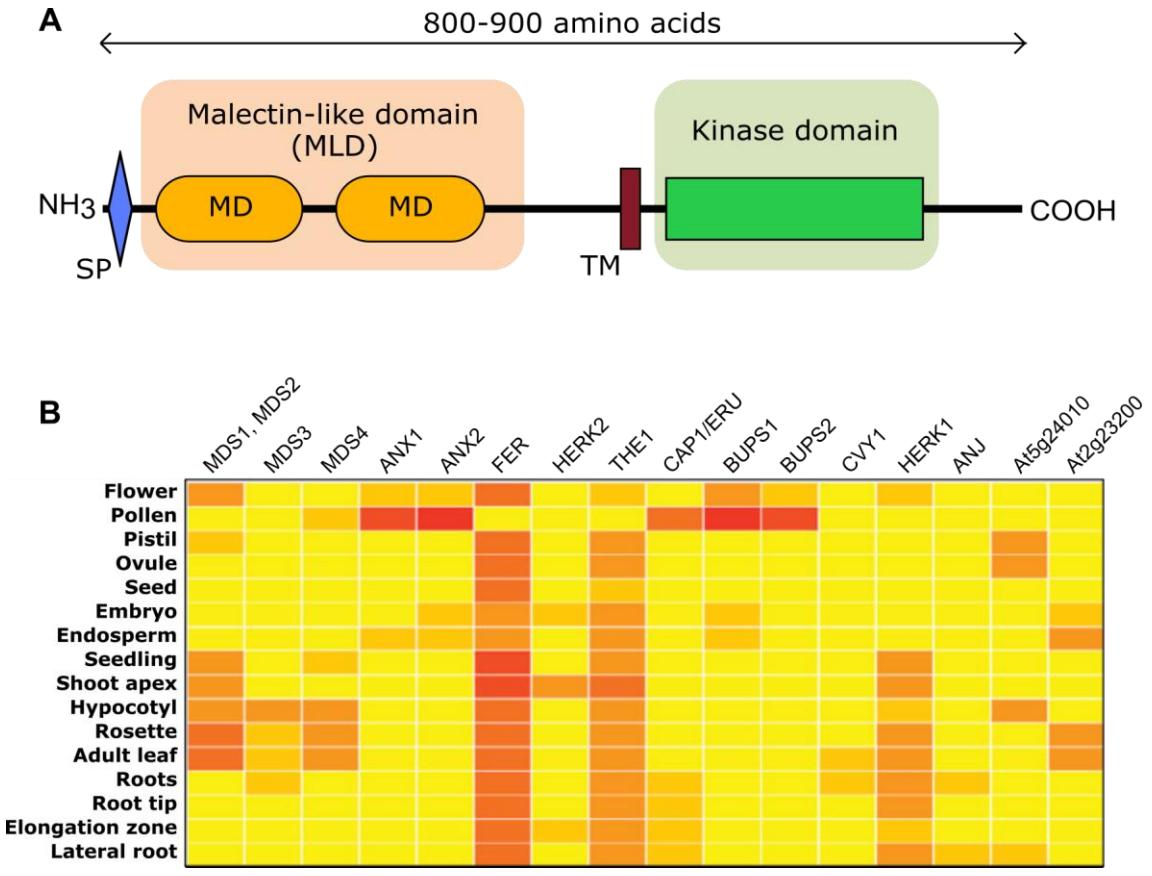

Figure 3.1 CrRLK1L domain organisation and gene expression heatmap. A, typical domain organisation of the CrRLK1L family of proteins. Domains are represented by boxes and length coverage is based on the FERONIA protein of Arabidopsis. SP, signal peptide; MD, malectin domain; TM, transmembrane domain. Adapted from [123]. **B**, heatmap of the relative expression potential of CrRLK1L genes of Arabidopsis in multiple tissues. Expression potential is represented by a colour gradient, with red indicating 100% of expression potential and yellow 0% of expression potential. Data was collected from the Genevestigator microarray database. Adapted from [51].

3.1.2 CrRLK1L proteins control multiple developmental processes in plants

Homologs of this subfamily of RLKs can be found in the genomes of all lineages of land plants, with an expansion in number from earliest to latest diverging lineages, as exemplified by the liverworts (one CrRLK1L in Marchantia) and flowering plants (17 CrRLK1Ls in Arabidopsis; [123]). In liverworts, the CrRLK1L protein is required for rhizoid tip growth stability, as mutants in this gene fail to maintain growth of these root hair-like structures [124]. With the increase in developmental complexity during land plant evolution, the CrRLK1Ls have been recruited to a variety of processes including tip growth, cell expansion, reproduction, response to pathogens and abiotic stresses (as reviewed in [123]).

Functions have been assigned to 14 of the 17 CrRLK1Ls in the model flowering plant Arabidopsis. FER is expressed in most plant tissues and is required for tip growth in root hairs and trichomes, cell expansion in roots and petioles, cell shape in leaf epidermis, maternal control of fertilisation and responses to abscisic acid (ABA), amongst other functions (Figure 3.1B; [30, 32-33, 60, 74, 97, 125]). $[Ca^{+2}]_{CYT}$-ASSOCIATED PROTEIN KINASE 1/ERULUS (CAP1/ERU; hereon referred to as ERULUS/ERU) is a key regulator of tip growth in root hairs and pollen tubes [67, 75-77], while CURVY1 (CVY1) controls trichome and epidermal cell morphology [81]. THE1 monitors cell wall integrity status and regulates cell elongation and lateral root initiation accordingly [61, 63, 82]. THE1, HERCULES RECEPTOR KINASE 1 (HERK1) and HERK2 were described as redundant regulators of cell elongation in hypocotyls and petioles [112, 126]. According to recent findings the *the1* mutant allele used in these studies is not a knock-out mutant but rather mimics THE1 over-expression [82]; further confirmation is therefore required to elucidate the role of these CrRLK1Ls in cell elongation (see Section 3.3). Two pairs of redundant CrRLK1Ls control pollen tube growth stability, ANXUR1 (ANX1) and ANX2, and BUDDHA'S PAPER SEAL1 (BUPS1) and BUPS2 [62, 65-66]. Finally, MEDOS1 (MDS1), MDS2, MDS3 and MDS4 influence the response to metal ions in roots and hypocotyls [87].

3.1.3 Functional redundancy in the Arabidopsis CrRLK1L family

Based on reporter lines and publicly available expression datasets, the CrRLK1Ls display diverse expression patterns. Expression in some cases is restricted to a narrow developmental window (*ANX1*, *ANX2*, *BUPS1* and *BUPS2*, whose expression is mostly restricted to the reproductive stage); expression of other CrRLK1L genes is restricted

to certain organs or structures (for example *MDS3*, *MDS3*, *HERK2*, *ERU*, *AT5G24010* and *AT2G23200*); meanwhile a handful of family members are expressed throughout most developmental stages (e.g. *FER*, *THE1* and *HERK1*; Figure 3.1B; [51]).

Based on amino acid sequence similarity, the 17 CrRLK1Ls in Arabidopsis can be separated in two groups (Figure 3.2). The first contains all characterised members to date and presents the highest homology to CrRLK1Ls from early divergent lineages of land plants, suggesting they may have evolved and diversified from the ancestral CrRLK1L function [123]. A second clade comprises the MDS members which can be grouped in two pairs of CrRLK1Ls with high amino acid similarity that cluster as two consecutive gene tandems on the fifth chromosome of Arabidopsis (Figure 3.2). Functional redundancy between CrRLK1Ls with tight phylogenetic relationships has been reported for ANX1/ANX2 and BUPS1/BUPS2 in controlling pollen tube growth stability [62, 65-66]. When phylogeny and expression data are taken into consideration, certain gene combinations arise as interesting candidates in which to explore functional redundancy in certain developmental processes. Expressed in the same tissues under similar conditions, CrRLK1L clusters including AT5G24010-AT2G23200, CVY1-HERK1-AT5G59700 (ANJEA/ANJ; first characterised in this thesis), MDS1-MDS2 and MDS3-MDS4 constitute potential candidates for functional redundancy (Figure 3.1B).

3.1.4 Aims

This chapter reports on confirmation, generation and screening of multiple CrRLK1L T-DNA insertion lines. Carried out during the first year of this research project, these experiments led to the identification of a reproductive defect associated with *HERK1* and *ANJEA*, explored in further detail in Chapter 4. The results presented in this chapter should be regarded as a record of initial tests that confirm published results and show promising new avenues of research. However, these results are of a preliminary nature and, as such, should be interpreted with caution and confirmed further before conclusions are drawn. Additional preliminary assays are summarised in the Annexe 1 of this thesis.

Given the interest in this subfamily of RLKs as putative signalling hubs in plant development and based on the hypothesis of possible functional redundancy between CrRLK1Ls, multiple Arabidopsis CrRLK1L T-DNA insertion lines were obtained and several higher order mutants were generated through genetic crosses. These lines were initially screened with the aim of i) confirming previously reported defects in CrRLK1L mutant lines and ii) identifying new functions for CrRLK1Ls in plant

development or iii) in response to exogenous cues (i.e. hormones or stress).

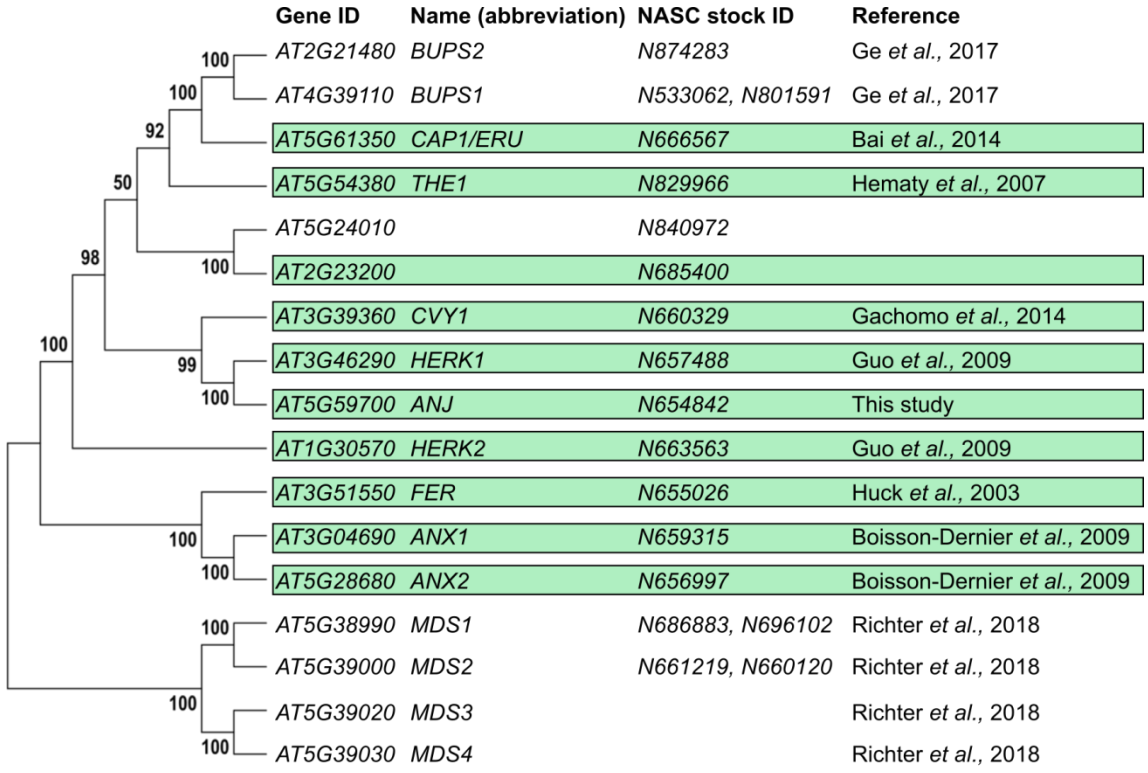

Figure 3.2 Summary of the Arabidopsis CrRLK1Ls studied in this chapter; phylogenetic relationships and T-DNA insertion lines used. Phylogenetic analysis of the CrRLK1L proteins in *A. thaliana* is based on full-length amino acid sequences, aligned using ClustalX [127] and a Neighbour-Joining phylogenetic tree generated with the software MEGA5.2 [128-129]. The percentage of replicates where associated taxa clustered in the bootstrap test is shown next to each branch (1000 replicates). All CrRLK1L members in *A. thaliana* (*AT4G39110*|*BUPS1*, *AT2G21480*|*BUPS2*, *AT5G61350*|*CAP1*/*ERU*, *AT5G54380*|*THE1*, *AT2G23200*, *AT5G24010*, *AT2G39360*|*CVY1*, *AT3G46290*|*HERK1*, *AT5G59700*|*ANJ*, *AT1G30570*|*HERK2*, *AT3G51550*|*FER*, *AT3G04690*|*ANX1*, *AT5G28680*|*ANX2*, *AT5G39000*|*MDS2*, *AT5G38990*|*MDS1*¸ *AT5G39020*|*MDS3*, *AT5G39030*|*MDS4*) were included in this analysis. T-DNA insertion lines obtained from the Nottingham Arabidopsis Stock Centre (NASC) for each CrRLK1L are listed here. T-DNA insertion lines for genes *MDS3* and *MDS4* were unavailable. Genes for which a homozygous T-DNA insertion line was obtained and analysed in this thesis are highlighted in green.

3.2 Results

3.2.1 Confirmation of single homozygous CrRLK1L T-DNA insertion lines and generation of double homozygous lines

An initial set of 15 T-DNA insertion lines was obtained from the Nottingham Arabidopsis Stock Centre (NASC; Figure 3.2). Using PCR-based genotyping, 10 of these lines were confirmed as homozygous for the T-DNA insertions whereas the remaining five were genotyped as wild-type (insertion lines for *BUPS1*, *BUPS2*, *AT5G24010*, *MDS1* and *MDS2*). Additional T-DNA insertion lines were only available for *BUPS1* and *AT5G24010* but were also confirmed as wild-type by genotyping PCRs for their corresponding gene of interest (Figure 3.2; Table 3.1). Therefore, the subset of 10 homozygous T-DNA insertion lines was studied in all following experiments. Due to an interesting preliminary phenotype observed in *herk2* roots (see Annexe 1), it was decided to create multiple double homozygous lines with a combination of *herk2* with an additional CrRLK1L insertion line (Table 3.1). In addition to the *herk2 crrlk1l* double mutants, other CrRLK1L double mutants were generated, including combinations between *the1-4*, *herk1* and *herk2* based on previous reports in which redundancy in controlling cell elongation was proposed (Table 3.1; [112, 126]). A *herk1 herk2 the1-4* triple homozygous line was also generated to study the interaction between these three genes during germination (Table 3.1). Finally, double homozygous *herk1 at5g59700* (*anjea; anj*) and *herk1 cvy1* lines were obtained based on the close phylogenetic relationship between these genes (Table 3.1).

3.2.2 Confirmation of published developmental defects and preliminary screens

In recent years, the scientific community has become aware of the necessity to improve our practises to ensure reproducibility [130-132]. We therefore sought to investigate previously described phenotypes for the set of homozygous CrRLK1L T-DNA lines aiming to identify putative new regulators and provide independent confirmation of the involvement of already characterised CrRLK1Ls in such developmental processes.

3.2.2.1 Defects in root hair growth in *eru* and *fer-5*

Two of the 10 confirmed homozygous T-DNA lines in this project have been linked to defects in root hair growth. Firstly, ERU was described as a regulator of root hair

Table 3.1 Confirmed homozygous insertion lines included in this chapter and associated developmental mutant phenotypes.

Confirmed homozygous line	First described	Impaired developmental processes confirmed in this chapter
fer-5	[74]	Root hair growth, trichome morphology
fer-4	[74]	Petiole length
herk1	[126]	
herk2	[126]	
the1-4	[126]	
cvy1	[81]	
cap1/eru	[75]	Root hair growth
anx1	[65]	
anx2	[65]	
anj	This study	
at2g23200	This study	
herk2 fer-5	This study	Root hair growth, trichome morphology
herk2 cvy1	This study	
herk2 the1-4	This study	ABA-induced delay of germination
herk2 cap1/eru	This study	Root hair growth
herk2 anj	This study	
herk2 at2g23200	This study	
herk1 herk2	This study	
herk1 the1-4	[126]	ABA-induced delay of germination, petiole length
herk1 herk2 the1-4	[126]	ABA-induced delay of germination, petiole length
herk1 anj	This study	Seed set
herk1 cvy1	This study	

development in Arabidopsis. *eru* mutant plants displayed a pronounced reduction in root hair length due to a loss of growth stability at the tip and consequent burst [75, 77]. Secondly, *fer* mutant plants presented defective root hair growth and impaired responsiveness to exogenous addition of auxins (*fer* root hairs remained short whereas Col-0 wild-type (WT) increased in length upon auxin addition; [74]). We could recapitulate these defects in root hair growth in *eru* and *fer-5* lines (Figure 3.3A-B). In control conditions, *eru* root hairs were significantly shorter than WT while *fer-5* root hair length remained at WT levels (Figure 3.3A-B). When exposed to exogenous auxins (125 nM of 1-naphtaleneacetic acid; NAA), root hairs in both *fer-5* and *eru* mutant lines displayed a significant reduction in length compared to WT (Figure 3.3A-B). These

lines were analysed in parallel to additional single and double homozygous lines, however only *eru*, *fer-5*, and double homozygous lines containing these mutations (*herk2 eru* and *herk2 fer-5*) presented statistically significant differences with WT (Annexe 1). We were therefore able to reproduce previous experiments and add independent evidence of the involvement of these two CrRLK1Ls in controlling root hair tip growth.

3.2.2.2 Distorted cell shape in *cvy1* and *fer-5*

FER has been linked to multiple other developmental processes, however the T-DNA line chosen for the initial screens presented in this chapter corresponds to the weak allele *fer-5* (NASC ID: N655026; [74]). In addition to the root hair defect, trichome morphology defects were also observed in this *fer* T-DNA line [74]. Similarly, CVY1 was reported to regulate cell shape as *cvy1* plants presented severely distorted trichomes and leaf pavement cells, as well a faster transition to the flowering stage and higher seed yield [81]. To confirm these published phenotypes, we grew *fer-5* and *cvy1* plants to maturity, cleared mature rosette leaves and observed trichome and pavement cell shape morphology in a qualitative screen. Pavement cells in *cvy1* leaves were normal and no severe distortion of cell shape could be observed in the adaxial or abaxial epidermis (Figure 3.3C). Where distorted trichomes were abundant in *fer-5* leaves, *cvy1* trichomes were found to develop normally (Figure 3.3D). Furthermore, *cvy1* plants flowered at the same time and produced similar seed yields to WT plants when grown to maturity in several replicates during the course of this project (data not shown). Therefore, while we could confirm the trichome defect in *fer-5* mutant plants, we could not reproduce the mutant phenotypes linked to *cvy1* [81]. Importantly, the *cvy1* T-DNA line used in these assays is the line used by Gachomo and colleagues (NASC ID: N660329; [81]), thus ruling out allelic differences as the cause of the discrepancies. Of the additional CrRLK1L T-DNA lines screened qualitatively for pavement cell and trichome defects only the double homozygous *herk2 fer-5* presented qualitative differences in trichome morphology (lines analysed: *cvy1*, *fer-5*, *eru*, *herk1*, *herk2*, *the1-4*, *anj*, *at2g23200*, *herk2 cvy1*, *herk2 fer-5*, *herk2 eru*, *herk2 anj* and *herk2 at2g23200*; not shown).

3.2.2.3 Impaired petiole elongation in *herk1 the1-4*, *herk1 herk2 the1-4* and *fer-4*

Several CrRLK1L receptors regulate petiole elongation including FER, HERK1, HERK2 and THE1 [112, 126]. HERK1, HERK2 and THE1 were described as redundant regulators of cell expansion in petioles as double homozygous *herk1 the1-4* displayed

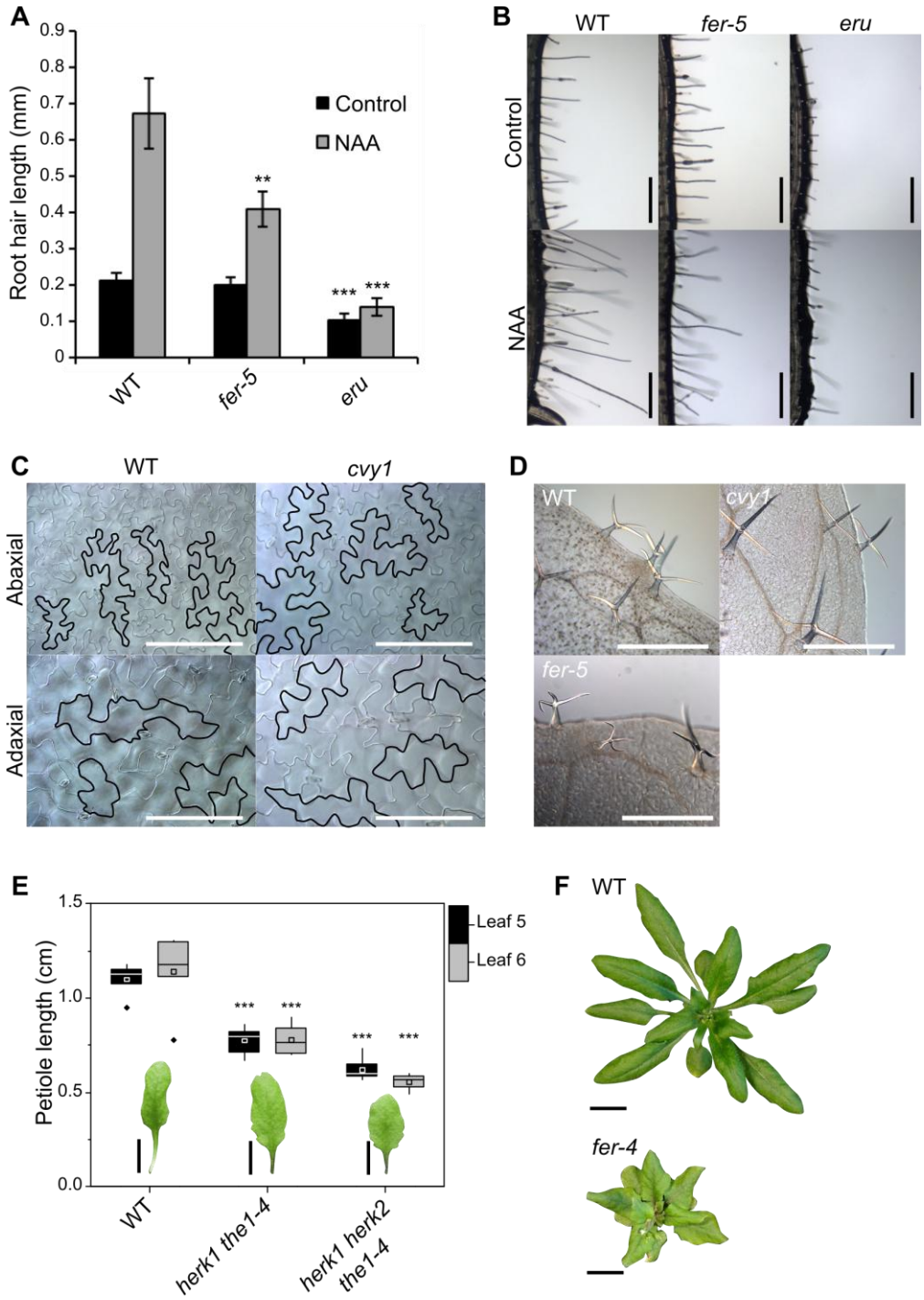

Figure 3.3 Confirmation of previously described developmental defects in CrRLK1L T-DNA insertion lines. A, root hair length in CrRLK1L insertion lines *eru* and *fer-5*. Plants were grown on vertical, half-strength Murashige and Skoog (MS) plates in control or auxin (125 nM NAA) supplemented conditions for 6 days. 50 hairs were measured from four seedlings per line; n = 4 for each line. **B**, representative photographs from the root hair zone of the primary root of Col-0 wild-type (WT) and insertion lines that displayed impaired root hair development. Scale bars represent 200 µm. **C**, pavement cell morphology in the adaxial and abaxial epidermis as seen in mature cleared leaves in differential interference contrast (DIC) microscopy images. Scale bars represent 150 µm. **D**, trichome morphology in *cvy1* and *fer-5* insertion lines in mature cleared leaves. Scale bars represent 500 µm. **E**, petiole length of rosette leaves five and six measured from six plants and representative photograph of a leaf 6 for each genotype.

Scale bars represent 1 cm. **F**, representative photographs of WT and *fer-4* homozygous plant at 21 days after germination in which the dwarf phenotype of *fer-4* plants can be observed. Scale bars represent 1 cm. Significant differences were tested in two-sample Student's *t* tests (**, p<0.01; ***, p<0.001).

a short petiole phenotype which was more pronounced in triple homozygous *herk1 herk2 the1-4* plants [112, 126]. Although these lines were not among the initial set generated for these preliminary screens, they were subsequently obtained to characterise their responsiveness to ABA during germination (Section 3.2.3). This was taken as an opportunity to confirm previously reported results regarding their role in petiole expansion. Plants were grown on soil under our standard conditions until bolting, rosette leaves were detached from the stem at the base of the petiole, photographed, and petioles measured. We could reproduce the results published by Guo and colleagues for *herk1 the1-4* and *herk1 herk2 the1-4*, which display a reduction in petiole length in the double mutant that is more pronounced in the triple mutant (Figure 3.3E; [112, 126]). During the course of these preliminary assays, the hypomorphic allele *fer-5* was used which does not have a petiole expansion defect (Annexe 1). The loss-of-function *fer-4* mutant has been reported to have a petiole elongation defect in rosette leaves [74, 112]. We subsequently obtained the *fer-4* line given the relevance of its reproductive defect to the results presented in Chapter 4, which allowed us to qualitatively confirm a defect in petiole elongation for this particular allele (Figure 3.3F). Additionally, we quantified petiole length in several single and double homozygous CrRLK1L T-DNA lines but found no additional mutant lines with this developmental defect (*cvy1*, *fer-5*, *eru*, *herk1*, *herk2*, *the1-4*, *anj*, *at2g23200*, *herk2 cvy1*, *herk2 fer-5*, *herk2 eru*, *herk2 anj* and *herk2 at2g23200*; Annexe 1).

3.2.3 *herk1*, *herk2* and *the1-4* affect sensitivity to ABA during germination

CrRLK1L receptors have been linked to responses to several plant hormones including brassinosteroids, auxins and ABA [74, 97, 126]. Whereas the connection between CrRLK1Ls and brassinosteroids and auxins awaits further clarification, it has been established that FER acts as a negative regulator of ABA signalling [97-98]. *fer* loss-of-function mutants are hypersensitive to ABA, present constitutively closed stomata, increased production of reactive oxygen species in stomata, show enhanced shortening of roots and hypersensitivity to ABA-mediated inhibition of germination [97]. FER triggers the phosphorylation and activation of a core negative regulator of the ABA signalling ABA INSENSITIVE 2 (ABI2; [97]). In turn, in a negative feedback loop ABI2 directly dephosphorylates FER to dampen the RALF1-triggered, FER-mediated activation of ABI2 [98].

3.2.3.1 ABA-mediated inhibition of germination is enhanced in *herk2 the1-4*

To identify additional ABA response regulators within the CrRLK1L family of Arabidopsis, we subjected a set of CrRLK1L T-DNA insertion lines to germination assays in the presence of ABA. Double homozygous insertion line *herk2 the1-4* displayed a significant delay in germination when seeds were exposed to 1 and 2 µM ABA in pilot experiments (Annexe 1). In the light of these preliminary results, we confirmed the *herk2 the1-4* hypersensitive response to ABA during germination and pursued its characterisation further. The germination assay was repeated using the lines *herk2*, *the1-4* and the double mutant *herk2 the1-4* to i) confirm we could reproduce the result obtained in the pilot experiment, and ii) determine whether the ABA hypersensitivity is caused by an interaction of the two mutations when present in the same genetic background. At three days after stratification, more than 90% of the seedlings from all lines had expanded green cotyledons in control conditions (Figure 3.4A-B). In the presence of 1 µM ABA, a delay in germination in the *herk2 the1-4* line was apparent when compared to Col-0 wild-type (WT) and single T-DNA insertion lines *herk2* and *the1-4* (Figure 3.4A, C).

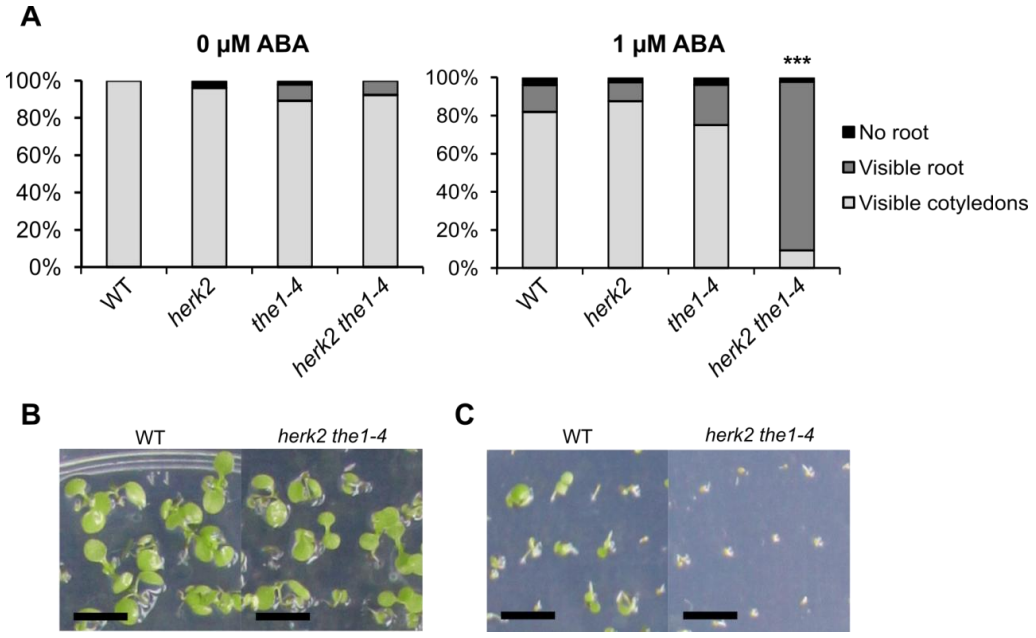

Figure 3.4 Impaired germination of the *herk2 the1-4* insertion line in the presence of ABA. Seeds from the *herk2*, *the1-4*, and *herk2 the1-4* insertion lines were sown on MS plates containing 0, 1 and 2 µM ABA, stratified for three days and incubated in our standard growth conditions for 3 days. **A**, the percentage of germination (n = 40-60) was recorded in three different categories: seeds in which the root tip had not fractured the seed coat (no germination), those in which the root had grown outside of the seed coat (root emergence) and those in which the cotyledons had emerged (green cotyledons). **B**, representative photograph of Col-0 wild-type (WT) and *herk2 the1-4* seedlings at three days after stratification in control conditions and, **C**, 1 µM ABA. Scale bars represent 1 cm. *** $p<0.001$ (Fisher's exact tests).

3.2.3.2 Exploring *herk2 the1-4* hypersensitivity to ABA beyond germination

Our results supported a germination delay in *herk2 the1-4* seeds when exposed to exogenous ABA, indicative of hypersensitivity to ABA in this particular line. Because the single T-DNA lines of *herk2* and *the1-4* had a comparable phenotype to WT, this result was suggestive of functional redundancy between these two CrRLK1Ls in controlling ABA sensitivity during this particular developmental window (Figure 3.4). *HERK2* and *THE1* expression patterns extend beyond the seed germination stage of development and it was therefore hypothesised that the hypersensitivity to ABA in *herk2 the1-4* could also be present at later stages (Figure 3.1B; [126]). Preliminary experiments were carried out on mature leaves and roots to test this hypothesis.

Firstly, the loss of relative fresh weight of mature detached leaves from *herk2 the1-4* plants was tracked after bolting as a proxy for stomatal responses to desiccation, a process that relies on ABA signalling [133-134]. No significant differences were found between WT and *herk2 the1-4* detached leaves in the rate of weight loss at early or later time points (Figure 3.5A), suggesting HERK2 and THE1 are not involved in ABA responses to desiccation in mature leaves.

Secondly, the effect of exogenous ABA on root growth in *herk2 the1-4* seedlings was studied. Exogenous ABA at concentrations of 1 µM or lower induce root elongation while higher concentrations have the opposite effect [135]. Seeds from *herk2 the1-4* were stratified at 4°C for four days on plates without ABA and germinated under our standard conditions on vertical plates for four days. Seedlings were then transferred to plates supplemented with 0, 1, 5 and 10 µM ABA, and root elongation since transfer was measured after four days. No significant differences were found between *herk2 the1-4* roots and WT in the ABA supplemented conditions, indicative of a lack of hypersensitivity to these concentrations of exogenous ABA in root elongation in this double mutant (Figure 3.5B-C). A small but significant difference was found in control conditions in which *herk2 the1-4* roots presented an increased elongation after transfer (Figure 3.5B-C). This result suggests *herk2 the1-4* roots grow faster than WT, which could be caused by an increased sensitivity to endogenous ABA levels. These experiments require replication before conclusions are drawn, but nevertheless constitute an interesting future research direction.

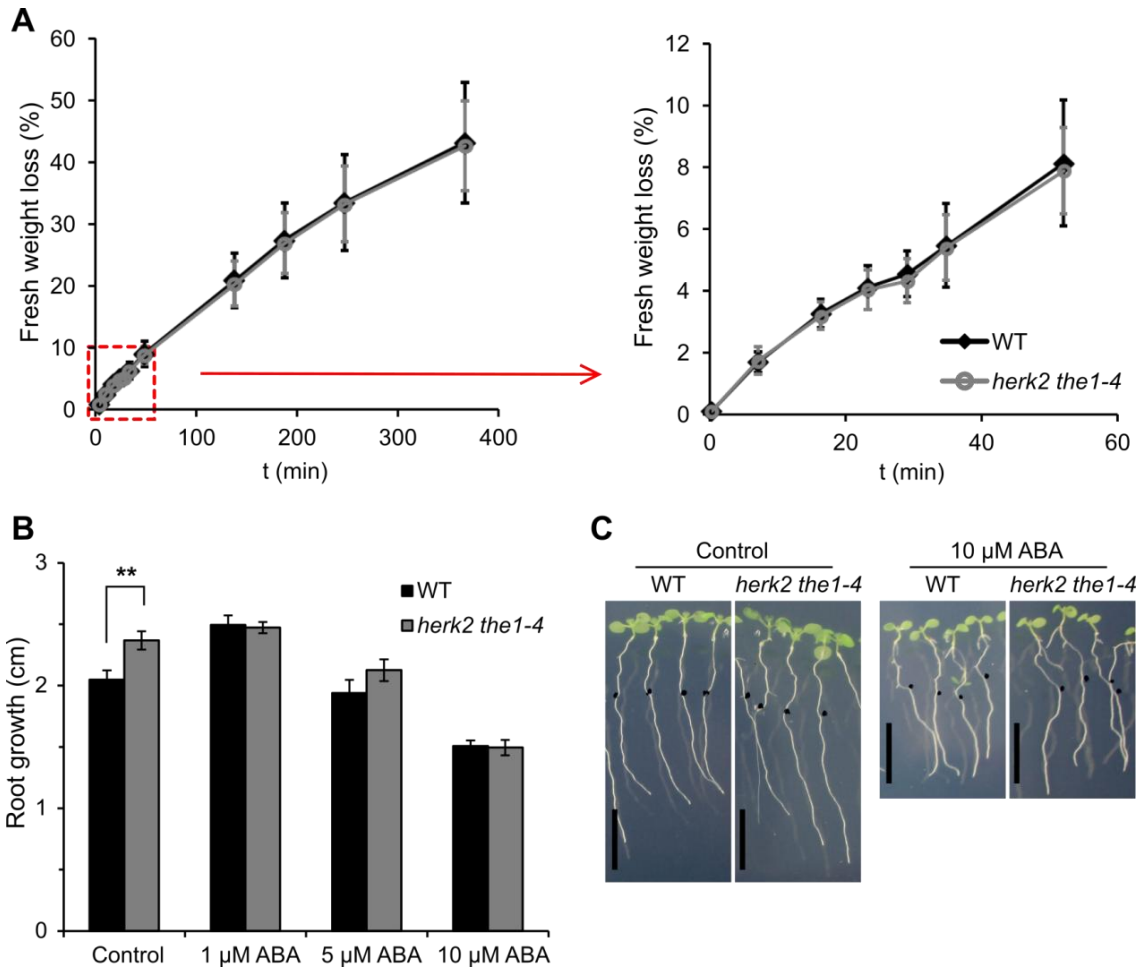

Figure 3.5 Fresh weight loss and root elongation in response to ABA in *herk2 the1-4*. **A**, percentage of fresh weight loss in detached mature leaves (four leaves from four plants per line) at multiple time points during the first hour after detachment (left panel) and during the whole experimental time course (right panel). Data presented are means and standard deviation. No statistically significant difference was found between genotypes at any time point using Student's *t* tests. **B**, effect of exogenous ABA on root growth. Seeds were germinated on vertical control plates and grown under standard conditions for four days, then 8-10 seedlings were transferred to each condition (0, 1, 5, 10 µM ABA), root tip positions were marked and the plants allowed to grow for another four days. Data presented are means and standard deviation. Student's *t* tests comparing genotypes under each condition were carried out (**, $p<0.01$). **C**, representative photographs of seedlings analysed in B in control and 10 µM ABA after 4 days of growth in test conditions. Scale bars represent 1 cm.

3.2.3.3 HERK1, HERK2 and THE1 as putative regulators of sensitivity to ABA during germination

Guo and colleagues characterised HERK1, HERK2 and THE1 as redundant regulators of cell elongation in petioles and hypocotyls as *herk1 the1-4* and *herk1 herk2 the1-4* plants display a dwarf phenotype, similar to *fer-4* mutant allele [112, 126]. Based on this evidence, we wanted to test whether HERK1 could influence the sensitivity to ABA during germination along with HERK2 and THE1. The remaining combinations of

double and triple homozygous mutants for these three CrRLK1Ls were isolated (double homozygous *herk1 herk2*, *herk1 the1-4* and triple homozygous *herk1 herk2 the1-4*) and subsequently screened for hypersensitivity to ABA during germination.

To determine the degree of hypersensitivity, lower concentrations of ABA were used in this experiment (0, 0.25 and 0.5 µM ABA; Figure 3.6A-C). After three days of growth, a delay in germination was observed in plates supplemented with 0.5 µM ABA where the T-DNA lines *herk1 the1-4*, *herk2 the1-4* and *herk1 herk2 the1-4* presented a more pronounced sensitivity to the exogenous hormone (Figure 3.6C-D). Interestingly, the *herk1 herk2* line displayed a WT phenotype in these assays (Figure 3.6), as well as a WT petiole elongation phenotype when plants were grown to maturity (not shown). These results suggest that i) ABA concentrations equal to or lower than 0.25 µM do not induce delayed germination in these mutant lines under the conditions tested here, and ii) the three CrRLK1Ls HERK1, HERK2 and THE1 may regulate germination sensitivity to ABA, with THE1 acting redundantly with HERK1 and HERK2.

Although the data presented here only represents one replicate, the hypersensitivity to ABA in germination of the lines *herk1 the1-4*, *herk2 the1-4* and *herk1 herk2 the1-4* was successfully reproduced in multiple subsequent experiments carried out by a summer intern and a MBiolSci student. To elucidate the role of these CrRLK1Ls in ABA-related processes several experiments were carried out during these short-term student projects analysing *herk1, herk2 and the1-4* single mutants, as well as double and triple insertion lines. Experiments included osmotic and saline stress during germination and drought tolerance assays. Interestingly, despite large variability between experiments, the triple mutant *herk1 herk2 the1-4* was consistently more resistant to drought, maintaining turgor in rosette leaves for longer and displaying the highest degree of survival after rewatering in several independent assays (data not shown). Although these results could be indicative of an increased responsiveness to ABA-mediated desiccation tolerance, the dwarf phenotype of *herk1 herk2 the1-4* plants could also contribute through differences in leaf architecture which could in turn also affect water loss.

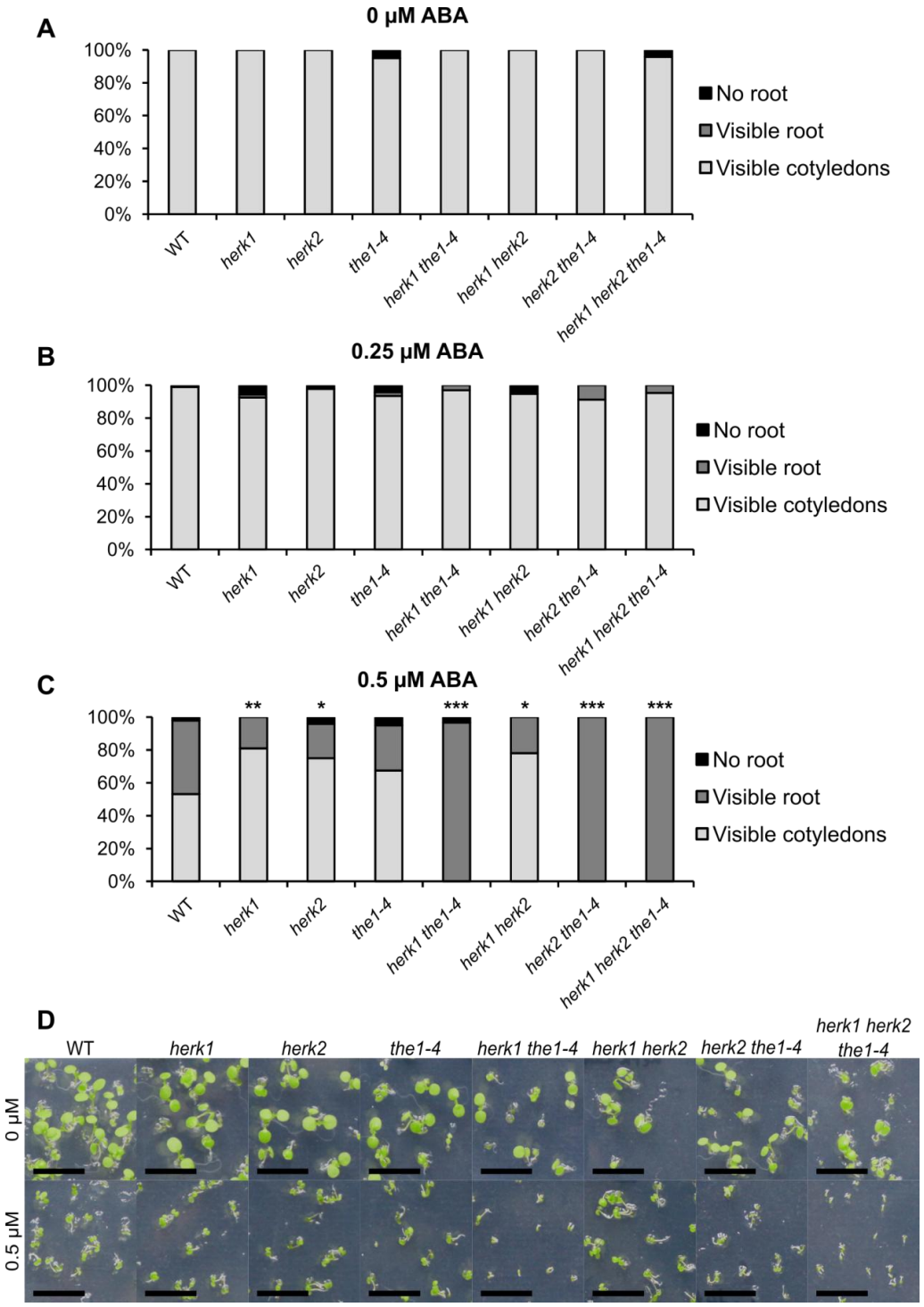

Figure 3.6 Hypersensitivity to ABA during germination in additional *herk1*, *herk2* and *the1-4* mutants. Seeds from Col-0 wild-type, *herk1*, *herk2*, *the1-4*, *herk1 the1-4*, *herk1 herk2*, *herk2 the1-4* and *herk1 herk2 the1-4* insertion lines were sown on MS plates containing 0, 0.25 and 0.5 µM ABA (**A**, **B** and **C**, respectively); stratified for three days and incubated in our standard growth conditions for three days. Percentage of germination (n = 20-90) at three different levels was recorded: seeds in which the root tip had not fractured the seed coat (no germination), those in which the root had grown outside of the seed coat (root emergence) and those in which the cotyledons had emerged (green cotyledons). **D**, representative photographs of all genotypes in control and 0.5 µM ABA at three days after germination are shown. *, $p<0.05$; **, $p<0.01$; ***, $p<0.001$ (Fisher's exact tests). Scale bars represent 1 cm.

3.2.4 Seed production defect in *herk1 anj* plants

Based on the close phylogenetic relationship between the CrRLK1Ls HERK1, ANJ we isolated double homozygous *herk1 anj* plants in an attempt to unravel developmental defects controlled by these CrRLK1Ls that may be masked by functional redundancy in single insertion lines. A reproductive defect was observed in homozygous *herk1 anj* lines, which presented shorter siliques than WT. When compared to WT, *herk1 anj* plants showed a reduction in seed production per silique, as quantified from mature siliques prior to dehiscence (Figure 3.7). The reduction in seeds per silique (mean of 52.8 in WT and 15 in *herk1 anj* in this particular experiment) could have multiple causes, including i) defects in gametophyte development, ii) defects in in pollen tube germination, growth or guidance, iii) impaired fertilisation or iv) impaired seed development. Additionally, no qualitative reproductive defects were observed in a homozygous *herk1 cvy1* line, also isolated as part of our attempt to explore the HERK1-ANJ-CVY1 clade, suggesting CVY1 may not function in redundancy with HERK1 in reproduction. It remains to be tested whether HERK1 and CVY1, or ANJ and CVY1 redundantly control other aspects of plant development. Confirmation of the *herk1 anj* reproductive phenotype and a detailed description of the role of HERK1 and ANJ in fertilisation was pursued further and is presented in Chapter 4.

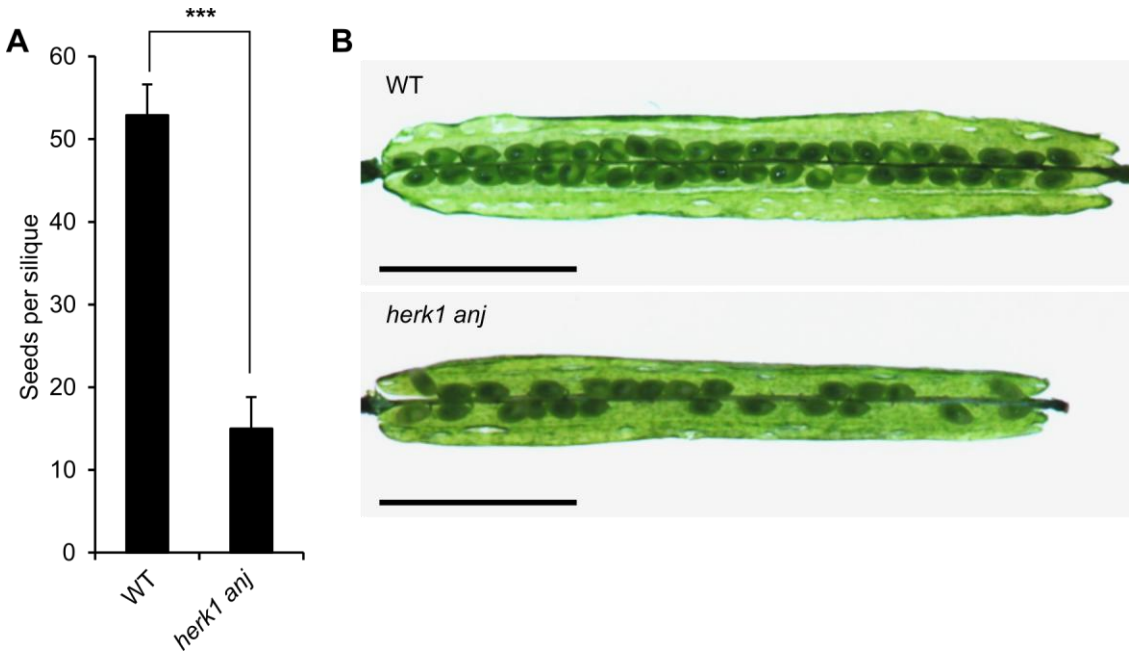

Figure 3.7 The *herk1 anj* double homozygous T-DNA insertion line displays a reduced seed set phenotype. A, seed content per silique in Col-0 wild-type (WT) and *herk1 anj* siliques. Bars represent mean seed content per silique and SD (n = 5) from each line. Significant differences were tested in two-sample Student's *t* tests (***, p<0.001). **B**, representative images from dissected maturing siliques prior to dehiscence from WT and *herk1 anj* plants.

3.3 Discussion

In this chapter, reverse genetics were applied to identify new functions for members of the CrRLK1L family of receptors in Arabidopsis. Under the hypothesis of functional redundancy between related members of this receptor family, multiple order mutants were generated to unravel novel regulatory functions in plant development. Starting with the confirmation of 10 single T-DNA insertion lines, a set of double and triple homozygous lines were generated through genetic crosses. Initially, subsets of these lines (depending on availability) were screened in pilot assays, aiming to confirm previously published developmental defects and potentially unravel related phenotypes in uncharacterised mutant lines. Some of these initial tests are described in detail in the supplemental information (Annexe 1) given their preliminary nature. As such, they should not be interpreted as definitive. They require further replication in optimal conditions and the use of a larger number of biological replicates.

We were able to reproduce previously reported results regarding developmental defects in the CrRLK1L mutant lines *fer* (impaired root hair growth in response to auxins, distorted trichomes and dwarf rosette phenotype; as described in [70, 74, 112]), *eru* (defective root hair growth; [75-77]), and in the double and triple insertion lines *herk1 the1-4* and *herk1 herk2 the1-4* (short petioles; [112, 126]). Conversely, we were unable to reproduce any of the developmental aberrations described for the *cvy1* mutant (distorted trichomes and pavement cells [81]). The results presented here are not exact replicates of the published experiments but rather constitute an attempt to reproduce their results using our standard growth conditions. It is therefore possible that *cvy1* defects are environment-dependant and only appear when plants are grown under the conditions used by Gachomo and colleagues [81]. In their study, plants were grown with 24h illumination at 24°C and pavement cells were analysed from plate-grown seedlings. No explicit information on growth stage or conditions was found for the trichome morphology analysis [81]. Given that our plants were grown in soil with 16 hours per day of ~120 $\mu mols^{-1}m^{-2}$ light and 60% humidity at 23°C and pavement cells and trichomes were observed in mature leaves, it is possible that *cvy1* phenotype is restricted to an earlier developmental stage or that it may be triggered by high humidity (if plate grown seedlings were used), continuous light or higher temperatures. If this were the case, it could facilitate an interesting unexplored research path linking the CrRLK1Ls with adaptation to changes in the growth environment. Results presented in this chapter regarding the *cvy1* mutant are qualitative. A quantitative approach to studying cell shape in pavement cells and trichomes (i.e. by quantifying number of

lobes per square mm and number of branches per trichome) could help us clarify whether there are more subtle defects in *cvy1* plants grown under our conditions.

Results presented in this chapter suggested an interplay between ABA signalling and HERK1, HERK2 and THE1 during germination. Guo and colleagues described these three CrRLK1Ls as redundant regulators of cell expansion, and therefore we hypothesised that they could also act redundantly during germination [112, 126]. This interpretation has been recently challenged by the characterisation of the *the1-4* allele (used in the present study and by Guo and colleagues; NASC ID: N829966; [112, 126]) as a hypermorphic allele rather than a loss-of-function mutant [82]. The *the1-4* allele generates a truncated version of THE1 that lacks the kinase domain and mimics THE1 over-expression, thus inhibiting cell elongation in response to cell wall damage [82, 136]. The current interpretation is that the *herk1* and *herk1 herk2* mutations may trigger cell wall composition modifications that could be sensed by the truncated version of THE1 in *the1-4* background. In turn, this would promote cell elongation inhibition leading to the dwarf phenotypes of *herk1 the1-4* and *herk1 herk2 the1-4* plants [136]. In the light of this evidence our results need to be reinterpreted. Functional redundancy between *HERK1*, *HERK2* and *THE1* in responses to ABA during germination and drought is unlikely. Redundancy between *HERK1* and *HERK2* is not a plausible explanation in this context given that mutations in either of these genes appear to prime the plant to respond in a hypersensitive manner to ABA in *the1-4* background, as seen in *herk1 the1-4* and *herk2 the1-4* lines. These findings highlight the importance of understanding the consequence of T-DNA insertions in the lines used in our experiments. Verifying that mutant lines are true knock-outs should constitute common practise, for instance, by reintroducing the wild-type gene in the mutant background or demonstrating that multiple independent mutant alleles produce a similar experimental outcome.

Generation of double T-DNA insertion lines in CrRLK1L genes with close phylogenetic relationships proved successful and allowed us to identify a reproductive defect in *herk1 anj* mutant plants. Five CrRLK1L receptors have been thoroughly studied in the context of reproduction: FER, ANX1, ANX2, BUPS1 and BUPS2 [60, 62, 65-66]. FER controls fertilisation from the female gametophyte by ensuring pollen tube burst and subsequent release of the sperm cells within the embryo sac [60]. ANX1/ANX2 and BUPS1/BUPS2 constitute two pairs of redundant CrRLK1Ls that are required for pollen tube tip growth stability [62, 65-66]. The *herk1 anj* seed production defect was reminiscent of *fer*, *anx1 anx2* and *bups1 bups2* knock-out lines which often fail to

complete fertilisation and therefore display a reduced seed set. Due to the importance of reproduction and the possible implication of two additional CrRLK1Ls in this process, the *herk1 anj* reproductive defect was selected for in-depth analysis. The subsequent description of the role of HERK1 and ANJ in reproduction is presented in Chapter 4.

3.3.1 Future work

Identification of novel functions for this family of receptors in plant development awaits a more intensive, quantitative analysis of selected developmental processes as initiated here for the subset of mutant lines. Production of mutant lines for additional CrRLK1L genes via targeted mutagenesis (i.e. using the CRISPR/Cas9 system; [137-138]) would allow us to uncover functions masked by functional redundancy with CrRLK1L genes lacking available mutant lines. For instance, generation of higher order mutant lines in the sister genes *AT2G23200* and *AT5G24010* would likely succeed at revealing roles for these as yet uncharacterised CrRLK1Ls. This approach relies on the hypothesis that sequence similarity can be indicative of functional redundancy between proteins. Complementing this methodology with the generation of transcriptional reporter lines to identify expression patterns during development and testing induction or repression of expression upon selected stimuli would help us target functionally-related members of this family of proteins. Additionally, expressing fluorescently-tagged fusions of these proteins under their native promoters would complement results from transcriptional reporters and inform us about their subcellular localisation, which should be overlapping between redundant proteins.

Confirming these results linking HERK1, HERK2 and THE1 to sensitivity to exogenous ABA during germination requires several further experiments. First, given the recent findings about the *the1-4* allele, it will be informative to test whether in this particular developmental context this allele also behaves like a THE1 over-expression line, by transforming *herk1* and *herk1 herk2* mutant lines with the THE1 over-expression construct and analysing their responsiveness to ABA during germination. Second, it is necessary to repeat the experiments presented here using true knock-out *the1* lines (such as *the1-6*; [82]) to see whether they display opposite phenotypes to those observed in the over-expression or hypermorphic mutant line. Finally, revisiting the experiments published by Guo and colleagues [112, 126] and repeating those assays with a *the1* knock-out allele will help us understand whether these three receptors work cooperatively in such developmental processes, or whether the cell elongation defects reflect an indirect response to the imposed condition of a truncated version of THE1 in the *the1-4* background.

3.3.2 Conclusions

T-DNA insertional mutant collections have provided invaluable resources to the plant biology community for almost two decades [139-141]. The results presented in this chapter reflect the usefulness of combining these collections with a reverse genetics approach to unravel new regulatory roles for genes of interest. This approach allowed us to assign putative new roles in ABA-mediated responses during germination and in reproduction for several CrRLK1L receptors. Here we provide preliminary evidence to support that CrRLK1L receptors are versatile signalling factors that play crucial roles in diverse processes during plant development.

Chapter 4

HERCULES RECEPTOR KINASE 1 and ANJEA are female determinants of pollen tube reception

4.1 Introduction

Flowering plants rely on sexual reproduction to produce the next generation of individuals. Plant sexual reproduction depends on the process of double fertilisation in which haploid gametes fuse to generate a diploid zygote and triploid endosperm that through subsequent cell division, expansion and differentiation generate the embryo and surrounding seed tissues. In flowering plants, gametes are enclosed in a multicellular structure, the gametophyte. Male gametophytes develop in the anthers of the flowers as pollen grains and comprise a haploid vegetative cell and two gametes known as the sperm cells. Sperm cells are contained in the cytoplasm of the vegetative cell, tightly associated with the vegetative cell nucleus, and act as passive cargo during the processes of pollen tube germination, growth and targeting of ovules (Figure 4.1A; [142]). Female gametophytes develop within the ovules and are composed of seven cells: three haploid antipodal cells, two haploid synergid cells, a diploid gamete, the central cell, and a haploid gamete or egg cell (Figure 4.1B). Whereas the antipodal cells' role in reproduction is not well understood, specific roles have been assigned to the remaining female gametophyte cells. Synergid cells are key during pollen tube attraction, induction of pollen tube burst, consequent release of sperm cells and block of attraction of multiple pollen tubes (polytubey; [143-144]). The central cell undergoes fertilisation by one of the sperm cells, and the resulting triploid cell divides and differentiates into the endosperm, one of the main components of the seed that ensures nutrition of the developing embryo and, in some species, seedling at early stages of development and germination [145]. The egg cell is fertilised by the second sperm cell to generate a diploid cell (zygote) that gives rise to the embryo. In the

following sections, I summarise the molecular events required for efficient fertilisation in flowering plants.

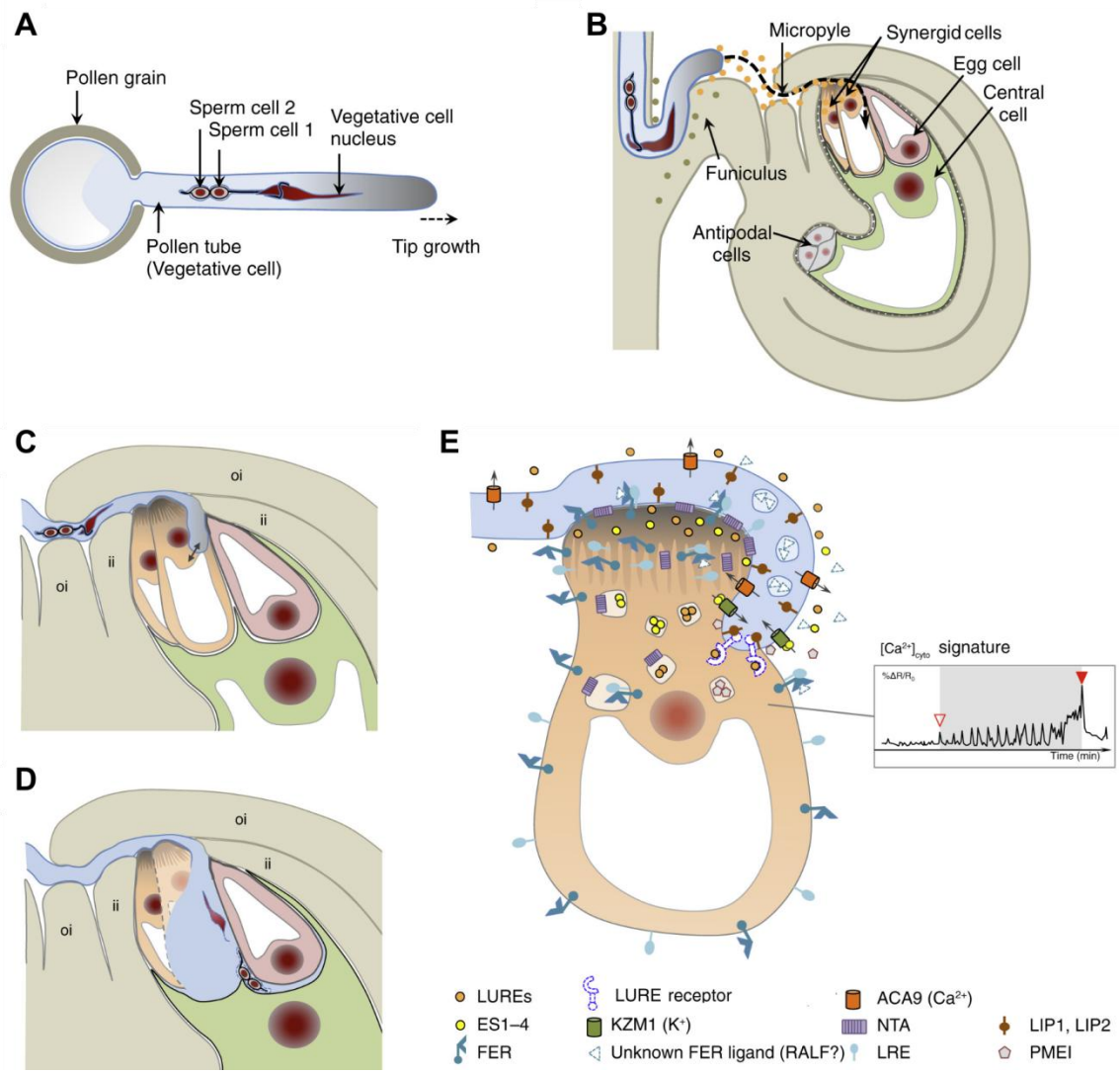

Figure 4.1 Pollen tube reception in Arabidopsis. **A**, diagram of a germinated pollen tube. All components of the male gametophyte are depicted here. **B**, representation of a mature Arabidopsis ovule connected to the ovary tissues through the funiculus with an arriving pollen tube (in light blue). All cells comprising the female gametophyte are presented in the diagram and the secretion of attractant molecules is represented by punctate particles at the micropyle. **C** and **D**, cartoon representation of the pollen tube reception event in early and late stages, respectively. oi, outer integument; ii, inner integument. Colour schemes follow the representation in B. **E**, schematic representation of some of the molecular components involved in the dialogue between a synergid cell (depicted in light brown) and an arriving pollen tube (in light blue). Depiction of a representative synergid Ca^{2+} signature during pollen tube reception is included on the right and a legend for all components represented in the diagram is included below. Figure taken from [146].

4.1.1 Pollen tube germination, growth and attraction

Sperm cell motility has been lost during the evolution of certain lineages of land plants

and remains, for instance, in mosses in which flagellated sperm cells that can move autonomously are produced [147]. On the other hand, flowering plants developed pollen grains as a mechanism to protect male gametes from desiccation and allow their dispersal on land [147]. Sperm cells in pollen grains are non-motile and therefore depend fully on the pollen tube to reach the female gametophyte and allow fertilisation. There are multiple steps that the pollen grains/tubes need to accomplish efficiently between their release from the anthers and the release of the sperm cells into the female gametophyte (see [148] for a detailed review):

Firstly, the pollen grain needs to adhere to the papillae cells of a receptive stigma, a process in which pollen grain coat proteins are important regulators [149]. Secondly, the pollen grain undergoes hydration, sourcing water and nutrients from the stigmatic tissues to allow pollen tube germination [150]. Pollen grain-stigma interactions promote rapid pollen germination, where the pollen tube emerges, penetrates the stigmatic cuticle and grows through the stigma and towards the pistil [151]. Stigma-to-ovary concentration gradients of proteins like chemocyanin and plantacyanin, thought to influence reactive oxygen species (ROS) production, contribute to the directional growth towards the ovary of the pollen tube in the pistil [152-153]. Pollen-pistil communication is also necessary to provide the pollen tubes with the competence to sense attraction signals from the ovules, as reflected by significant changes to the transcriptome of pollen tubes grown through a pistil in semi-*in vivo* assays and those grown *in vitro* [154].

Once the pollen tubes reach the ovary, the ovules within are responsible for the directionality of pollen tube growth [155]. While our understanding about long-range attraction signals towards the ovule is still limited, several short-range pollen tube attractant molecules have been identified [156]. Synergid cells are responsible for the synthesis and secretion of the attractant LURE peptides, known to mediate the attraction of pollen tubes towards the female gametophyte at the micropyle of the ovule (Figure 4.1B; [157]). LURE peptides belong to the defensin-like (DEFL) cysteine-rich family of peptides and present high divergence in amino acid sequence between closely related species, explaining the species-dependant attraction of pollen tubes by LURE peptides [158]. Multiple receptor-like kinases (RLKs) have been reported to bind LUREs in two independent studies. One study described three leucine-rich repeat (LRR) RLKs MALE DISCOVERER 1 (MDIS1), MDIS1-INTERACTING RLK 1 (MIK1) and MIK2 to mediate LURE perception in Arabidopsis through heterodimerisation of these LRR-RLKs (MDIS1-MIK1, MDIS1-MIK2; [159]). A second study characterised an

additional LRR-RLK, POLLEN-SPECIFIC RECEPTOR KINASE 6 (PRK6), as a pollen tube tip-specific receptor for LURE peptides in Arabidopsis, with structural and detailed biochemical evidence supporting PRK6's role as a true LURE receptor [160-161]. Additional components of this signalling pathway include the membrane anchored cytoplasmic kinases LOST IN POLLEN TUBE GUIDANCE 1 (LIP1) and LIP2, which present reduced sensitivity to LURE peptides *in vitro* and defects in guidance *in vivo* [162]. Sensing of LUREs at the growing tip of the pollen tube likely activates focalisation of the cell wall remodelling mechanisms towards areas with a higher LURE signalling input, therefore promoting a change in growth directionality towards the source of these peptides [156].

Tip growth is a specialised form of cell expansion and constitutes the only source for pollen tube growth (see [73] for a detailed review). A tightly controlled regulation of pollen tube tip growth as the tubes grow within the female reproductive tissues is therefore required to ensure successful transport of the sperm to the ovules [163]. Processes like production of ROS, Ca^{2+} gradients, cytoskeleton remodelling, and RLK-mediated sensing of autocrine small secreted peptides have a central role in controlling pollen tube growth [62, 68, 79-80, 163]. A detailed description of the molecular regulation of this process is included in Chapter 5.

4.1.2 Reception of the pollen tube in the ovule and release of sperm cells

Short-range attraction of pollen tubes mediated by the synergid cells leads to the pollen tube reception at the female gametophyte [156]. Pollen tubes enter the micropyle and reach what is believed to be the point of highest concentration of attraction molecules, the filiform apparatus of the synergid cells [164]. The filiform apparatus is a thickened cell wall structure with unique characteristics (i.e. accumulation of callose [165]), located at the outermost pole of the synergid cells, that also constitutes the first contact point between male and female gametophytes [166]. Pollen tubes arrest growth momentarily after reaching the filiform apparatus, resume growth alongside or between the synergid cells and towards the egg and central cells area of the ovule, and conclude their journey through the termination of the pollen tube, or pollen tube bust - indispensable for sperm cell release and subsequent fertilisation (Figure 4.1C-E; [72]). Communication between the arriving pollen tube and the synergids is thought to control every phase of pollen tube reception. Multiple signals are thought to play an important role in this process, including mechanical forces, ions, ROS and small peptides [148]. Although the involvement of some of those cues remains speculative, enlightening discoveries have been made in the past decade about the regulation of pollen tube

reception.

One member of the *Catharanthus roseus* RLK 1-like (CrRLK1L) family, FERONIA (FER), was first characterised in the context of pollen tube reception control in Arabidopsis [59-60]. *fer* mutants were found to present a fertility defect caused by pollen tube overgrowth at the synergid cell area of the female gametophyte [60]. The pollen tube overgrowth phenomenon implies a defect in communication between pollen tube and female gametophyte, resulting in impaired pollen tube burst. When pollen tubes fail to terminate, the sperm cells are not released into the ovule, thus impeding fertilisation. FER is widely expressed throughout most tissues and stages of plant development except for the pollen, including several layers of the ovule where it specifically accumulates in the synergid cells' filiform apparatus [60]. ROS accumulates at the synergid cell area of mature ovules prior to pollen tube arrival via FER-dependent NADPH oxidase activation [68]. Interestingly, pharmacological scavenging of ROS from the ovule during pollen tube arrival induced pollen tube overgrowth, suggesting a possible role for FER-mediated ovular ROS accumulation in controlling pollen tube burst [68]. FER has also been found to form a complex at the filiform apparatus with the synergid cell-specific glycosylphosphatidylinositol (GPI)-anchored protein LORELEI (LRE; [70-71]). *lre* mutants also fail to induce pollen tube termination and ROS production in the ovule, suggesting that FER and LRE form a receptor complex required to receive the pollen tube [70-71].

NORTIA (NTA) is a synergid cell-specific, endomembrane compartment-localised member of the MILDEW RESISTANCE LOCUS O (MLO)-like family [69, 167]. Similarly to FER and LRE, NTA was identified due to the pollen tube overgrowth-induced reduced fertility phenotype observed in *nta* mutants [69]. NTA is a 7-pass membrane protein with a calmodulin-binding domain, believed to bind calmodulin in a Ca^{2+}-dependent manner [69, 168]. The second messenger Ca^{2+} also plays an important role in the synergid cells during pollen tube reception [72]. Specific signatures in the synergids' Ca^{2+} concentration take place as the pollen tube contacts the synergids and grows along them, culminating with a Ca^{2+} spike that coincides with pollen tube burst and degeneration of the receptive synergid [72]. NTA influences the amplitude of such signatures and concentration spike during pollen tube reception and is therefore regarded as a Ca^{2+} oscillation modulator [72]. Because depleting Ca^{2+} from the ovule with pharmacological treatments results in pollen tube overgrowth [68], the current hypothesis is that NTA regulates pollen tube reception by ensuring proper Ca^{2+} signalling in the synergid. Additionally, NTA was found to relocalise towards the filiform

apparatus area upon pollen tube reception in a FER-dependent manner, implicating that NTA acts downstream of FER in this pathway [69]. The consequence and significance of this relocalisation awaits further clarification.

Additional regulators of pollen tube reception include TURAN (TUN) and EVAN (EVN), a uridine diphosphate (UDP)-glycosyltransferase and a dolichol kinase, respectively, involved in endoplasmic reticulum protein N-glycosylation [165]. TUN and EVN are required for the female control of pollen tube burst from the synergid cells and are speculated to mediate glycosylation of FER, LRE or NTA which would in consequence explain the pollen tube overgrowth observed in *tun* and *evn* mutants [165]. The *abstinence by mutual consent* (*amc*) mutant also displays a pollen tube overgrowth phenotype, however in *amc* mutants the defect only occurs when both male and female gametophytes involved are mutant [169]. The *amc* mutation affects a peroxin in charge of regulating protein import to peroxisomes, therefore suggesting this organelle may be of importance for pollen tube reception [169]. Finally, one case of paternal control of pollen tube termination has been reported; a triple mutation affecting three MYB transcription factors, MYB97, MYB101 and MYB120 [170]. Contrary to the rest of paternal regulators of pollen tube growth stability which present a premature pollen tube burst phenotype, pollen mutant in these three MYBs reach the ovules normally but often fail to terminate and overgrow in the female gametophyte [170]. Identifying the target genes of this set of transcription factors in pollen will undoubtedly reveal key components of the paternal signalling pathway that controls pollen tube burst.

In maize, DEFENSIN-LIKE cysteine-rich small peptides EMBRYO SAC 1-4 (ES1-4) are responsible for pollen tube burst upon contact with the synergid cells [171-172]. ES1-4 accumulate in the synergids and are secreted during pollen tube arrival [172]. *In vitro* experiments showed ES4 induces depolarisation of the plasma membrane, a process in which the potassium channel K^+ CHANNEL ZEA MAYS 1 (KZM1) is involved as well [172]. Pectin methylesterase inhibitors (PMEIs) are also thought to be involved in destabilising the cell wall at the tip of the pollen tube, as they were found to localise specifically at the apical region of the pollen tube where they are thought to impair pectin methylesterases function [173-174].

In Arabidopsis, recent reports suggest a role for a small secreted peptide belonging to the RAPID ALKALINISATION FACTOR (RALF) family, RALFL34, as a putative ovular trigger of pollen tube rupture [62]. RALFL34 was shown to i) bind directly the extracellular domain of the pollen tube expressed CrRLK1Ls BUDDHA'S PAPER SEAL 1 (BUPS1), BUPS2, ANXUR1 (ANX1) and ANX2 in pull down assays, ii) to promote

rapid burst of pollen tubes grown *in vitro* and iii) to compete with pollen expressed RALFL4 and RALFL19 for binding to the abovementioned CrRLK1Ls [62]. Given the involvement of BUPS1/2, ANX1/2 and RALFL4/19 in ensuring pollen tube growth stability (see Section 5.1 of Chapter 5 of this thesis for a more detailed explanation), the standing hypothesis proposes that RALFL34 induces pollen tube burst at the female gametophyte by blocking RALFL4/19-BUPS/ANX autocrine signalling that prevents premature pollen tube burst [62, 175]. Lack of a pollen tube overgrowth defect in *ralfl34* mutants and localisation of RALFL34-GFP in the inner integument of the ovule prior to fertilisation instead of the synergid cells impede a straightforward interpretation of these results [62]. It is possible that RALFL34 acts in redundancy with additional ovule-expressed RALFLs, and that RALFL34 may be processed and transported outside of the inner integument and into the female gametophyte to induce pollen tube burst upon pollen tube-synergid cell dialogue during pollen tube reception. These scenarios remain speculative and their exploration will provide exciting results in the future.

4.1.3 Posterior events

Minutes after release, sperm cells undergo attachment to the egg cell and central cell surfaces prior to their respective fusions [176]. In most plant species analysed, including Arabidopsis, the sperm cells show no preference towards either female gamete, and the process through which they specifically attach to the surfaces of the egg cell and central cells is thought to involve cell surface charges and rapidly evolving cell surface effectors [177-178]. One sperm cell fuses with the egg cell, and soon after the second sperm cells fuses with the central cell [179]. The cytoskeleton rearranges to orchestrate the transport of the sperm cell nuclei towards the egg and central nuclei for fusion [180]. An additional cell fusion event has been recently reported, taking place between the persistent synergid cell and the central cell soon after the first division of the fertilised central cell [144]. This fusion is crucial to block the attraction of additional pollen tubes (polytubey) into the already fertilised ovule; the attractant molecules that remain in the persistent synergid cell are diluted in a larger cell volume through fusion [144].

4.1.4 Aims

This chapter reports on the characterisation of the CrRLK1L receptors HERCULES RECEPTOR KINASE 1 (HERK1) and ANJEA (ANJ) as maternal determinants of pollen tube reception in Arabidopsis.

Several experimental approaches were undertaken to identify the cause of the reduced fertility observed in *herk1 anj* mutant plants, assign a new function to these two proteins and expand our understanding about the control of development mediated by CrRLK1Ls, including: i) reverse genetics, ii) microscopic examination, iii) use of genetic reporters, iv) multiple staining techniques and v) biochemical assays.

Results included in this chapter regarding the protein-protein interaction assays were performed in collaboration with Noel Blanco Touriñán (Yeast 2 hybrid (Y2H); Blázquez-Alabadí Lab, Instituto de Biología Molecular y Celular de Plantas, (IBMCP), Spain) and Thomas A. DeFalco (Co-immunoprecipitation assays; Zipfel Lab, University of Zurich, Switzerland).

4.2 Results

4.2.1 Reduced seed set in *herk1 anj* double mutants

A reverse genetics approach using multiple T-DNA insertion lines targeting CrRLK1L genes yielded the identification of a reproductive phenotype in *herk1 anj* double mutant plants (section 3.2.4; see Chapter 3 for details on the preliminary phenotypic screen of CrRLK1L T-DNA lines). The *herk1 anj* homozygous line presents T-DNA insertions in the coding regions of the CrRLK1Ls *HERCULES RECEPTOR KINASE 1* (*HERK1*; *AT3G46290*) and *ANJEA* (*ANJ*; *AT5G59700*; Figure 4.2A). The mutant line *herk1* used in this study (NASC stock ID: N657488) had been described to knock out *HERK1* expression in previous reports [112, 126]. The *anj* T-DNA line studied here and used to generate the double *herk1 anj* mutant (NASC stock ID: N654842) had not been characterised, therefore I used RT-PCR to verify that the insertion abolishes *ANJ* gene expression. Briefly, RNA extracted from floral tissue from five pooled plants per line (Col-0 WT, *anj* and *herk1 anj*) was retrotranscribed into first strand cDNA, and presence of the transcripts of interest (*ANJ* and *FER* as a positive control) was subsequently assessed by PCR using primers specific to the genes of interest (see Annexe Table 2 for the primers sequence). The *ANJ*-specific amplicon was absent from *anj* and *herk1 anj* cDNA samples, indicating that the *anj* T-DNA insertion impedes expression of this gene (Figure 4.2B).

Preliminary results included in the third chapter of this thesis suggested a fertility defect in the double mutant *herk1 anj*, as these plants presented shorter siliques that contained fewer seeds than WT plants. To confirm these results and further investigate the contribution of each T-DNA insertion, seed counts on maturing siliques from Col-0

WT, *herk1, anj* and *herk1 anj* plants were carried out prior to dehiscence. Briefly, five maturing siliques from the main inflorescence stem were harvested per plant examined (avoiding the first five siliques produced in the inflorescence due to their low fertility) and developing seeds were exposed through manual dissection. In agreement with the preliminary results, seed production per silique was strongly reduced in *herk1 anj* plants, whereas single mutants *herk1* and *anj* were not affected and produced siliques full of seeds with comparable numbers to WT (Figure 4.2C-D). 75% identity and 86% similarity at the protein level between these two homologous CrRLK1Ls suggests functional redundancy could explain the lack of reproductive defects in the single T-DNA insertion lines.

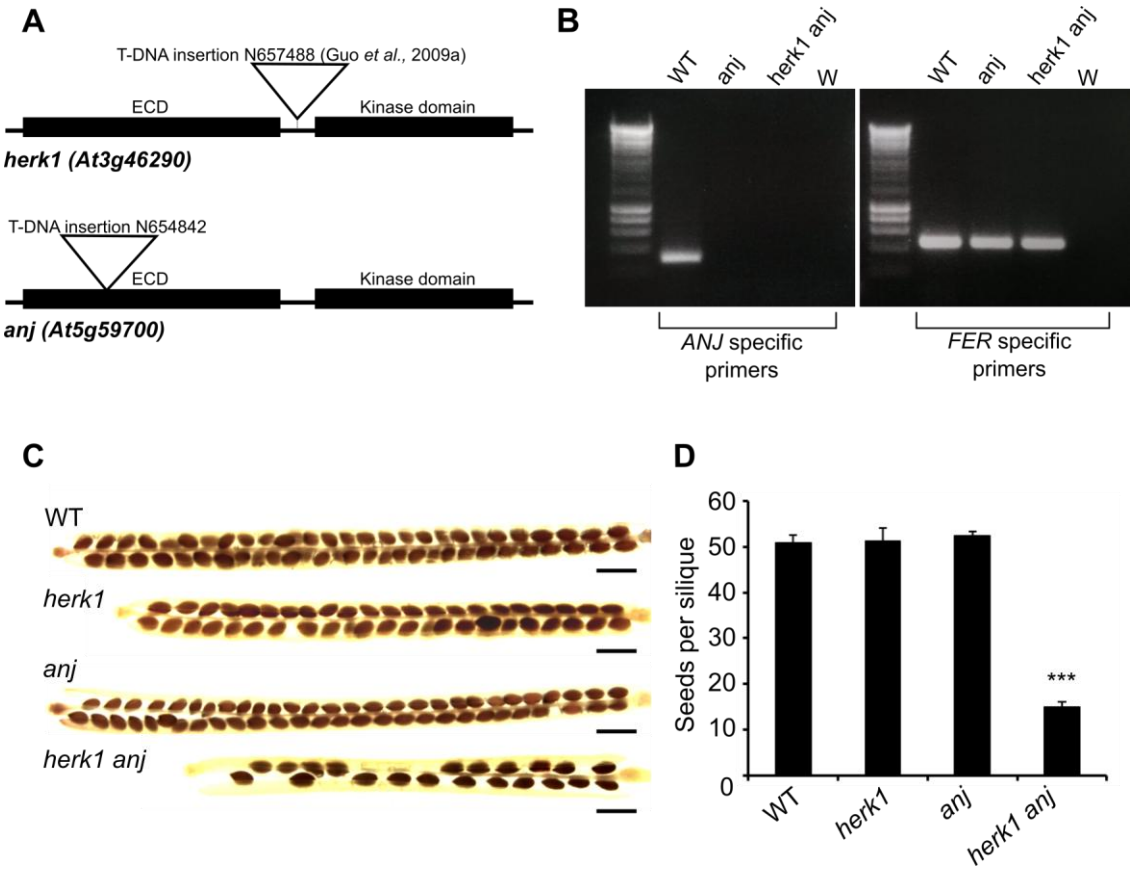

Figure 4.2 *anj* T-DNA insertion knocks out *ANJ* expression and seed set defect in *herk1 anj* plants. A, domain organisation of HERK1 and ANJ with T-DNA insertion sites indicated in the lines *herk1* and *anj* used in the present study. **B**, analysis of ANJ gene expression by RT-PCR in *anj*, *herk1 anj* and Col-0 WT plants. RNA was extracted from pooled inflorescences of five plants per line. W, water control. **C**, representative photographs of mature siliques from WT, *herk1*, *anj* and *herk1 anj* prior to dehiscence. Siliques were cleared in 0.4M NaOH, 1% Triton X-100. Scale bar = 1 mm. **D**, quantification of the number of developing seeds per silique in WT, *herk1*, *anj* and *herk1 anj* plants. Seeds from maturing green siliques were exposed under a dissection microscope and photographed. *n* = 4 (four independent experiments with at least three plants per line and five siliques per plant). Data presented are means ± SEM. *** $p<0.001$ (Student's *t*-test).

4.2.2 Maternally-derived pollen tube overgrowth causes the reproductive defect in *herk1 anj* plants

Impairment of multiple reproductive processes could explain the low seed set per silique observed in the *herk1 anj* double homozygous line, including i) development of male or female gametophytes, ii) pollen germination, iii) pollen tube growth, iv) pollen tube targeting of ovules, v) pollen tube burst at the female gametophyte, vi) attachment or fusion of the sperm cells to the female gametes and vii) early post-fertilisation processes. Aniline blue staining of pollen tubes was used to track pollen tube germination, growth inside of the ovary and targeting of ovules to identify whether the reproductive phenotype in *herk1 anj* was caused by defects in steps ii)-v). Similarly to WT, ovules in *herk1 anj* ovaries from self-pollinated flowers were efficiently targeted by pollen tubes suggesting steps ii)-iv) were unaffected in this mutant (Figure 4.3A). Closer examination of the ovules in aniline blue stained ovaries revealed a pollen tube overgrowth phenotype in *herk1 anj* ovules, with 83% of ovules exhibiting pollen tube overgrowth (Figure 4.3B-D). This high proportion of pollen tube overgrowth events contrasts with low frequencies observed in Col-0 WT, *herk1* and *anj* single mutant lines (less than 2%; Figure 4.3D).

Pollen tube overgrowth causes fertility defects in multiple mutants such as *fer*, *lre*, *nta*, *tun* and *evn*, among others [59-60, 69, 71, 165]. In these mutants, pollen tubes reach the female gametophyte normally but fail to communicate with the synergids to trigger pollen tube termination (or burst) which concludes the journey of the pollen tube and releases the two sperm cells into the ovule to allow fertilisation. The frequency of pollen tube overgrowth events in *herk1 anj* is higher than the reduction in seed set as quantified from maturing siliques (Figures 4.3D and 4.2D; 83% and 71%, respectively). These frequencies indicate that the reproductive defect caused by disruption of *HERK1* and *ANJ* expression is not fully penetrant as 29% of seeds can still be recovered. Furthermore, the pollen tube overgrowth does not result in impairment of fertilisation in 12% of the cases. Infrequent release of the sperm cells into the ovule after pollen tube overgrowth could explain this discrepancy in frequencies, although this hypothesis has not been tested yet. An additional explanation that could increase the chances of sperm cell release is the attraction of further pollen tubes to an already targeted ovule, a phenomenon known as polytubey. Polytubey has been found in mutants defective in fertilisation and is caused by prolonged emission of attractant molecules after the first pollen tube reception event, usually explained by the lack of degeneration of the synergid cells following pollen tube burst and double fertilisation [59, 143-144, 181].

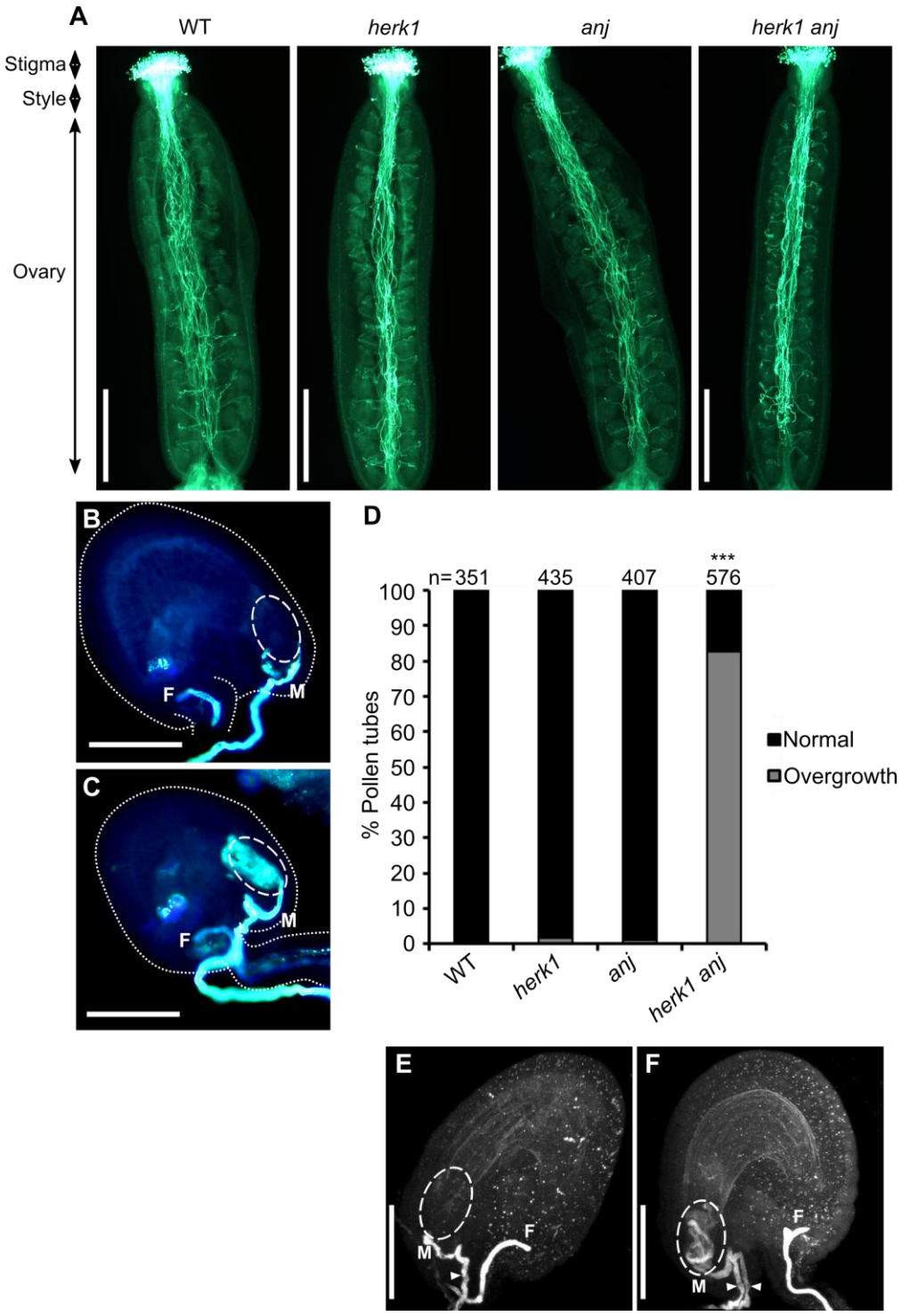

Figure 4.3 Aniline blue staining of pollen tubes reveals a pollen tube overgrowth defect in *herk1 anj* ovules. A, aniline blue staining of pollen tubes in self-pollinated stage 16 flowers in WT Col-0, *herk1*, *anj* and *herk1 anj* plants. Scale bars = 500 µm. **B** and **C**, representative images of ovules with normal reception of a pollen tube and pollen tube overgrowth, respectively. Scale bars = 50 µm. **D**, Percentage of pollen tubes with normal reception at the female gametophyte (black bars) and with overgrowth (grey bars) as assessed by aniline blue staining. 15 self-pollinated stage 16 flowers from WT, *herk1*, *anj* and *herk1 anj* were analysed. *** $p<0.001$ (χ-square tests). **E** and **F**, representative images of a normal pollen tube reception event in WT and a *herk1* anj ovule displaying pollen tube overgrowth and attraction of multiple

pollen tubes, respectively. Images are maximum intensity projections across several z-planes obtained by confocal imaging of aniline blue stained ovules. Scale bars = 50 µm. M, micropyle. F, funiculus. White arrowheads mark individual pollen tubes. Dashed lines delineate the synergid cell area.

Polytubey was also found in *herk1 anj* ovules from self-pollinated flowers (Figure 4.3E-F), although gathering of quantitative data regarding the frequency of this phenomenon has not been pursued.

With the exception of the triple mutant in *MYB97*, *MYB101* and *MYB120*, all reproductive mutations characterised by pollen tube overgrowth present a maternal origin [146]. To investigate the parental origin of the pollen tube overgrowth observed in *herk1 anj,* reciprocal crosses were performed between Col-0 WT and *herk1 anj,* with subsequent staining of pollen tubes performed one day after pollination. Reciprocal crosses revealed the reproductive phenotype in *herk1 anj* plants has a maternal origin, as only crosses in which *herk1 anj* was used as female donor resulted in pollen tube overgrowth (Figure 4.4). Frequencies of pollen tube overgrowth observed indicate that there is no partial paternal effect in the *herk1 anj* reproductive defect (Figure 4.4). These results suggested that multiple CrRLK1L receptors (HERK1 and ANJ in addition to FER) control the process of pollen tube reception at the female gametophyte in Arabidopsis.

A genetic complementation approach was undertaken to verify that the mutant phenotype observed in *herk1 anj* plants is caused by disruption of the *HERK1* and *ANJ* genes and not due to additional unidentified insertions. To this end, *pANJ::ANJ-GFP* and *pHERK1::HERK1* constructs were generated and used to test complementation of *herk1 anj* alongside a *pFER::HERK1-GFP* construct (kindly provided by U. Grossniklaus; University of Zurich), given that *pHERK1::HERK1-GFP* resulted in bacterial toxicity and *FER* is known to be expressed in most female reproductive structures [59-60]. *Agrobacterium*-mediated floral dip was used to transform *herk1 anj* plants with the abovementioned constructs and complementation of the pollen tube overgrowth defect was assessed in the T1 generation by aniline blue staining of pollen tubes from self-pollinated flowers. 100% complementation would be expected from a sporophytic recessive mutation in T1 generation while, alternatively, a 50% complementation would result from a gametophytic defect and a single insertion event. Multiple independent T1 lines were analysed and approximately a 50% complementation of the pollen tube overgrowth defect was observed for each of the three constructs tested (Figure 4.5). These results indicate that i) the *herk1 anj*

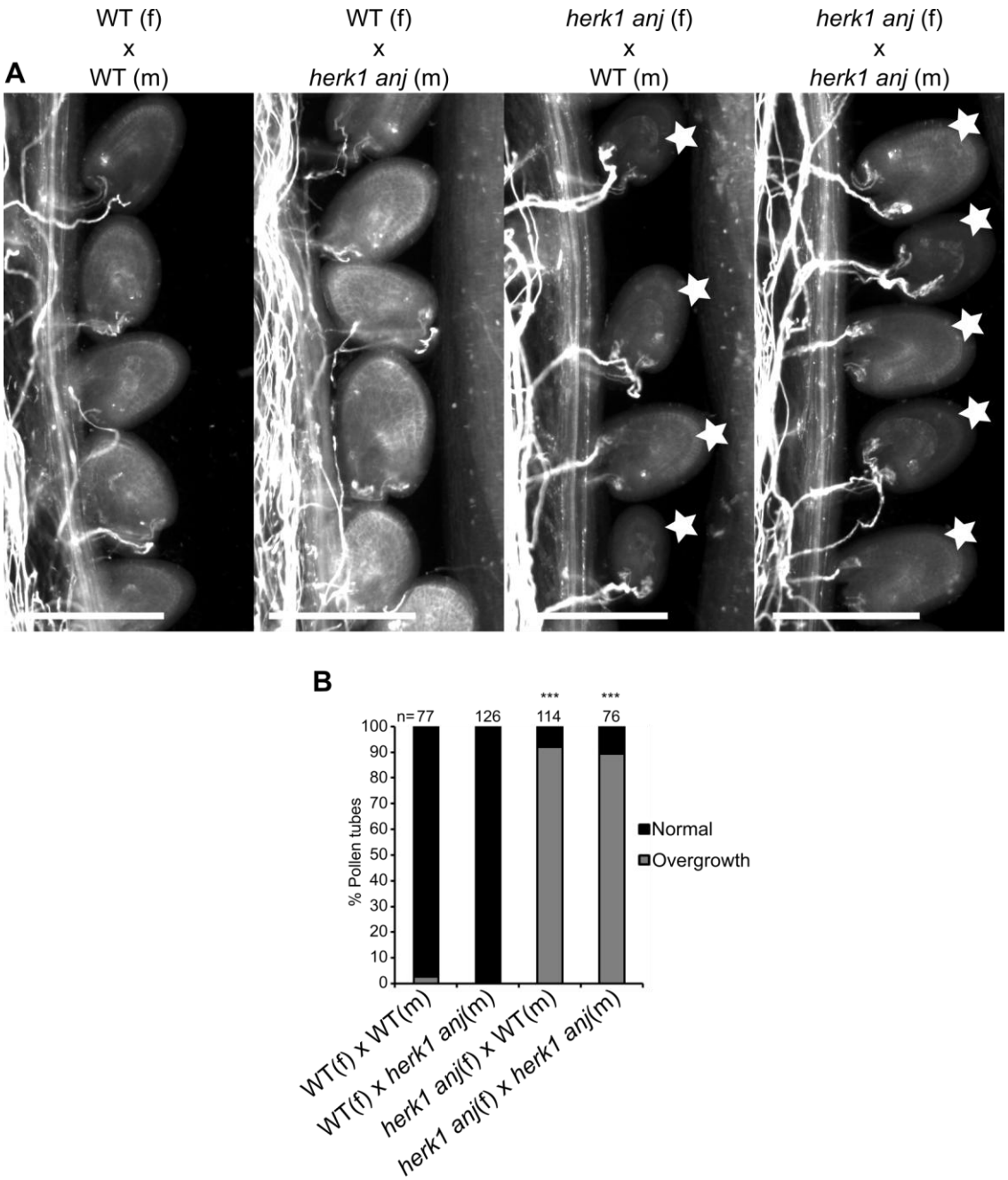

Figure 4.4 Reciprocal crosses between *herk1 anj* and WT plants indicate a maternal origin of the reproductive defect. A, representative images of aniline blue stained ovaries at 24 hours after pollination in the reciprocal crosses indicated in the figure. White stars highlight ovules displaying pollen tube overgrowth. Scale bars = 200 µm. **B**, quantification of normal pollen tube reception and overgrowth in reciprocal crosses between WT Col-0 and *herk1 anj* plants with at least two siliques per cross. *** $p<0.001$ (χ-square tests).

reproductive defect is caused by the disruption of these two CrRLK1Ls, ii) the phenotype has a gametophytic origin and iii) the constructs used in this complementation experiment are suitable for examining HERK1-GFP and ANJ-GFP cellular localisation in the female gametophyte.

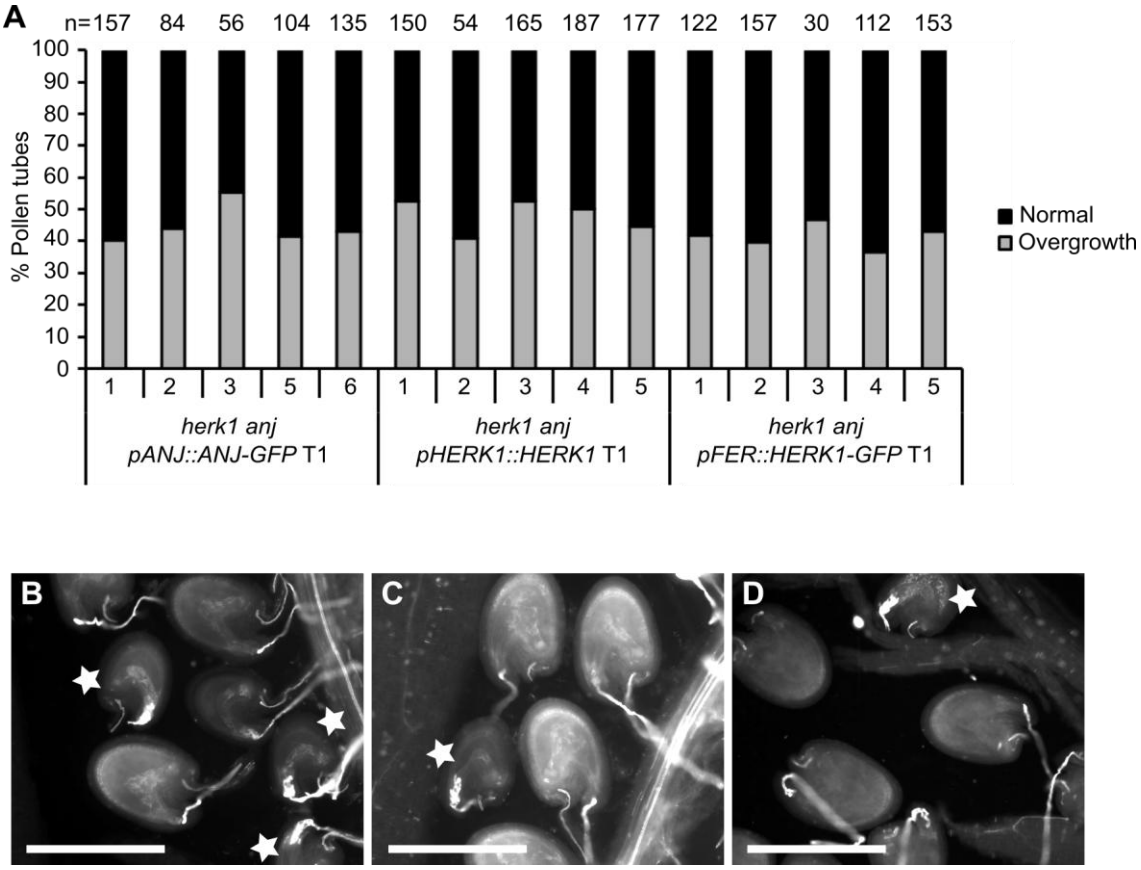

Figure 4.5 Complementation of the *herk1 anj* pollen tube overgrowth defect in T1 plants with ANJ-GFP, HERK1 and HERK1-GFP. A, quantification of normal pollen tube reception events (black bars) and pollen tube overgrowth (grey bars) in siliques from five independent T1 *herk1 anj* plants transformed with *pANJ::ANJ-GFP*, *pHERK1::HERK1* and *pFER::HERK1-GFP*. Data from control lines were not collected in this experiment. At least three siliques per line were analysed. **B**, **C** and **D**, representative images of the aniline blue stained carpels analysed in A. Images correspond to *herk1 anj* plants expressing *pANJ::ANJ-GFP*, *pHERK1::HERK1* and *pFER::HERK1-GFP* in B, C and D, respectively. White stars highlight ovules displaying pollen tube overgrowth. Scale bars = 200 µm.

4.2.3 HERK1 and ANJ are filiform apparatus localised effectors

To gain a deeper understanding about the function of HERK1 and ANJ, transcriptional and translational reporter lines were produced to study expression patterns and cellular localisation. β-glucuronidase (GUS)-based transcriptional reporter constructs were generated using GateWay technology. First, a promoter sequence comprising 2kb upstream of the ATG start codon for each gene was amplified from genomic DNA with a 5' terminal CACC extension and cloned into the entry vector *pENTR/D-TOPO*. *pHERK1* and *pANJ* were then recombined into the destination vector *pGWB433* via LR-recombination, generating the respective *pHERK1::GUS* and *pANJ::GUS* constructs. These reporter constructs were transformed into Col-0 WT Arabidopsis plants via *Agrobacterium*-mediated floral dip [182]. T1 and T2 plants were used to

examine the expression patterns of *HERK1* and *ANJ* with GUS histochemical staining of floral tissues [121]. Overlapping expression patterns of *pHERK1::GUS* and *pANJ::GUS* were observed in the junction of the stigma and style, along the funiculus and at the synergid cell area of the ovule (Figure 4.6A-B). *pHERK1::GUS* expression was also found in the style, ovary walls, stamens and some developing pollen grains (Figure 4.6C-E). *pANJ::GUS* expression was detected in stigmas and stamens (Figure 4.6F-H). HERK1 and ANJ reproductive function should be executed at overlapping areas of expression in the female gametophyte given their functional redundancy and the maternal gametophytic origin of the *herk1 anj* reproductive phenotype. The synergid cell area of the female gametophyte therefore arose as a strong candidate for HERK1 and ANJ control of pollen tube reception.

Expression data obtained with the GUS transcriptional reporter lines was complemented with the analysis of the GFP translational reporter lines used in the complementation experiments *pANJ::ANJ-GFP* and *pFER::HERK1-GFP* (section 4.2.2). Microscopic examination of dissected mature ovules from emasculated flowers of each reporter line was carried out rapidly after dissection in an epifluorescence microscope. In agreement with the GUS assays, ANJ-GFP fluorescent signal in the female gametophyte was found to accumulate in the synergid cell, being particularly strong in the filiform apparatus (Figure 4.7A-B). Additionally, HERK1-GFP was also found to accumulate in the filiform apparatus of the synergid cells when expressed under the *pFER* promoter (Figure 4.7C-D), suggesting the control of pollen tube burst by HERK1 and ANJ in the female gametophyte is executed from the filiform apparatus of the synergid cells. Interestingly, previously characterised regulators of pollen tube reception FER and LRE also accumulate specifically at the filiform apparatus, where they are believed to form a receptor complex that mediates male-female gametophytic communications [60, 70-71, 183]. A scenario in which a higher order receptor complex regulates pollen tube reception at the synergid cells arose as an attractive option to explore based on the similarity of the mutant phenotypes, overlapping expression patterns and subcellular localisation in the synergid cells of these four membrane receptors FER, LRE, HERK1 and ANJ.

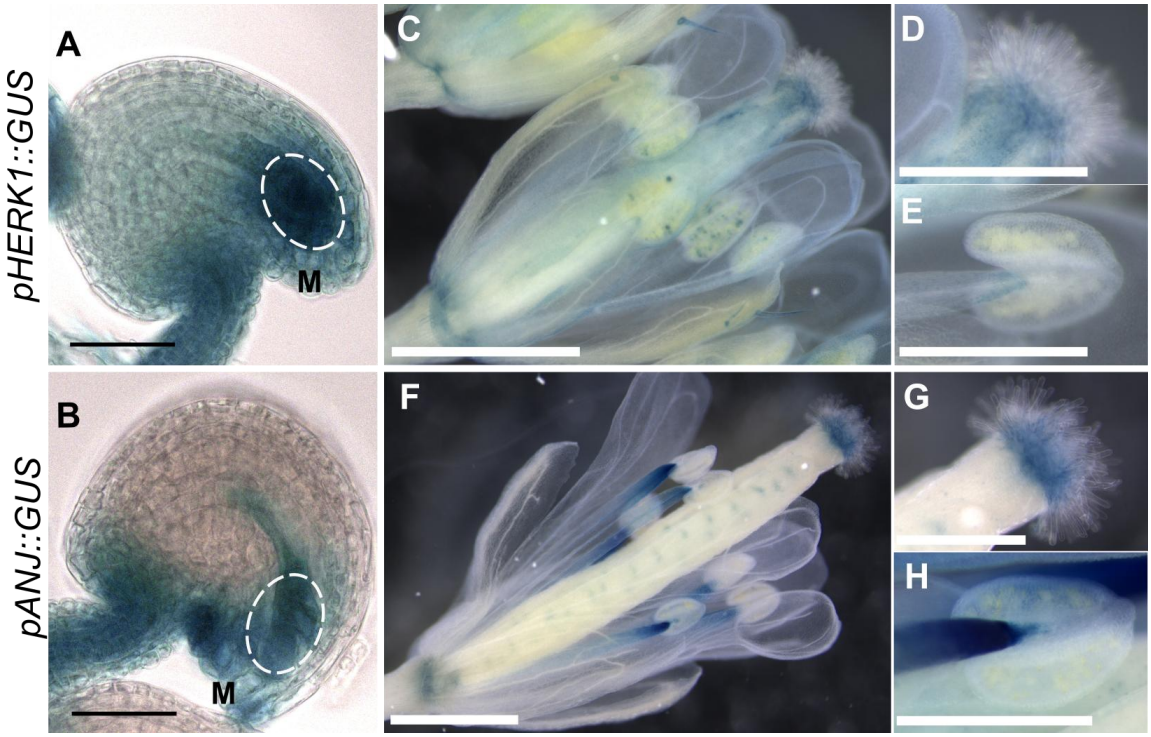

Figure 4.6 GUS histochemical assays reveal *HERK1* and *ANJ* expression patterns in ovules and floral tissues. A and **B**, expression of *pHERK1::GUS* and *pANJ::GUS* in mature ovules. M, micropyle. Dashed lines delineate the synergid cells area of the ovule. **C**, **D** and **E**, representative images of the expression pattern in flowers of *HERK1* as shown by *pHERK1::GUS*. Mature stigma and anther are shown in D and E, respectively. GUS activity in at least four T1 lines was examined. **F**, **G** and **H**, representative images of the expression pattern in flowers of *ANJ* as shown by *pANJ::GUS*. A mature stigma and anther are shown in G and H, respectively. GUS activity in at least four T1 lines was examined. Scale bars = 25 µm in A and B; 1 mm in C and F; 0.5 mm in D, E, G and H.

4.2.4 Ovule development in *herk1 anj* plants is normal

The defect in pollen tube reception observed in *herk1 anj* ovules could be explained through two main hypotheses: i) morphological abnormalities in ovular development or ii) a defect in signalling specific to the pollen tube termination process. Morphological abnormalities in the development of the female gametophyte could in turn affect the subcellular distribution of key players in the pollen tube burst signalling pathway therefore impeding proper communication between gametophytes (see section 4.2.7). A signalling defect specific to the regulation of pollen tube burst would imply HERK1 and ANJ are direct regulators of the communication between pollen tube and synergid cells, similar to FER and LRE.

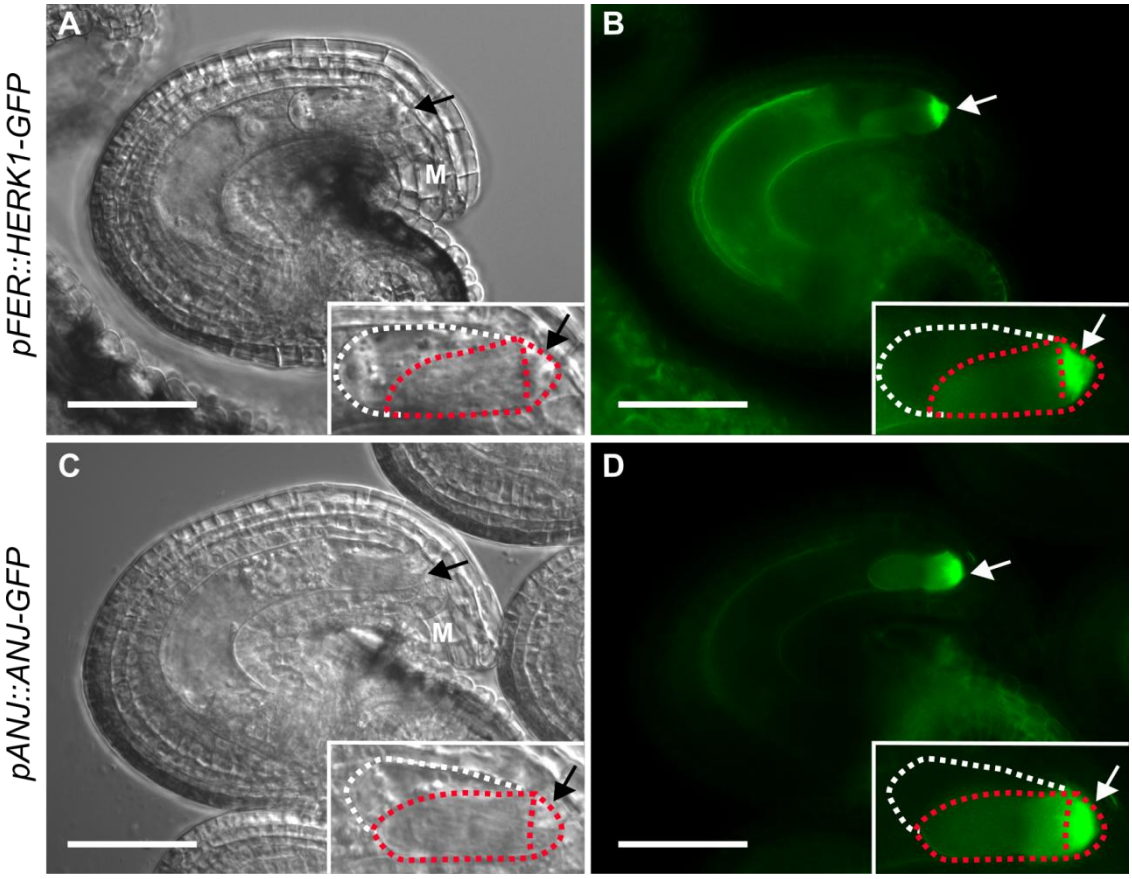

Figure 4.7 HERK1-GFP and ANJ-GFP accumulate at the filiform apparatus of the synergid cells. A and **B**, representative differential interference contrast (DIC) image of a mature ovule expressing *pFER::HERK1-GFP* and corresponding fluorescence image showing accumulation of HERK1-GFP at the filiform apparatus, respectively. **C** and **D**, representative DIC image of a mature ovule expressing *pANJ::ANJ-GFP* and corresponding fluorescence image displaying ANJ-GFP accumulation at the filiform apparatus, respectively. M, micropyle. White dotted line delineates the egg cell. Red dotted line delineates the synergid cell and filiform apparatus. Arrows indicate the filiform apparatus. Scale bars = 50 µm.

In brief, development of the mature female gametophyte involves the generation of seven cells that comprise the gamete's single egg cell, two central cells, two accessory synergid cells, and three antipodal cells. During the maturation of the female gametophyte, the antipodal cells, and egg and synergid cells need to differentiate on opposite poles of the gametophyte, with the synergids and egg cell located at the outermost position next to the ovular opening, or micropyle. The central cell nuclei also undergo a migration towards the micropylar pole until in close proximity with the egg cell. Subsequently, the two haploid central cell nuclei fuse to generate a diploid central cell nucleus (see Chapter 1 for a detailed description; [184]). As the synergid cells mature, a filiform apparatus develops at the micropylar end of each synergid. Ultrastructural analysis of this enlarged cell wall structure revealed an intricate system of cell wall, membrane and cytoplasmic projections that is also known to accumulate

callose [165-166, 185]. The synergid cells express pollen tube reception regulators FER, LRE and NTA, with their respective subcellular locations being crucial to control this process (see section 4.2.7; [69-70]).

The female gametophyte structure of *herk1 anj* ovules, and in particular, the synergid cells' structure was studied to identify possible morphological defects that could explain the pollen tube overgrowth phenotype. First, the structure and cellular organisation of the mature female gametophyte was analysed in *herk1 anj* ovules from stage 14 flowers using Christensen's confocal microscopy method [120]. Analysis of mature ovules of *herk1 anj* revealed no differences in the structure of the female gametophyte compared with WT Col-0 as all components were present in the expected orientation and with indistinguishable morphology (Figure 4.8A).

Second, competency of *herk1 anj* synergid cells to express the only downstream component of the pollen tube reception pathway identified to date, NTA, was tested with the transcriptional reporter pNTA>>TdTomato (kindly provided by M. Bayer; Max Planck Institute for Developmental Biology, Tübingen, Germany). Multiple T1 transformants were selected and ovules from stage 14 flowers dissected for analysis using epifluorescence microscopy. Nuclear TdTomato fluorescence was observed in *herk1 anj* female gametophytes in the nuclei of both synergid cells, indicating that the *herk1 anj* mutation does not impair the synergid cells' competency to transcribe the downstream regulator NTA (Figure 4.8B). Finally, callose deposition at the filiform apparatus was examined with SR2200 staining in dissected mature live ovules. Epifluorescence microscopy imaging of the stained ovules revealed no qualitative differences in callose accumulation between WT Col-0 and *herk1 anj* mature ovules, suggesting this process is not impaired in the *herk1 anj* mutant background (Figure 4.8C).

4.2.5 Production of ROS in the female gametophyte of *herk1 anj* plants

ROS production has a central role in regulating reproduction as its homeostasis is key in ensuring pollen tube growth stability as well as intergametophytic communications during pollen tube reception in the ovule. Pollen tube tip growth relies on constant, tip-focused production of ROS by the membrane NADPH oxidases Rboh H/J that is thought to trigger Ca^{2+} mobilisation to maintain a positive feedback loop [79, 186-187].

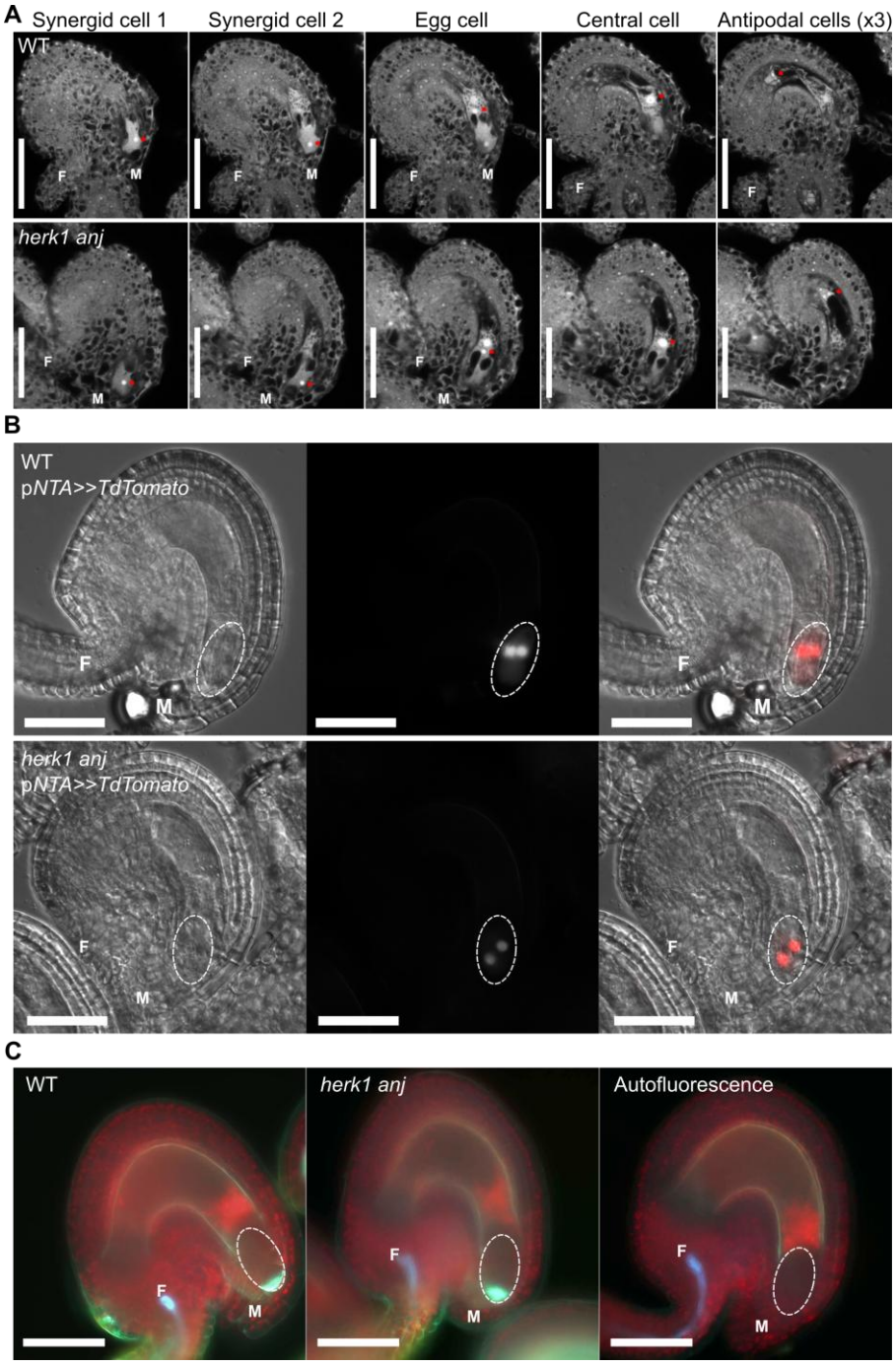

Figure 4.8 Structure of the female gametophyte in *herk1 anj* plants. A, series of consecutive z-planes of representative mature ovules from WT Col-0 and *herk1 anj* displaying normal female gametophyte structure. Ovaries from unpollinated stage 14 flowers were dissected and ovules exposed by removing the ovary walls. Dissected ovaries were fixed and cleared as per [120]. Red asterisks mark the nuclei of each component of the mature female gametophyte. **B**, representative DIC and corresponding fluorescence and merged images of mature ovules from WT and *herk1 anj* T1 plants expressing *pNTA>>TdTomato* displaying accumulation of TdTomato in the nucleus of each synergid cell. **C**, representative images of mature ovules stained with SR2200 displaying accumulation of callose at the filiform apparatus (white fluorescence). Background autofluorescence of an unstained ovule can be seen in the right panel. Scale bars = 50 µm. M, micropyle. F, funiculus. Dashed lines delineate the synergid cells area of the ovule.

Conversely, exogenous ROS induces a Ca^{2+} influx peak at the pollen tube tip that results in pollen tube burst in *in vitro* assays [68]. ROS have been described to accumulate at the synergid cell region of mature fertile ovules in a FER and LRE-dependent manner [68]. Pharmacological depletion of ROS from the female gametophyte during pollen tube reception results in pollen tube overgrowth in WT ovules [68], further supporting the link between ROS and pollen tube burst. Due to the absence of ovular ROS production and the pollen tube overgrowth phenotype displayed in *fer* and *lre* mutants, a link between ovular ROS accumulation and pollen tube termination was established [68].

Characterisation of ovular ROS production in *herk1 anj* was pursued to shed light onto the regulatory roles of HERK1 and ANJ in the pollen tube reception process as well as to gather evidence of their positioning within the synergid cell signalling pathway. To this end, a H_2DCF-DA ROS staining protocol was set up to interrogate ROS production in dissected ovules based on Duan and colleagues report [68]. Briefly, ovules from unpollinated mature carpels were exposed under a dissection microscope and immediately transferred to staining solution, incubated for 15 minutes, washed several times for 5 minutes and subsequently imaged with epifluorescence microscopy. Ovules from six carpels per line were categorised depending on the H_2DCF-DA signal at the micropyle as assessed by visual examination (no signal, low, moderate or high; Figure 4.9A). First, ovules from stage 14 flowers were analysed as they were reported to present high levels of ovular ROS production in WT [68]. *fer-4* and *lre-5* ovules were analysed in parallel to *herk1 anj* as negative controls for ROS production. A severe reduction in the proportion of ROS-positive ovules was observed in *fer-4*, while *herk1 anj* and *lre-5* were found to display a less marked but significant reduction in ROS production when compared to WT Col-0 (Figure 4.9B).

Flower stages are defined by relative comparison of flower features; for instance, stage 14 flowers are those in which anthesis has recently occurred, anthers pigmentation is turning yellow, are still located below the stigma and have not yet dehisced. Previous studies found correlations between the morphological flower stage and the stage of development of their respective ovules, so flower stage could be used as a proxy for ovular development [188], the direct assessment of which is more time consuming and destructive [120]. Notably, flower development coordination is highly variable between different growth conditions and even within one inflorescence at different stages of the inflorescence growth. It is therefore crucial to choose a particular stage of plant growth and to verify the correspondence between flower stage and ovular development under

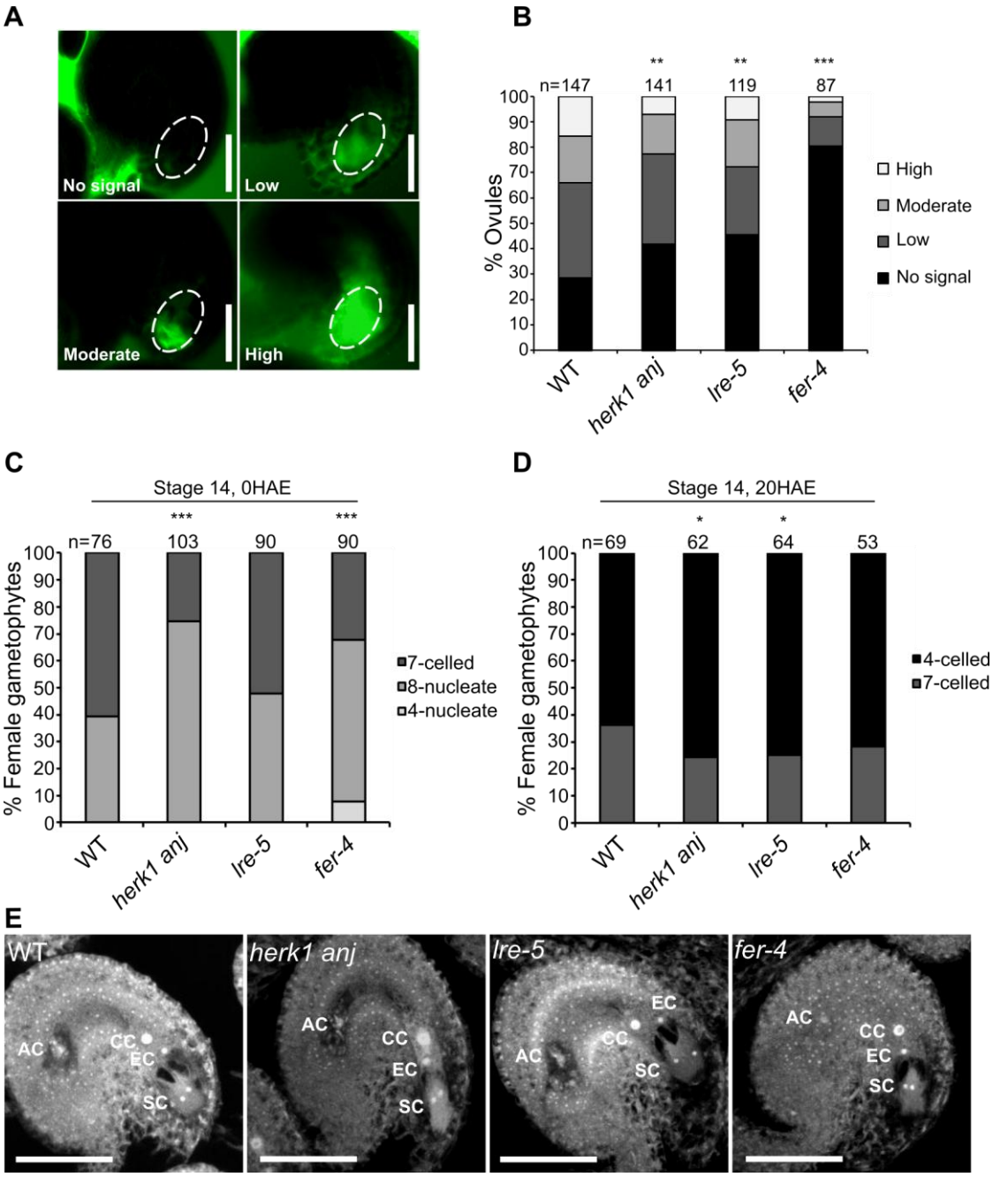

Figure 4.9 H_2DCF-DA staining of ovular ROS in *herk1 anj*, *lre-5* and *fer-4* in stage 14 flowers and female gametophyte structure at 0 and 20 hours after emasculation. A, representative images of ovular ROS production from each category applied in this study. Scale bars = 25 µm. Dashed lines delineate the synergid cells area. **B**, quantification of ROS production in the synergid cell area of WT Col-0, *herk1 anj*, *lre-5* and *fer-4* ovules from stage 14 flowers. Categories listed in the legend relate to A. Ovules analysed from six siliques per line. ** p<0.01; *** p<0.001 (χ-square tests). **C** and **D**, Female gametophyte developmental stage in ovules from stage 14 flowers in WT, *herk1 anj*, *lre-5* and *fer-4* as assessed by confocal microscopy at 0 and 20 hours after emasculation, respectively. Ovules analysed from five siliques per line. * p<0.05 ; *** p<0.001 (χ-square tests). **E**, representative images of the mature female gametophyte in WT, *herk1 anj*, *lre-5* and *fer-4* ovules showing no major defects in its development as assessed by confocal microscopy as per [120]. Images are maximum intensity projections across multiple z-planes from one representative ovule per genotype. Scale bars = 50 µm. AC, antipodal cells; CC, central cell; EC, egg cell; SC, synergid cells.

the particular growth conditions used in each experiment. Thus, ovules from stage 14 flowers were analysed with Christensen's protocol as per the female gametophyte structure analysis (see section 4.2.4; [120]), and assigned to the different stages of ovule development (Figure 4.9C). A large proportion of ovules in pre-fertile stages of development (eight-nucleate and younger) were found in all genotypes, with *herk1 anj* and *fer-4* displaying a small delay in comparison to WT (Figure 4.9C). Aiming to allow all ovules to reach maturity, stage 14 flowers were emasculated and ovule development was assessed 20 hours later. At 20 hours after emasculation, all ovules analysed had reached maturity in all genotypes tested (7-celled or 4-celled female gametophytes; Figure 4.9D), indicating that 20 hours after emasculation of stage 14 flowers represents a more meaningful time point to study ROS production at mature, fertile female gametophytes under our particular conditions.

Consequently, staining of ovular ROS was repeated at 20 hours after emasculation and, interestingly, while the reduction in ROS production was recapitulated in *fer-4* ovules, *herk1 anj* and *lre-5* ovules produced normal levels of ROS (Figure 4.10A-B). Pollen tube overgrowth was found to occur at the same rate in *herk1 anj*, *lre-5* and *fer-4* under these particular conditions by analysis of aniline blue stained pollen tubes in carpels hand pollinated 20 hours after emasculation (Figure 4.10C), indicating that normal levels of ROS accumulation in *herk1 anj* and *lre-5* are not sufficient to rescue the reproductive defect. In the light of this results it seems plausible that HERK1, ANJ and LRE are not essential for the accumulation of ROS at the synergid cells prior to pollen tube arrival. It is nevertheless possible that HERK1, ANJ and LRE may influence ROS homeostasis during male-female gametophyte communication after pollen tube arrival; however this hypothesis cannot be tested with the *in vitro* system used in the experiments presented here.

These results suggest that only FER is required for ROS accumulation in the synergid cells prior to pollen tube arrival, contrary to previous evidence pointing at a role for LRE in controlling this process as well [68]. One possible explanation is that LRE control of ROS production in ovules may only take place under certain environmental conditions. ROS experiments at 0 and 20 hours after emasculation were repeated three times with similar results, indicating that the method followed in the present work is sufficiently robust to consistently detect large reductions in ROS production as those found in *fer-4* mutants. It is likely that H_2DCF-DA-based assays are not sensitive enough to detect smaller reductions that could take place in *herk1 anj* and *lre-5*. The use of genetically-encoded ROS reporters and live imaging techniques in fertilisation impaired mutants

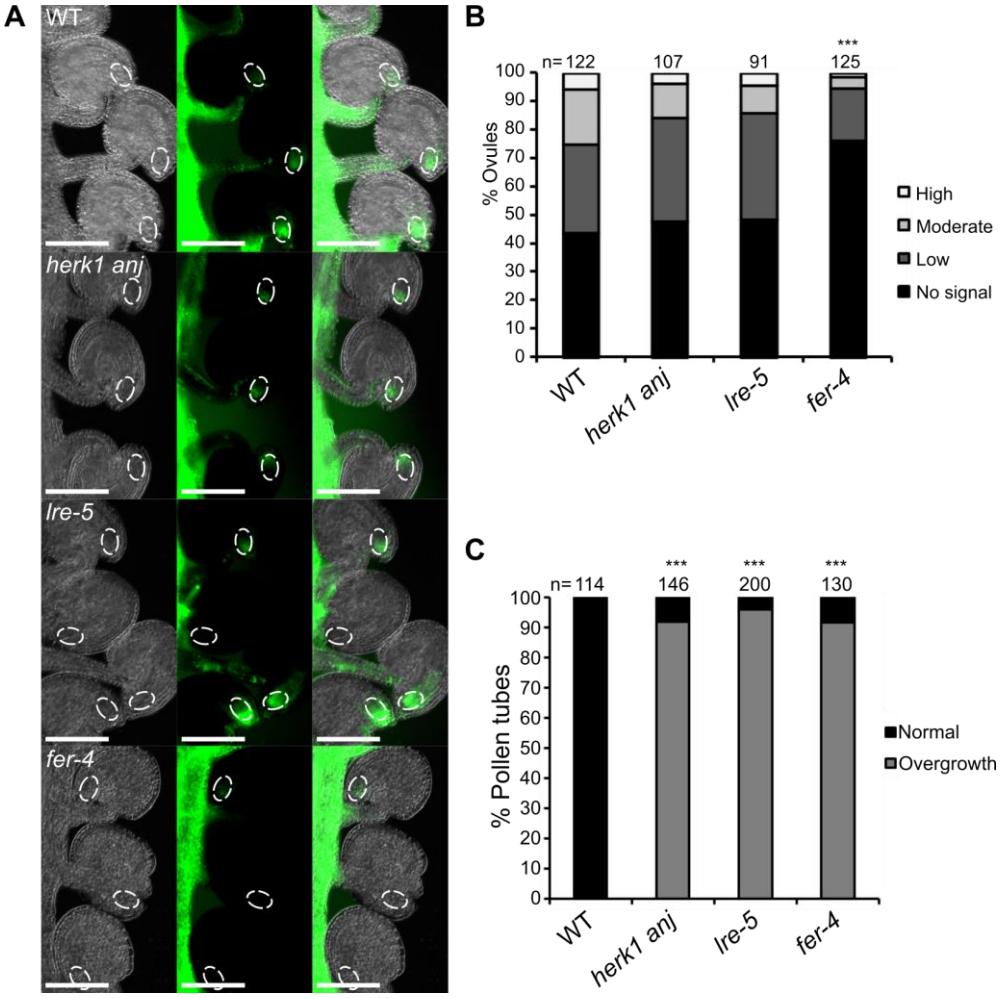

Figure 4.10 Ovular ROS production in *herk1 anj*, *lre-5* and *fer-4* mature ovules and pollen tube overgrowth defect 20 hours after emasculation. A, representative images of H_2DCF-DA staining of ROS in dissected ovaries from WT Col-0, *herk1 anj*, *lre-5* and *fer-4* 20 hours after emasculation of stage 14 flowers. Left to right: DIC, H_2DCF-DA fluorescence and merged images. Scale bars = 100 µm. Dashed lines delineate the synergid cells area of the ovule. **B**, quantification of ROS production in the synergid cell area of ovules in WT, *herk1 anj*, *lre-5* and *fer-4* 20 hours after emasculation. Categories in the legend relate to Figure 4.9A. Ovules dissected from at least five siliques per line. *** $p<0.001$ (χ-square tests). **C**, quantification of normal pollen tube reception events (black bars) and pollen tube overgrowth (grey bars) in carpels manually self-pollinated 20 hours after emasculation. Fertilisation events counted from at least three siliques per line. *** $p<0.001$ (χ-square tests).

would provide a more detailed picture of the contribution of each element of this signalling pathway to ROS production during pollen tube reception. Genetic reporters *p35S::cHyper* and *pUBQ10::GRX-roGFP2* were transformed into Col-0 wild-type and *herk1 anj* plants to attempt to visualise ROS and redox status live during pollen tube reception, respectively (kindly provided by Alex Costa, University of Milan; [189-190]). Unfortunately these reporter constructs did not present clear expression in the synergid cells precluding any further experiments in the context of pollen tube reception with said lines.

4.2.6 Localisation of pollen tube reception effectors in *herk1 anj* synergid cells

Specific subcellular localisation in the synergid cells of FER, LRE and NTA is a requirement to ensure proper regulation of the pollen tube reception process. Whereas FER and LRE are membrane proteins localised at the filiform apparatus of the synergid cell [60, 71, 183], NTA localises in endomembrane compartments throughout the synergid cell cytoplasm prior to pollen tube arrival [69]. A dual role as FER co-receptor and chaperone has been proposed for LRE based on protein interaction experiments and observation of FER mislocalisation in *lre* mutants in which FER-GFP fluorescence could be seen throughout the entire synergid cytoplasm instead of accumulating in the filiform apparatus in approximately 50% of the ovules [70].

Due to the close relationship of FER, HERK1 and ANJ as receptors of the CrRLK1L family, their overlapping subcellular localisation in the synergid cells, and their involvement in pollen tube reception control, a scenario where subcellular localisation of HERK1 and ANJ would be controlled in a similar manner arose as a strong hypothesis. The effects of the *herk1* and *anj* mutations on the localisation of the already described effectors of pollen tube reception and the role of LRE in controlling HERK1 and ANJ localisation in addition to FER were tested with fluorescent translational reporters. Constructs *pFER::HERK1-GFP*, *pANJ::ANJ-GFP* (used in the complementation experiments), *pFER::FER-GFP*, *pLRE::LRE-Citrine* and *pMYB98::NTA-GFP* were transformed into the WT Col-0, *herk1 anj* and *lre-5* backgrounds. The *pFER::FER-GFP* reporter construct was generated following the same cloning strategy used to produce *pANJ::ANJ-GFP* (Section 4.2.3), whereas *pLRE::LRE-Citrine* and *pMYB98::NTA-GFP* were kindly provided by U. Grossniklaus (University of Zurich; [165]) and S. Kessler (Purdue University; [167]), respectively. Transgenic lines were obtained through the floral dip method and T1 lines were analysed for each construct and background [106]. Analysis of mature, virgin *herk1 anj* ovules revealed no defects in the subcellular localisation of FER, LRE or NTA (Figure 4.11), indicating that the pollen tube overgrowth defect in *herk1 anj* is not caused by mislocalisation of these effectors. Conversely, *lre-5* did not impair HERK1 or ANJ accumulation in the filiform apparatus or NTA distribution throughout the synergid cytoplasm (Figure 4.11). Suprisingly, the *lre-5* mutation also did not modify FER localisation in the synergid cells and fluorescence was observed at the filiform apparatus area of the synergids in contrast to previous reports (Figure 4.11; ovules from three siliques per transformant and five independent transformants were

observed; [70]), suggesting LRE role as FER chaperone could be dependent on environmental factors.

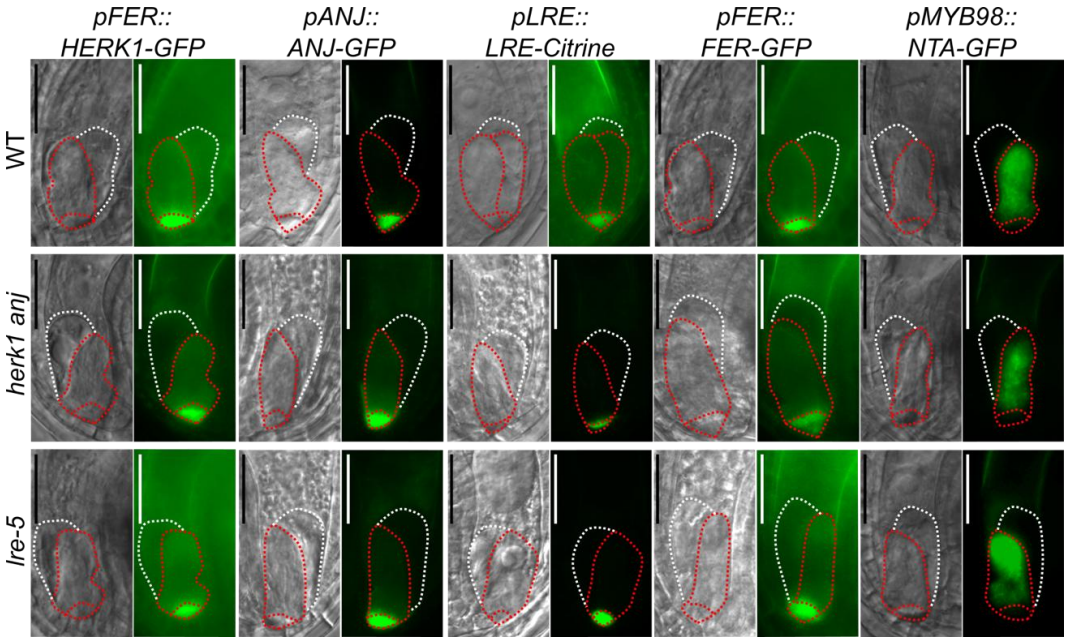

Figure 4.11 Synergid cell subcellular localisation of the pollen tube reception effectors is unaffected in *herk1 anj* plants prior to pollination. Representative DIC and corresponding fluorescence images of the synergid cells of mature ovules expressing *pFER::HERK1-GFP*, *pANJ::ANJ-GFP*, *pLRE-LRE-Citrine*, *pFER::FER-GFP* and *pMYB98::NTA-GFP* in WT Col-0, *herk1 anj* and *lre-5* plants. White dotted lines delineate the egg cell. Red dotted lines delineate the synergid cells and filiform apparatus, respectively. Scale bars = 25 µm.

4.2.7 NTA relocalisation after pollen tube arrival

Downstream of the receptors FER and LRE in the control of pollen tube reception, NTA modulates the amplitude of the Ca^{2+} signatures that take place in the synergid cells as the pollen tube grows along the receptive synergid [72]. Interestingly, upon pollen tube arrival at the female gametophyte, NTA's cellular distribution changes as it accumulates in the filiform apparatus [69]. NTA relocalisation depends on functional FER in the synergid cell, suggesting NTA acts downstream of FER in the pollen tube reception pathway [69], although clarification of the biological meaning of NTA relocalisation awaits further investigation.

NTA relocalisation upon pollen tube arrival in *herk1 anj* was tested using fluorescent translational reporters of NTA expressed specifically in the synergid cells under the synergid cell-specific transcription factor MYB98 promoter and timed pollinations. Plants carrying the *pMYB98::NTA-GFP* reporter construct were selected and stage 14 flowers were emasculated and allowed to mature for an additional 24 hours.

Emasculated flowers were hand pollinated and ovules were dissected after eight hours to allow pollen tubes to target the NTA-GFP-expressing ovules. Staining of callose in live ovules with SR2200 was used to visualise pollen tubes and the filiform apparatus. A shift in the fluorescence towards the filiform apparatus after pollen tube arrival could be recapitulated in WT Col-0 ovules [69], however this response was absent in most *herk1 anj* ovules observed (Figure 4.12A). Relative fluorescence intensity across the length of the synergid cell of ovules that had received a pollen tube was also recorded. A significant decrease in relative intensity was only registered in WT, whereas *herk1 anj* relative intensity stayed at the same level as that registered for virgin ovules (Figure 4.12B). These results suggest that similar to FER, HERK1 and ANJ could be required for and therefore acting upstream of the relocalisation of NTA upon pollen tube arrival at the female gametophyte.

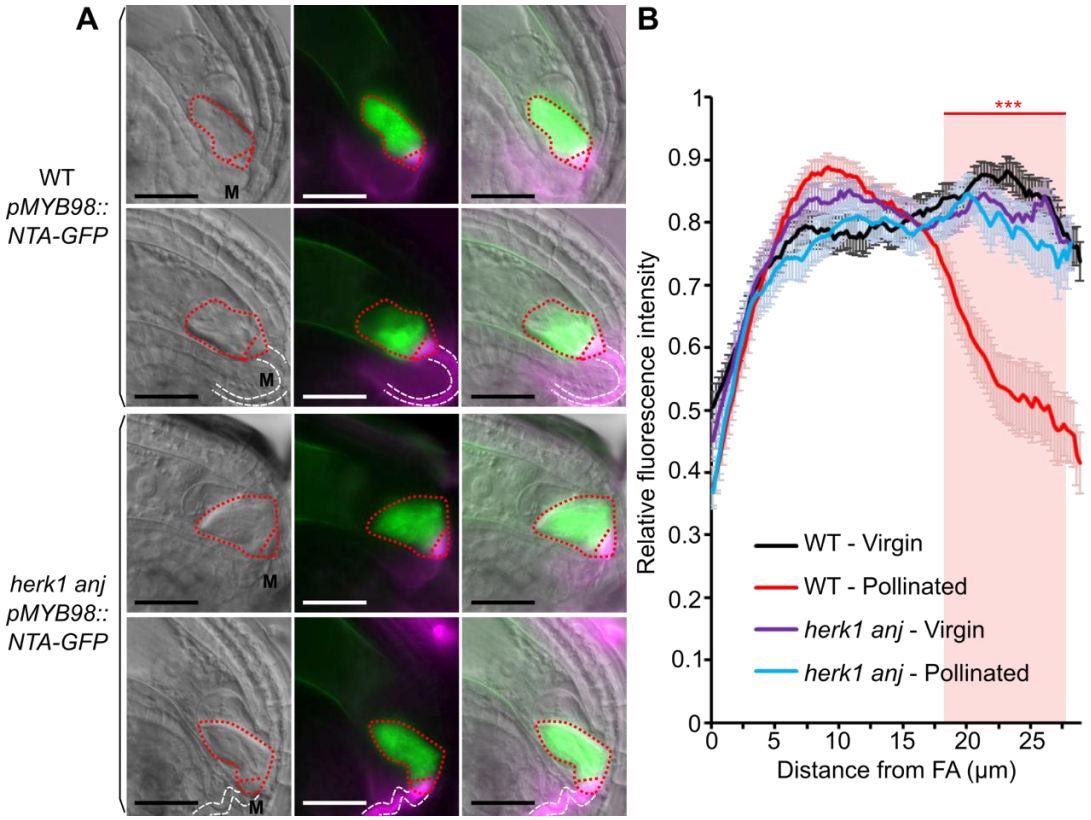

Figure 4.12 NTA relocalisation upon pollen tube arrival is absent in *herk1 anj* mutants. A, Localisation of NTA in the synergid cell before and after pollen tube arrival (upper and lower panels, respectively) in WT Col-0 and *herk1 anj* mature ovules expressing pMYB98::NTA-GFP. Left to right, panels correspond to representative DIC, combined fluorescence of GFP and SR2200 stained callose and merged images. Scale bars = 25 µm. Red dotted lines delineate the synergid cell and filiform appratus. White dotted lines delineate the pollen tube. M, micropyle. **B**, quantification of the profile of relative fluorescence along the synergid cells of WT and *herk1 anj* ovules, before (virgin) and after (pollinated) pollen arrival. Data shown are means ± SEM, n = 25. *** p<0.001 (Student's *t*-test). FA, filiform apparatus.

Additionally, detailed microscopic examination of NTA-GFP in WT Col-0 synergid cells after pollen tube arrival did not show a clear relocalisation to the filiform apparatus as commonly interpreted from previous reports [69]. Instead, pollen tube reception appeared to trigger NTA-GFP redistribution within the cytoplasmic region towards the filiform apparatus (Figure 4.13). These experiments were repeated using a reporter line with fluorescently tagged pollen tubes as male parent and similar results were obtained (data not shown). A more detailed description of this process using confocal microscopy and live imaging of the pollen tube reception event would be invaluable to clarify the exact timing of NTA relocalisation and the extent of the overlap with the filiform apparatus.

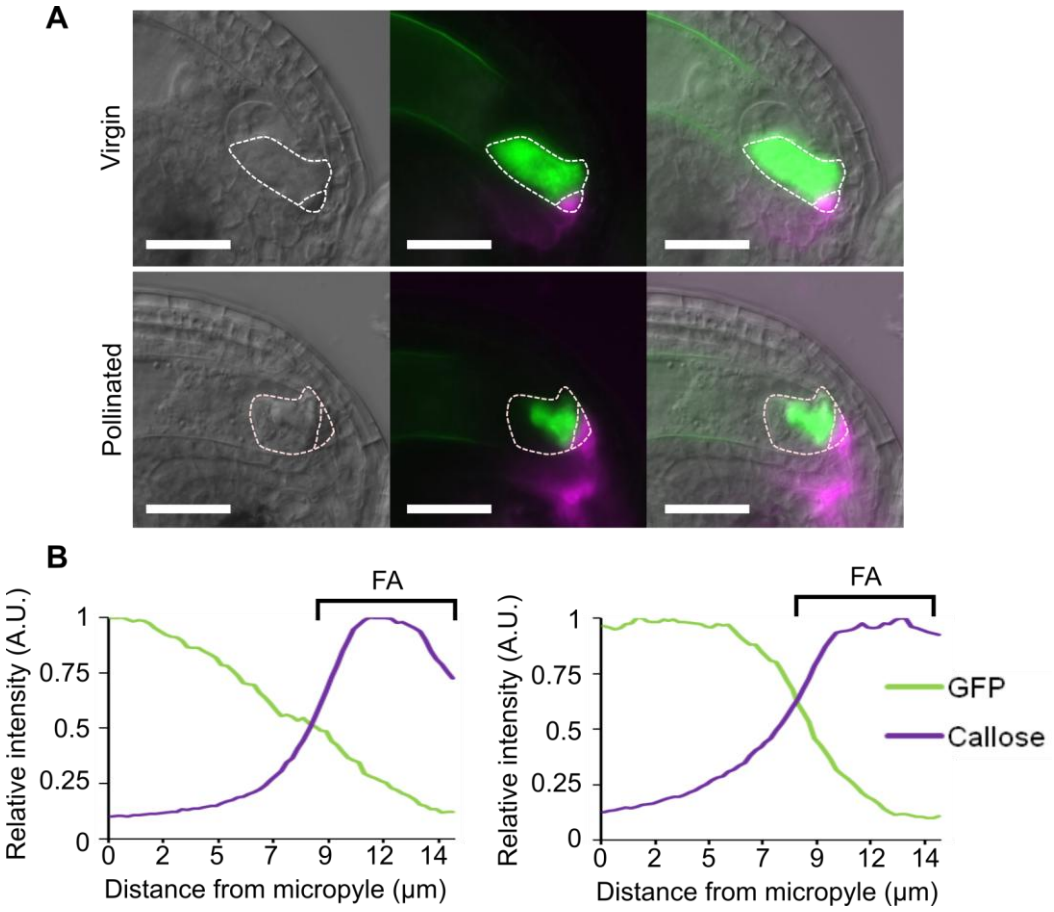

Figure 4.13 NTA relocalisation is excluded from the filiform apparatus. A, representative DIC, fluorescence and merged images of the localisation of NTA-GFP in the synergid cells of WT Col-0 virgin and fertilised ovules (upper and lower panels, respectively). SR2200 staining of callose in live ovules was used to identify ovules that had received a pollen tube. Scale bars = 25 µm. White dotted lines delineate the synergid cells and filiform apparatus as per the corresponding DIC image. **B**, relative fluorescence intensity profiles for the GFP and callose channels of the filiform apparatus and adjacent synergid cell cytoplasmic region in virgin and fertilised ovules presented in A (left and right panels, respectively). Profiles show no qualitative increase in the GFP fluorescence in the filiform apparatus region after pollen tube reception.

4.2.8 Kinase-dead versions of HERK1 and ANJ rescue *herk1 anj* reproductive phenotype

Activation of downstream signalling upon sensing of external cues by RLKs often relies on the catalytic activity of their intracellular kinase domain. Kinase activity results in the phosphorylation of direct interaction partners of the cytosolic kinase domain which often involve other RLKs, cytoplasmic receptor kinases and mitogen-activated protein kinases among many others [18, 191]. The kinase domain of some RLKs is not catalytically active and, in other cases, the kinase activity of catalytically-active RLKs is not required for particular processes they regulate [57]. Studying whether the kinase activity is required is an important step towards understanding how an RLK regulates the process of interest. To this end, kinase-dead (KD) versions of HERK1 and ANJ were cloned in the constructs used previously in the complementation experiments (*pHERK1::HERK1* and *pANJ::ANJ-GFP*; section 4.2.2) and the resulting constructs were introduced in *herk1 anj* mutants to test rescue of the fertility phenotype. HERK1-KD and ANJ-KD were generated by PCR-based targeted mutagenesis of the activation loop residues D606N/K608R of ANJ and D609N/K611R of HERK1 [110].

Complementation of the gametophytic fertility defect in *herk1 anj* in the T1 generation in plants with a single insertion of the complementation construct would result in a 50% recovery of the reproductive phenotype. Approximately 50% of pollen tube reception events were normal in T1 hemizygous *herk1 anj* plants carrying either *pHERK1:HERK1-KD* or *pANJ::ANJ-KD-GFP* as analysed by aniline blue staining of pollen tubes in self pollinated flowers (Figure 4.14A). Furthermore, isolated T2 homozygous plants displayed full complementation of the reproductive phenotype to WT levels in both HERK1-KD and ANJ-KD-GFP expressing plants, which rendered almost complete absence of pollen tube overgrowth events and siliques full of developing seeds (Figure 4.14A-B). These results suggest that the kinase activity of HERK1 and ANJ is not essential for their role in controlling pollen tube reception at the synergid cells, similarly to what has been described for FER previously [192].

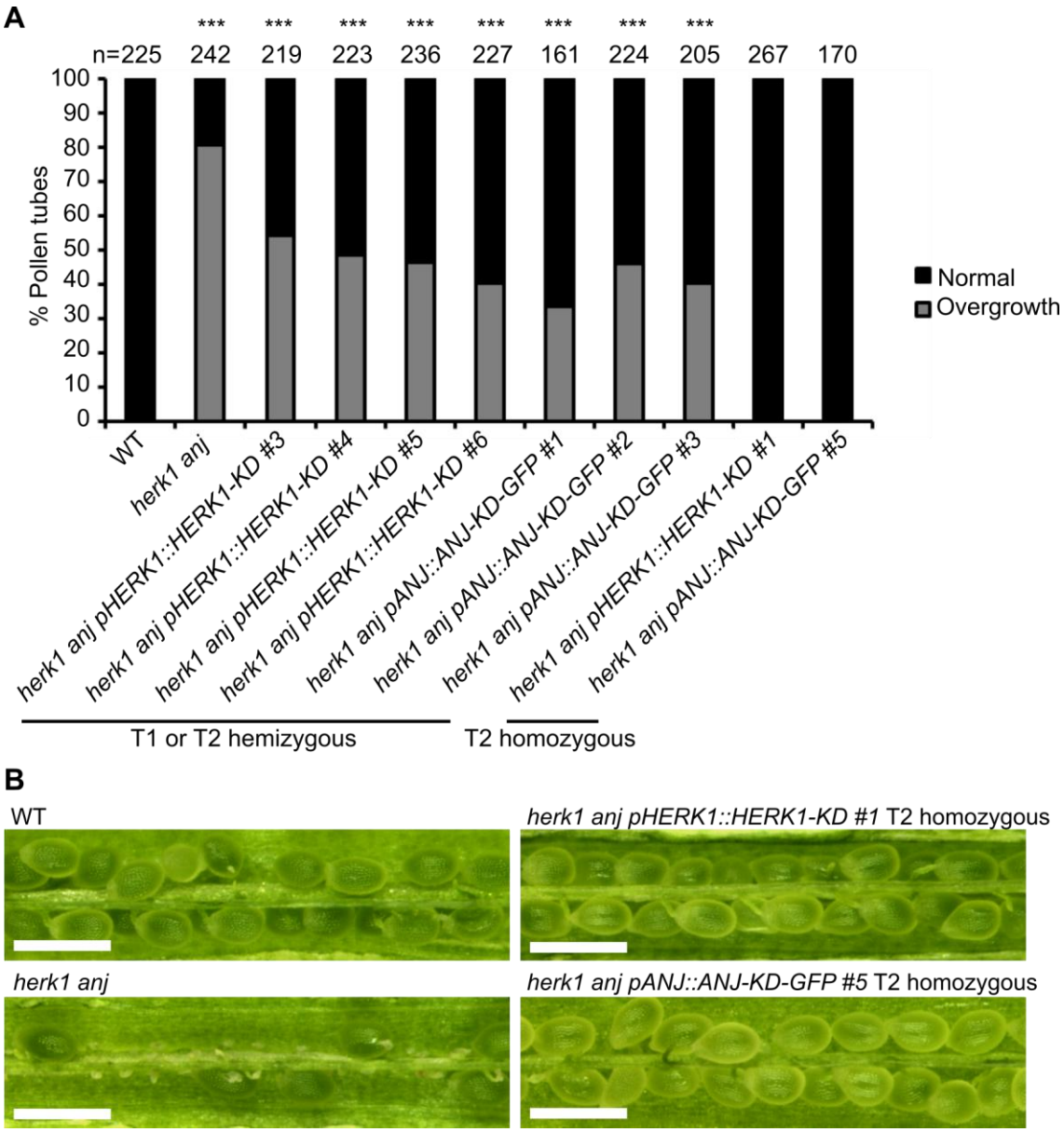

Figure 4.14 Kinase-dead HERK1 and ANJ rescue the pollen tube overgrowth and seed set phenotypes of *herk1 anj*. A, quantification of normal pollen tube reception events (black bars) and pollen tube overgrowth (grey bars) in WT Col-0, *herk1 anj* and T1 or T2 *herk1 anj* plants expressing *pHERK1::HERK1-KD* or *pANJ::ANJ-KD-GFP*. At least three self-pollinated siliques per line were analysed. *** p<0.001 (χ-square tests). **B**, representative photographs of developing seeds in dissected self-pollinated siliques from WT, *herk1 anj* and T2 homozygous *herk1 anj* plants expressing *pHERK1::HERK1-KD* or *pANJ::ANJ-KD-GFP* showing full complementation of the seed production phenotype of *herk1 anj*. Scale bars = 500 µm.

4.2.9 HERK1 and ANJ interact with LRE

LRE and its homolog LORELEI-LIKE GPI-ANCHORED PROTEIN 1 (LLG1) mediate processes like fertilisation and pathogen responses with their RLK interaction partners FER, FLAGELLIN SENSING 2 (FLS2) and EF-TU RECEPTOR (EFR; [70, 89]). LRE and LLG1 are attached to the apoplastic side of the plasma membrane through a GPI anchor and interact with the extracellular juxtamembrane region of their respective RLK interactors [70, 89]. Despite the elusive proof of direct binding between LRE and LLG1 to the signals sensed by their interactor RLKs, evidence suggests these GPI-anchored proteins are required for sensing of extracellular cues or stabilisation of the RLK at the plasma membrane, as i) mutants in LRE or LLG1 display phenotypically similar defects as mutants in their respective RLK co-receptors, and ii) plasma membrane localisation of the co-receptor is altered in the absence of LRE or LLG1 [70-71, 89, 183, 193]. Based on the latter, LRE and LLG1 are regarded as chaperones that ensure proper delivery of the RLK to the plasma membrane [70].

The similarity of the reproductive phenotype between *herk1 anj* and *lre* mutants, overlapping cellular localisation of HERK1, ANJ and LRE in the synergid cells and the homology between HERK1, ANJ and LRE co-receptor FER, made the possiblility of receptor complexes of HERK1-LRE and ANJ-LRE an attractive scenario to test. A yeast two hybrid (Y2H) system was chosen to test direct interaction *in vitro* between the extracellular juxtamembrane regions of HERK1 and ANJ (HERK1exJM, ANJexJM, respectively; as per [70]) and LRE (amino acids 23-138; as per [70]). Interactions were detected between HERK1exJM and LRE(23-138), as well as between ANJexJM and LRE(23-138), suggesting the respective proteins might also interact physically in the synergid cell of Arabidopsis (Figure 4.15A). A co-immunoprecipitation (CoIP) assay was chosen to verify these interactions *in planta*. In brief, tagged versions of the proteins of interest were transiently co-expressed in *Nicotiana benthamiana* leaves following *Agrobacterium* infiltration, the proteins were subsequently extracted and interactions detected based on their capacity to co-precipitate. To this end, over-expression constructs *p35S::HERK1-GFP, p35S::HERK1-MYC*, *p35S::ANJ-GFP*, *p35S::ANJ-MYC* and *p35S::HA-LRE* constructs were generated.

Several difficulties were encountered in the use of these constructs to test co-immunoprecipitation: first, the *ANJ* over-expression constructs yielded undetectable expression of ANJ-GFP or ANJ-MYC in *Nicotiana* leaves, which therefore hindered testing of the ANJ-LRE interaction *in planta*. Second, the HERK1-tag

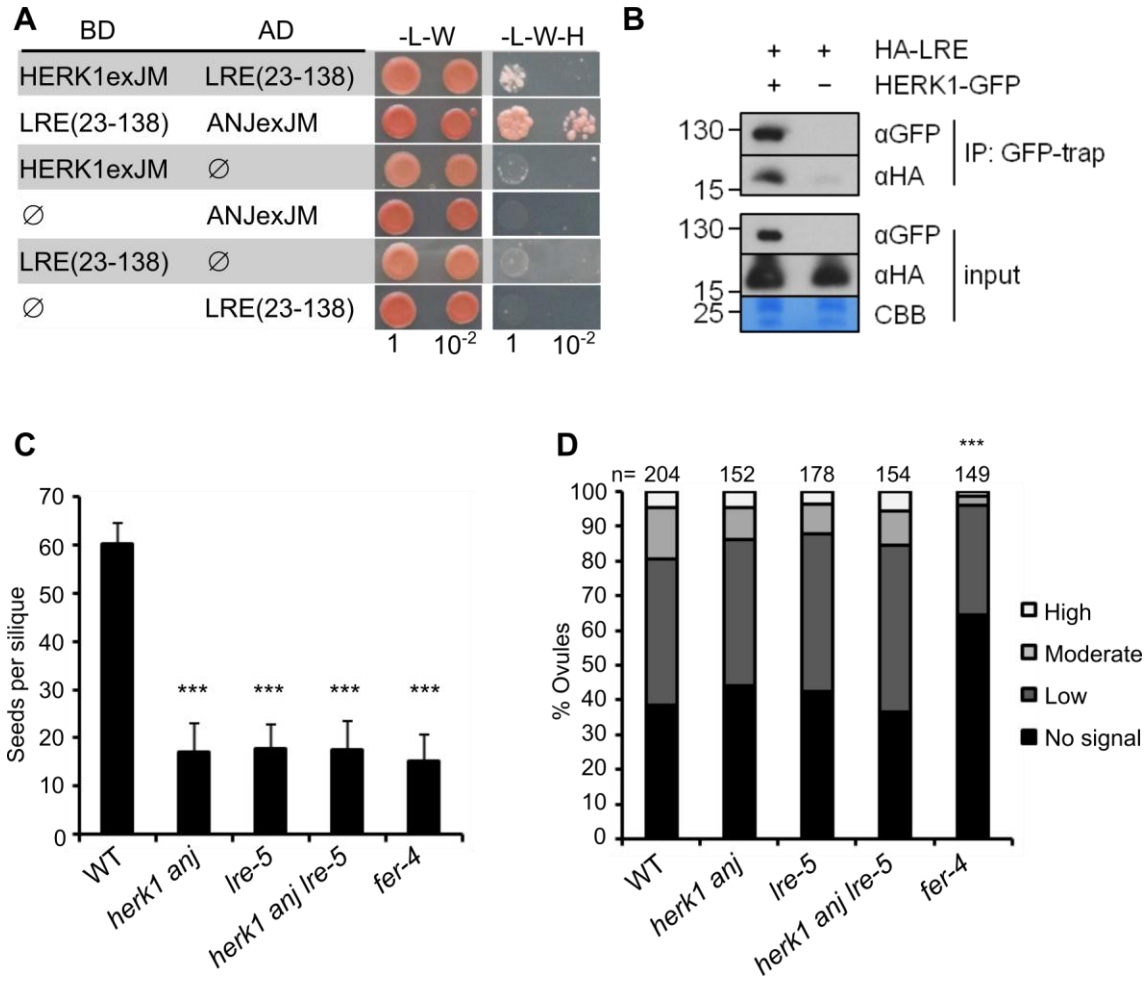

Figure 4.15 HERK1 and ANJ interact with LRE, and seed set and ROS production in triple mutant *herk1 anj lre-5*. **A**, yeast two hybrid assays of the extracellular juxtamembrane domains of HERK1 and ANJ (HERK1exJM and ANJexJM, respectively) with LRE (residues 23-138; signal peptide and C-terminal domains excluded). Ø represents negative controls where no sequence was cloned into the activating domain (AD) or DNA-binding domain (BD) constructs. -L-W-H, growth medium depleted of leucine (-L), tryptophan (-W) and histidine (-H). **B**, co-immunoprecipitation of HA-LRE with HERK1-GFP following 2 days of transient expression in *N. benthamiana* leaves. Numbers indicate MW marker sizes in kDa. Assays were performed twice with similar results. **C**, quantification of developing seeds per silique in WT Col-0, *herk1 anj*, *lre-5*, *herk1 anj lre-5* and *fer-4* plants. Developing siliques were dissected and photographed under a stereomicroscope. n = 5. Data presented are means ± SD. *** p<0.001 (Student's *t*-test). **D**, quantification of the H_2CDF-DA staining of ROS in ovules from WT Col-0, *herk1 anj*, *lre-5*, *herk1 anj lre-5* and *fer-4* plants at 20 HAE. Categories listed in the legend refer to Figure 4.9A. At least five siliques were analysed per line. *** p<0.001 (χ-square tests).

over-expression constructs resulted in bacterial toxicity when introduced in multiple *Agrobacterium* strains as no colonies harbouring the constructs were recovered. This issue was successfully overcome by expressing HERK1-GFP in *Nicotiana* with the *pFER::HERK1-GFP* construct used in complementation experiments (section 4.2.2) which allowed testing co-immunoprecipitation between LRE and HERK1. HA-LRE co-immunoprecipitated with HERK1-GFP therefore confirming the Y2H results and

indicating that HERK1 and LRE interact *in planta* (Figure 4.15B). A *pFER::ANJ-GFP* construct has also been generated given *pFER* success in expressing HERK1-GFP in *Nicotiana* in order to overcome ANJ-tag expression issues and test co-immunoprecipitation with HA-LRE. Interactions *in planta* between ANJ and LRE are expected based on the strong Y2H interaction and the high degree of homology between HERK1 and ANJ, however these hypotheses await experimental confirmation.

A genetic approach was undertaken to provide complementary evidence of the interaction between HERK1, ANJ and LRE in the reproductive context. A triple homozygous *herk1 anj lre-5* line was generated by crossing the *herk1 anj* and *lre-5* mutant lines. PCR genotyping of the F2 and F3 generations of this cross yielded the identification of a triple homozygous *herk1 anj lre-5* plant in the F3 generation. Phenotyping of this line revealed no additive effect to the seed production phenotype in *herk1 anj lre-5* in comparison to the progenitor lines (Figure 4.15C), supporting a role for these three receptors in the same signalling pathway, possibly acting as co-receptors at the filiform apparatus of the synergid cell based on the protein interaction results. Interestingly, the reduction in fertility in these lines is also comparable to that observed for the *fer-4* mutant when grown in parallel under our conditions (Figure 4.15C). Additionally, ovular ROS production was measured in *herk1 anj lre-5* plants to test whether knocking out multiple effectors of this signalling pathway could lead to a ROS production defect as seen in *fer-4* ovules. *herk1 anj lre-5* mature ovules were found to produce WT levels of ROS in the synergid cell area prior to fertilisation (Figure 4.15D), indicating that ROS production appears to be only FER-dependent under our conditions.

The results presented here suggest that LRE may form receptor complexes with HERK1 and ANJ, similar to what has been described for FER [70]. Tripartite receptor complexes comprising HERK1, LRE and FER or ANJ, LRE and FER therefore arose as an interesting scenario and multiple approaches were put in place to test this hypothesis. First, a biomolecular fluorescent complementation (BiFC) assay was chosen to test the formation of homo- and heterodimers of the CrRLK1Ls HERK1, ANJ and FER in *Nicotiana* leaf epidermal cells following *Agrobacterium*-mediated transient co-expression. Over-expression constructs with *p35S* driven expression of nYFP or cYFP C-terminal-tagged HERK1, ANJ and FER were generated to this end. Reconstitution of the split YFP protein *in planta* is indicative of direct interaction between interaction partners in BiFC assays and it is typically assessed two or three days post-inoculation to allow for protein expression. Unfortunately, all constructs

tested resulted in a strong hypersensitive-like response in *Nicotiana* leaves at three days after inoculation (Figure 4.16A). At two days after infiltration a noticeable hypersensitive response was absent in most inoculated leaves and reconstitution of YFP fluorescence was assessed by examination of the leaf epidermis with epifluorescence microscopy. Noticeably and despite the lack of obvious symptoms of stress in the selected leaves, high levels of autofluorescence were observed in leaves infiltrated with *p35S::CrRLK1L-splitYFP*-harbouring *Agrobacterium*, hindering the observation of YFP fluorescence where present (Figure 4.16B). These observations indicated that i) the over-expression of these CrRLK1Ls in *Nicotiana* following *Agrobacterium* infiltration likely resulted in the activation of cellular signalling pathways that led to cell death and ii) microscopic symptoms were evident at two days after inoculation. Hypothetically, the CrRLK1Ls could be accumulating gradually in the cell before cellular toxicity pathways are activated after a threshold is reached; earlier time points following inoculation were therefore explored. Tracking of YFP fluorescence reconstitution by homodimerisation of IMPAIRED IN BABA-INDUCED DISEASE IMMUNITY 1 (IBI1) was used as a proxy to establish the earliest time point at which the selected expression cassette system yields enough protein expression to detect an interaction (*IBI1 pEarlygate201* and *202* constructs were kindly provided by R. Schwarzenbacher, University of Sheffield). Expression and maturation times of different proteins can vary largely [194], and therefore the use of IBI1 can only be interpreted as a rough estimate to select the temporal window in which to probe YFP fluorescence reconstitution. At 39 hours post infiltration, faint but noticeable YFP fluorescence reconstitution was observed in the IBI1 control samples whereas no fluorescence could be observed for any of the CrRLK1L interactions tested (Figure 4.16C). Small areas of high autofluorescence could be observed in some regions of the inoculated leaves at 39 hours after infiltration indicating that the hypersensitive response was already being triggered (data not shown). This suggested that either i) cell toxicity occurs during early stages of over-expression before interactions between the CrRLK1L members tested could be detected, or ii) there is no interaction between these CrRLK1Ls in this heterologous system. Complementary approaches are currently being undertaken to test interaction between these CrRLK1Ls including co-immunoprecipitation assays following transient expression in *Nicotiana* and a genetic approach aiming to obtain a triple homozygous *herk1 anj fer-4* and quadruple homozygous *herk1 anj fer-4 lre-5* plants, with the goal of characterising genetic interactions between these receptors in the context of fertilisation. Triple homozygous *herk1 anj lre-5* was crossed with *fer-4* and the F2 and F3 generations are currently being genotyped to identify triple and quadruple mutants.

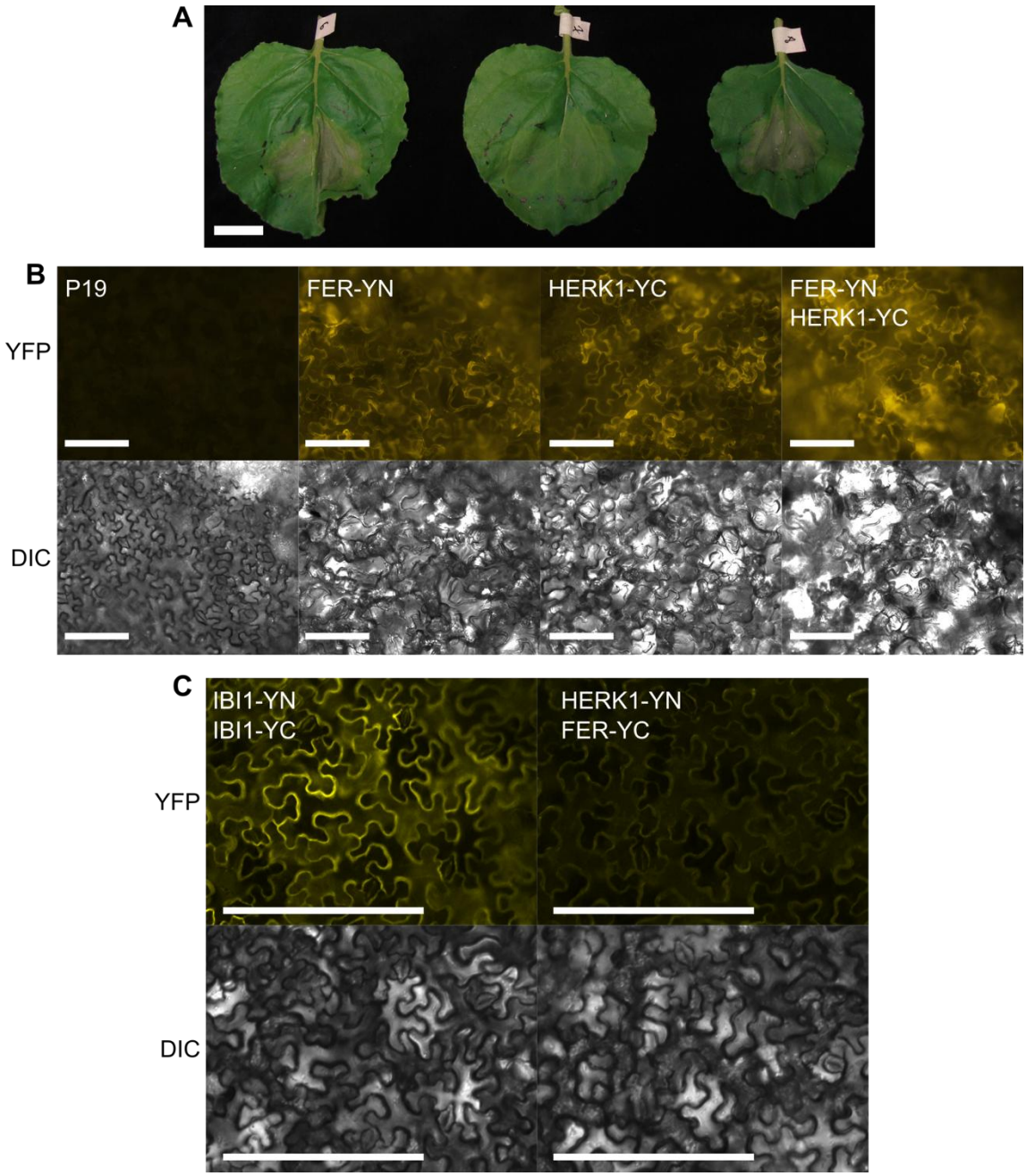

Figure 4.16 Induction of hypersensitive responses following transient over-expression of HERK1, ANJ and FER in BiFC assays. A, photograph of representative *Nicotiana* leaves displaying a hypersensitive response following three days of transient over-expression of *CrRLK1L-split YFP* constructs. Scale bars = 1 cm. **B**, CrRLK1L overexpression-triggered autofluorescence in *Nicotiana* leaves as seen under an epifluorescence microscope. Expression of single *CrRLK1L-split YFP* and their combinations in co-infiltrations triggered epidermal cell disruption and autofluorescence two days after infiltration as seen in the YFP channel and corresponding DIC images (upper and lower panels, respectively). FER-nYFP, HERK1-cYFP and their co-expression are included here as representative examples. Samples infiltrated only with the RNA silencing suppressor P19 were used as controls for background fluorescence. Scale bars = 250 µm. **C**, example of YFP fluorescence reconstitution in IBI1-nYFP/IBI1-cYFP coinfiltrated *Nicotiana* leaves and background levels of autofluorescence seen in the *CrRLK1L-split YFP* 39 hours after infiltration (HERK1-nYFP and FER-cYFP were used as a representative example). Scale bars = 250 µm.

4.2.10 *HERK1* and *ANJ* expression patterns beyond reproduction

Exploring the expression patterns of genes of interest represents an interesting approach to identify candidate regulators of the development of certain organs or structures as expression within the relevant tissue is normally a prerequisite. The reproductive phenotype in *herk1 anj* plants explored in the previous sections of this chapter demonstrates that HERK1 and ANJ execute a redundant control of fertilisation; however, additional roles in development for these CrRLK1Ls are also possible. Publicly available gene expression databases are a useful resource to obtain preliminary information about the expression pattern of genes in different stages of development and upon selected stimuli. The Arabidopsis EFP Browser database reflects a widespread expression pattern for *HERK1* across most tissues and stages of development, except for the pollen, whereas *ANJ* expression appears to be very low, restricted to seeds, flowers, roots and inflorescence stems; and absent from rosette leaves and pollen (http://bar.utoronto.ca/efp/cgi-bin/efpWeb.cgi).

Transcriptional reporter lines *pHERK1::GUS* and *pANJ::GUS* were used to identify interesting expression patterns of these two CrRLK1Ls across multiple organs and stages of plant development including roots, hypocotyl and leaves in young seedlings grown *in vitro*, as well as fully expanded mature rosette leaves and inflorescence stems from plants grown on soil. Analysis of these reporter lines in the T1 and T2 generations led to the identification of characteristic expression patterns for *HERK1* and *ANJ*. Notably, the strength of the *ANJ* promoter appeared to be significantly weaker than that of *HERK1* as an overnight incubation in staining solution was required to obtain qualitatively GUS staining intensities in *pANJ::GUS* reporter lines similar to *pHERK1::GUS* lines after four hours of incubation (data not shown). Overlapping expression patterns identified include trichomes in seedlings and mature plants, root vasculature, pedicels, pistils and junctions between pedicels and inflorescence stems (Figure 4.17). *pHERK1* activity was also detected in leaves and leaf margins in seedlings and mature plants, hypocotyls, root hairs and root tips (Figure 4.17). Conversely, *pANJ::GUS* expression was detected in stomata in pedicels and inflorescence stems and the stigma papillae (Figure 4.17B). These results suggest that HERK1 and ANJ could be executing regulatory functions in multiple tissues in addition to the female gametophyte. Detailed examination of relevant structures and exposure to stress could potentially uncover defects in *herk1 anj* plants and allow the identification of new functions for these two CrRLK1Ls.

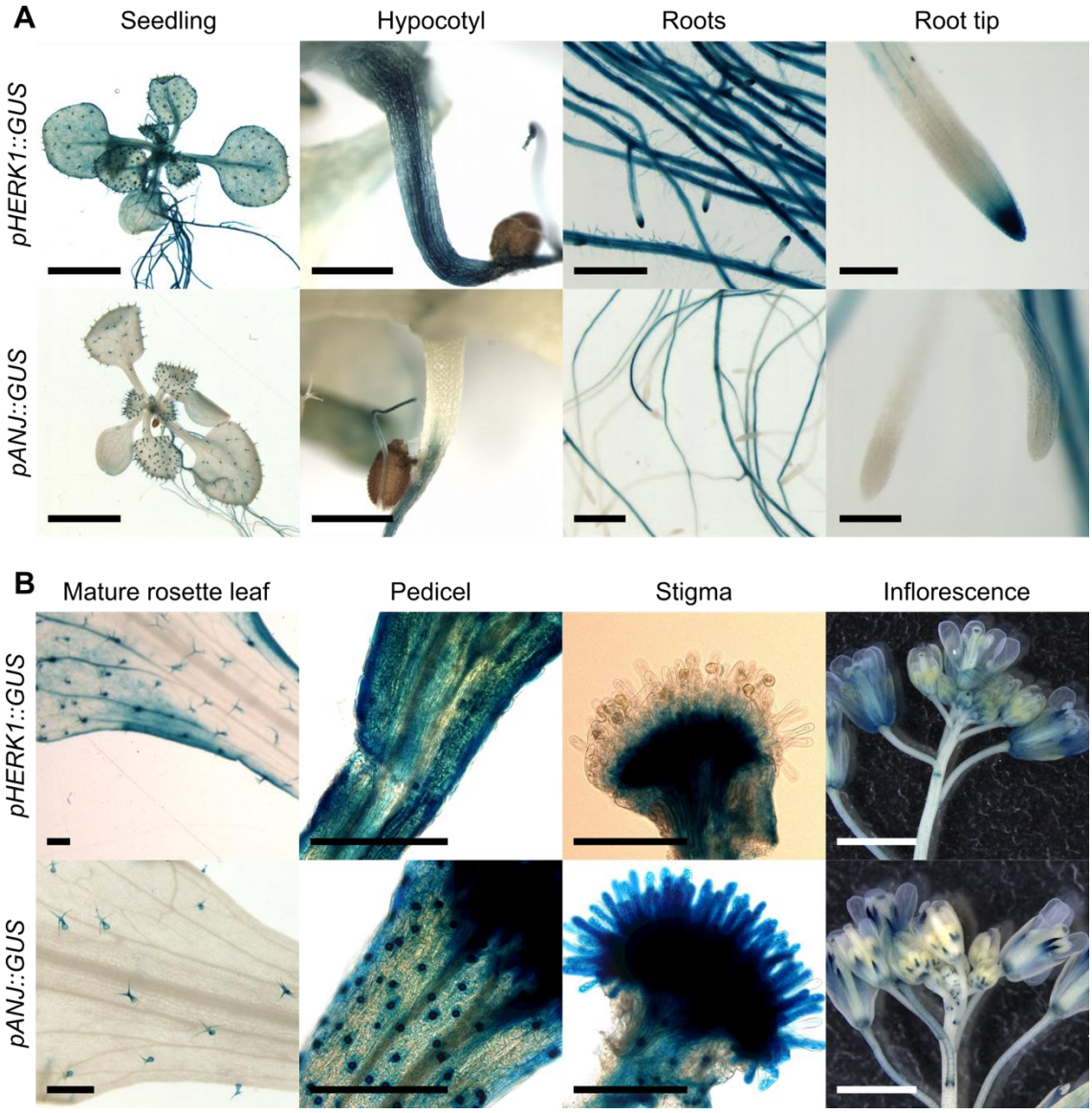

Figure 4.17 Expression pattern of *HERK1* and *ANJ* beyond ovules. A, representative images of the expression pattern of HERK1 and ANJ as indicated by *pHERK1::GUS* and *pANJ::GUS* in seedlings, hypocotyls, roots and root tips after six hours of incubation and subsequent clearing and fixing. GUS activity was examined in at least four T1 lines. Scale bars = 5 mm in seedlings; 1 mm in hypocotyls and roots; 250 µm in root tips. **B**, Expression patterns in mature rosette leaves, pedicels, stigmas and inflorescences after six hours of incubation. GUS activity was examined in at least four T1 lines. Scale bars = 5 mm in rosette leaves; 250 µm in pedicels and stigmas; 2.5 mm in inflorescences.

4.2.11 *herk1 anj* plants produce bigger seeds

In many crops, seeds are the main product and seed size one of the key factors influencing the final yield. Seed size control can originate from several tissues including the seed coat and embryo, as well as from environmental cues. Control on seed size executed by the seed coat represents a form of maternal control as the seed coat develops from the maternal ovular integuments, which surround the female

gametophyte and after fertilisation divide, expand and differentiate to give rise to the seed coat (see [195] for a detailed review of this topic). The CrRLK1L FER is highly expressed in the integument cells after fertilisation and negatively regulates cell expansion of this cell layer, therefore constraining seed growth [196]. These findings explain the larger seed size observed in *fer-4* seeds and the molecular mechanism is thought to involve downstream, FER-mediated RHO OF PLANTS (ROP) GUANINE NUCLEOTIDE EXCHANGE FACTOR 1 (ROPGEF1) signalling [196].

Notably, during the course of the multiple experiments presented in this chapter, seeds from the *herk1 anj* mutant appeared to be bigger in size than WT and the respective single insertion lines *herk1* and *anj* (Figure 4.18A). In order to quantify these differences, seeds were harvested from healthy Col-0 WT, *herk1*, *anj* and *herk1 anj* plants grown in parallel and subsequently allowed to desiccate for a month. Over 50 seeds per line were photographed in triplicate under a steromicroscope and the area of each individual seed was then calculated using the image analysis software ImageJ. Significant differences were assessed with Student's *t* tests and *herk1 anj* seeds were found to be 24±14% larger than WT while *herk1* seeds were 6±10% smaller than WT. Furthermore, seed weight was measured by quantifying the weight of 200 seeds per line in triplicate and statistically significant differences with WT Col-0 were obtained for *herk1 anj* (51±11% heavier) and *anj* (13±2% heavier). Together, these preliminary results suggest that HERK1 and ANJ could be executing redundant control of seed size similar to their homolog FER. Analysis of HERK1 and ANJ expression patterns during seed development, microscopic analysis of developing seeds in *herk1 anj* mutants and complemented lines as well as a more thorough analysis of seed characteristics at different times after harvest would be necessary to confirm the involvement of HERK1 and ANJ in this particular developmental process. Besides, the fertility phenotype in these mutants should be taken into account to rule out indirect effects on seed size development. For instance, given that approximately 70% of the ovules do not develop into seeds in the *herk1 anj* siliques, developing seeds could lack potential spatial constraints imposed by neighbouring seeds. Furthermore, increased availability of resources per seed could also promote larger seeds. Analysing seed size in WT Col-0 siliques with reduced seed set per silique following minimal pollination would constitute a useful approach to control for these possible side effects on seed size that reduced fertility could have in *herk1 anj* plants.

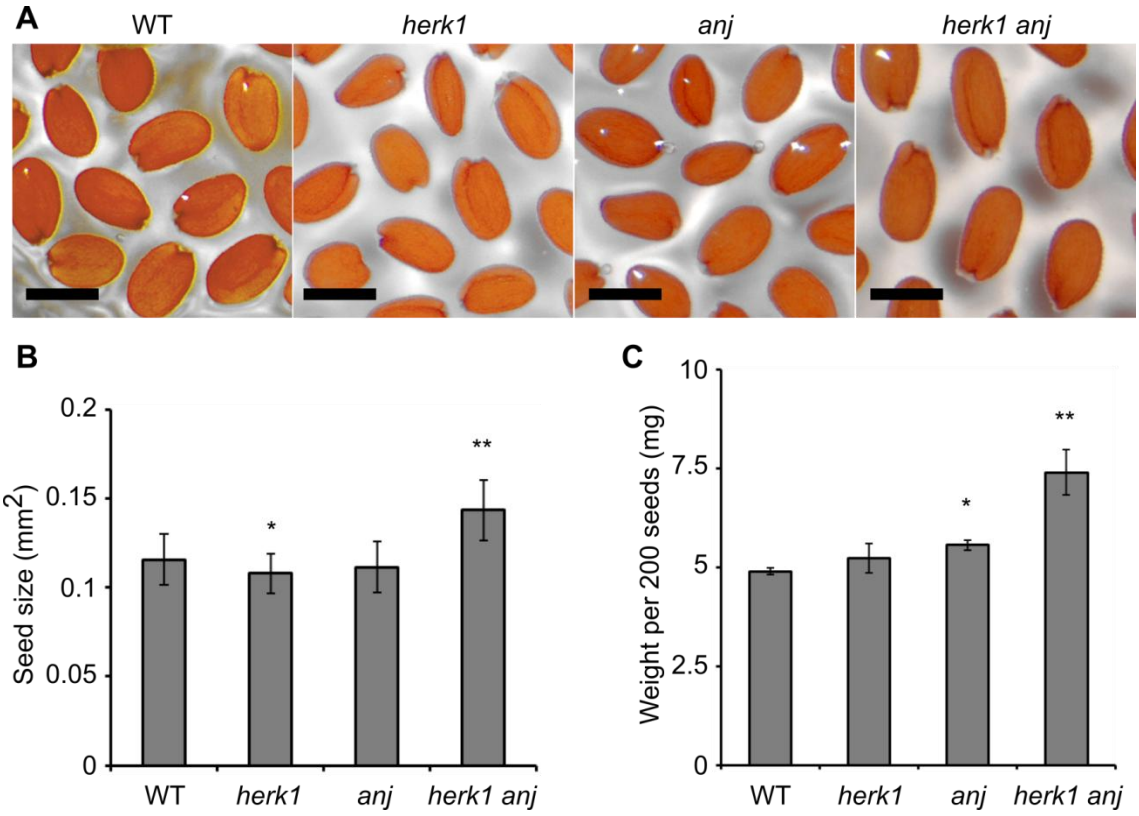

Figure 4.18 Analysis of seed size and weight in *herk1 anj* plants. A, representative photographs of seeds from WT Col-0, *herk1*, *anj* and *herk1 anj* plants. Dry seeds were submerged in water, placed on a microscope slide and photographed under a stereomicroscope. Scale bars = 500 µm. **B**, quantification of seed size in terms of area occupied by individual seeds from WT, *herk1*, *anj* and *herk1 anj*. Data presented corresponds to means ± SD from three independent measurements (n = 3) of the mean seed size from over 50 seeds. * p<0.05, ** p<0.01 (Student's *t*-test). **C**, quantification of the weight per 200 seeds from WT, *herk1*, *anj* and *herk1 anj*. Data presented corresponds to means ± SD from three independent measurements (n = 3) of the weight of 200 seeds. * p<0.05, ** p<0.01 (Student's *t*-test).

4.2.12 Vegetative growth and petiole elongation is unaltered *herk1 anj* plants

Several CrRLK1Ls have been linked to cellular expansion during development including FER, HERK1, HERK2 and THE1 [112, 126]. *fer* knockdown mutants, *herk1 the1-4,* and *herk1 herk2 the1-4* mutants display a dwarf phenotype caused by reduced cell elongation in petioles [112, 126]. HERK1, HERK2 and THE1 were initially proposed to redundantly regulate cell elongation [112, 126]; this hypothesis has been challenged by recent reports in which the *the1-4* allele used in previous studies was characterised as a hypermorphic allele that mimics THE1 over-expression [82]. In the light of these results, functional redundancy between these three CrRLK1Ls in the context of cell expansion awaits clarification (see Chapter 3 for additional results and discussion about HERK1, HERK2 and THE1 interactions).

Growth during the vegetative and reproductive stages of development does not appear to be impaired in *herk1 anj* mutants, as seedlings, rosettes and flowering plants look qualitatively similar to WT (Figure 4.19). Additionally, petiole elongation was characterised in *herk1 anj* plants based on previous evidence suggestive of HERK1 influence on cell elongation in petioles [112, 126]. Plants from *herk1 anj, herk1 the1-4* and *herk1 herk2 the1-4* lines were grown in parallel with Col-0 WT until bolting, rosette leaves were detached from the stem and petiole length quantified for each leaf position (leaves 1 to 10). No differences were found at any leaf position between WT and *herk1 anj*, while *herk1 the1-4* and *herk1 herk2 the1-4* mutants presented significantly shorter petioles than WT at every leaf position in the rosette (Figure 4.20). These results indicate that the *herk1 anj* mutation does not affect petiole elongation in the rosette leaves.

4.3 Discussion

This chapter summarises the description of the CrRLK1Ls HERK1 and ANJ as maternal determinants for fertilisation in Arabidopsis. Genetic, biochemical and histochemical approaches were used investigate the role of HERK1 and ANJ in fertilisation, yielding the characterisation of these CrRLK1Ls as redundant regulators of pollen tube reception at the synergid cell. For fertilisation to occur, male and female gametophytes engage in a tightly controlled dialogue that mediates pollen tube growth towards the ovule, pollen tube termination and subsequent release of the sperm cells into the female gametophyte [146]. Plants defective in HERK1 and ANJ present a female gametophytic fertility phenotype resulting in impaired seed production from most ovules. A pollen tube overgrowth defect was found to underlie the fertility phenotype in *herk1 anj* plants, suggestive of a block in the communication between male and female gametophytes during pollen tube reception. Analysis of expression patterns, cellular localisation and complementation experiments suggested HERK1 and ANJ regulate pollen tube reception from the filiform apparatus of the synergid cells, where they accumulate prior to fertilisation. Microscopic examination revealed no severe abnormalities in the structure of the female gametophyte in *herk1 anj* plants, suggesting a signalling defect underlies the reproductive phenotype of this mutant. Experiments to position HERK1 and ANJ in the pollen reception signalling cascade revealed that i) the synergid subcellular localisation of previously characterised effectors FER, LRE and NTA is not affected by the *herk1 anj* mutation, ii) LRE does not influence HERK1 and ANJ polar localisation within the filiform apparatus of the

Figure 4.19 The *herk1 anj* mutation does not have a major impact on plant growth. A, **C** and **E**, photographs from representative 10 days old WT Col-0, *herk1 anj* and *fer-4* seedlings germinated on soil. **B**, **D** and **F**, photographs of representative 21 day old WT, *herk1 anj* and *fer-4* plants. **G**, representative WT and *herk1 anj* plants (left and right, respectively) at 5 weeks old. *fer-4* plants were included in **E** and **F** as an example of stunted growth induced by disruption of a CrRLK1L member. Scale bars = 1.5 cm.

synergid cell, iii) functional HERK1 and ANJ are required for proper relocalisation of NTA following pollen tube reception, iv) ovular accumulation of ROS prior to pollen tube arrival is not impaired in *herk1 anj* plants, and v) the kinase activity of HERK1 and ANJ is dispensable in the reproductive context. Finally, detection of direct interactions between the extracellular domains of HERK1 and ANJ with LRE suggested HERK1 and ANJ may form receptor complexes with LRE at the filiform apparatus to mediate pollen tube-synergid cell communication.

As RLKs, HERK1 and ANJ primary function at the synergid cells may be the detection of pollen-derived cues during pollen tube reception and their transduction into intracellular responses to induce pollen tube burst. Although the nature of said cues is as yet unknown, extensive research on additional members of the CrRLK1L family in Arabidopsis in the last decade has allowed the identification of certain candidates to fulfil this role [136]. FER is the best characterised CrRLK1L member to date and various studies point at a multifaceted role in extracellular signal recognition for FER [136].

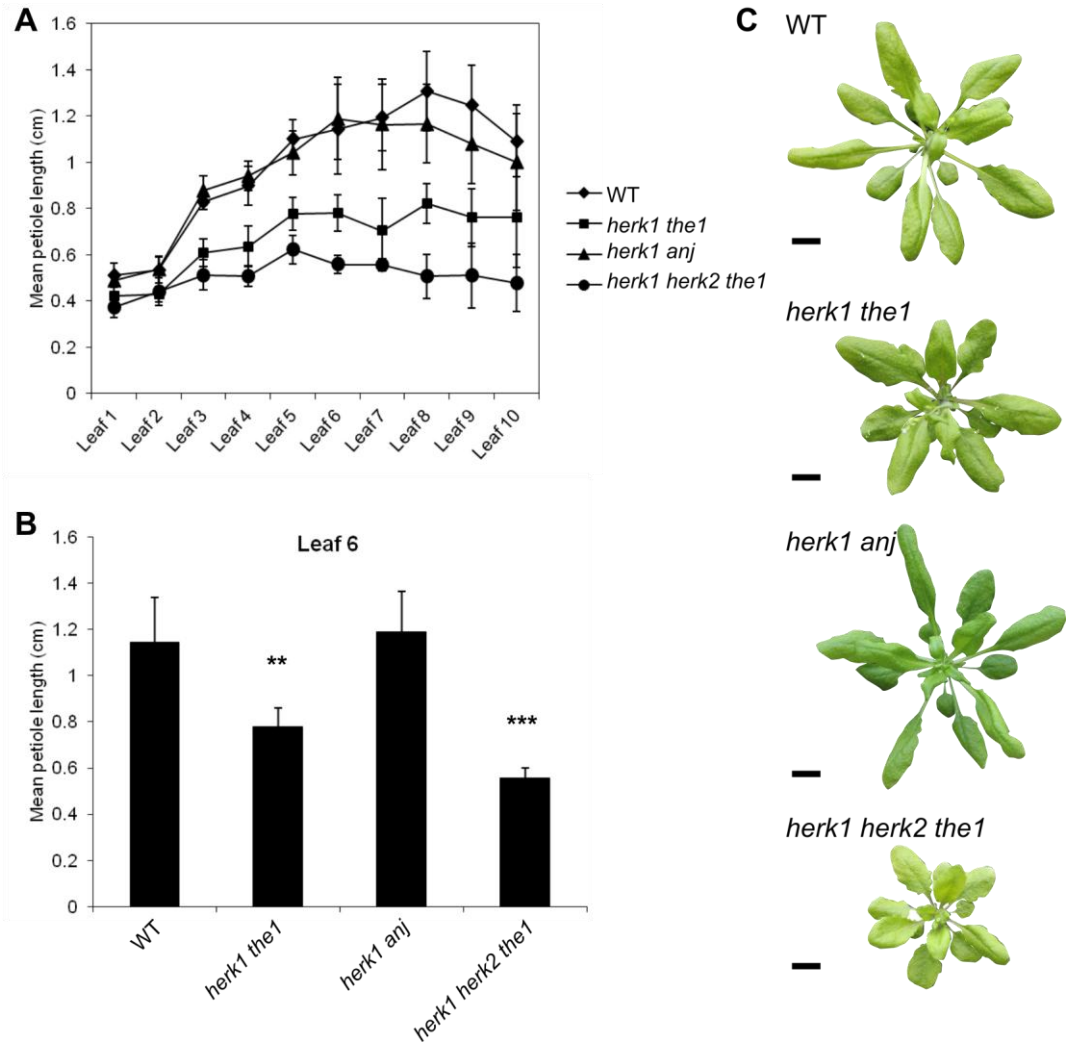

Figure 4.20 *herk1 anj* petioles elongate normally. A, quantification of petiole length in rosette leaves 1-10 (leaf 1 as the first true leaf in the rosette) from WT Col-0, *herk1 the1-4*, *herk1 anj* and *herk1 herk2 the1-4* mutant plants at initiation of bolting. Data presented are means ± SD from 6 plants per line (n = 6). No statistically significant differences were found at any leaf position between WT and *herk1 anj* in Student's *t* tests. **B**, example of mean petiole lengths in WT, *herk1 the1-4*, *herk1 anj* and *herk1 herk2 the1-4* mutants in leaf 6 extracted from dataset presented in A. Data presented are means ± SD from 6 plants per line (n = 6). ** $p<0.01$, *** $p<0.001$ (comparisons with WT in Student's *t*-test). **C**, representative WT, *herk1 the1-4*, *herk1 anj* and *herk1 herk2 the1-4* plants at initiation of bolting. Scale bars = 1 cm.

The extracellular domain of FER has been reported to interact physically with multiple elements including other RLKs, GPI-anchored proteins, small secreted peptides and cell wall components, making FER a versatile signalling hub that coordinates the response to multiple external cues from the plasma membrane [31-33, 64, 70, 197]. Cysteine-rich small secreted peptides belonging to the rapid alkalinisation factor (RALF) family are known to control processes like cell elongation and responses to pathogens through FER [32-33]. Interestingly, multiple reports support a tight connection between the CrRLK1L and RALF peptide families as multiple receptor-

peptide pairs have been described in addition to the founding pair of FER-RALF1 [32]. CrRLK1Ls BUPS1, BUPS2, ANX1 and ANX2 bind autocrine pollen peptides RALFL4 and RALFL19 at the pollen tube tip to sustain pollen tube growth stability, as disruption of either redundant pair BUPS1/BUPS2, ANX1/ANX2 or RALFL4/RALFL19 results in premature pollen tube burst [62]. Very recently THE1 has been reported to bind RALFL34 to directly mediate lateral root initiation [63]. These findings suggest that sensing RALF peptides could be a core function of the extracellular domain of the CrRLK1Ls as there is growing evidence that members from distinct subclades within the CrRLK1L phylogeny retain the capacity despite low sequence similarity of the extracellular CrRLK1L domains (see Figure 3.2 for a protein-based CrRLK1L phylogeny in Arabidopsis). Therefore, HERK1 and ANJ could also control male-female gametophyte communications by sensing pollen tube-derived or autocrine RALF signals. For instance, given that RALFL4 and RALFL19 are secreted at the tip of the growing pollen tube, it is possible that upon arrival to the female gametophyte these RALFs may diffuse within the filiform apparatus and trigger synergid responses via HERK1 and ANJ or FER. Conversely, sensing of autocrine RALF signals constitute another possible alternative as several RALF peptides are expressed in ovular tissues according to gene expression databases (i.e. RALFL14, RALFL24, RALFL31, RALFL34; GENEVESTIGATOR, https://genevestigator.com/gv/). The role of RALF peptides as putative regulators of fertilisation was also explored during the final year of this research project and relevant results were included in the following chapter of the present thesis (Chapter 5).

Changes in the mechanical and biochemical properties of the filiform apparatus cell wall upon pollen tube arrival constitute another category of candidate signals sensed by HERK1 and ANJ. As a fast tip-growing structure, the cell wall of the pollen tube differs from most other cell types in composition and dynamicity, specifically at the tip where continuous cell wall remodelling takes place [198]. During early stages of pollen tube reception, the pollen tube grows within the micropyle towards the female gametophyte until establishing direct contact with the source of the LURE attractants, the filiform apparatus of the synergid cells [199]. Direct physical contact between pollen tube and filiform apparatus and subsequent growth along the receptive synergid cell will unequivocally impose changes in the mechanical and biochemical properties of the filiform apparatus as the pollen tube cell wall undergoes dynamic remodelling promoting its growth between the synergid and the integument. The malectin-like domain present in the extracellular region of the CrRLK1Ls has been shown to mediate direct binding between FER, ANX1/2, BUPS1/2 and polygalacturonic acid, the building

block of pectin and one of the main components of plant cell walls [31, 64]. Interaction between FER and the cell wall supported the hypothesis of FER as a putative link between cell wall integrity and cellular adaptation as exemplified in previous reports describing impaired mechanosensing and adaptation to saline stress in *fer* mutant roots [125]. Similarly, HERK1 and ANJ could be sensing disruptions in the filiform apparatus intricate cell wall structure through their malectin-like domains together with FER, priming the synergid cells to respond and communicate with the received pollen tube to trigger pollen tube burst.

RLK signal transduction often involves homo- or heterodimerisation with other RLKs or receptor proteins at the plasma membrane upon exposure to ligands [200-201]. Phenotyping of relevant mutants, study of cellular localisation and protein interaction results presented in this chapter suggest that HERK1-LRE and ANJ-LRE receptor complexes may be formed at the synergid cells to mediate male-female gametophyte communication. Previously, interaction between FER and LRE, as well as between FER and LLG1 had been reported suggesting LRE proteins and CrRLK1Ls may constitute a common co-receptor unit [70]. Testing direct interactions between LRE proteins and CrRLK1L ligands such as RALF peptides or cell wall components, as well as whether the presence of LRE proteins influence CrRLK1L affinities to said ligands would prove useful in determining the mechanism of action of the LRE proteins. Interestingly, uncharacterised LRE proteins LLG2 and LLG3 are specifically expressed in pollen tubes according to gene expression databases (Arabidopsis EFP Browser; http://bar.utoronto.ca/efp/cgi-bin/efpWeb.cgi). Testing whether single and/or double mutants in these LRE proteins display pollen tube growth defects and whether they may be interacting with pollen CrRLK1Ls like BUPS1, BUPS2, ANX1 and ANX2 would likely provide further evidence to support a CrRLK1L-LRE protein receptor unit. Additionally, CrRLK1L heterocomplexes have also been reported in the context of pollen tube growth between BUPS and ANX proteins [62]. How these CrRLK1L heterocomplexes impact sensing of extracellular cues or downstream signalling remains to be explored. These findings open interesting questions about the CrRLK1L signalling at the synergid cells including i) whether FER may be interacting directly with HERK1 and ANJ, ii) whether FER, HERK1 and ANJ competitively interact with LRE or iii) whether LRE is capable of interacting with both CrRLK1Ls simultaneously and therefore represents a molecular bridge that allows tripartite FER-LRE-HERK1/ANJ complexes formation. Unfortunately, attempts to identify direct interactions between CrRLK1Ls FER, HERK1 and ANJ using BiFC were unsuccessful due to early induction of a hypersensitive-like response in *Nicotiana* leaves that hampered the interpretation

of results. Co-immunoprecipitation of these receptors is currently being tested and will hopefully shed light on the possibility of CrRLK1L complexes regulating fertility from the filiform apparatus.

ROS are thought to play a central role in regulating the communication between gametophytes and pollen tube burst in the ovule as a consequence. First, ROS production at the tip of growing pollen tubes is known to be crucial in maintaining tip growth stability as disruption of ROS homeostasis results in pollen tube burst *in vitro*. Second, ROS accumulates at the entrance of the female gametophyte during fertile stages of ovule development. Furthermore, depletion of ovular ROS by addition of exogenous inhibitors of NADPH oxidases results in pollen tube overgrowth indicating a connection between ROS and the regulation of pollen tube termination. Accumulation of ROS at the synergid cell area prior to pollen tube arrival was shown to depend on functional FER and LRE, suggesting ROS accumulation could be a downstream event during the pollen tube reception signalling cascade [68]. Having identified HERK1 and ANJ as redundant regulators of pollen tube reception in the synergid cells, and based on previous findings on FER and LRE, testing whether ROS accumulation prior to pollen tube reception is affected in *herk1 anj* ovules became a priority in the characterisation of these CrRLK1Ls. Histochemical staining of mature live ovules showed ROS production does not depend on functional HERK1 and ANJ. Surprisingly, while ROS dependency on functional FER could be confirmed, the assays presented here could not detect any decrease of ROS in *lre* mutants in mature ovules as previously reported. Experiments testing ROS production in *herk1 anj*, *lre-5* and *fer-4* mutants were repeated three times and similar results were obtained, indicating that these assays work robustly and suggesting that discrepancies between this thesis and previous reports may be as a result of differencies in experimental protocols or plant growth environments. Further, ROS accumulation in the ovules of triple mutants *herk1 anj lre-5* also displayed WT levels, supporting further that ROS production appears to be only FER-dependent under our growth conditions. A dual role for FER in the synergid cells in inducing ROS accumulation and independently controlling pollen tube reception together with LRE, HERK1 and ANJ could explain these findings. Observing the dynamics of ROS production in the synergids as the pollen tube reception takes place using genetically-encoded ROS reporters would allow detailed examination of this process and detection of transient differences in these mutants that the *in vitro* system used here cannot provide.

Dynamic changes in Ca^{2+} concentration in the synergids take place during the different

stages of pollen tube reception, resulting in specific Ca^{2+} signatures required for correct pollen tube termination [72]. FER, LRE and NTA were shown to influence different aspects of these signatures during pollen tube reception by mechanisms still unknown [72]. Based on the findings presented here describing a dependency of NTA relocalisation on functional HERK1 and ANJ, and given the involvement of NTA as a modulator of the amplitude of the Ca^{2+} signatures, it is possible that HERK1 and ANJ also influence Ca^{2+} dynamics during pollen tube reception [69, 72]. The underlying mechanism connecting signal perception at the filiform apparatus by these three CrRLK1Ls and LRE with downstream events like ROS production, induction of Ca^{2+} signatures and relocalisation of NTA remains elusive. Induction of downstream signalling cascades by RLKs often involves activation of their intracellular kinase domain and subsequent phosphorylation of interaction partners. FER kinase activity is dispensable in the context of fertility as shown in previous reports [192], and interestingly, so are HERK1 and ANJ kinase activities, as kinase-dead versions of these two CrRLK1Ls can fully complement the fertility defect in *herk1 anj* plants. Besides, the reproductive phenotype of *fer* mutants could also be rescued with a chimeric protein comprising the FER extracellular domain and HERK1 kinase domain [192], suggesting that the kinase domain of FER, HERK1 and possibly ANJ are equivalent and may control pollen tube reception through induction of an identical signalling pathway. Recent reports have found that whereas the kinase-dead FER was able to rescue the fertility defect in *fer* plants, the response to RALF1 in root-cell elongation requires FER kinase activity [202], exemplifying how one CrRLK1L protein can transduce signals through multiple mechanisms in a context dependent manner. It would therefore be very informative to test whether kinase-dead FER is able to complement the ROS accumulation phenotype in ovules prior to pollen tube arrival as it could aid understanding whether FER's roles in ROS accumulation and control of pollen tube reception can be separated.

4.3.1 Future work

Clarifying the mechanism through which HERK1 and ANJ mediate the reception of the pollen tube requires further experimentation. First, investigating the possibility of tripartite receptor complexes FER-LRE-HERK1 and FER-LRE-ANJ would require i) studying the capacity of these receptors to interact with one another by Y2H and/or co-immunoprecipitation, ii) generating triple and quadruple mutants *herk1 anj fer-4* and *herk1 anj lre-5 fer-4* to subsequently iii) demonstrate that there is no additive effect to the reproductive phenotype in seed production or pollen tube reception. Additionally,

testing complementation of the reproductive phenotypes in these mutants with chimeric proteins comprising combinations of the extracellular and intracellular domains of FER, HERK1 and ANJ would confirm whether there is redundancy in sensing of stimuli and transduction of signals between these CrRLK1Ls.

Generation of stably transformed lines expressing synergid cell-specific reporters of ROS and redox status would probe further into the regulation of downstream events controlled by HERK1 and ANJ during pollen tube reception. Observation of the pollen tube reception in live imaging experiments in mutant backgrounds using ratiometric reporters such as Hyper and GRXroGFP2 (sensors of hydrogen peroxide and redox potential, respectively; [190, 203]) would provide the temporal resolution required to test whether fluctuations in the production of ROS or changes in the synergid cell redox status depend on functional HERK1 and ANJ. Similarly, recording Ca^{2+} fluctuations in the synergid cells during pollen tube reception in *herk1 anj* plants would shed light on a possible role for these two CrRLK1Ls in modulating Ca^{2+} signatures as has been described for FER, LRE and NTA [72]. Furthermore, exposing these reporter lines to a variety of stimuli could be useful to further our understanding on the nature of the signals sensed at the filiform apparatus by these receptors. Dissected live ovules could be exposed to different purified cell wall components, RALF peptides, changes in pH, ROS, among others, to observe synergid cell responses in Ca^{2+}, ROS and redox status in multiple mutant backgrounds. Absence of, or differences in responses to stimuli in certain mutants would suggest possible receptor-signal partners that could be subsequently verified by genetic and biochemical approaches.

Recent reports have established a direct link between CrRLK1Ls and cell wall integrity by characterising FER as a pectin binding receptor as well as by describing how ERULUS (ERU) maintains cell wall integrity in root hairs by inducing modifications of pectin through pectin methylesterases activity modulation [31, 64, 77]. In fact, *eru* mutation influences the amount of de-esterified homogalacturonan in root hair cell walls, suggesting that the CrRLK1Ls are capable of sensing changes in the cell wall as well as inducing its remodelling [77]. Interestingly, the RALF-CrRLK1L signalling module that controls pollen tube growth also influences pollen tube cell wall composition [80]. It would be very informative to study in detail whether HERK1 and ANJ affect the composition of the filiform apparatus beyond callose accumulation. Detecting presence of different types of cell wall components in the synergid cells of fertilisation mutants by immunostaining using antibodies specific to different cell wall epitopes would allow the identification of putative cell wall components critical for the

function of the filiform apparatus during pollen tube reception, which could yield the addition of a new branch to the signalling network controlling this process.

Finally, long term plans could include the generation of mutagenised populations of Arabidopsis seeds using ethyl methanesulphonate (EMS) in the *herk1 anj* mutant background. The resulting population could be screened for suppression of the fertility defect in terms of seed production per silique and interesting individuals sequenced to obtain candidate genes that could have an important role in the HERK1/ANJ signalling pathway.

4.3.2 Conclusions

This chapter summarises the characterisation of the CrRLK1Ls HERK1 and ANJ as female determinants of pollen tube reception in Arabidopsis, therefore constituting the first study in which functions have been assigned to these genes in the context of reproduction. The work presented here yielded the identification of two novel synergid cell regulators of pollen tube overgrowth and highlight the relevance of the CrRLK1L family in controlling several aspects of reproduction in Arabidopsis.

Chapter 5

Control of reproduction by rapid alkalinisation factor peptides

5.1 Introduction

The development of plant structures requires active coordination of cell division, growth and differentiation between distal and closely located cells. Plant cells engage in communication to ensure coordinated development and response to external stimuli by exchanging hormones and inducing biochemical changes in their surroundings that can be sensed by neighbouring cells [204]. The plant hormones first identified were small molecules like auxins, cytokinins or gibberellins. Research during the past two decades has drawn the attention to small secreted peptides and has placed them as central hormonal regulators of a variety of processes in plant development [205].

Plant small secreted peptides are usually sensed by receptor-like kinases (RLKs; [206]) and can be classified into different categories depending on the maturation process they undergo to produce the final, biologically-active peptide. Maturation typically involves a first step of proteolytic cleavage of the signal peptide, followed by multiple steps of post-translational modifications comprising further proteolytic processing to release the shorter active peptide as well as formation of disulfide bonds, tyrosine sulfation, proline hydroxylation, etc (see [207] for a detailed review on plant peptide maturation). Small post-translationally modified peptides undergo N-terminal removal and contain few or no cysteine residues implying that disulfide bonds are not required for their structural maturation. This class includes the CLV3/EMBRYO SURROUNDING REGION-RELATED (CLE) family of peptides known to control the production of stem cells in meristematic regions [208]. Cysteine-rich peptides constitute the second category of small secreted peptides in plants and are characterised by presenting multiple cysteine residues in the mature peptide region, often in pairs, of known relevance for their mature structural conformation. Peptides from the LURE and rapid alkalinisation factor (RALF) families belong to this group, regulators of pollen tube guidance and cell expansion, respectively [209].

RALF peptides were first identified in tobacco cell cultures as activators of medium alkalinisation at very low concentrations without induction of defence responses [210]. This founding study demonstrated the prevalence of the RALF peptides across multiple plant species and found that purified RALF peptides from tomato induce stunted root growth in tomato and Arabidopsis seedlings [210]. Independent studies found similar alkalinisation properties in RALF peptides derived from poplar and sugarcane, further supporting the role of this family of peptides in regulating apoplastic pH [211-212]. Furthermore, characterisation of RALF peptides in *Solanum* suggested their involvement in controlling pollen tube growth and female gametophyte development [213-215]. While these studies highlighted the importance of this family of cysteine-rich peptides in plant development, research in Arabidopsis has nevertheless provided biochemical and genetic evidence of the versatility of the RALF peptides in controlling multiple aspects of plant development as well as their intimate association with the *Catharanthus roseus* RLK 1-like (CrRLK1L) receptors.

5.1.1 RALF peptide family evolution and domain diversity

Analysis of the proteomes of species in multiple lineages of the plant kingdom revealed the prevalence of the RALF peptides across land plants and absence in earlier divergent lineages like chlorophytes or charophytes, suggesting RALFs could represent an innovation of land plants [123]. An expansion in RALF gene number has taken place during land plant evolution, most remarkably after the divergence between monocots and eudicots [216-217]. It has been proposed that the common ancestor of eudicots and monocots harboured five RALF genes that through genome duplication events and tandem expansions gave rise to the large RALF families found in present day angiosperms [216]. RALF gene number in extant representatives of the earliest divergent groups of land plants vary between one and three [123]; meanwhile, representatives of angiosperm lineages like Amborella (representative of the earliest divergent angiosperms), Arabidopsis (Brassicaceae, eudicot) and rice (Poaceae, monocot) present 9, 37 and 16, respectively, exemplifying the remarkable expansion of this gene family during land plant evolution and specifically within some eudicot clades (see Figure 5.1 for Arabidopsis RALFs; [216-217]). Interestingly, whereas monocot RALF gene number correlates with the general trend of genome expansion, eudicot RALFs expansion cannot be explained by genome duplication events alone and have undergone a substantial expansion through tandem duplications, accounting for more than 50% of RALF genes in Arabidopsis, for instance [216-217].

Canonical RALF peptide structure comprises a prepropeptide of 85-125 amino acids

containing the N-terminal signal peptide (thought to direct these peptides towards the apoplastic route of secretion), a variable domain and a C-terminal mature peptide of approximately 50 amino acids [210]. RALFs are thought to be proteolytically processed to release the mature peptide in the Golgi apparatus by serine proteases that recognise a RRXL motif near the N-terminus of the mature peptide region of the propeptide [33, 218-219]. Additionally, a YISY motif commonly found in the mature peptide region of RALFs has been proposed to play an important role in receptor recognition [220], although this hypothesis awaits confirmation by structural analysis of RALF-receptor complexes.

Large-scale bioinformatic analysis of proteomes from more than 50 species identified four distinct clades of RALFs (I-IV) that present significant differences within the mature peptide region, suggesting differences in terms of receptor binding affinity between clades [217]. Angiosperms present members of each clade (I-IV), whereas RALF members from early divergent lineages of land plants are restricted to cluster III, suggesting members from this group could carry out ancestral RALF functions [217]. Clade IV constitutes the most divergent group with several unique characteristics: i) they rarely have the YISY motif and instead present XIXY, ii) the RRXL protease recognition site is usually absent, iii) the variable region of the propeptide lacks several features which results in a remarkable reduction in prepropeptide length to approximately 88 amino acids, iv) different biochemical properties are predicted for clade IV propeptides, v) they are over-represented within the Brassicaceae family, accounting for more than 50% of Arabidopsis RALFs (Figure 5.1), and vi) their expression patterns reveal inflorescence-specific roles for this clade of RALFs [217]. In the light of this evidence it has been suggested that clade IV RALFs should be considered a functionally divergent type of peptides as they may not be proteolytically processed and are likely to signal through different receptors than clades I-III [217].

5.1.2 RALF peptides in Arabidopsis

37 RALF-encoding genes are found in the genome of *Arabidopsis thaliana*, 22 out of which have been classified as cluster IV RALFs (Figure 5.1; [217]). Tight phylogenetic RALF clusters including *RALFL10*, *RALFL11*, *RALFL12* and *RALFL13*, *RALFL25* and *RALFL26*, or *RALFL8* and *RALFL9* exemplify the importance of tandem duplications in the expansion of Arabidopsis cluster IV RALFs (Figure 5.1). To date, only one cluster IV RALF, RALFL8, has been characterised in responses to combined biotic and abiotic stresses by investigating the impact of *RALFL8* over-expression during plant

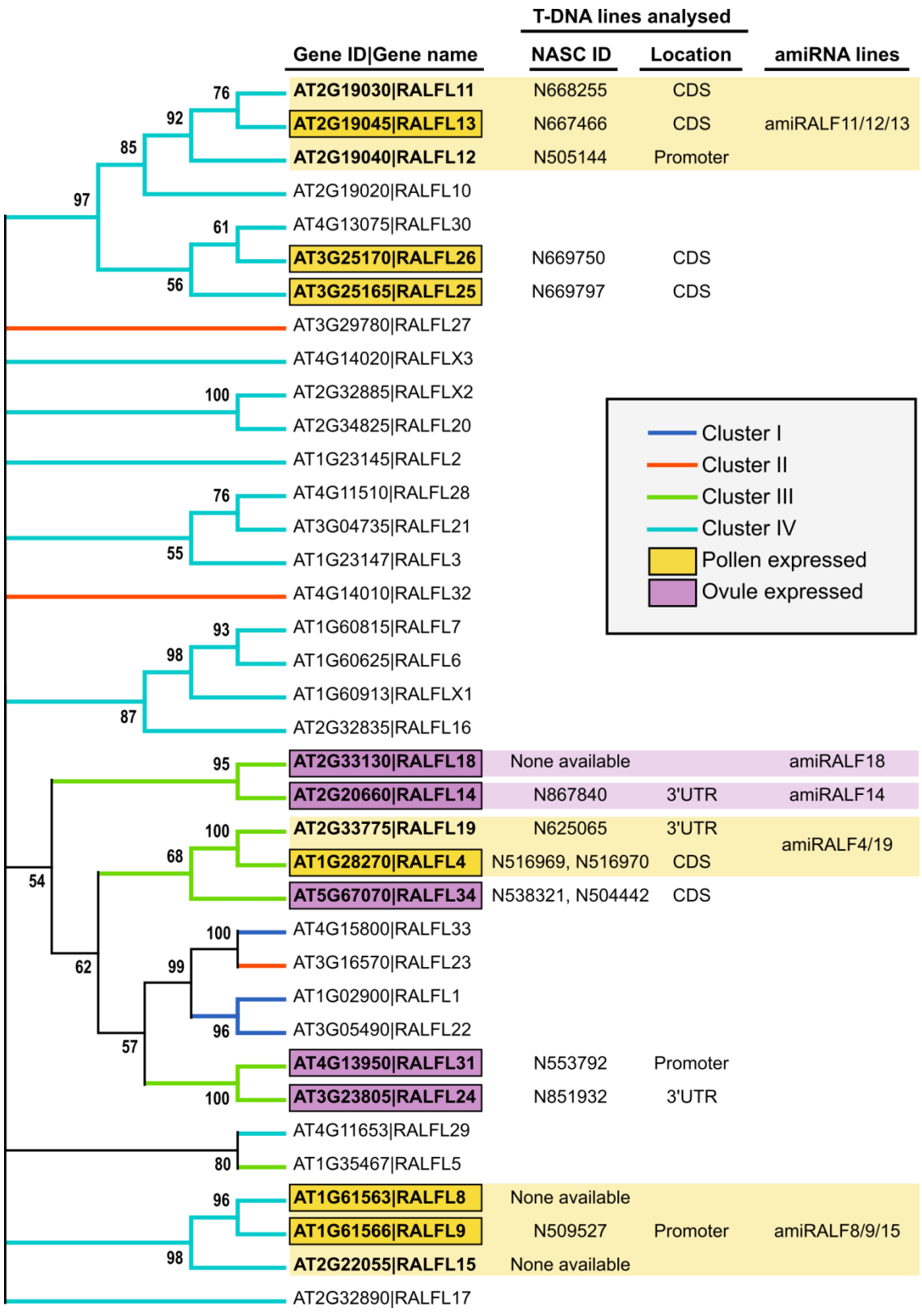

Figure 5.1 The RALF family in Arabidopsis and putative regulators of reproduction. Phylogenetic analysis of the RALF proteins in *A. thaliana* based on full-length amino acid sequences, aligned using ClustalX [127] and a Neighbour-Joining phylogenetic tree generated with the software MEGA5.2 [128-129]. The percentage of replicates where associated taxa clustered in the bootstrap test is shown next to each branch (1000 replicates). Branches with

bootstrap values below 50 were condensed. RALF members in *Arabidopsis thaliana* (AT1G02900|RALFL1, AT1G23145|RALFL2, AT1G23147|RALFL3, AT1G28270|RALFL4, AT1G35467|RALFL5, AT1G60625|RALFL6, AT1G60815|RALFL7, AT1G61563|RALFL8, AT1G61566|RALFL9, AT2G19020|RALFL10, AT2G19030|RALFL11, AT2G19040|RALFL12, AT2G19045|RALFL13, AT2G20660|RALFL14, AT2G22055|RALFL15, AT2G32835|RALFL16, AT2G32890|RALFL17, AT2G33130|RALFL18, AT2G33775|RALFL19, AT2G34825|RALFL20, AT3G04735|RALFL21, AT3G05490|RALFL22, AT3G16570|RALFL23, AT3G23805|RALFL24, AT3G25165|RALFL25, AT3G25170|RALFL26, AT3G29780|RALFL27, AT4G11510|RALFL28, AT4G11653|RALFL29, AT4G13075|RALFL30, AT4G13950|RALFL31, AT4G14010|RALFL32, AT4G15800|RALFL33, AT5G67070|RALFL34, AT1G60913|RALFLX1, AT2G32885|RALFLX2 and AT4G14020|RALFLX3) were included in this analysis. Coloured branches indicate the RALF cluster each Arabidopsis member belongs to, as per [217]. T-DNA insertion lines obtained from the Nottingham Arabidopsis Stock Centre (NASC) for each RALF are listed here, along with their respective predicted insertion site. Genes with pollen or ovule expression according to GENEVESTIGATOR [221] and the Arabidopsis EFP Browser (http://bar.utoronto.ca/efp/cgi-bin/efpWeb.cgi) are highlighted in yellow and purple boxes, respectively. Clusters of RALFs targeted by pollen or ovule-specific amiRNA lines are highlighted with light yellow or light purple boxes, respectively.

development and in response to biotic and abiotic stress [222]. Therefore, despite the prevalence of the cluster IV RALFs in Arabidopsis, functional and mechanistic characterisation of these RALFs remains elusive.

Arabidopsis RALF proteins from clades I-III have been thoroughly investigated during the last decade, shaping our current understanding of the function and regulation of plant development executed by these cysteine-rich peptides. First, the effect of exogenously applied RALFs in multiple aspects of plant development was investigated, including root and hypocotyl elongation, lateral root production, pollen tube germination, among others. These assays suggested RALF1, and RALFL19, 22, 23, 24, 31 and 34 could induce alkalinisation of growth media, inhibit hypocotyl and root elongation, as well as reduce lateral root density [212, 223-224]. Additionally, RALF1 was shown to induce rapid changes in cytoplasmic Ca^{2+} concentrations [225]. Second, over-expression of *RALF1* and *RALFL23* lead to aerial and root dwarfism and incapacity to acidify the growth medium, whereas knocking down their expression resulted in the opposite effect [218, 224]. These results evidenced the tight relationship between Arabidopsis clade I-III RALFs and the control of cell elongation via modulation of apoplastic pH. Finally, a direct link between RALF signalling and apoplastic pH regulation was identified through a phosphoproteomics screen aiming to decipher cellular signalling cascades activated upon exposure of roots to exogenous RALF1 [32]. Haruta and colleagues found that proton ATPase 2 (AHA2) phosphopeptides increased in abundance after RALF1 treatment, suggesting that RALF1 activates phosphorylation of AHA2 which could in turn inhibit its proton pump activity resulting in increased apoplastic pH and subsequent inhibition of cell elongation [32].

Multiple lines of evidence portray the CrRLK1L receptor family as RALF peptide receptors. The identification of FERONIA (FER) as a RALF1 receptor by Haruta and colleagues was the first connection between CrRLK1Ls and RALF peptides [32]. FER phosphopeptides were also found to increase in abundance upon RALF1 treatment in seedlings, suggesting RALF1 triggers FER phosphorylation [32]. Given the almost complete insensitivity to exogenous RALF1 observed in *fer* knock-out mutants in terms of root elongation inhibition, and based on the detection of a physical interaction between the FER extracellular domain and RALF1, FER was proposed as a RALF1 receptor at the plasma membrane [32]. The identification of FER as a RALF1 receptor suggested the CrRLK1Ls, of which 17 are found in Arabidopsis, could function as RALF peptide sensors (see chapters 3 and 4 for a detailed description of the CrRLK1L family in Arabidopsis). This hypothesis was further strengthened by the characterisation of FER as a RALFL23 receptor in the context of immunity [33]. Furthermore, in the past year five additional CrRLK1Ls have been reported to mediate sensing of three Arabidopsis RALFs closely related to RALF1 and RALFL23 to control pollen tube growth and lateral root initiation [62-63]. These findings are covered in detail in the discussion of the present chapter (section 5.3).

5.1.3 Aims

The identification of HERCULES RECEPTOR KINASE 1 (HERK1) and ANJEA (ANJ) CrRLK1Ls as female determinants of fertility during this PhD project opened possible scenarios worth testing to further our understanding in the regulation of fertility executed by these CrRLK1Ls (see the discussion section in Chapter 4). One such hypothesis was the possible involvement of RALF peptides in the control of pollen tube reception mediated by HERK1 and ANJ in the synergid cells of the ovule. When this side project was conceived the only CrRLK1L reported ligands were RALF1 in the context of cell elongation in roots and RALFL23 in immunity [32-33]. Besides, previous evidence linked RALF peptides and pollen tube germination and growth, as well as to the induction of Ca^{2+} fluxes, key process in the synergid cells during pollen tube reception [213, 223, 225]. Therefore, testing whether RALF peptides secreted from pollen tubes or ovular tissues in response to pollen tube arrival could be responsible for the activation of HERK1 and ANJ or FER-mediated signalling arose as an exciting question to explore.

The main aims pursued in the present chapter were i) to identify interesting candidates for the regulation of fertilisation within the Arabidopsis RALF family by analysing gene expression databases, generation of lines with impaired RALF expression and

examination for defects in seed production as a proxy for failed fertilisation; ii) to identify lines defective in reproduction that presented a pollen tube overgrowth; iii) to generate reporter lines that allow complementation of the reproductive defects as well as characterisation of expression patterns and cellular localisation; and finally and as a longer term goal, iv) to test direct interaction between such RALF peptides and the synergid cell CrRLK1Ls HERK1, ANJ and FER and analyse sensitivity to such peptides in *herk1 anj* and *fer* mutant backgrounds. The initial screen for fertility impairment of *ralf* mutants yielded the identification of two RALFs, RALFL4 and RALFL19, as putative regulators of reproduction. Although none of the lines analysed resulted in pollen tube overgrowth defects, studying the role of RALFL4 and RALFL19 in pollen tube growth constituted an exciting opportunity to shed light on the regulation of reproduction by RALF peptides and their characterisation was therefore pursued.

5.2 Results

5.2.1 Identification of candidate RALFs and generation of *ralf* artificial microRNA lines

The first step towards the identification of putative RALF regulators of reproduction was to select a subset of candidates among the 37 RALF peptides in Arabidopsis based on likelihood of expression in either pollen tubes or ovaries. To this end, public gene expression databases GENEVESTIGATOR [221] and the Arabidopsis EFP Browser (http://bar.utoronto.ca/efp/cgi-bin/efpWeb.cgi) were explored and RALF genes displaying pollen- or ovary-enriched expression were selected. This initial reproductive RALF subset included *RALFL4*, *8*, *9*, *13*, *25* and *26* as pollen-expressed RALFs, and *RALFL14*, *18*, *24*, *31* and *34* as ovary-expressed RALFs (Figure 5.1). Among them, *RALFL14* and *RALFL18* were expected to be female gametophyte-expressed according to previous reports [226]. Additionally, despite the lack of expression data for some RALF genes and in order to avoid masking of interesting phenotypes by functional redundancy between homologous RALFs, *RALFL11*, *12*, 15 and *RALFL19* were included in this initial subset (Figure 5.1).

A reverse genetics approach could be helpful in unravelling possible regulatory functions in reproduction and thus the Nottingham Arabidopsis Stock Centre (NASC) catalogue was probed for T-DNA insertion lines in which the selected RALF genes were disrupted. Unfortunately, due to the relatively small size of these peptides it was not possible to obtain T-DNA insertion lines disrupting the coding sequence (less than 400 bp) for all RALFs. T-DNA insertion lines disrupting coding sequences, 5' or 3'

untranslated regions as well as promoter regions (with insertions located less than 1 kb upstream of the start codon) were obtained as they could interfere with gene expression (Figure 5.1; no T-DNA lines were available for *RALFL8*, *15* or *18*). However, based on the phylogenetic relationships between the selected set of RALFs, differential functions could be expected from the clades comprising *RALFL11*, *12* and *13*; *RALFL25* and *26*; *RALFL4* and *19*; *RALFL14* and *18*; and *RALFL8*, *9* and *15*, as well as functional redundancy between members within each of these clades (Figure 5.1). Functional redundancy between closely related RALFs would mask mutant phenotypes in single insertion lines and thus the generation of double or triple insertion lines would be necessary. While this constituted a feasible approach for the clades comprising *RALFL4* and *RALFL19*, and *RALFL24* and *RALFL31*, chromosomal proximity between members of the other clades for which T-DNA lines were obtained would hinder the generation of mutants of higher degree. To overcome this issue a second approach was undertaken to knock down gene expression of RALF clusters of interest using artificial microRNAs (amiRNAs; [109]). Briefly, amiRNAs targeting RALF clusters of interest were designed using WMD3 (http://wmd3.weigelworld.org/cgi-bin/webapp.cgi; [227]) and cloned in the Arabidopsis precursor MIR319a backbone under pollen- or ovule-specific promoters. The pollen-specific *LAT52* promoter (*pLAT52*; [228]) and the synergid cell specific *NORTIA* promoter (*pNTA*; [69]) were chosen to target amiRNA expression to pollen tubes and mature ovules, respectively. All female regulators of pollen tube reception in Arabidopsis identified to date are expressed in the synergid cells (see Chapter 4), which made *pNTA* a robust candidate to interfere with putative ovular RALF regulators of pollen tube reception. amiRNA constructs targeting the clusters *RALFL11*,*12* and *13*, *RALFL4* and *19*, and *RALFL8*, *9* and *15* were successfully designed (Figure 5.2A). Unfortunately, no specific *RALFL14* and *18* amiRNAs could be designed using WMD3 and therefore individual *RALFL14* amiRNA and *RALFL18* amiRNA constructs were generated instead (Figure 5.2A).

Five RALF amiRNA constructs were transformed into WT Col-0 plants by the floral dip method and the T1 generation of seeds was screened for transformants carrying the desired construct [106]. T1 transformants were successfully isolated for amiRALF11/12/13, amiRALF8/9/15 and amiRALF14 (Figure 5.2A). Unfortunately, no transformants were rescued from the T1 generation of amiRALF4/19 and amiRALF18 (Figure 5.2A; over 1 mL of dry T1 seeds from four healthy T0 plants per construct were screened for transformants). Transformations for all amiRNA constructs were carried out in parallel using plants grown under the same conditions, suggesting the constructs amiRALF4/19 and amiRALF18 could have a negative impact in the process of

A

amiRNA line	Promoter	Target genes	T1 plants analysed?
amiRALF11/12/13	*pLAT52*	*AT2G19030|RALFL11* *AT2G19045|RALFL13* *AT2G19040|RALFL12*	Yes
amiRALF4/19	*pLAT52*	*AT2G33775|RALFL19* *AT1G28270|RALFL4*	No transformants recovered
amiRALF8/9/15	*pLAT52*	*AT1G61563|RALFL8* *AT1G61566|RALFL9* *AT2G22055|RALFL15*	Yes
amiRALF18	*pNTA*	*AT2G33130|RALFL18*	No transformants recovered
amiRALF14	*pNTA*	*AT2G20660|RALFL14*	Yes

B

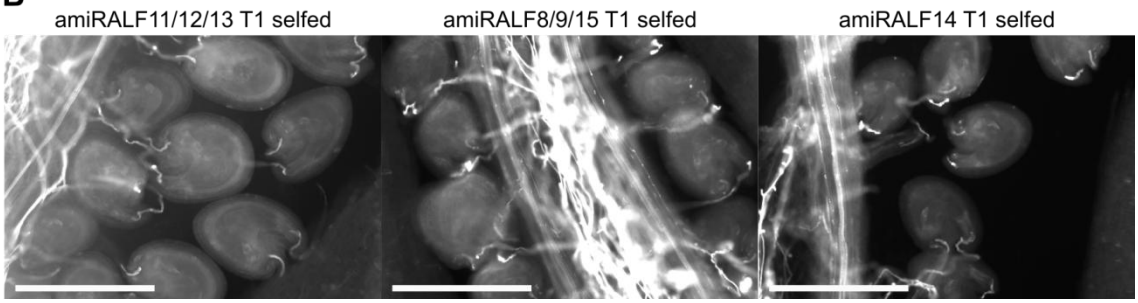

Figure 5.2 Pollen and ovule-specific RALF amiRNA lines. A, summary of amiRNA lines generated including promoter used, RALFs targeted and recovery of transformants in the T1 generation. **B**, representative images of aniline blue-stained pollen tubes in self-pollinated T1 plants harbouring RALF amiRNA constructs (indicated above the corresponding image). No pollen tube overgrowth events were recorded indicating that pollen tube reception may not be affected in these lines. Ovules from two to three carpels per plant and three independent T1 plants were analysed for each amiRNA construct. Scale bars = 200 µm.

reproduction or embryo development. The floral dip method relies on stable transformation of the female gametophyte of the T0 plants and therefore synergid cell specific expression of amiRALF18 could have impaired the capacity of transformed ovules to undergo fertilisation of develop seeds [229]. Conversely, while pollen does not undergo stable transformation with the floral dip method, reports have shown transient expression of the construct takes place in pollen which, if obstructive of pollen development, could have in turn minimised the transformation success by blocking reproduction in transformed flowers [230].

Plants carrying the constructs amiRALF11/12/13, amiRALF8/9/15 and amiRALF14 were subjected to aniline blue staining of pollen tubes in self-pollinated carpels to identify defects in pollen tube reception. In the T1 generation 50% of pollen tubes or

ovules (*pLAT52* or *pNTA*-driven constructs, respectively) would express the corresponding amiRNA in single insertion lines, allowing the identification of reproductive defects caused by RALF knock-down. At least two carpels per plant and three independent T1 plants per line (approximately 300 ovules) were analysed, however no defects in pollen tube reception were observed for amiRALF11/12/13, amiRALF8/9/15 or amiRALF14 (Figure 5.2B). Whereas it is possible that the RALF clades including *RALFL11*,*12* and *13*; *RALFL8*,*9* and *15*; and *RALFL14* may not be involved in the reception of pollen tubes, several considerations should be taken into account when interpreting these results: first, functional redundancy between the RALFs targeted in these amiRNA lines and additional untargeted RALFs could be masking reproductive mutant phenotypes; second, specific targeting amiRALFL14 to synergid cells could have been insufficient to impair RALF14 function in the female gametophyte (*pRALFL14* was reported to be active synergids, egg cell and central cells; [226]); third, gene expression levels of the corresponding RALFs were not quantified for the T1 lines analysed and therefore, insufficient reduction in *RALF* expression is also possible. In conclusion, although no defects in pollen tube reception were observed in these amiRNA lines, it is not possible to rule out functions for these RALFs in controlling fertilisation due to the preliminary nature of the results presented in this section.

5.2.2 Confirmation of RALF T-DNA insertion lines, generation of double insertion lines and screen for reproductive defects

A set of 14 T-DNA insertion lines was obtained from NASC to identify possible defects in pollen tube reception associated with disrupted RALF gene expression (Figure 5.1). Analysis of two consecutive generations by genotyping PCR allowed the isolation of individuals homozygous T-DNA insertion lines targeting *RALFL4*, *9*, *14*, *19*, *24*, *25* and *31* (*ralfl4*/N516969; *ralfl9*/N509527; *ralfl14*/N867840; *ralfl19*/N625065; *ralfl24*/N851932; *ralfl25*/N669797; *ralfl31*/N553792; respectively). T-DNA lines targeting *RALFL11*, *12*, *13*, *26* and *34* were unfortunately found to be incorrect as all individuals analysed lacked T-DNA insertions in the expected regions (more than 10 individuals genotyped per line), therefore hindering the generation of multiple order mutants targeting the likely redundant RALFs RALFL11, 12 and 13, as well as RALFL25 and 26. The confirmed set of RALF T-DNA lines nevertheless allowed pursuing the generation of double mutants *ralfl4 ralfl19* and *ralfl24 ralfl31*, likely redundant pairs in pollen and ovules, respectively. The respective single homozygous lines were crossed and generation F2 was genotyped, yielding the isolation of homozygous *ralfl24 ralfl31*.

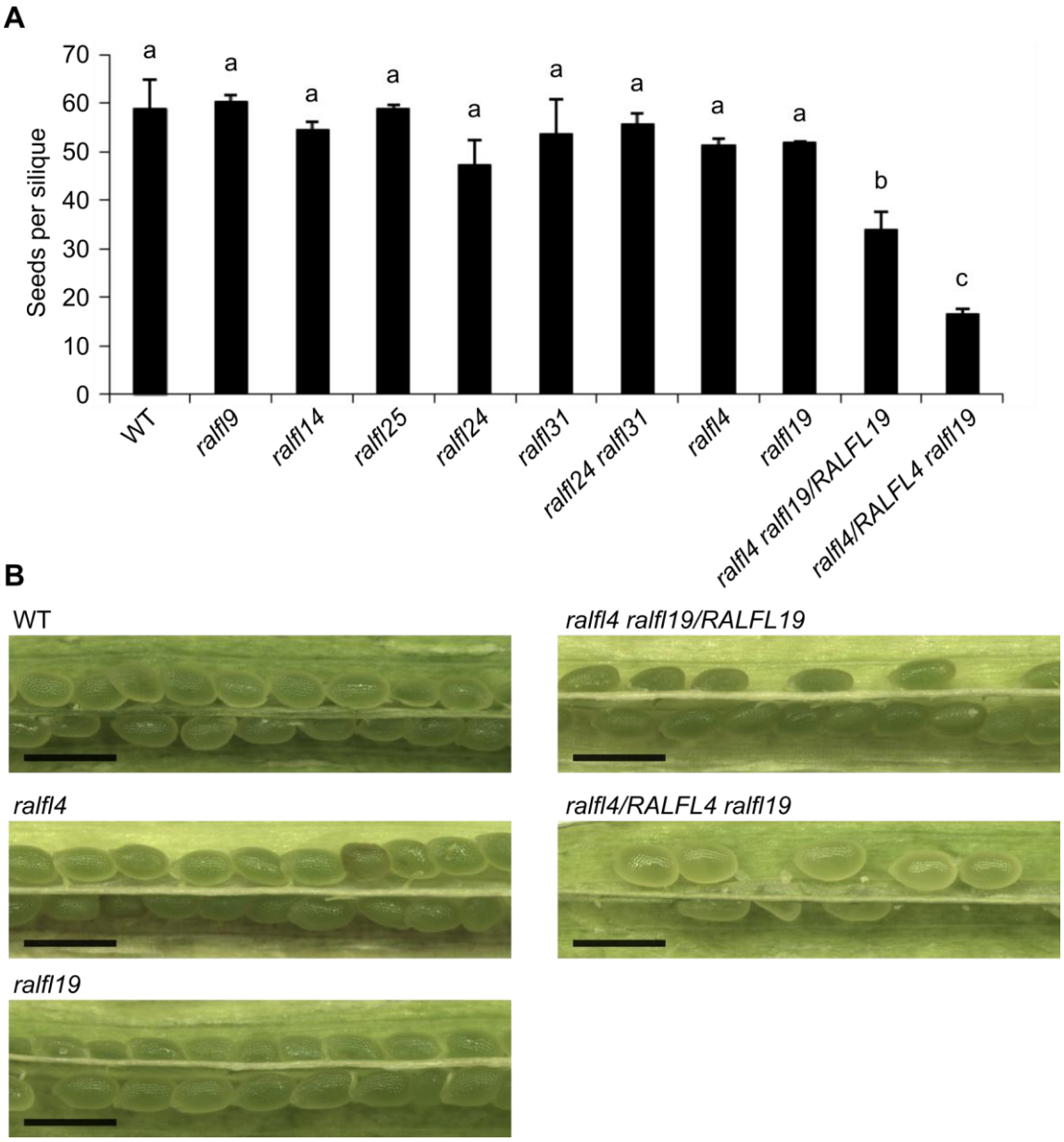

Figure 5.3 Analysis of seed set in single and double RALF T-DNA insertion lines reveal a reproductive defect in *ralfl4 ralfl19* insertion lines. A, quantification of seed production per silique. Fully expanded maturing siliques were harvested prior to dehiscence, dissected to expose the developing seeds and photographed under a stereomicroscope. Seeds were counted from five siliques per plant and three plants per line (n = 3). Data presented are means ± SD (One-way ANOVA followed by Tukey's significant difference test; $p<0.05$). **B**, representative photographs of dissected maturing siliques of WT Col-0, *ralfl4*, *ralfl19*, *ralfl4 ralfl19/RALFL19* and *ralfl4/RALFL4 ralfl19* lines that illustrate the seed production defect in the double T-DNA insertion lines. Scale bars = 1 mm.

Although no double homozygous *ralfl4 ralfl19* were found, the identification of *ralfl4*/*ralfl4 ralfl19*/*RALFL19* and *ralfl4*/*RALFL4 ralfl19*/*ralfl19* plants allowed the characterisation of gametophytic defects as 50% of the pollen grains are *ralfl4 ralfl19* in these plants.

Seed production per silique was quantified in the confirmed lines *ralfl9*, *ralfl14*, *ralfl25*, *ralfl24*, *ralfl31*, *ralfl24 ralfl31*, *ralfl4*, *ralfl19*, *ralfl4*/*ralfl4 ralfl19*/*RALFL19* and *ralfl4*/*RALFL4 ralfl19*/*ralfl19*. Reductions in seed set was interpreted as a proxy for underlying defects in fertilisation. While the single homozygous insertion lines tested and double homozygous *ralfl24 ralfl31* presented normal seed production per silique, both *ralfl4 ralfl19* homozygous/hemizygous lines displayed a significant reduction in seed set (Figure 5.3A). Dissected maturing siliques from *ralfl4*/*ralfl4 ralfl19*/*RALFL19* and *ralfl4*/*RALFL4 ralfl19*/*ralfl19* lines displayed multiple empty seed positions per silique in which ovules had not developed into seeds, suggesting the *ralfl4 ralfl19* mutation impaired fertilisation or early events during seed development (Figure 5.3B). Interestingly, the reduction in seed set was more pronounced in *ralfl4*/*RALFL4 ralfl19*/*ralfl19* than *ralfl4*/*ralfl4 ralfl19*/*RALFL19* (Figure 5.3A), and whereas this suggests *ralfl4* and *ralfl19* could have different impacts on fertility, replication of this experiment would be required to rule out possible overlooked sources of variation.

The elusiveness of double homozygous *ralfl4 ralfl19* individuals in the segregating F2 population analysed also suggested a possible requirement of functional RALF4 or RALFL19 for proper reproduction. To further confirm this hypothesis, segregation of the *ralfl4* and *ralfl19* insertions in the progeny of *ralfl4*/*ralfl4 ralfl19*/*RALFL19* and *ralfl4*/*RALFL4 ralfl19*/ralfl19 plants was analysed by genotyping PCR. Notably, while 25% of their progeny would be expected to be double homozygous, no *ralfl4 ralfl19* double homozygous individuals were isolated from either progeny (72 individuals analysed, collectively), suggesting that the double homozygous mutation is lethal (Figure 5.4). Interestingly, instead of the 1:2:1 ratio expected of Mendelian segregation of the mutations, a 1:1:0 ratio was observed instead for *ralfl4* and *ralfl19* segregating mutations (Figure 5.4). Such deviation from the expected ratio could reflect impaired transmission of the double mutation through either gametophyte, most likely through the pollen based on the predicted expression patterns for *RALFL4* and *RALFL19* (Figures 5.4 and 5.1). Collectively, these results portrayed RALFL4 and RALFL19 as potential male regulators of reproduction.

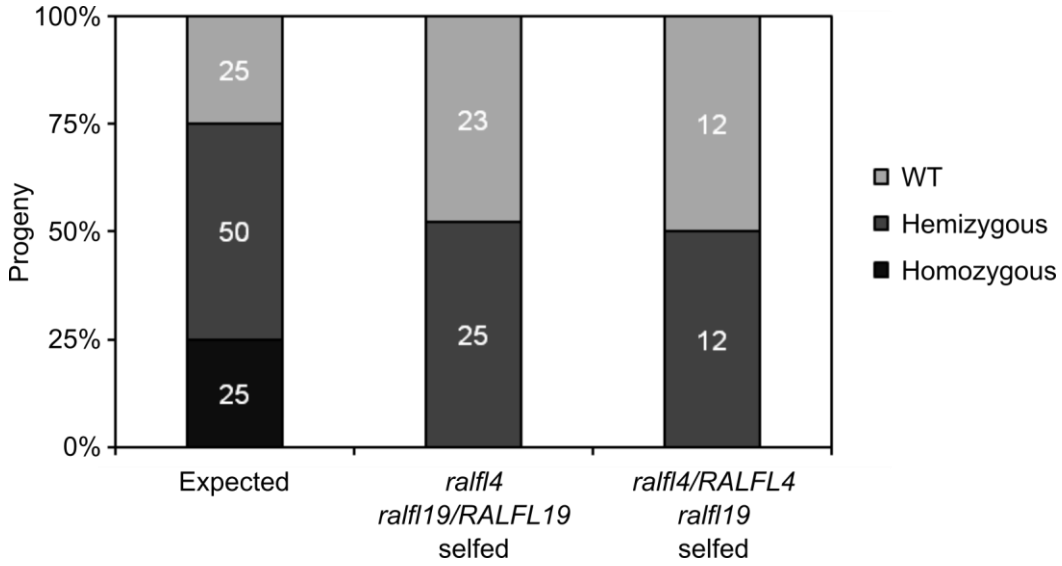

Figure 5.4 *ralfl4* and *ralfl19* mutations block the transmission of *ralfl19* and *ralfl4* T-DNA insertions, respectively. Analysis of segregation of the *ralfl19 and ralfl4* mutations in the progeny of hemizygous plants in *ralfl4* or *ralfl19* homozygous backgrounds, respectively. The column on the left exemplifies the ratio of WT, hemizygous and homozygous individuals expected from mutations that follow a Mendelian segregation ratio (1:2:1). Genotyping of the progeny of *ralfl4 ralfl19/RALFL19* and *ralfl4/RALFL4 ralfl19* selfed plants (n = 48 and 24, respectively) reveals a block in the transmission of the segregating mutations as no double homozygous individuals can be recovered.

5.2.3 RALFL4 and RALFL19 are required to sustain pollen tube tip growth in pistils

The reduction in seed production per silique observed in *ralfl4 ralfl19* segregating mutants implies these two RALFs are required for reproduction. Defects in a variety of processes could be responsible for the reduction observed in seed set, including i) gametophyte development, ii) pollen tube hydration and germination, iii) pollen tube growth, iv) communication between pollen tube and female sporophytic tissues, v) attraction of pollen tubes towards the female gametophyte, vi) intergametophytic communication and pollen tube termination, vii) fusion of gametes and viii) early defects in embryo and endosperm development (see section 4.1 of the present thesis or refer to [146, 156, 164, 231] for review). Based on the predicted expression pattern and the segregation of the respective mutations of these peptides presented in the previous section a male gametophytic defect was expected. Aiming to discern which of these steps were affected by the *ralfl4 ralfl19* mutations, pollen tube growth within female reproductive tissues was studied in the segregating mutants *ralfl4*/*ralfl4 ralfl19*/*RALFL19* and *ralfl4*/*RALFL4 ralfl19*/*ralfl19*. Aniline blue-stained, self-pollinated carpels were observed by epifluorescence microscopy to identify defects in pollen tube growth. Two carpels per plant and three plants per line were analysed and no defects

in pollen tube reception in the female gametophyte could be found; however, remarkable morphological abnormalities were observed in pollen tubes growing within the stylar tissues (Figure 5.5A). *ralfl4 ralfl19* pollen tubes appeared to generate large vesicles during their growth within the style, suggesting the tip growth that governs pollen tube growth was impaired, resulting in a loss of growth polarity (Figure 5.5A). Additionally, pollen tube morphology defects were also found when Col-0 WT plants were used as female acceptors of *ralfl4 ralfl19* segregating pollen, supporting further that RALFL4 and RALFL19 are required for stable pollen tube growth within the stylar tissues (Figure 5.5B).

Interestingly, the pollen tube growth phenotype observed in *ralfl4 ralfl19* segregating mutants was reminiscent of what had been described for the CrRLK1Ls ANXUR1 (ANX1) and ANX2 [65-66]. ANX1 and ANX2 were characterised as functionally redundant, pollen tube specific CrRLK1Ls that control pollen tube growth stability from the pollen tube plasma membrane as *anx1 anx2* pollen tubes failed to grow *in vitro* and *in vivo* [65-66]. ANX1 and ANX2 were known to maintain pollen tube growth stability via NADPH oxidase production of reactive oxygen species (ROS) in pollen tubes and the receptor-like cytoplasmic kinase MARIS (MRI; [78-79]). Additionally, ANX1 and ANX2 were hypothesised to control pollen tube growth by ensuring cell wall integrity as *ANX1* over-expressing pollen tubes were found to over-accumulate cell wall materials [79]. ANX1 and ANX2 are the most closely related Arabidopsis CrRLK1Ls to FER (see Chapter 3, Figure 3.2), receptor of RALF1 in the context of root growth and RALFL23 to modulate plant immunity, and RALF1, RALFL23, 4 and 19 are part of the same RALF cluster (Figure 5.1; [32-33]). In the light of this evidence and the preliminary results presented in this chapter, whether RALFL4 and RALFL19 represented the pollen tube specific signals sensed by ANX1 and ANX2 to maintain pollen tube growth stability constituted an exciting hypothesis to test.

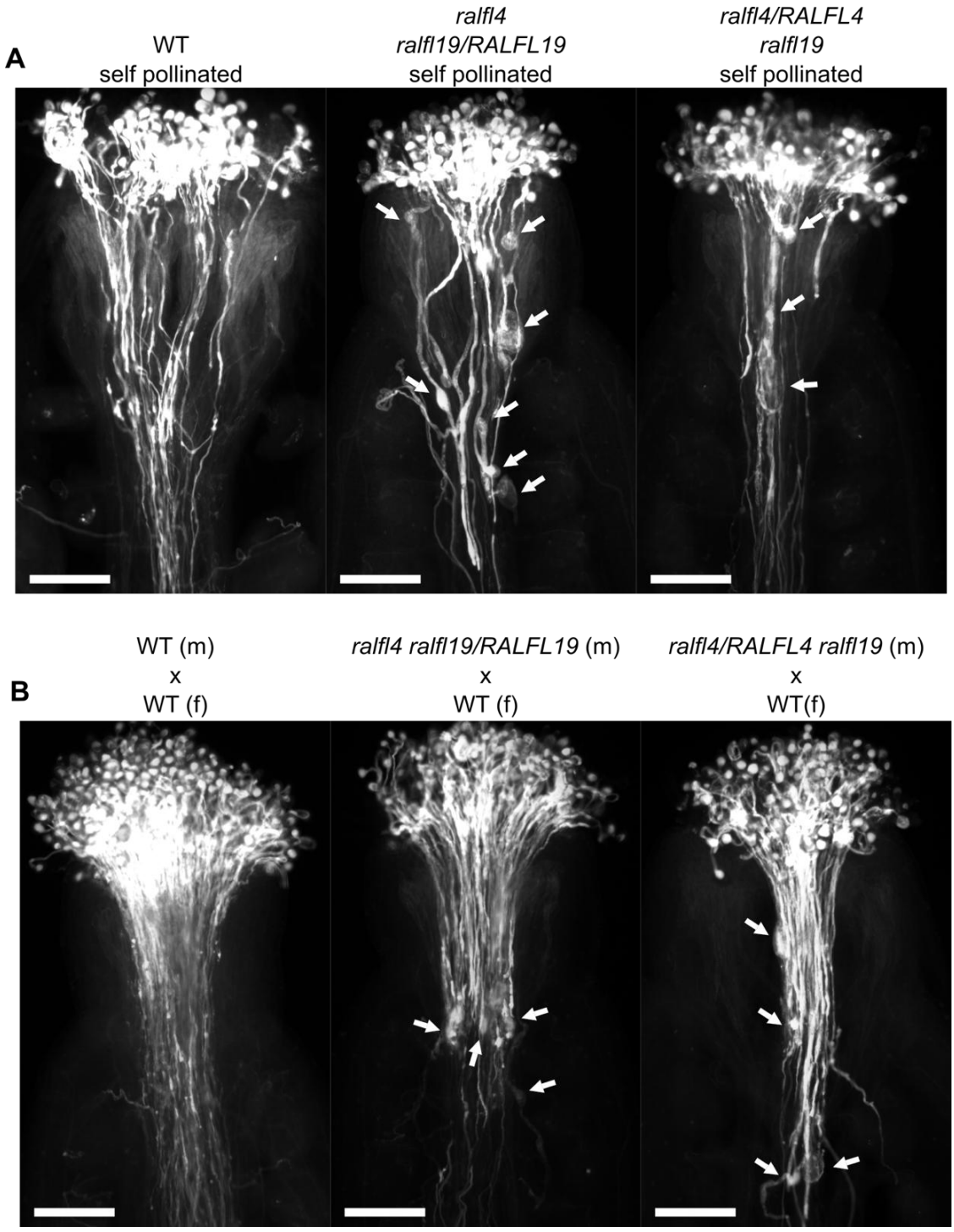

Figure 5.5 *ralfl4 ralfl19* mutation impairs pollen tube growth in pistils. A, representative images of aniline blue-stained pollen tubes growing in the pistils of WT Col-0, *ralfl4 ralfl19/RALFL19* and *ralfl4/RALFL4 ralfl19* selfed plants. White arrows indicate pollen tube abnormalities suggestive of loss of tip growth polarity. Scale bars = 100 µm. **B**, representative images of aniline blue-stained pollen tubes of WT, *ralfl4 ralfl19/RALFL19* and *ralfl4/RALFL4 ralfl19* growing on WT carpels. Pollen tube abnormalities are only observed in the pollen tubes of *ralfl4 ralfl19* mutant lines (white arrows), suggesting RALFL4 and RALFL19 influence pollen tube growth paternally. Scale bars = 100 µm.

5.2.4 RALFL4 and RALFL19 expression is mostly restricted to pollen grains

To gain insight into the role of RALFL4 and RALFL19 in the control of reproduction, transcriptional reporter lines based on *promoter::β-glucuronidase* (*GUS*) transcriptional fusions were generated to identify *RALFL4* and *RALFL19* expression patterns. Briefly, promoter regions comprising 2052 and 2079 bp upstream of the ATG start codon of *RALFL4* and *RALFL19*, respectively, were amplified from genomic DNA and cloned into entry vector *pENTR/D-TOPO*. *pRALFL4* and *pRALFL19* were subsequently transferred to destination vector *pGWB433* via LR recombination resulting in the final reporter constructs *pRALFL4::GUS* and *pRALFL19::GUS* [114]. Final constructs were transformed into Arabidopsis Col-0 WT plants by the floral dip method and transformants carrying the reporter cassettes were selected in the T1 generation by resistance to kanamycin [106].

Histochemical detection of GUS activity in T1 transformants in aerial tissues revealed strong *pRALFL4* and *pRALFL19* activity in pollen grains in anthers prior to anthesis, indicating that these RALF peptides likely accumulate in the pollen grain before pollen tube germination (Figure 5.6A and D). Detailed observation of flowers suggested *pRALFL4* and *pRALFL19* are not active in maternal tissues, in agreement with publicly available microarray data (Figure 5.6B and E; Figure 5.1). GUS activity was absent in rosette leaves, inflorescence stems and flower organs other than anthers in *pRALFL4::GUS* lines (Figure 5.6A-C). *pRALFL19* expression was not restricted to anthers and instead GUS activity could be seen in the vasculature of leaves, sepals as well as very weak activity in inflorescence stems (Figure 5.6 D-E). These observations suggested that RALFL4 and RALFL19 are pollen-derived factors required for pollen tube growth stability in female sporophytic tissues and that, in a non-reproductive context, RALFL19 is likely executing additional functions in the development of the vasculature in aerial organs of Arabidopsis.

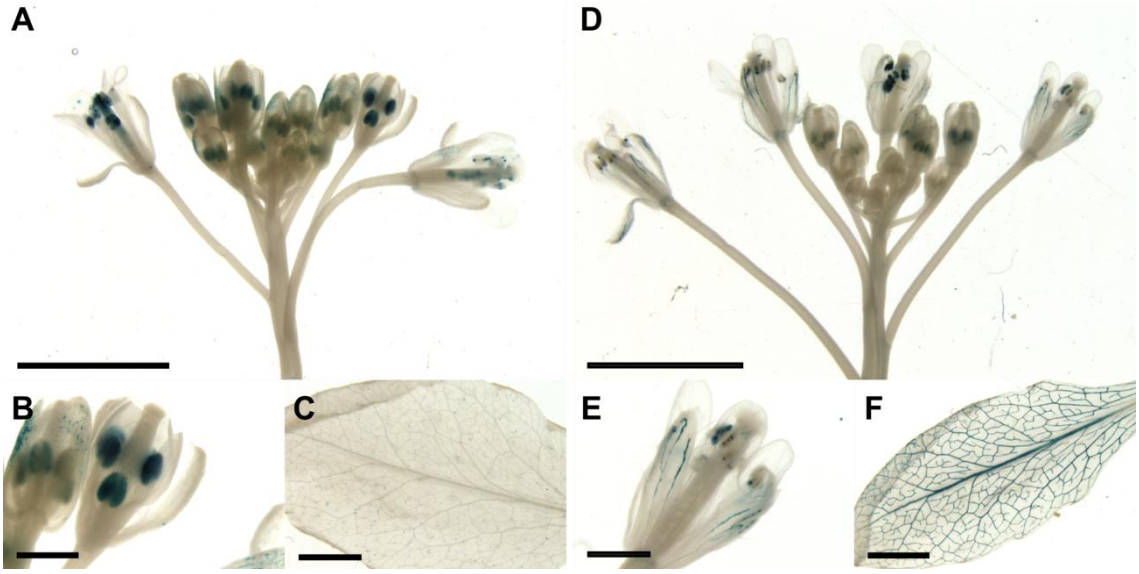

Figure 5.6 Transcriptional reporter lines reveal pollen-specific expression of *RALFL4* and *RALFL19* in reproductive organs. β-glucuronidase (GUS) histochemical analysis of T1 WT Col-0 plants harbouring a *pRALFL4::GUS* or *pRALFL19::GUS* construct (A-B and D-E, respectively). Photographs of representative inflorescences (A and D), detail of a flower (B and D) and mature rosette leaves (C and F) are presented here. *pRALFL4* activity was detected in pollen grains and within pollinated carpels exclusively (**A**-**B**). *pRALFL19* expression was found in pollen grains, pollinated carpels and in the vasculature of stems, leaves and sepals and (**D**-**F**). More than four independent T1 lines were analysed for each construct and identical expression patterns were observed. Scale bars = 5 mm (A, C, D and F); 1 mm (B and E).

5.2.5 RALFL4 and RALFL19 accumulate at the tip of pollen tubes *in vitro*

In addition to the transcriptional reporter lines described in the previous section, translational reporter lines were generated for RALF4 and RALFL19 in order to study the expression and cellular localisation of these RALF peptides in pollen grains and pollen tubes. In brief, genomic regions spanning the promoter and coding sequence excluding the stop codon of *RALFL4* and *RALFL19* were amplified and cloned via KpnI/BamHI digests into a pGreenIIS-based backbone. The resulting constructs contained the promoter and coding sequence in frame with a C-terminal GFP, constituting *pRALFL4::RALFL4-GFP* and *pRALFL19::RALFL19-GFP* reporter constructs. These constructs were transformed into Col-0 WT plants by the floral dip method and transformants were selected in the T1 generation by screening for resistance to basta conferred by said constructs.

Analysis of five independent T1 transformants per reporter line confirmed the results obtained with the GUS transcriptional reporters as strong fluorescence from both RALFL4-GFP and RALFL19-GFP could be observed in pollen grains prior to germination as seen in Figure 5.7A and C, where the reporter constructs are

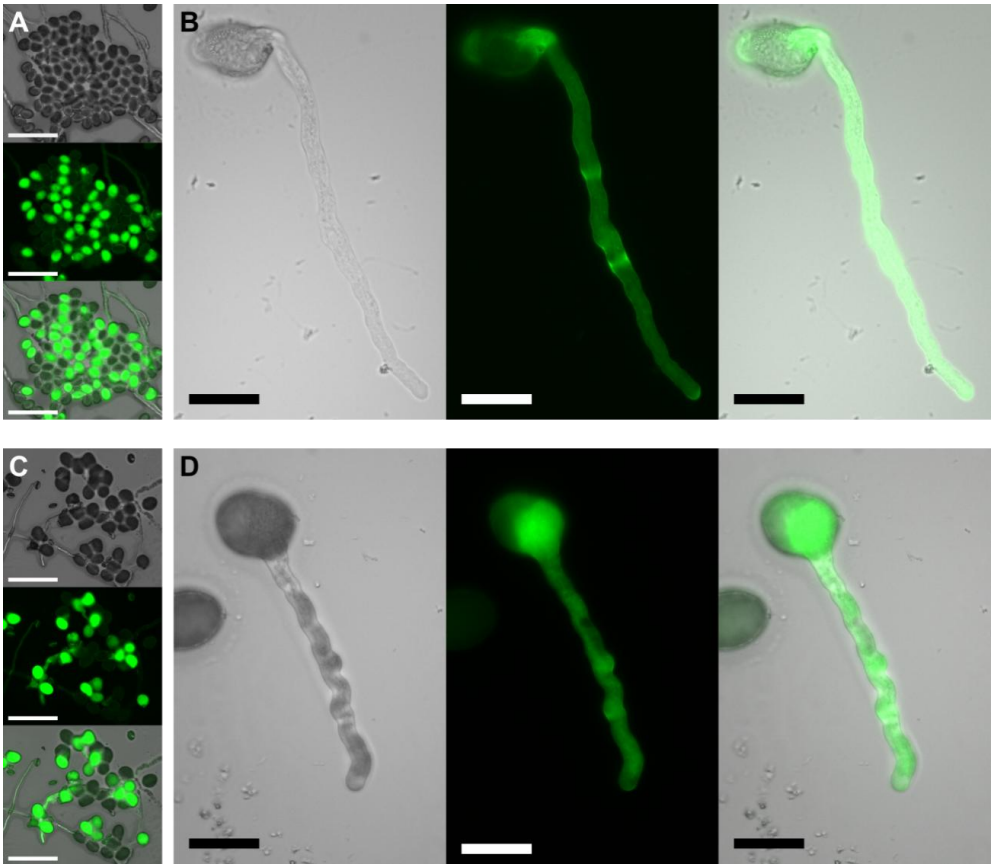

Figure 5.7 RALFL4-GFP and RALFL19-GFP accumulate in the cytoplasm of pollen grains and pollen tubes. WT Col-0 plants expressing translational reporter constructs *pRALFL4::RALFL4-GFP* or *pRALFL19::RALFL19-GFP* were analysed in the T1 generation. Representative images of *in vitro* germinated pollen grains expressing RALFL4-GFP and RALFL19-GFP are shown in A-B and C-D, respectively. **A** and **C** show images of pollen grains and germinating pollen tubes *in vitro* in which segregation of *pRALFL4::RALFL4-GFP* and *pRALFL19::RALFL19-GFP* constructs can be observed. Scale bars = 100 µm. **B** and **D** show germinated pollen tubes growing *in vitro* displaying RALFL4-GFP and RALFL19-GFP localised throughout the whole pollen tube cytoplasm. Scale bars = 25 µm. Images correspond to differential interference contrast microscopy (DIC), GFP fluorescence and merged images (top to bottom in A and C; left to right in B and D).

segregating in pollen grains from T1 plants. To study the cellular localisation of RALFL4-GFP and RALFL19-GFP in pollen tubes, an *in vitro* assay for pollen tube germination was set up in which, in brief, freshly dehisced anthers from T1 reporter plants were gently rubbed on a thin layer of solid pollen tube germination medium (10% sucrose, 0.01% boric acid, 1mM MgSO4, 5mM CaCl2, 5mM KCl and 1.5% of agarose, pH 7.5; as per [104]), and incubated in a high humidity chamber for 4-6 hours to allow for pollen tube hydration and germination. Growing pollen tubes were subsequently examined by direct observation of the *in vitro* sample under an epifluorescence microscope. RALFL4-GFP and RALFL19-GFP fluorescence could be observed throughout the cytoplasm of the growing pollen tubes whereas the pollen grain GFP

fluorescence appeared to diminish after germination, suggesting that these RALFs are redistributed throughout the growing pollen tube cytoplasm as it expands from the pollen grain (Figure 5.7B and D). Interestingly, detailed examination of the pollen tube tip area revealed that RALFL4-GFP and RALFL19-GFP accumulate at the periphery of the pollen tube tip (see Figure 5.8 for an example). Specific localisation of RALFL4 and RALFL19 at the tip of growing pollen tubes fits in the proposed model in which this pair of RALFs would be secreted at the tip of growing pollen tubes and sensed by receptors ANX1 and ANX2 to maintain pollen tube cell wall integrity.

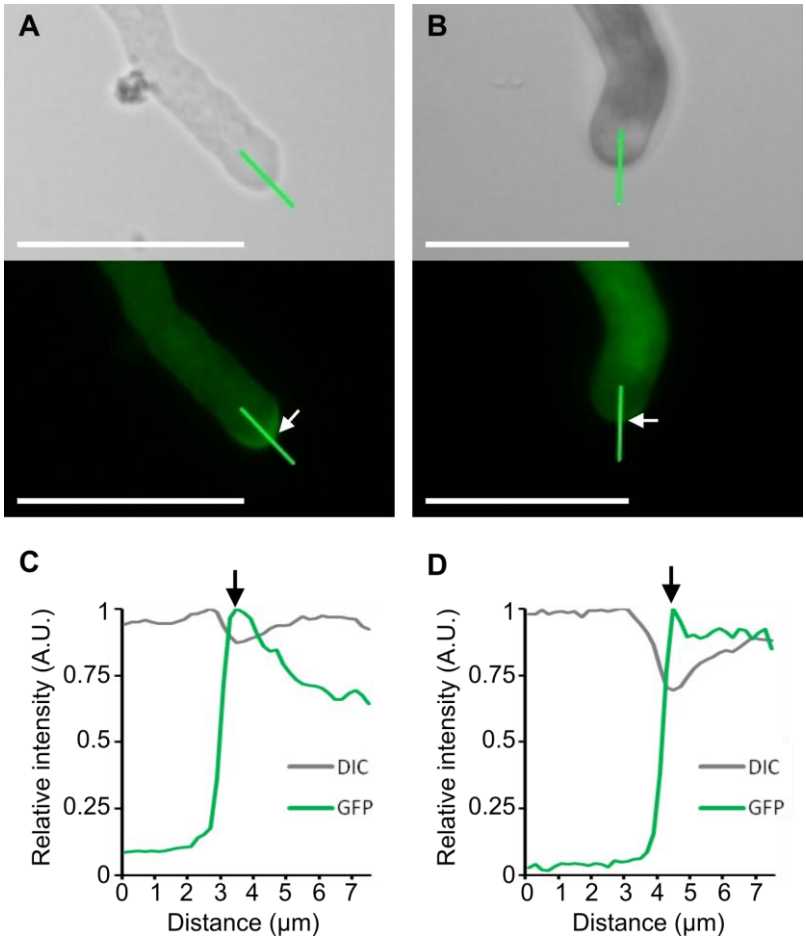

Figure 5.8 RALFL4-GFP and RALFL19-GFP accumulate at the pollen tube tip. A, detail of the tip of a RALFL4-GFP-expressing pollen tube germinated *in vitro*. Upper panel shows the DIC image and lower panel the corresponding fluorescence image. Green line, region of interest in which the intensity profile was recorded. White arrow, pollen tube tip. Scale bars = 25 µm. **B**, detail of the tip of a RALFL19-GFP-expressing pollen tube germinated *in vitro*. Upper panel shows the DIC image and lower panel the corresponding fluorescence image. Green line, region of interest in which the intensity profile was recorded. White arrow, pollen tube tip. Scale bars = 25 µm. **C**, relative intensity profiles along the region of interest in the DIC and fluorescence images shown in A (grey and green lines, respectively). Black arrow points at the section corresponding to the pollen tube tip periphery. **D**, relative intensity profiles along the region of interest in the DIC and fluorescence images shown in B (grey and green lines, respectively). Black arrow points at the section corresponding to the pollen tube tip periphery.

5.3 Discussion

The present chapter summarises preliminary results obtained in the characterisation of selected members of the Arabidopsis family of RALF peptides as regulators of reproduction. Based on the identification of CrRLK1Ls HERK1 and ANJ as synergid cell determinants of pollen tube reception (see chapter 4) and the characterisation of CrRLK1Ls as receptors of RALF peptides in previous reports [32-33], RALF peptides constituted interesting candidates to fulfil the role of signal sensed by CrRLK1Ls HERK1, ANJ and FER during pollen tube reception. Among the 37 RALF-encoding genes present in Arabidopsis genome, 15 RALFs were shortlisted as potential regulators of reproduction given their pollen- or ovary-enriched expression profiles according to publicly available gene expression databases.

A dual reverse genetics approach involving the study of T-DNA insertion lines and the generation of amiRNA lines was chosen to unravel functions in reproduction of said RALFs. The small gene size of these cysteine-rich peptides complicated the selection of T-DNA lines disrupting the coding sequence of each of the 15 RALFs and, consequently, lines with predicted insertions in coding and neighbouring regions (5' and 3' transcribed untranslated regions as well as in promoters) were obtained for 12 out of 15 shortlisted RALFs. Of these, a subset of seven T-DNA lines could be confirmed to disrupt the respective RALF genes (lines *ralfl4*, *ralfl9*, *ralfl14*, *ralfl19*, *ralfl24*, *ralfl25* and *ralfl31*). High chances of functional redundancy between phylogenetically-related RALFs among the 15 candidates based on protein similarity and predicted overlapping expression patterns prompted the generation of amiRNA-based knock-down lines targeting the putative functionally redundant RALF clades. No evidence of defective pollen tube reception was found for the amiRNA lines that were successfully generated. T-DNA lines *ralfl4*, *ralfl19*, *ralfl24* and *ralfl31* were used to generate double mutants *ralfl4 ralfl19* and *ralfl24 ralfl31*. While double homozygous mutants *ralfl24 ralfl31* were isolated, *ralfl4 ralfl19* double homozygous remained elusive and therefore plants homozygous for one mutation and hemizygous for the second were analysed (*ralfl4*/*ralfl4 ralfl19*/*RALFL19* and *ralfl4*/*RALFL4 ralfl19*/*ralfl19*). Notably, the double mutants *ralfl4 ralfl19* presented a significant reduction in seed production per silique and analysis of segregation of both mutations suggested the double mutation impaired its gametophytic transmission. Transcriptional reporter lines supported gene expression databases predictions about *RALFL4* and *RALFL19* expression patterns being specific of pollen, suggesting the reproductive defect in *ralfl4 ralfl19* mutants stems from a male gametophytic defect. Pollen tubes harbouring *ralfl4*

and *ralfl19* T-DNA insertions displayed remarkable morphological defects as they grew through the stylar tissues, suggestive of a possible loss of tip growth polarity. Furthermore, translational reporter lines indicated that RALFL4 and RALFL19 may be transported to the periphery of the tip of growing pollen tubes *in vitro*, supporting a possible role for these peptides in regulating tip growth.

This preliminary characterisation of RALFL4 and RALFL19 suggested these peptides could constitute the signal sensed by ANX1 and ANX2: pollen specific CrRLK1Ls that maintain pollen tube growth stability [65-66]. A detailed experimental plan had been drafted to pursue the characterisation of these RALFs as novel regulators of pollen tube growth including: i) testing complementation of the *ralfl4 ralfl19* mutants with *pRALFL4::RALFL4*, *pRALFL19::RALFL19*, *pRALFL4::RALFL4-GFP* and *pRALFL19:RALFL19-GFP* to confirm the pollen tube defect is caused by disruption of *RALFL4* and *RALFL19* expression as well as to ascertain the cellular localisation observed in the GFP reporter lines is representative of the true localisation of these peptides; ii) minimal pollination assays to quantify the frequency of pollen tube burst and abnormalities in the segregating *ralfl4 ralfl19* mutants; iii) confirming the defect in transmission of the *ralfl4* and *ralfl19* mutations has a paternal origin by genotyping the progeny of reciprocal crosses between WT Col-0 and the segregating *ralfl4 ralfl19* mutants; iv) characterise the *ralfl4 ralfl19* mutants pollen tube growth in *in vitro* assays looking for morphological distortions and burst; v) apply a genetic approach to test whether RALFL4 and RALFL19 are controlling pollen tube growth via the ANX1/ANX2 signalling pathway by expressing the dominant MARIS^{R240C} variant and testing rescue of the pollen tube defect in *ralfl4 ralfl19* mutants [78]; vi) produce recombinant RALFL4 and RALFL19 and test rescue of the pollen tube defects *in vitro* of the *ralfl4 ralfl19* mutants as well as mutants in the components of the ANX1/ANX2 signalling pathway [65-66, 78-79]; and finally vii) test physical interaction between these RALFs and ANX1 and ANX2 ectodomains.

Early in the development of this branch of the present thesis, two articles reporting thorough characterisation of RALFL4 and RALFL19 confirmed the role of this RALF pair as regulators of pollen tube growth stability [62, 80]. Mecchia, Ge and colleagues reported the characterisation of RALFL4 and RALFL19 as functionally redundant regulators of pollen tube growth [62, 80]. Their results confirmed this chapter's preliminary evidence as they found pollen tubes defective in RALFL4 and RALFL19 burst at the stigmatic surface or soon after penetration in the stylar tissues [62, 80]. Besides, Mecchia and colleagues observed differences in the cell wall composition of

pollen tubes with impaired *RALFL4* and *RALFL19* expression, as well as binding to the apical region and internalisation of RALFL4 in pollen tubes *in vitro* [80]. Rescue of the *ralfl4 ralfl19* fertility defect by expression of the dominant MARIS^{R240C} variant confirmed these peptides control pollen tube growth through the ANXUR-MARIS signalling pathway [78, 80]. Furthermore, RALFL4 and RALFL19 were found to physically interact with the ectodomains of ANX1, ANX2, as well as with BUDDHA'S PAPER SEAL 1 (BUPS1) and BUPS2, two novel pollen-specific CrRLK1Ls that are required for pollen tube growth [62]. Direct interactions between the ANX and BUPS ectodomains were also reported, suggesting these two groups of redundant CrRLK1Ls may form heterocomplexes that mediate sensing of RALFL4 and RALFL19 [62]. RALFL4 was also found to interact with LEUCINE-RICH REPEAT EXTENSINS (LRXs), cell wall integrity modulators that are required for correct pollen tube growth and sensing of RALF4 [80, 232-233], suggesting RALFs, LRXs and CrRLK1Ls may cooperate at the apical region of pollen tubes to maintain growth.

Very recently, the characterisation of an additional RALF-CrRLK1L ligand-receptor pair has been reported in lateral root initiation in Arabidopsis [63]. THESEUS1 (THE1) and RALFL34 fine tune cell division in the pericycle of Arabidopsis during lateral root initiation, thus expanding the list of RALF receptors to five CrRLK1Ls (FER, ANX1, ANX2, BUPS1, BUPS2 and THE1), responsible for the perception of at least five of these cysteine-rich peptides (RALF1, RALFL23, RALFL4, RALFL19 and RALFL34; [32-33, 62-63]). It now appears evident that the RALF peptides are sensed by the CrRLK1L receptor family to modulate various developmental processes. Investigating the mechanism through which these receptors integrate RALF and pectin sensing and how interactions between CrRLK1Ls with co-receptors and other membrane interactors influence their signalling will prove invaluable in understanding how cell wall integrity is maintained during cell expansion, differentiation, and defence against pathogens.

5.3.1 Future work

The role of RALFL4 and RALFL19 as pollen tube tip growth stability regulators has been thoroughly characterised [62, 80], however functions for these two peptides in additional reproductive processes awaits further investigation. For instance, RALFL4 and RALFL19 could also be of importance for the process of pollen tube reception in the female gametophyte. Ovular RALFL34 has been proposed to mediate induction of pollen tube rupture in the female gametophyte via ANX and BUPS receptors as low concentrations of RALFL34 induce rapid pollen tube burst *in vitro* and interactions between RALFL34 and ANX1/2 and BUPS1/2 ectodomains have been detected [62].

The exact mechanism through which FER, HERK1 and ANJ perceive pollen tube arrival and prime the synergid cells to induce pollen tube burst and concurrent receptive synergid degeneration is still unknown. Given that RALFL4 and RALFL19 are secreted at the pollen tube tip [62, 80], diffusion of these peptides to the filiform apparatus during pollen tube arrival is likely to occur. RALFL4 and RALFL19 could then trigger FER, HERK1 and ANJ signalling, which could in turn prompt the maturation and secretion of RALFL34 from the inner integument to the apoplastic region surrounding the female gametophyte where the pollen tube is thought to grow. The establishment of *in vitro* assays in which ovules expressing synergid cell specific reporters of Ca^{2+} and ROS are exposed to recombinant RALFL4 and RALFL19 could provide an indication of whether these peptides impact synergid signalling and whether FER, HERK1 and ANJ mediate such responses.

Preliminary results presented in this chapter show that *RALFL19* is expressed beyond pollen grains in the vasculature of leaves, sepals and stems. This suggests RALFL19 may be executing additional functions in the development of vascular tissues. Investigating RALFL19 involvement in vascular development would be an interesting path to follow as no RALFs or CrRLK1Ls have been linked to vasculature development to date. Additionally, exploring the expression of *RALFL4* and *RALFL19* in roots and other tissues, as well as upon certain stimuli like biotic and abiotic stresses would be very informative. This is of particular relevance given that ANX1 and ANX2, receptors of RALFL4 and RALFL19, although first described as pollen-specific CrRLK1Ls, have recently been demonstrated to mediate immunity during other stages of plant development and their expression profiles to be responsive to biotic stress [91]. Thus, subjecting *RALFL4* and *RALFL19* reporter lines to stimuli such as cold, heat, wounding and pathogen-associated molecular patterns could provide evidence for the involvement of these peptides in processes beyond reproduction. An interesting resource to generate to investigate additional functions of this RALF pair would be pollen-specific complemented lines in which *RALFL4* and *RALFL19* expression is restricted to pollen tubes by using pollen-specific promoters like *pLAT52* [228]. This would facilitate the characterisation of defects in double homozygous *ralfl4 ralfl19* by overcoming the severe reproductive impairment reported for these plants [62, 80]. This approach would allow the use of genetically-encoded reporters of subcellular localisation of known effectors, hormones and secondary messenger molecules like Ca^{2+} and ROS.

It is clear that we are only beginning to understand how this versatile family of peptides

governs different aspects of plant development. It is especially unclear how cluster IV RALFs are processed, perceived and, consequently, how they impact plant development. An amiRNA line targeting the cluster IV RALFL11, 12 and 13 was successfully generated in the present study and while no defects in pollen tube reception were observed in the preliminary analysis of this line, defects in other aspects of pollen maturation and pollen tube growth should not be ruled out until thorough characterisation of this line has been completed. Targeted mutagenesis of phylogenetically-related RALFs using the CRISPR/Cas9 system in combination with the generation of transcriptional and translational reporter lines would prove advantageous to obtain genetic evidence of putative functions of these RALFs [137-138].

5.3.2 Conclusions

This chapter has reported the preliminary results of a side project of this thesis conceived with the intention of identifying putative ligands of HERK1 and ANJ during the process of pollen tube reception within the RALF family of peptides. Whereas no candidate RALFs were found to control pollen tube reception, a preliminary screen of *ralf* mutants yielded the identification of RALFL4 and RALFL19 as potential regulators of pollen tube growth stability. These results were later confirmed by Mecchia, Ge and colleagues in two publications in *Science* in which these two RALFs were thoroughly characterised and put in context within the pollen tube growth signalling cascade [62, 80]. Together, these findings strengthen the connection between CrRLK1Ls and RALFs in controlling plant reproduction.

Chapter 6

General discussion

6.1 Summary of findings

Fertilisation, cell expansion and modulation of immunity are only a few of the many processes directly regulated by the *Catharanthus roseus* receptor-like kinase (RLK) 1-like (CrRLK1L) family in Arabidopsis. Extensive scrutiny of these RLKs over the last decade has portrayed them as versatile signalling hubs on which the plant cell relies to maintain homeostasis upon a multitude of external and internal cues (i.e. cell wall disruption, pathogenic signals, endogenous developmental signals and hormones). At the onset of this project, the aim was to use *Arabidopsis thaliana* as a model to explore the landscape of CrRLK1L functions in plant development and assign new functions to uncharacterised or previously studied CrRLK1Ls. The identification of HERCULES RECEPTOR KINASE 1 (HERK1) and ANJEA (ANJ) as novel reproduction determinants drew our attention and an in-depth characterisation of this pair of CrRLK1Ls in the reproductive context became the main objective of this dissertation. Experiments were designed to identify how HERK1 and ANJ regulate reproduction, whether they are functionally redundant, and to establish a link with the established FERONIA (FER), LORELEI (LRE) and NORTIA (NTA) signalling pathway. Finally, exciting results suggesting HERK1 and ANJ control pollen tube reception in a similar way to FER were obtained which, given the growing body of evidence indicating CrRLK1Ls are RAPID ALKALINISATION FACTOR (RALF) receptors, prompted a side project to investigate the Arabidopsis RALF family in search of putative HERK1, ANJ or FER reproductive ligands.

The first results chapter of this dissertation presented a compilation of preliminary assays to discover new developmental roles for a set of CrRLK1Ls (Chapter 3). These tests yielded the identification of novel functions for four CrRLK1Ls as HERK1, HERK2 and THESEUS1 (THE1) were found to influence seed germination sensitivity to exogenous abscisic acid (ABA), while HERK1 and ANJ regulate reproduction. The former was pursued further through a set of experiments that aimed to confirm the preliminary results and to deepen our understanding of the extent of the link between ABA sensitivity and CrRLK1Ls HERK1, HERK2 and THE1. Later description of the *the1-4* mutant used in this thesis as a hypermorphic allele challenged the interpretation

of ABA hypersensitivity as a result of functional redundancy between HERK1, HERK2 and THE1 [82]. Currently it is hypothesised that disruption of *HERK1* or *HERK2* primes the plant to respond in a hypersensitive manner to ABA when the truncated *THE1* gene product of *the1-4* mutation is present in the cell [82]. THE1 was reported to sense cell wall integrity disruptions and trigger inhibition of cell expansion, production of reactive oxygen species (ROS) and lignification [61, 234]. Changes in cell wall composition due to *HERK1* or *HERK2* loss of function are therefore a possible explanation for the dwarf phenotype of *herk1 the1-4* and *herk1 herk2 the1-4* mutants while remaining a less likely explanation of the ABA hypersensitivity. Exploring the sensitivity to ABA of true *the1* knockouts would shed light on the relationship between these CrRLK1Ls and this hormone. THE1 has recently been linked to cell expansion in roots and the initiation of lateral roots, processes in which THE1 acts as RALFL34 receptor [63]. Interestingly, RALFL34 signalling is partially dependent on FER, suggesting that THE1-mediated sensing of RALFL34 relies on FER [63], the underlying mechanism of which awaits clarification. Given the direct modulation of ABA signalling by FER via downstream activation of PROTEIN PHOSPHATASES 2C (PP2Cs; [97-98]), another possible scenario involves a complex CrRLK1L-interdependency in which putative CrRLK1L heterocomplexes (FER-HERK1/HERK2/THE1) would be required to maintain ABA homeostasis.

The characterisation of HERK1 and ANJ as redundant determinants of fertilisation constitutes the main research of this thesis (Chapter 4). Histochemical assays allowed the identification of the pollen tube reception phase as the stage at which HERK1 and ANJ influence reproduction. Pollen tube reception can be defined as the process during which the pollen tube enters the ovule through the micropylar pore attracted by LURE signals and establishes direct contact with the female gametophyte (Figure 6.1A-B), engaging in a molecular dialogue that concludes with the pollen tube termination and release of sperm cells to allow double fertilisation (see Figure 6.1C-F and Section 6.2 for diagram and proposed models, respectively). Crosses and genetic reporters indicated HERK1 and ANJ act as female regulators of pollen tube reception, more specifically as synergid cell, filiform apparatus-located receptors. Mutant phenotypes and subcellular localisation in the synergids suggested a common signalling pathway between HERK1/ANJ and the previously characterised FER and LRE effectors [60, 71]. Parallels between these pathways were investigated through a series of experiments from which several main conclusion could be drawn as, prior to pollen tube arrival to the female gametophyte i) there is no interdependence in synergid cellular localisation between HERK1/ANJ and other pollen tube reception effectors

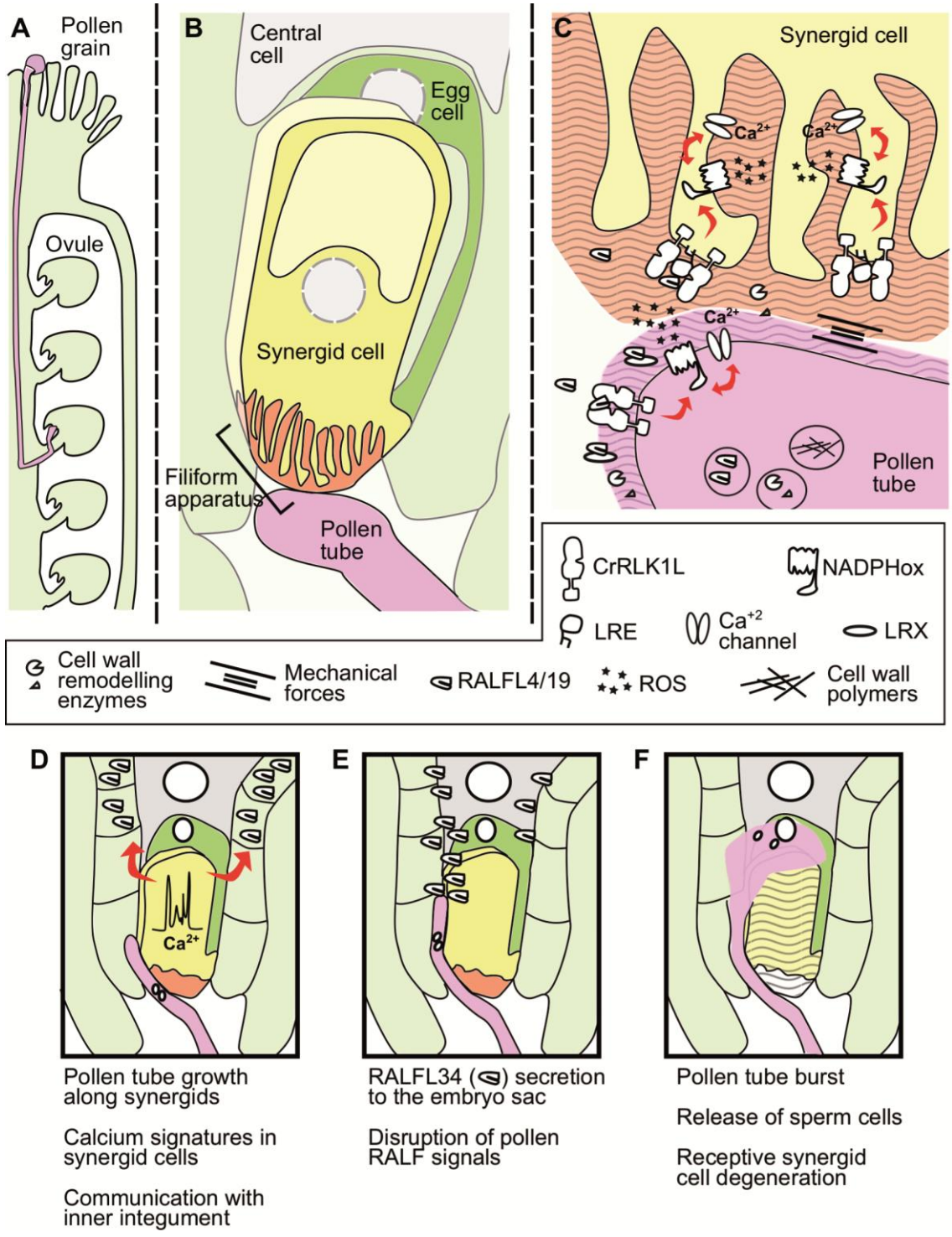

Figure 6.1 CrRLK1Ls and RALF peptides control multiple steps of reproduction. A, pollen grain germinated on the stigma surface and pollen tube growth within the ovary to target one ovule. Pollen grain and tube in pink; carpel tissues in light green. **B**, diagram of the micropylar region of an ovule during early stages of pollen tube reception. Integument layers surrounding the female gametophyte appear in light green. **C**, representation of molecular events involved in pollen tube tip growth and pollen tube reception at the filiform apparatus of the synergid cells. In pollen tubes (pink), ANX-BUPS heterodimers appear at the apical region; secretion of RALF peptides, cell wall materials and cell wall remodelling enzymes is also represented. Putative FER-LRE-HERK1 or ANJ complexes appear in the filiform apparatus (orange) of the synergid cell (yellow). Pollen tube-derived RALF signals and biochemical changes or mechanical stress

to the filiform apparatus cell wall are proposed as tentative signals perceived by FER and HERK1/ANJ CrRLK1Ls during pollen tube reception. **D-F**, stepwise representation of posterior stages of pollen tube reception at the female gametophyte. A putative mechanism of pollen tube reception and induction of pollen tube burst is proposed: pollen tube-induced Ca^{2+} signatures in the synergid cells would be sensed by neighbouring integument cells that accumulate RALFL34; secretion of mature RALFL34 to the embryo sac apoplast would allow contact between the pollen tube tip and the peptide, disrupting tube growth stability; pollen tube bursts and receptive synergid cell degenerates, allowing fertilisation.

tested (FER, LRE, NTA); and ii) FER, but not HERK1/ANJ or LRE affect the production of ROS at the micropyle in mature ovules under our growth conditions; whereas during pollen tube reception iii) HERK1/ANJ, like FER [69], affect the relocalisation of NTA in the synergids; and iv) HERK1/ANJ kinase activity is dispensable in the control of pollen tube reception, similarly to what has been reported for FER [192, 202]. These results suggested HERK1/ANJ and FER-LRE pathways share a high degree of similarity as mutants in these signalling elements displayed similar defects with the exception of the impairment of ROS production which appeared to depend on FER alone under our conditions, contrary to previous reports in which both FER and LRE are required for ROS production at the micropyle [68]. In the light of this evidence, the identification of possible protein interactions between these filiform apparatus receptors was pursued. Yeast two hybrid and co-immunoprecipitation assays indicated HERK1-LRE and ANJ-LRE complexes may form during the reception of pollen tubes. Based on previously reported FER-LRE complexes [70], our findings prompted HERK1/ANJ-LRE-FER tripartite complexes as a tentative signalling unit that mediates intergametophytic communication, a hypothesis that awaits experimental confirmation.

Finally, in the quest for pollen tube reception ligands of the synergid cell CrRLK1Ls HERK1, ANJ and FER, a reverse genetics screen of a set of RALF peptides was undertaken based on expression profiles (Chapter 5). Reproductive impairment was identified in plants lacking functional *RALFL4* and *RALFL19*, pollen tube expressed peptides according to expression databases. This RALF pair was found to influence reproduction by ensuring pollen tube growth through the stigma and style tissues, suggesting RALFL4 and RALFL19 are pollen tube growth stability factors. Because no RALFs had been genetically characterised in the process of pollen tube growth, experiments were set out to shed light on the function of these two RALFs in controlling pollen tube growth despite a lack of evidence for the involvement of RALFL4/19 in the process of pollen tube reception. Detailed examination of the RALFL4/19-defective pollen tubes suggested these peptides are involved in controlling the anisotropic pollen tube tip growth as they travel through female tissues. Crosses and analysis of the progeny of segregating mutants showed that RALFL4/19 control pollen tube growth

from the pollen tubes and that loss of both peptides blocks fertilisation. Genetic reporters confirmed *RALFL4* and *RALFL19* are pollen grain and pollen tube-expressed peptides, in agreement with gene expression databases. Additionally, examination of the subcellular localisation of fluorescent fusion proteins in pollen tubes grown *in vitro* indicated RALFL4 and RALFL19 are likely accumulating at the apical region of the pollen tubes, supporting a tip growth regulation role for these peptides. Publications by Mecchia, Ge and colleagues confirmed the findings presented in Chapter 5 of this dissertation and provided a thorough characterisation of these RALFs as regulators of pollen tube growth in a signalling pathway that involves CrRLK1Ls ANXUR1 (ANX1), ANX2, BUDDHA'S PAPER SEAL 1 (BUPS1), BUPS2 and LEUCINE-RICH REPEAT EXTENSINS (LRXs; [62, 80]; see Figure 6.1C-F and Section 6.2 for further detail).

In summary, this PhD project set out to further our understanding of the regulation of development as executed by CrRLK1Ls, and was successful in assigning putative new functions to three members of the Arabidopsis CrRLK1L family during germination, adding two novel CrRLK1Ls to the synergid cells' pollen tube reception toolbox and identifying a redundant pair of RALFs as pollen tube growth effectors. As a whole, experiments presented in this thesis provided new insights into CrRLK1L signalling and have set up a basis for future research that could help us comprehend the mechanisms underlying fertilisation and other CrRLK1L-dependent processes in plant development.

6.2 Towards a CrRLK1L signalling mechanism for pollen tube reception

This section discusses possible scenarios during pollen tube reception in the female gametophyte based on our current understanding of the molecular events underlying both pollen tube growth and synergid cell activation. Briefly, pollen tubes are attracted towards the female gametophyte by synergid cell-secreted peptidic signals, as part of a direct exchange of signals between the male and female gametophytes. A molecular dialogue takes place during pollen tube reception, in which the pollen tube grows along the synergid cells until pollen tube burst is triggered, resulting in the release of the male gametes into the embryo sac, allowing subsequent double fertilisation (Figure 6.1 C-F; see Chapter 4 introduction for detailed review). Multiple factors have been identified as pollen tube reception effectors most of which reside in the synergid cells; however, a clear signalling pathway that links all of the steps of pollen tube reception remains elusive. Three main questions remain to be answered in relation to this process:

i) **What is the nature of the signal received by the synergid cell-specific receptors HERK1, ANJ, FER and LRE?** It is commonly understood that these filiform apparatus-located membrane receptors must constitute the first layer of signal transducers in intergametophytic communication given their outermost physical localisation in the female gametophyte. As RLKs, HERK1, ANJ and FER have the potential to play the main role in informing the synergid cells of the presence of the pollen tubes, with LRE possibly acting as a co-receptor [70]. Based on previous reports, sensing of RALF peptides and cell wall materials like pectin are the two main signal candidates and a case can be made for either candidate [30-33, 62-63]. RALF peptides are known to be expressed in ovules and pollen tubes based on gene expression databases and genetic evidence (see Chapter 5). While the characterisation of ovule-derived RALF peptides involved in pollen tube reception remains elusive, the pollen tube growth stability regulators RALFL4 and RALFL19 arise as promising candidates [62, 80]. This redundant RALF pair is secreted by the growing pollen tube at the apical region and continuously internalised after binding to pollen LRXs and CrRLK1Ls ANX1/2 and BUPS1/2, maintaining pollen tube growth (Figure 6.1C; [62, 80]). Based on live imaging of the reception of pollen tubes, when the pollen tube arrives at the synergid cells its growth slows down for some time before speed is restored as it grows along the synergid cells between the female gametophyte and surrounding integument layer of the ovule (Figure 6.1B-F; [72]). This evidences a prolonged physical contact between the pollen tube tip and the filiform apparatus area, which could tentatively allow the diffusion of RALFL4/19 which could in turn reach the synergid cell HERK1, ANJ and FER RLKs and act as signals of pollen tube arrival (Figure 6.1C). Affecting the capacity of pollen tubes to sustain their growth, defects during pollen tube arrival in *ralfl4 ralfl19* mutants cannot be found due to premature burst. It is however worth noting that the fertility defect displayed by lines with low expression levels of *RALFL4* and *RALFL19* can be partially rescued by a dominant mutation of the downstream pollen tube growth signalling component MARIS (MARIS^{R240C}; [80]). This indicates that pollen tubes with constitutively active pollen tube growth signalling and very low levels of *RALFL4* and *RALFL19* expression are effectively received by the female gametophyte, although given the incomplete rescue of fertility and elusive evidence of lack of pollen tube growth in these complemented lines, it is possible to argue that low levels of RALFL4/19 are sufficient for the female gametophyte to recognise arrival of the pollen tube. Testing complementation of true *ralfl4 ralfl19* knockout lines by MARIS^{R240C} and whether these RALFs can interact with HERK1, ANJ and/or FER ectodomains could prove whether these peptides are involved in the pollen tube reception.

Cell wall perturbations are the second potential candidate signal perceived by the synergid CrRLK1Ls during pollen tube reception. As a tip growing cell, the apical region of the pollen tubes is constantly undergoing cell wall remodelling to accommodate newly deposited cell wall materials while presenting a cell wall composition different from stationary cell types as it needs to be flexible enough to allow tip growth and sufficiently strong to withstand turgor pressure [73]. Therefore, pollen tube apical regions are constantly degrading and secreting cell wall components, as well as maintaining a tip-focused, NADPH oxidase-mediated ROS production gradient that impacts the calcium transport dynamics at the apical region (Figure 6.1C; [65-66, 78-79]). Although these features are cause and consequence of the pollen tube growth, plant tissues directly in contact with the growing pollen tube tip are also subject to the effect of these biochemical modifications to some extent. It is likely that the presence of cell wall remodelling enzymes, ROS production and calcium concentration fluctuations impose changes to the filiform apparatus cell wall structure as pollen tube arrival occurs. Disruption of the filiform apparatus cell wall homeostasis could be potentially sensed by the synergid CrRLK1Ls, as has been reported for FER in salt stress-induced cell wall damage in roots [64]. Furthermore, pollen tube growth upon the filiform apparatus and along the synergid cells is likely to impose mechanical stress, another possible source of cell wall integrity disruption and a process in which FER has also been implicated in roots [125].

ii) **How is the pollen tube arrival signal transmitted to downstream synergid effectors?** During pollen tube reception, the synergid cells undergo dynamic calcium concentration changes that culminate in a calcium concentration peak coincident with pollen tube burst and receptive synergid degeneration [72]. It has been shown that FER, LRE and NTA influence the development and amplitude of the calcium signatures which argues the perception of pollen tubes by the synergid CrRLK1Ls is transduced into downstream changes in calcium dynamics [72]. The exact mechanism of signal transduction in the synergid cells is yet to be characterised although there is some evidence pointing at activation of RHO OF PLANTS (ROP) signalling, which could in turn activate membrane NADPH oxidases to produce ROS and would subsequently alter calcium channel activity (Figure 6.1C; [68]). This mechanism is based around the hypothesis of conservation of signalling pathways between FER control of root hairs and pollen tube reception. However, root hair signalling relies on FER kinase activity to phosphorylate downstream ROP GUANINE EXCHANGE FACTORS (ROPGEFs) which in turn activate ROP signalling to sustain root hair tip ROS production [74]. A similar pathway for pollen tube reception would

therefore require FER kinase capacity to phosphorylate downstream signalling components and interestingly, genetic evidence pointed to a dispensability of FER kinase activity in the reproductive context [192, 202].

In a similar line of evidence, results presented in this dissertation also indicate that the kinase activities of HERK1 and ANJ are not essential for their reproductive functions, raising the question of whether these CrRLK1Ls are actively transducing the pollen tube reception signal or acting as a co-receptors for additional unidentified RLKs that execute the kinase activity. Alternatively, it is possible that FER and HERK1/ANJ form heterocomplexes at the synergids and that the kinase activity of either interactor is sufficient for pollen tube reception. Testing protein interactions between these CrRLK1Ls and complementation of the pollen tube overgrowth phenotype in triple *herk1 anj fer-4* mutants with kinase-dead versions of FER and HERK1/ANJ would prove very informative and allow confirmation or rejection of this hypothesis. Additional unidentified synergid CrRLK1L interactors could include members of the LEUCINE-RICH REPEAT (LRR) RLK family, known to interact with FER, ANX1 and ANX2 in the context of immunity against bacterial pathogens [33, 91]. In support of this hypothesis, the seeming conservation between pollen tube reception at the synergid cells and response to pathogens is noteworthy, with both including callose accumulation, production of ROS and calcium fluctuations as well as the involvement of MILDEW RESISTANCE LOCUS O (MLO) proteins like NTA and homologs [69].

iii) **How is pollen tube burst triggered?** Pollen tube burst can be triggered *in vitro* following exposure to ROS, changes in osmotic pressure and the ovular peptide RALFL34 [62, 74, 186]. There is nevertheless no evidence to date of the direct induction of pollen tube burst by these elements *in vivo*. It has been shown that pharmacological depletion of free calcium or NADPH oxidase activity in the female gametophyte can impair pollen tube burst in the female gametophyte, indicating that free calcium and NADPH oxidase production of ROS are important elements for pollen tube reception [68]. Live imaging of calcium dynamics during pollen tube reception in the synergids argued the importance of calcium signatures during the reception of pollen tubes [72]. Given that pollen tubes require the maintenance of calcium homeostasis to sustain growth, changes in the calcium dynamics in the synergid cells could be registered by the pollen tube, and integrated in a way that leads to pollen tube burst. It is likely that prolonged disruption of pollen tube endogenous calcium dynamics as the pollen tubes grow along the synergid cell entails cumulative damage that concludes with pollen tube burst. However, recent studies have identified the ovule-

derived RALFL34 as a putative trigger of pollen tube burst as it is able to bind pollen tube CrRLK1Ls ANX1, ANX2, BUPS1 and BUPS2 with high affinity and can induce pollen tube burst *in vitro* after short exposures [62]. While genetic reporters show an ovule-specific expression pattern for *RALFL34*, mutants in this peptide are fully fertile, suggesting that either RALFL34 does not control pollen tube reception or it executes this function redundantly with additional ovular RALFs. According to Ge and colleagues, RALFL34 expression in the ovule is restricted to the central cell-surrounding cells of the integument layer, where fluorescent fusion proteins of this peptide appear to accumulate in the cytoplasm [62]. If this peptide is the trigger for pollen tube burst in redundancy with other ovular RALFs, pollen tube arrival should be specifically signalled to the integument cells expressing RALFL34 to promote its exocytosis to the embryo sac apoplast, from where RALFL34 could diffuse towards the pollen tube tip and induce its rupture (Figure 6.1D-F). Given the direct physical contact between synergid cells, growing pollen tube and the integument layer of cells in the ovule, calcium signatures produced in the synergids could be registered by the integument and transduced into secretion of RALFL34 and redundant peptides (Figure 6.1D-E). RALFL34 could consequently bind pollen CrRLK1Ls, disrupt RALFL4/19 signalling and induce pollen tube burst as has been proposed previously (Figure 6.1F). Importantly, disruption of the RALFL4/19 signalling cascade that ensures pollen tube growth stability is not sufficient to explain pollen tube burst as paternal pollen tube reception mutants that do not affect pollen tube growth stability have been reported. The *myb97 myb101 myb120* mutant displays a pollen tube overgrowth phenotype in the female gametophyte while presenting normal pollen tube growth and targeting of ovules [170]. Therefore, targets of this set of MYB transcription factors constitute pollen tube burst-specific effectors that are required for pollen tube termination and could include a parallel ANX/BUPS downstream signalling cascade that is only activated in the presence of RALFL34. Alternatively, MYB targets could represent the pollen tube derived signal perceived by the synergid cell CrRLK1Ls as the exact step of pollen tube reception at which the *myb97 myb101 myb120* mutant is affected is currently unknown. Subjecting *myb97 myb101 myb120* mutant pollen tubes to RALFL34 *in vitro* as well as characterising the synergid cell calcium signatures during reception of *myb97 myb101 myb120* mutant pollen tubes would allow us to identify the defective stage in this mutant and shed some light on the interplay between these signalling pathways.

6.3 Outlook

The regulatory scope of CrRLK1L proteins reaches beyond fertilisation as their cell wall integrity and RALF receptor roles are integral in the control of multiple processes in all stages of plant development. The use of the *Arabidopsis thaliana* as a model has proven successful in providing the scientific community with detailed molecular insights into CrRLK1L functions and signalling mechanisms. It will be of the utmost interest to start applying the knowledge generated with the model flowering plant to improve crop species of commercial and nutritional importance worldwide. At the intersection of multiple hormonal, developmental and environmental signalling cascades, the CrRLK1L proteins are candidate elements to fine tune specific plant responses in crops to our benefit. Indeed, several publications have reported the characterisation of certain CrRLK1Ls in species other than Arabidopsis, revealing they regulate similar processes to those described for the model plant. For instance, CrRLK1Ls in strawberry and apple were found to control the timing of fruit ripening by modulating ABA and ethylene signalling cascades, respectively [235-237]; pear CrRLK1Ls are key in controlling pollen tube elongation and rupture [238]; cotton fibre development, a tip growth-mediated process, was also found to be tightly associated with several CrRLK1Ls [239]; tomato heat stress responses are regulated by a brassinosteroid-induced, CrRLK1L-dependent process that involves activation of NADPH oxidases to generate ROS [240]; and finally, the common bean defence-related Co-4 cluster of genes contain several CrRLK1Ls, the transcription of which has been found to be differentially modulated upon exposure to pathogens, suggesting a link in the regulation of pathogen responses [241]. These findings evidence that, albeit subject to differences rooted in the phylogenetic distance between Arabidopsis and those species, the CrRLK1L functions in controlling ABA and ethylene signalling, abiotic and biotic stress responses appear to be conserved across plants. Additionally, research on crop species like rice has allowed the identification of further functions of the CrRLK1Ls like the repression of cell death in reproductive contexts [242]. As the main product of staple crops like rice, maize or wheat, effective seed production under varying environmental conditions is at the centre of attention of the scientific community. Pursuing the characterisation of crop CrRLK1Ls in the context of reproduction would likely help us optimise seed production under multiple conditions given the involvement of CrRLK1Ls in multiple aspects of fertilisation and stress tolerance as evidenced by multiple reports, including this dissertation. Current and future work will undoubtedly produce fruitful research into the use of these versatile signalling elements to improve the crops we rely on.

Cited literature

1. Mitrophanov, A.Y. and E.A. Groisman, *Signal integration in bacterial two-component regulatory systems.* Genes Dev, 2008. **22**(19): p. 2601-11.
2. Grefen, C. and K. Harter, *Plant two-component systems: principles, functions, complexity and cross talk.* Planta, 2004. **219**(5): p. 733-42.
3. Nongpiur, R., et al., *Histidine kinases in plants: cross talk between hormone and stress responses.* Plant Signal Behav, 2012. **7**(10): p. 1230-7.
4. Kabbara, S., T. Schmulling, and N. Papon, *CHASEing Cytokinin Receptors in Plants, Bacteria, Fungi, and Beyond.* Trends Plant Sci, 2018. **23**(3): p. 179-181.
5. Lacey, R.F. and B.M. Binder, *How plants sense ethylene gas--the ethylene receptors.* J Inorg Biochem, 2014. **133**: p. 58-62.
6. Milligan, G. and E. Kostenis, *Heterotrimeric G-proteins: a short history.* Br J Pharmacol, 2006. **147 Suppl 1**: p. S46-55.
7. Oldham, W.M. and H.E. Hamm, *Heterotrimeric G protein activation by G-protein-coupled receptors.* Nat Rev Mol Cell Biol, 2008. **9**(1): p. 60-71.
8. Urano, D. and A.M. Jones, *Heterotrimeric G protein-coupled signaling in plants.* Annu Rev Plant Biol, 2014. **65**: p. 365-84.
9. Trusov, Y. and J.R. Botella, *Plant G-Proteins Come of Age: Breaking the Bond with Animal Models.* Front Chem, 2016. **4**: p. 24.
10. Taddese, B., et al., *Do plants contain g protein-coupled receptors?* Plant Physiol, 2014. **164**(1): p. 287-307.
11. Roy Choudhury, S. and S. Pandey, *Interaction of Heterotrimeric G-Protein Components with Receptor-like Kinases in Plants: An Alternative to the Established Signaling Paradigm?* Mol Plant, 2016. **9**(8): p. 1093-1095.
12. Johnston, C.A., et al., *GTPase acceleration as the rate-limiting step in Arabidopsis G protein-coupled sugar signaling.* Proc Natl Acad Sci U S A, 2007. **104**(44): p. 17317-22.
13. Jaiswal, D.K., et al., *Time-dependent, glucose-regulated Arabidopsis Regulator of G-protein Signaling 1 network.* Current Plant Biology, 2016. **5**: p. 25-35.
14. Yu, Y., D. Chakravorty, and S.M. Assmann, *The G Protein beta-Subunit, AGB1, Interacts with FERONIA in RALF1-Regulated Stomatal Movement.* Plant Physiol, 2018. **176**(3): p. 2426-2440.
15. Liang, X., et al., *Arabidopsis heterotrimeric G proteins regulate immunity by directly coupling to the FLS2 receptor.* Elife, 2016. **5**: p. e13568.
16. Peng, Y., et al., *BRI1 and BAK1 interact with G proteins and regulate sugar-*

responsive growth and development in Arabidopsis. Nat Commun, 2018. **9**(1): p. 1522.

17. Shiu, S.H. and A.B. Bleecker, *Receptor-like kinases from Arabidopsis form a monophyletic gene family related to animal receptor kinases.* Proc Natl Acad Sci U S A, 2001. **98**(19): p. 10763-8.
18. Shiu, S.H. and A.B. Bleecker, *Plant receptor-like kinase gene family: diversity, function, and signaling.* Sci STKE, 2001. **2001**(113): p. re22.
19. Shiu, S.H. and A.B. Bleecker, *Expansion of the receptor-like kinase/Pelle gene family and receptor-like proteins in Arabidopsis.* Plant Physiol, 2003. **132**(2): p. 530-43.
20. Jill Harrison, C., *Development and genetics in the evolution of land plant body plans.* Philos Trans R Soc Lond B Biol Sci, 2017. **372**(1713).
21. Shiu, S.H., et al., *Comparative analysis of the receptor-like kinase family in Arabidopsis and rice.* Plant Cell, 2004. **16**(5): p. 1220-34.
22. Kobe, B. and J. Deisenhofer, *The leucine-rich repeat: a versatile binding motif.* Trends Biochem Sci, 1994. **19**(10): p. 415-21.
23. Kinoshita, T., et al., *Binding of brassinosteroids to the extracellular domain of plant receptor kinase BRI1.* Nature, 2005. **433**(7022): p. 167-71.
24. She, J., et al., *Structural insight into brassinosteroid perception by BRI1.* Nature, 2011. **474**(7352): p. 472-6.
25. Ogawa, M., et al., *Arabidopsis CLV3 peptide directly binds CLV1 ectodomain.* Science, 2008. **319**(5861): p. 294.
26. Santiago, J., et al., *Mechanistic insight into a peptide hormone signaling complex mediating floral organ abscission.* Elife, 2016. **5**.
27. Chinchilla, D., et al., *The Arabidopsis receptor kinase FLS2 binds flg22 and determines the specificity of flagellin perception.* Plant Cell, 2006. **18**(2): p. 465-76.
28. Zipfel, C., et al., *Perception of the bacterial PAMP EF-Tu by the receptor EFR restricts Agrobacterium-mediated transformation.* Cell, 2006. **125**(4): p. 749-60.
29. Anderson, C.M., et al., *WAKs: cell wall-associated kinases linking the cytoplasm to the extracellular matrix.* Plant Mol Biol, 2001. **47**(1-2): p. 197-206.
30. Feng, W., et al., *The FERONIA Receptor Kinase Maintains Cell-Wall Integrity during Salt Stress through Ca2+ Signaling.* Current Biology, 2018. **28**(5): p. 666-+.
31. Lin, W., et al., *FERONIA's sensing of cell wall pectin activates ROP GTPase signaling in Arabidopsis.* bioRxiv, 2018.
32. Haruta, M., et al., *A peptide hormone and its receptor protein kinase regulate*

plant cell expansion. Science, 2014. **343**(6169): p. 408-11.

33. Stegmann, M., et al., *The receptor kinase FER is a RALF-regulated scaffold controlling plant immune signaling.* Science, 2017. **355**(6322): p. 287-+.
34. Liu, T., et al., *Chitin-induced dimerization activates a plant immune receptor.* Science, 2012. **336**(6085): p. 1160-4.
35. Petutschnig, E.K., et al., *The lysin motif receptor-like kinase (LysM-RLK) CERK1 is a major chitin-binding protein in Arabidopsis thaliana and subject to chitin-induced phosphorylation.* J Biol Chem, 2010. **285**(37): p. 28902-11.
36. Iizasa, E., M. Mitsutomi, and Y. Nagano, *Direct binding of a plant LysM receptor-like kinase, LysM RLK1/CERK1, to chitin in vitro.* J Biol Chem, 2010. **285**(5): p. 2996-3004.
37. Yekondi, S., et al., *Nonredundant functions of Arabidopsis LecRK-V.2 and LecRK-VII.1 in controlling stomatal immunity and jasmonate-mediated stomatal closure.* New Phytol, 2018. **218**(1): p. 253-268.
38. Balague, C., et al., *The Arabidopsis thaliana lectin receptor kinase LecRK-I.9 is required for full resistance to Pseudomonas syringae and affects jasmonate signalling.* Mol Plant Pathol, 2017. **18**(7): p. 937-948.
39. Hohmann, U., K. Lau, and M. Hothorn, *The Structural Basis of Ligand Perception and Signal Activation by Receptor Kinases.* Annu Rev Plant Biol, 2017. **68**: p. 109-137.
40. Wang, J., et al., *Structural Insight into Recognition of Plant Peptide Hormones by Plant Receptor Kinases*, in *Plant Structural Biology: Hormonal Regulations*, J. Hejátko and T. Hakoshima, Editors. 2018, Springer International Publishing: Cham. p. 31-46.
41. Tang, J., et al., *Structural basis for recognition of an endogenous peptide by the plant receptor kinase PEPR1.* Cell Res, 2015. **25**(1): p. 110-20.
42. Torii, K.U., *Leucine-rich repeat receptor kinases in plants: structure, function, and signal transduction pathways.* Int Rev Cytol, 2004. **234**: p. 1-46.
43. Matsubayashi, Y., et al., *An LRR receptor kinase involved in perception of a peptide plant hormone, phytosulfokine.* Science, 2002. **296**(5572): p. 1470-2.
44. Wong, J.E., et al., *An intermolecular binding mechanism involving multiple LysM domains mediates carbohydrate recognition by an endopeptidase.* Acta Crystallogr D Biol Crystallogr, 2015. **71**(Pt 3): p. 592-605.
45. Ma, R., et al., *Structural basis for specific self-incompatibility response in Brassica.* Cell Res, 2016. **26**(12): p. 1320-1329.
46. Kachroo, A., M.E. Nasrallah, and J.B. Nasrallah, *Self-incompatibility in the Brassicaceae: receptor-ligand signaling and cell-to-cell communication.* Plant

Cell, 2002. **14 Suppl**: p. S227-38.

47. Du, S., L.J. Qu, and J. Xiao, *Crystal structures of the extracellular domains of the CrRLK1L receptor-like kinases ANXUR1 and ANXUR2.* Protein Sci, 2018. **27**(4): p. 886-892.
48. Moussu, S., et al., *Crystal structures of two tandem malectin-like receptor kinases involved in plant reproduction.* Acta Crystallogr D Struct Biol, 2018. **74**(Pt 7): p. 671-680.
49. Schallus, T., et al., *Malectin: a novel carbohydrate-binding protein of the endoplasmic reticulum and a candidate player in the early steps of protein N-glycosylation.* Mol Biol Cell, 2008. **19**(8): p. 3404-14.
50. Boisson-Dernier, A., S.A. Kessler, and U. Grossniklaus, *The walls have ears: the role of plant CrRLK1Ls in sensing and transducing extracellular signals.* J Exp Bot, 2011. **62**(5): p. 1581-91.
51. Lindner, H., et al., *CrRLK1L receptor-like kinases: not just another brick in the wall.* Curr Opin Plant Biol, 2012. **15**(6): p. 659-69.
52. Smith, L.M., K. Bomblies, and D. Weigel, *Complex evolutionary events at a tandem cluster of Arabidopsis thaliana genes resulting in a single-locus genetic incompatibility.* PLoS Genet, 2011. **7**(7): p. e1002164.
53. Yeh, Y.H., et al., *The Arabidopsis Malectin-Like/LRR-RLK IOS1 Is Critical for BAK1-Dependent and BAK1-Independent Pattern-Triggered Immunity.* Plant Cell, 2016. **28**(7): p. 1701-21.
54. Yang, X., F. Deng, and K.M. Ramonell, *Receptor-like kinases and receptor-like proteins: keys to pathogen recognition and defense signaling in plant innate immunity.* Frontiers in Biology, 2012. **7**(2): p. 155-166.
55. Wang, J., et al., *Allosteric receptor activation by the plant peptide hormone phytosulfokine.* Nature, 2015. **525**(7568): p. 265-8.
56. Sun, Y., et al., *Structural basis for flg22-induced activation of the Arabidopsis FLS2-BAK1 immune complex.* Science, 2013. **342**(6158): p. 624-8.
57. Castells, E. and J.M. Casacuberta, *Signalling through kinase-defective domains: the prevalence of atypical receptor-like kinases in plants.* J Exp Bot, 2007. **58**(13): p. 3503-11.
58. Schulze-Muth, P., et al., *Novel type of receptor-like protein kinase from a higher plant (Catharanthus roseus). cDNA, gene, intramolecular autophosphorylation, and identification of a threonine important for auto- and substrate phosphorylation.* J Biol Chem, 1996. **271**(43): p. 26684-9.
59. Huck, N., et al., *The Arabidopsis mutant feronia disrupts the female gametophytic control of pollen tube reception.* Development, 2003. **130**(10): p.

2149-2159.

60. Escobar-Restrepo, J.M., et al., *The FERONIA receptor-like kinase mediates male-female interactions during pollen tube reception.* Science, 2007. **317**(5838): p. 656-60.
61. Hematy, K., et al., *A receptor-like kinase mediates the response of Arabidopsis cells to the inhibition of cellulose synthesis.* Curr Biol, 2007. **17**(11): p. 922-31.
62. Ge, Z.X., et al., *Arabidopsis pollen tube integrity and sperm release are regulated by RALF-mediated signaling.* Science, 2017. **358**(6370): p. 1596-1599.
63. Gonneau, M., et al., *Receptor Kinase THESEUS1 Is a Rapid Alkalinization Factor 34 Receptor in Arabidopsis.* Current Biology, 2018.
64. Feng, W., et al., *The FERONIA Receptor Kinase Maintains Cell-Wall Integrity during Salt Stress through Ca(2+) Signaling.* Curr Biol, 2018. **28**(5): p. 666-675 e5.
65. Boisson-Dernier, A., et al., *Disruption of the pollen-expressed FERONIA homologs ANXUR1 and ANXUR2 triggers pollen tube discharge.* Development, 2009. **136**(19): p. 3279-88.
66. Miyazaki, S., et al., *ANXUR1 and 2, sister genes to FERONIA/SIRENE, are male factors for coordinated fertilization.* Curr Biol, 2009. **19**(15): p. 1327-31.
67. Schoenaers, S., et al., *The Kinase ERULUS Controls Pollen Tube Targeting and Growth in Arabidopsis thaliana.* Frontiers in Plant Science, 2017. **8**.
68. Duan, Q., et al., *Reactive oxygen species mediate pollen tube rupture to release sperm for fertilization in Arabidopsis.* Nat Commun, 2014. **5**: p. 3129.
69. Kessler, S.A., et al., *Conserved molecular components for pollen tube reception and fungal invasion.* Science, 2010. **330**(6006): p. 968-71.
70. Li, C., et al., *Glycosylphosphatidylinositol-anchored proteins as chaperones and co-receptors for FERONIA receptor kinase signaling in Arabidopsis.* Elife, 2015. **4**.
71. Tsukamoto, T., et al., *A role for LORELEI, a putative glycosylphosphatidylinositol-anchored protein, in Arabidopsis thaliana double fertilization and early seed development.* The Plant Journal, 2010. **62**(4): p. 571-588.
72. Ngo, Q.A., et al., *A Calcium Dialog Mediated by the FERONIA Signal Transduction Pathway Controls Plant Sperm Delivery.* Developmental Cell, 2014. **29**(4): p. 491-500.
73. Rounds, C.M. and M. Bezanilla, *Growth mechanisms in tip-growing plant cells.* Annu Rev Plant Biol, 2013. **64**: p. 243-65.

74. Duan, Q., et al., *FERONIA receptor-like kinase regulates RHO GTPase signaling of root hair development.* Proc Natl Acad Sci U S A, 2010. **107**(41): p. 17821-6.
75. Bai, L., et al., *A Receptor-Like Kinase Mediates Ammonium Homeostasis and Is Important for the Polar Growth of Root Hairs in Arabidopsis.* Plant Cell, 2014. **26**(4): p. 1497-1511.
76. Bai, L., et al., *Arabidopsis CAP1-mediated ammonium sensing required reactive oxygen species in plant cell growth.* Plant Signal Behav, 2014. **9**.
77. Schoenaers, S., et al., *The Auxin-Regulated CrRLK1L Kinase ERULUS Controls Cell Wall Composition during Root Hair Tip Growth.* Curr Biol, 2018. **28**(5): p. 722-732 e6.
78. Boisson-Dernier, A., et al., *Receptor-like cytoplasmic kinase MARIS functions downstream of CrRLK1L-dependent signaling during tip growth.* Proc Natl Acad Sci U S A, 2015. **112**(39): p. 12211-6.
79. Boisson-Dernier, A., et al., *ANXUR receptor-like kinases coordinate cell wall integrity with growth at the pollen tube tip via NADPH oxidases.* PLoS Biol, 2013. **11**(11): p. e1001719.
80. Mecchia, M.A., et al., *RALF4/19 peptides interact with LRX proteins to control pollen tube growth in Arabidopsis.* Science, 2017. **358**(6370): p. 1600-1603.
81. Gachomo, E.W., et al., *The Arabidopsis CURVY1 (CVY1) gene encoding a novel receptor-like protein kinase regulates cell morphogenesis, flowering time and seed production.* BMC Plant Biol, 2014. **14**: p. 221.
82. Merz, D., et al., *T-DNA alleles of the receptor kinase THESEUS1 with opposing effects on cell wall integrity signaling.* J Exp Bot, 2017. **68**(16): p. 4583-4593.
83. Du, C., et al., *Receptor kinase complex transmits RALF peptide signal to inhibit root growth in Arabidopsis.* Proc Natl Acad Sci U S A, 2016. **113**(51): p. E8326-E8334.
84. Krzesłowska, M., *The cell wall in plant cell response to trace metals: polysaccharide remodeling and its role in defense strategy.* Acta Physiologiae Plantarum, 2011. **33**(1): p. 35-51.
85. Hocq, L., J. Pelloux, and V. Lefebvre, *Connecting Homogalacturonan-Type Pectin Remodeling to Acid Growth.* Trends Plant Sci, 2017. **22**(1): p. 20-29.
86. Richter, J., et al., *Role of CrRLK1L Cell Wall Sensors HERCULES1 and 2, THESEUS1, and FERONIA in Growth Adaptation Triggered by Heavy Metals and Trace Elements.* Front Plant Sci, 2017. **8**: p. 1554.
87. Richter, J., et al., *Multiplex mutagenesis of four clustered CrRLK1L with CRISPR/Cas9 exposes their growth regulatory roles in response to metal ions.*

Sci Rep, 2018. **8**(1): p. 12182.

88. Couto, D. and C. Zipfel, *Regulation of pattern recognition receptor signalling in plants.* Nature Reviews Immunology, 2016. **16**: p. 537.
89. Shen, Q.J., et al., *Arabidopsis glycosylphosphatidylinositol-anchored protein LLG1 associates with and modulates FLS2 to regulate innate immunity.* Proceedings of the National Academy of Sciences of the United States of America, 2017. **114**(22): p. 5749-5754.
90. Dressano, K., et al., *BAK1 is involved in AtRALF1-induced inhibition of root cell expansion.* PLoS Genet, 2017. **13**(10): p. e1007053.
91. Mang, H., et al., *Differential Regulation of Two-Tiered Plant Immunity and Sexual Reproduction by ANXUR Receptor-Like Kinases.* Plant Cell, 2017. **29**(12): p. 3140-3156.
92. Masachis, S., et al., *A fungal pathogen secretes plant alkalinizing peptides to increase infection.* Nat Microbiol, 2016. **1**(6): p. 16043.
93. Wu, H.M., et al., *RAC/ROP GTPases and auxin signaling.* Plant Cell, 2011. **23**(4): p. 1208-18.
94. Mao, D., et al., *FERONIA receptor kinase interacts with S-adenosylmethionine synthetase and suppresses S-adenosylmethionine production and ethylene biosynthesis in Arabidopsis.* Plant Cell Environ, 2015. **38**(12): p. 2566-74.
95. Deslauriers, S.D. and P.B. Larsen, *FERONIA is a key modulator of brassinosteroid and ethylene responsiveness in Arabidopsis hypocotyls.* Mol Plant, 2010. **3**(3): p. 626-40.
96. Wang, K.L., H. Li, and J.R. Ecker, *Ethylene biosynthesis and signaling networks.* Plant Cell, 2002. **14 Suppl**: p. S131-51.
97. Yu, F., et al., *FERONIA receptor kinase pathway suppresses abscisic acid signaling in Arabidopsis by activating ABI2 phosphatase.* Proc Natl Acad Sci U S A, 2012. **109**(36): p. 14693-8.
98. Chen, J., et al., *FERONIA interacts with ABI2-type phosphatases to facilitate signaling cross-talk between abscisic acid and RALF peptide in Arabidopsis.* Proc Natl Acad Sci U S A, 2016. **113**(37): p. E5519-27.
99. Xing, W., et al., *The structural basis for activation of plant immunity by bacterial effector protein AvrPto.* Nature, 2007. **449**(7159): p. 243-7.
100. Wang, K., *Preface. Agrobacterium protocols.* Methods Mol Biol, 2015. **1224**: p. vii-viii.
101. Murashige, T. and F. Skoog, *A Revised Medium for Rapid Growth and Bio Assays with Tobacco Tissue Cultures.* Physiologia Plantarum, 1962. **15**(3): p. 473-497.

102. Smyth, D.R., J.L. Bowman, and E.M. Meyerowitz, *Early Flower Development in Arabidopsis.* Plant Cell, 1990. **2**(8): p. 755-767.
103. Weigel, D. and J. Glazebrook, *Setting Up Arabidopsis Crosses.* Cold Spring Harbor Protocols, 2006. **2006**(5): p. pdb.prot4623.
104. Boavida, L.C. and S. McCormick, *Temperature as a determinant factor for increased and reproducible in vitro pollen germination in Arabidopsis thaliana.* Plant J, 2007. **52**(3): p. 570-82.
105. Green, M.R. and J. Sambrook, *Molecular cloning : a laboratory manual*. 2012, Cold Spring Harbor, N.Y.: Cold Spring Harbor Laboratory Press.
106. Bent, A., *Arabidopsis thaliana floral dip transformation method.* Methods Mol Biol, 2006. **343**: p. 87-103.
107. Clough, S.J. and A.F. Bent, *Floral dip: a simplified method for Agrobacterium-mediated transformation of Arabidopsis thaliana.* Plant J, 1998. **16**(6): p. 735-43.
108. Edwards, K., C. Johnstone, and C. Thompson, *A simple and rapid method for the preparation of plant genomic DNA for PCR analysis.* Nucleic Acids Res, 1991. **19**(6): p. 1349.
109. Schwab, R., et al., *Highly specific gene silencing by artificial microRNAs in Arabidopsis.* Plant Cell, 2006. **18**(5): p. 1121-33.
110. Ho, S.N., et al., *Site-Directed Mutagenesis by Overlap Extension Using the Polymerase Chain-Reaction.* Gene, 1989. **77**(1): p. 51-59.
111. Sessions, A., et al., *A high-throughput Arabidopsis reverse genetics system.* Plant Cell, 2002. **14**(12): p. 2985-94.
112. Guo, H., et al., *Three related receptor-like kinases are required for optimal cell elongation in Arabidopsis thaliana.* Proc Natl Acad Sci U S A, 2009. **106**(18): p. 7648-53.
113. Earley, K.W., et al., *Gateway-compatible vectors for plant functional genomics and proteomics.* Plant J, 2006. **45**(4): p. 616-29.
114. Nakagawa, T., et al., *Improved Gateway Binary Vectors: High-Performance Vectors for Creation of Fusion Constructs in Transgenic Analysis of Plants.* Bioscience, Biotechnology, and Biochemistry, 2007. **71**(8): p. 2095-2100.
115. Weigel, D. and J. Glazebrook, *Transformation of Agrobacterium Using Electroporation.* Cold Spring Harbor Protocols, 2006. **2006**(7): p. pdb.prot4665.
116. Weigel, D. and J. Glazebrook, *Transformation of Agrobacterium Using the Freeze-Thaw Method.* Cold Spring Harbor Protocols, 2006. **2006**(7): p. pdb.prot4666.
117. Waadt, R. and J. Kudla, *In Planta Visualization of Protein Interactions Using*

Bimolecular Fluorescence Complementation (BiFC). Cold Spring Harbor Protocols, 2008. **2008**(4): p. pdb.prot4995.

118. Lakatos, L., et al., *Molecular mechanism of RNA silencing suppression mediated by p19 protein of tombusviruses.* The EMBO journal, 2004. **23**(4): p. 876-884.
119. Mori, T., et al., *GENERATIVE CELL SPECIFIC 1 is essential for angiosperm fertilization.* Nature Cell Biology, 2005. **8**: p. 64.
120. Christensen, C.A., et al., *Megagametogenesis in Arabidopsis wild type and the Gf mutant.* Sexual Plant Reproduction, 1997. **10**(1): p. 49-64.
121. Li, X., *Histostaining for Tissue Expression Pattern of Promoter-driven GUS Activity in Arabidopsis.* Bio-protocol, 2011. **1**(13): p. e93.
122. Cheung, A.Y. and H.M. Wu, *THESEUS 1, FERONIA and relatives: a family of cell wall-sensing receptor kinases?* Curr Opin Plant Biol, 2011. **14**(6): p. 632-41.
123. Galindo-Trigo, S., J.E. Gray, and L.M. Smith, *Conserved Roles of CrRLK1L Receptor-Like Kinases in Cell Expansion and Reproduction from Algae to Angiosperms.* Front Plant Sci, 2016. **7**: p. 1269.
124. Honkanen, S., et al., *The Mechanism Forming the Cell Surface of Tip-Growing Rooting Cells Is Conserved among Land Plants.* Curr Biol, 2017. **27**(20): p. 3224.
125. Shih, H.W., et al., *The receptor-like kinase FERONIA is required for mechanical signal transduction in Arabidopsis seedlings.* Curr Biol, 2014. **24**(16): p. 1887-92.
126. Guo, H., et al., *A family of receptor-like kinases are regulated by BES1 and involved in plant growth in Arabidopsis thaliana.* Plant Signal Behav, 2009. **4**(8): p. 784-6.
127. Larkin, M.A., et al., *Clustal W and Clustal X version 2.0.* Bioinformatics, 2007. **23**(21): p. 2947-8.
128. Saitou, N. and M. Nei, *The neighbor-joining method: a new method for reconstructing phylogenetic trees.* Mol Biol Evol, 1987. **4**(4): p. 406-25.
129. Tamura, K., et al., *MEGA5: molecular evolutionary genetics analysis using maximum likelihood, evolutionary distance, and maximum parsimony methods.* Mol Biol Evol, 2011. **28**(10): p. 2731-9.
130. Fanelli, D., *Opinion: Is science really facing a reproducibility crisis, and do we need it to?* Proceedings of the National Academy of Sciences, 2018.
131. Casadevall, A. and F.C. Fang, *Reproducible Science.* Infection and Immunity, 2010. **78**(12): p. 4972-4975.
132. Baker, M., *1,500 scientists lift the lid on reproducibility.* Nature, 2016.

533(7604): p. 452-4.

133. Dodd, I.C., *Abscisic acid and stomatal closure: a hydraulic conductance conundrum?* New Phytol, 2013. **197**(1): p. 6-8.
134. Gaff, D.F. and B.R. Loveys, *Abscisic Acid Content and Effects During Dehydration of Detached Leaves of Desiccation Tolerant Plants.* Journal of Experimental Botany, 1984. **35**(9): p. 1350-1358.
135. Ghassemian, M., et al., *Regulation of abscisic acid signaling by the ethylene response pathway in Arabidopsis.* Plant Cell, 2000. **12**(7): p. 1117-26.
136. Franck, C.M., J. Westermann, and A. Boisson-Dernier, *Plant Malectin-Like Receptor Kinases: From Cell Wall Integrity to Immunity and Beyond.* Annu Rev Plant Biol, 2018. **69**: p. 301-328.
137. Bortesi, L. and R. Fischer, *The CRISPR/Cas9 system for plant genome editing and beyond.* Biotechnology Advances, 2015. **33**(1): p. 41-52.
138. Ran, F.A., et al., *Genome engineering using the CRISPR-Cas9 system.* Nature Protocols, 2013. **8**: p. 2281.
139. O'Malley, R.C., C.C. Barragan, and J.R. Ecker, *A User's Guide to the Arabidopsis T-DNA Insertion Mutant Collections*, in *Plant Functional Genomics: Methods and Protocols*, J.M. Alonso and A.N. Stepanova, Editors. 2015, Springer New York: New York, NY. p. 323-342.
140. O'Malley Ronan, C. and R. Ecker Joseph, *Linking genotype to phenotype using the Arabidopsis unimutant collection.* The Plant Journal, 2010. **61**(6): p. 928-940.
141. Alonso, J.M., et al., *Genome-wide Insertional mutagenesis of Arabidopsis thaliana.* Science, 2003. **301**(5633): p. 653-657.
142. Zhang, J., et al., *Sperm cells are passive cargo of the pollen tube in plant fertilization.* Nat Plants, 2017. **3**: p. 17079.
143. Maruyama, D., et al., *Independent Control by Each Female Gamete Prevents the Attraction of Multiple Pollen Tubes.* Developmental Cell, 2013. **25**(3): p. 317-323.
144. Maruyama, D., et al., *Rapid Elimination of the Persistent Synergid through a Cell Fusion Mechanism.* Cell, 2015. **161**(4): p. 907-918.
145. Yan, D.W., et al., *The Functions of the Endosperm During Seed Germination.* Plant and Cell Physiology, 2014. **55**(9): p. 1521-1533.
146. Dresselhaus, T., S. Sprunck, and G.M. Wessel, *Fertilization Mechanisms in Flowering Plants.* Current Biology, 2016. **26**(3): p. R125-R139.
147. Doyle, J.A., *Molecular and Fossil Evidence on the Origin of Angiosperms.* Annual Review of Earth and Planetary Sciences, Vol 40, 2012. **40**: p. 301-326.

148. Dresselhaus, T. and N. Franklin-Tong, *MaleFemale Crosstalk during Pollen Germination, Tube Growth and Guidance, and Double Fertilization.* Molecular Plant, 2013. **6**(4): p. 1018-1036.
149. Heizmann, P., D.T. Luu, and C. Dumas, *Pollen-stigma adhesion in the Brassicaceae.* Annals of Botany, 2000. **85**: p. 23-27.
150. Ma, J.F., et al., *Different regulatory processes control pollen hydration and germination in Arabidopsis.* Sexual Plant Reproduction, 2012. **25**(1): p. 77-82.
151. Edlund, A.F., R. Swanson, and D. Preuss, *Pollen and stigma structure and function: The role of diversity in pollination.* Plant Cell, 2004. **16**: p. S84-S97.
152. Kim, S., et al., *Chemocyanin, a small basic protein from the lily stigma, induces pollen tube chemotropism.* Proceedings of the National Academy of Sciences of the United States of America, 2003. **100**(26): p. 16125-16130.
153. Dong, J., S.T. Kim, and E.M. Lord, *Plantacyanin plays a role in reproduction in Arabidopsis.* Plant Physiology, 2005. **138**(2): p. 778-789.
154. Chen, Y.H., M.X. Zou, and Y.Y. Cao, *Transcriptome analysis of the Arabidopsis semi-In vivo pollen tube guidance system uncovers a distinct gene expression profile.* Journal of Plant Biology, 2014. **57**(2): p. 93-105.
155. Higashiyama, T., et al., *Pollen tube attraction by the synergid cell.* Science, 2001. **293**(5534): p. 1480-1483.
156. Higashiyama, T. and W.C. Yang, *Gametophytic Pollen Tube Guidance: Attractant Peptides, Gametic Controls, and Receptors.* Plant Physiology, 2017. **173**(1): p. 112-121.
157. Okuda, S., et al., *Defensin-like polypeptide LUREs are pollen tube attractants secreted from synergid cells.* Nature, 2009. **458**(7236): p. 357-U122.
158. Takeuchi, H. and T. Higashiyama, *A Species-Specific Cluster of Defensin-Like Genes Encodes Diffusible Pollen Tube Attractants in Arabidopsis.* Plos Biology, 2012. **10**(12).
159. Wang, T., et al., *A receptor heteromer mediates the male perception of female attractants in plants.* Nature, 2016. **531**(7593): p. 241-+.
160. Takeuchi, H. and T. Higashiyama, *Tip-localized receptors control pollen tube growth and LURE sensing in Arabidopsis.* Nature, 2016. **531**(7593): p. 245-+.
161. Zhang, X.X., et al., *Structural basis for receptor recognition of pollen tube attraction peptides.* Nature Communications, 2017. **8**.
162. Liu, J., et al., *Membrane-bound RLCKs LIP1 and LIP2 are essential male factors controlling male-female attraction in Arabidopsis.* Curr Biol, 2013. **23**(11): p. 993-8.
163. Krichevsky, A., et al., *How pollen tubes grow.* Developmental Biology, 2007.

303(2): p. 405-420.

164. Higashiyama, T. and H. Takeuchi, *The mechanism and key molecules involved in pollen tube guidance.* Annu Rev Plant Biol, 2015. **66**: p. 393-413.
165. Lindner, H., et al., *TURAN and EVAN Mediate Pollen Tube Reception in Arabidopsis Synergids through Protein Glycosylation.* Plos Biology, 2015. **13**(4).
166. Huang, B.-Q. and S.D. Russell, *Female Germ Unit: Organization, Isolation, and Function*, in *International Review of Cytology*, S.D. Russell and C. Dumas, Editors. 1992, Academic Press. p. 233-293.
167. Jones, D.S. and S.A. Kessler, *Cell type-dependent localization of MLO proteins.* Plant Signaling & Behavior, 2017. **12**(11).
168. Davis, T.C., et al., *Arabidopsis thaliana MLO genes are expressed in discrete domains during reproductive development.* Plant Reproduction, 2017. **30**(4): p. 185-195.
169. Boisson-Dernier, A., et al., *The peroxin loss-of-function mutation abstinence by mutual consent disrupts male-female gametophyte recognition.* Curr Biol, 2008. **18**(1): p. 63-8.
170. Leydon, A.R., et al., *Three MYB transcription factors control pollen tube differentiation required for sperm release.* Curr Biol, 2013. **23**(13): p. 1209-14.
171. Cordts, S., et al., *ZmES genes encode peptides with structural homology to defensins and are specifically expressed in the female gametophyte of maize.* Plant J, 2001. **25**(1): p. 103-14.
172. Amien, S., et al., *Defensin-like ZmES4 mediates pollen tube burst in maize via opening of the potassium channel KZM1.* PLoS Biol, 2010. **8**(6): p. e1000388.
173. Rockel, N., et al., *Elaborate spatial patterning of cell-wall PME and PMEI at the pollen tube tip involves PMEI endocytosis, and reflects the distribution of esterified and de-esterified pectins.* Plant J, 2008. **53**(1): p. 133-43.
174. Paynel, F., et al., *Kiwi fruit PMEI inhibits PME activity, modulates root elongation and induces pollen tube burst in Arabidopsis thaliana.* Plant Growth Regulation, 2014. **74**(3): p. 285-297.
175. Stegmann, M. and C. Zipfel, *Complex regulation of plant sex by peptides.* Science, 2017. **358**(6370): p. 1544-1545.
176. Hamamura, Y., et al., *Live-cell imaging reveals the dynamics of two sperm cells during double fertilization in Arabidopsis thaliana.* Curr Biol, 2011. **21**(6): p. 497-502.
177. Ingouff, M., et al., *The two male gametes share equal ability to fertilize the egg cell in Arabidopsis thaliana.* Curr Biol, 2009. **19**(1): p. R19-20.
178. Mori, T., et al., *Gamete attachment requires GEX2 for successful fertilization in*

Arabidopsis. Curr Biol, 2014. **24**(2): p. 170-5.

179. Sprunck, S., et al., *Egg cell-secreted EC1 triggers sperm cell activation during double fertilization.* Science, 2012. **338**(6110): p. 1093-7.
180. Kawashima, T., et al., *Dynamic F-actin movement is essential for fertilization in Arabidopsis thaliana.* Elife, 2014. **3**.
181. Beale, K.M., A.R. Leydon, and M.A. Johnson, *Gamete Fusion Is Required to Block Multiple Pollen Tubes from Entering an Arabidopsis Ovule.* Current Biology, 2012. **22**(12): p. 1090-1094.
182. Zhang, X., et al., *Agrobacterium-mediated transformation of Arabidopsis thaliana using the floral dip method.* Nat Protoc, 2006. **1**(2): p. 641-6.
183. Capron, A., et al., *Maternal Control of Male-Gamete Delivery in Arabidopsis Involves a Putative GPI-Anchored Protein Encoded by the LORELEI Gene.* Plant Cell, 2008. **20**(11): p. 3038-3049.
184. Yadegari, R. and G.N. Drews, *Female gametophyte development.* Plant Cell, 2004. **16**: p. S133-S141.
185. Kasahara, R.D., et al., *MYB98 is required for pollen tube guidance and synergid cell differentiation in Arabidopsis.* Plant Cell, 2005. **17**(11): p. 2981-92.
186. Potocky, M., et al., *Reactive oxygen species produced by NADPH oxidase are involved in pollen tube growth.* New Phytol, 2007. **174**(4): p. 742-51.
187. Wudick, M.M. and J.A. Feijo, *At the intersection: merging Ca2+ and ROS signaling pathways in pollen.* Mol Plant, 2014. **7**(11): p. 1595-1597.
188. Alvarez-Buylla, E.R., et al., *Flower Development.* The Arabidopsis Book / American Society of Plant Biologists, 2010. **8**: p. e0127.
189. Costa, A., et al., *H2O2 in plant peroxisomes: an in vivo analysis uncovers a Ca(2+)-dependent scavenging system.* Plant J, 2010. **62**(5): p. 760-72.
190. Aller, I., N. Rouhier, and A.J. Meyer, *Development of roGFP2-derived redox probes for measurement of the glutathione redox potential in the cytosol of severely glutathione-deficient rml1 seedlings.* Front Plant Sci, 2013. **4**: p. 506.
191. Wolf, S., *Plant cell wall signalling and receptor-like kinases.* Biochem J, 2017. **474**(4): p. 471-492.
192. Kessler, S.A., et al., *Functional analysis of related CrRLK1L receptor-like kinases in pollen tube reception.* EMBO Rep, 2015. **16**(1): p. 107-15.
193. Liu, X., et al., *The Role of LORELEI in Pollen Tube Reception at the Interface of the Synergid Cell and Pollen Tube Requires the Modified Eight-Cysteine Motif and the Receptor-Like Kinase FERONIA.* Plant Cell, 2016. **28**(5): p. 1035-52.
194. Dong, G.Q. and D.R. McMillen, *Effects of protein maturation on the noise in gene expression.* Phys Rev E Stat Nonlin Soft Matter Phys, 2008. **77**(2 Pt 1): p.

021908.

195. Li, N. and Y. Li, *Maternal control of seed size in plants.* J Exp Bot, 2015. **66**(4): p. 1087-97.
196. Yu, F., et al., *FERONIA receptor kinase controls seed size in Arabidopsis thaliana.* Mol Plant, 2014. **7**(5): p. 920-2.
197. Hou, Y.N., et al., *Maternal ENODLs Are Required for Pollen Tube Reception in Arabidopsis.* Current Biology, 2016. **26**(17): p. 2343-2350.
198. Chebli, Y., et al., *The Cell Wall of the Arabidopsis Pollen Tube-Spatial Distribution, Recycling, and Network Formation of Polysaccharides.* Plant Physiology, 2012. **160**(4): p. 1940-1955.
199. Higashiyama, T. and W.C. Yang, *Gametophytic Pollen Tube Guidance: Attractant Peptides, Gametic Controls, and Receptors.* Plant Physiol, 2017. **173**(1): p. 112-121.
200. Greeff, C., et al., *Receptor-like kinase complexes in plant innate immunity.* Frontiers in Plant Science, 2012. **3**.
201. Burkart, R.C. and Y. Stahl, *Dynamic complexity: plant receptor complexes at the plasma membrane.* Current Opinion in Plant Biology, 2017. **40**: p. 15-21.
202. Haruta, M., et al., *Comparison of the effects of a kinase-dead mutation of FERONIA on ovule fertilization and root growth of Arabidopsis.* FEBS Lett, 2018.
203. Hernández-Barrera, A., et al., *Chapter Fifteen - Using Hyper as a Molecular Probe to Visualize Hydrogen Peroxide in Living Plant Cells: A Method with Virtually Unlimited Potential in Plant Biology*, in *Methods in Enzymology*, E. Cadenas and L. Packer, Editors. 2013, Academic Press. p. 275-290.
204. Van Norman, J.M., N.W. Breakfield, and P.N. Benfey, *Intercellular communication during plant development.* Plant Cell, 2011. **23**(3): p. 855-64.
205. De Coninck, B. and I. De Smet, *Plant peptides - taking them to the next level.* J Exp Bot, 2016. **67**(16): p. 4791-5.
206. Zhang, H., et al., *Structural Insight into Recognition of Plant Peptide Hormones by Receptors.* Mol Plant, 2016. **9**(11): p. 1454-1463.
207. Tabata, R. and S. Sawa, *Maturation processes and structures of small secreted peptides in plants.* Front Plant Sci, 2014. **5**: p. 311.
208. Yamaguchi, Y.L., T. Ishida, and S. Sawa, *CLE peptides and their signaling pathways in plant development.* J Exp Bot, 2016. **67**(16): p. 4813-26.
209. Liu, X., et al., *Expansion and evolutionary patterns of cysteine-rich peptides in plants.* BMC Genomics, 2017. **18**(1): p. 610.
210. Pearce, G., et al., *RALF, a 5-kDa ubiquitous polypeptide in plants, arrests root*

growth and development. Proc Natl Acad Sci U S A, 2001. **98**(22): p. 12843-7.

211. Haruta, M. and C.P. Constabel, *Rapid alkalinization factors in poplar cell cultures. Peptide isolation, cDNA cloning, and differential expression in leaves and methyl jasmonate-treated cells.* Plant Physiol, 2003. **131**(2): p. 814-23.
212. Mingossi, F.B., et al., *SacRALF1, a peptide signal from the grass sugarcane (Saccharum spp.), is potentially involved in the regulation of tissue expansion.* Plant Mol Biol, 2010. **73**(3): p. 271-81.
213. Covey, P.A., et al., *A pollen-specific RALF from tomato that regulates pollen tube elongation.* Plant Physiol, 2010. **153**(2): p. 703-15.
214. Germain, H., et al., *Characterization of five RALF-like genes from Solanum chacoense provides support for a developmental role in plants.* Planta, 2005. **220**(3): p. 447-54.
215. Chevalier, E., A. Loubert-Hudon, and D.P. Matton, *ScRALF3, a secreted RALF-like peptide involved in cell-cell communication between the sporophyte and the female gametophyte in a solanaceous species.* Plant J, 2013. **73**(6): p. 1019-33.
216. Cao, J. and F. Shi, *Evolution of the RALF Gene Family in Plants: Gene Duplication and Selection Patterns.* Evolutionary Bioinformatics Online, 2012. **8**: p. 271-292.
217. Campbell, L. and S.R. Turner, *A Comprehensive Analysis of RALF Proteins in Green Plants Suggests There Are Two Distinct Functional Groups.* Front Plant Sci, 2017. **8**: p. 37.
218. Srivastava, R., et al., *Regulation and processing of a plant peptide hormone, AtRALF23, in Arabidopsis.* The Plant Journal, 2009. **59**(6): p. 930-939.
219. Matos, J.L., et al., *A conserved dibasic site is essential for correct processing of the peptide hormone AtRALF1 in Arabidopsis thaliana.* FEBS Lett, 2008. **582**(23-24): p. 3343-7.
220. Pearce, G., et al., *Structure-activity studies of RALF, Rapid Alkalinization Factor, reveal an essential--YISY--motif.* Peptides, 2010. **31**(11): p. 1973-7.
221. Hruz, T., et al., *Genevestigator v3: a reference expression database for the meta-analysis of transcriptomes.* Adv Bioinformatics, 2008. **2008**: p. 420747.
222. Atkinson, N.J., C.J. Lilley, and P.E. Urwin, *Identification of genes involved in the response of Arabidopsis to simultaneous biotic and abiotic stresses.* Plant Physiol, 2013. **162**(4): p. 2028-41.
223. Morato do Canto, A., et al., *Biological activity of nine recombinant AtRALF peptides: Implications for their perception and function in Arabidopsis.* Plant Physiology and Biochemistry, 2014. **75**: p. 45-54.

224. Bergonci, T., et al., *Arabidopsis thaliana RALF1 opposes brassinosteroid effects on root cell elongation and lateral root formation.* Journal of Experimental Botany, 2014. **65**(8): p. 2219-2230.
225. Haruta, M., et al., *A cytoplasmic Ca2+ functional assay for identifying and purifying endogenous cell signaling peptides in Arabidopsis seedlings: identification of AtRALF1 peptide.* Biochemistry, 2008. **47**(24): p. 6311-21.
226. Steffen, J.G., et al., *Identification of genes expressed in the Arabidopsis female gametophyte.* Plant J, 2007. **51**(2): p. 281-92.
227. Ossowski, S., R. Schwab, and D. Weigel, *Gene silencing in plants using artificial microRNAs and other small RNAs.* Plant J, 2008. **53**(4): p. 674-90.
228. Twell, D., et al., *Promoter analysis of genes that are coordinately expressed during pollen development reveals pollen-specific enhancer sequences and shared regulatory elements.* Genes Dev, 1991. **5**(3): p. 496-507.
229. Desfeux, C., S.J. Clough, and A.F. Bent, *Female reproductive tissues are the primary target of Agrobacterium-mediated transformation by the Arabidopsis floral-dip method.* Plant Physiol, 2000. **123**(3): p. 895-904.
230. Ye, G.N., et al., *Arabidopsis ovule is the target for Agrobacterium in planta vacuum infiltration transformation.* Plant J, 1999. **19**(3): p. 249-57.
231. Bleckmann, A., S. Alter, and T. Dresselhaus, *The beginning of a seed: regulatory mechanisms of double fertilization.* Frontiers in Plant Science, 2014. **5**.
232. Wang, X., et al., *Pollen-Expressed Leucine-Rich Repeat Extensins Are Essential for Pollen Germination and Growth.* Plant Physiol, 2018. **176**(3): p. 1993-2006.
233. Fabrice, T.N., et al., *LRX Proteins Play a Crucial Role in Pollen Grain and Pollen Tube Cell Wall Development.* Plant Physiol, 2018. **176**(3): p. 1981-1992.
234. Fujikura, U., et al., *Atkinesin-13A modulates cell-wall synthesis and cell expansion in Arabidopsis thaliana via the THESEUS1 pathway.* PLoS Genet, 2014. **10**(9): p. e1004627.
235. Jia, M., et al., *A FERONIA-Like Receptor Kinase Regulates Strawberry (Fragaria x ananassa) Fruit Ripening and Quality Formation.* Front Plant Sci, 2017. **8**: p. 1099.
236. Jia, M., et al., *Two FERONIA-Like Receptor Kinases Regulate Apple Fruit Ripening by Modulating Ethylene Production.* Front Plant Sci, 2017. **8**: p. 1406.
237. Li, B., J. Yan, and W. Jia, *FERONIA/FER-like receptor kinases integrate and modulate multiple signaling pathways in fruit development and ripening.* Plant Signal Behav, 2017. **12**(12): p. e1366397.

238. Kou, X., et al., *Evolution, expression analysis, and functional verification of Catharanthus roseus RLK1-like kinase (CrRLK1L) family proteins in pear (Pyrus bretchneideri).* Genomics, 2017. **109**(3-4): p. 290-301.
239. Niu, E., et al., *Genome-wide analysis of CrRLK1L gene family in Gossypium and identification of candidate CrRLK1L genes related to fiber development.* Mol Genet Genomics, 2016. **291**(3): p. 1137-54.
240. Yin, Y., et al., *BZR1 transcription factor regulates heat stress tolerance through FERONIA receptor-like kinases-mediated reactive oxygen species signaling in tomato.* Plant Cell Physiol, 2018.
241. Oblessuc, P.R., C. Francisco, and M. Melotto, *The Co-4 locus on chromosome Pv08 contains a unique cluster of 18 COK-4 genes and is regulated by immune response in common bean.* Theor Appl Genet, 2015. **128**(6): p. 1193-208.
242. Pu, C.X., et al., *The Rice Receptor-Like Kinases DWARF AND RUNTISH SPIKELET1 and 2 Repress Cell Death and Affect Sugar Utilization during Reproductive Development.* Plant Cell, 2017. **29**(1): p. 70-89.
243. *The Cytoskeleton and Signal Transduction: Role and Regulation of Plant Actin- And Microtubule-Binding Proteins*, in *Annual Plant Reviews online*.
244. *Microtubules and Microtubule-Associated Proteins*, in *Annual Plant Reviews online*.
245. Mucha, E., et al., *Rho proteins of plants--functional cycle and regulation of cytoskeletal dynamics.* Eur J Cell Biol, 2011. **90**(11): p. 934-43.
246. Wasteneys, G.O. and Z. Yang, *New Views on the Plant Cytoskeleton.* Plant Physiology, 2004. **136**(4): p. 3884-3891.
247. Baluska, F., et al., *Root hair formation: F-actin-dependent tip growth is initiated by local assembly of profilin-supported F-actin meshworks accumulated within expansin-enriched bulges.* Dev Biol, 2000. **227**(2): p. 618-32.
248. Rahman, A., et al., *Auxin, actin and growth of the Arabidopsis thaliana primary root.* Plant J, 2007. **50**(3): p. 514-28.
249. Rosero, A., V. Zarsky, and F. Cvrckova, *AtFH1 formin mutation affects actin filament and microtubule dynamics in Arabidopsis thaliana.* J Exp Bot, 2013. **64**(2): p. 585-97.
250. Lee, S.H. and H.T. Cho, *Auxin and Root Hair Morphogenesis*, in *Root Hairs*, A.M.C. Emons and T. Ketelaar, Editors. 2009, Springer Berlin Heidelberg: Berlin, Heidelberg. p. 45-64.

Annexe 1

A summary of preliminary results in the phenotypic characterisation of *Arabidopsis thaliana* CrRLK1L T-DNA insertion lines

A1.1 Introduction

In this supplemental annexe, I have summarised a set of experiments I carried out during the first year of my PhD project. Although they are preliminary in nature, these results complement the information presented in Chapter 3 and therefore constitute a valuable addition to this thesis. Assays presented here aimed to identify *Catharanthus roseus* receptor-like kinase 1-like (CrRLK1L) mutant lines with severe developmental defects in a rapid manner. They should be interpreted with caution and conclusions should not be drawn before these experiments are repeated in optimal conditions (increasing sample size, avoiding contaminations, using fresh seed stocks with identical history, etc). At the beginning, the focus of my research project was to study the evolution of the CrRLK1L proteins functions across land plants. To this end, I aimed to characterise the roles performed by these receptors in the moss *Physcomitrella patens*, an extant member of the bryophytes, an early divergent lineage of land plants, to then compare to the already characterised CrRLK1Ls in the flowering plant *Arabidopsis thaliana*. Additionally, gene swap experiments were planned to gather evidence about the possible conservation of CrRLK1L function across land plants. In these experiments a *P. patens* CrRLK1L gene would be expressed in an Arabidopsis CrRLK1L mutant background to test rescue of the phenotype, and vice versa. Therefore, a set of T-DNA insertion lines targeting CrRLK1L genes in Arabidopsis was obtained to identify mutant phenotypes to complement with the moss CrRLK1Ls. Generation of moss CrRLK1L knock-out and knock-down lines was also pursued through PEG-mediated transfection of *P. patens* protoplasts and homologous recombination-based gene targeting. This evo-devo branch of my PhD project was not pursued further due to multiple experimental difficulties encountered during the

generation of these initial moss CrRLK1L knock-out and knock-down lines and, most importantly, the identification of promising research projects describing new roles in development for Arabidopsis CrRLK1Ls (Chapters 3 and 4).

A1.1.1 Motivation and objectives

Characterising phenotypically the CrRLK1L T-DNA insertion lines of *A. thaliana* contributed to the initial objective of my PhD project (testing the functional conservation of the CrRLK1L family across land plant lineages) and to the secondary branch of my project, which consisted of exploring further the contribution of this family of receptors to the model plant's development. The main objectives pursued in this phenotypic screen were:

1. Identifying developmental defects caused by loss-of-function T-DNA insertion mutations in members of the *A. thaliana* CrRLK1L receptors to then complement with *Physcomitrella patens* homolog genes in order to test the functional conservation of these receptors from bryophytes to flowering plants. As reviewed in the introductory chapter (Chapter 1), the CrRLK1L receptors are involved in multiple developmental processes including tip growth in pollen tubes, root hairs and trichomes; and cell expansion in roots, hypocotyls, petioles and leaf epidermal pavement cells. Longitudinal cell expansion and tip growth were of particular interest for the initial evo-devo project given their occurrence in both model organisms used in this project, *A. thaliana* and the moss *P. patens*. They also constitute two of the main features of interest in the use of the *P. patens* as a model plant since i) the growth during its first life cycle stage, the generation of the filamentous tissue protonema, is strictly tip-growth driven; and ii) its structural simplicity during all life stages allows easy visualisation of cellular shape and growth. These facts directed our efforts towards identifying *A. thaliana* lines with developmental defects in such processes.

2. To gain deeper insights into the contribution of CrRLK1L receptors to *A. thaliana* development by: i) confirming the roles played by members that have previously been characterised, and by ii) unravelling the function of uncharacterised CrRLK1Ls. Reproducing experiments described in the literature with a set of CrRLK1L mutant lines is thus a useful approach to confirm published results under the available growth conditions and also to potentially identify novel functions for these receptors.

A1.1.2 Experimental overview

This project started with a set of *A. thaliana* T-DNA lines targeting 15 of the 17

CrRLK1Ls in the model plant, along with nearly all F1 seeds from the 105 possible crosses between those 15 lines (performed by my supervisor Lisa M. Smith prior to the start of my PhD). First, the 15 T-DNA insertion lines were genotyped to confirm or obtain homozygous insertion lines. For those lines in which the T-DNA insertion could not be detected, further lines were ordered if available and subsequently genotyped (see Chapter 3). F2 generation seeds were obtained for all the crosses in which both parental lines had been confirmed as homozygous. Then, selected double mutants were obtained by genotyping of their respective F2 or F3 generations. Based on published research where CrRLK1Ls were characterised, several phenotypic screens were carried out with different sets of single and/or double T-DNA insertion lines, depending on the selection stage of those lines at the time.

A1.2 Results and Discussion

A1.2.1 Cytoskeleton stability in roots (supplemental to section 3.2.1 from Chapter 3)

The cytoskeleton comprises actin filaments and microtubules and constitutes an intracellular, highly dynamic network that helps maintaining and modifying cell shape, organelle distribution, and transport of cell components [243-244]. As such, its components can be dynamically rearranged in response to environmental or developmental cues [243-245]. It has been established that several families of regulatory elements are in charge of detecting such cues and transmitting the signal to the cytoskeleton remodelling factors [246]. For instance, the signalling module composed by RLK-ROPGEF-ROP proteins is believed to play an active role in linking external cues to cytoskeleton remodelling [245]. Interestingly, members of the CrRLK1L family of receptors have been identified as direct interactors of ROPGEFs and described to direct downstream ROP protein activation to subsequently trigger downstream cellular responses [74, 97]. Besides, CrRLK1L CVY1 has been linked to cytoskeleton stability in epidermal leaf cells [81]. It is therefore possible that other members of this family of receptors play similar roles as those described for FER and CVY1.

In order to test this hypothesis, pilot experiments were carried out to test whether the CrRLK1L insertion lines presented defects in cytoskeleton stability in roots. Oryzalin and latrunculin-B (LatB) are microtubule and actin filament destabilising drugs, respectively. A concentration of 50 nM for both drugs was chosen as the condition upon which cytoskeleton stability impaired mutants should respond with cell distortion

in the elongation zone of the root, as described in multiple studies [247-249]. To study microtubule stability in roots, a pilot experiment was set up in which seeds were sown on half-strength Murashige and Skoog (MS), 1% agar plates supplemented with DMSO or 50 nM of oryzalin and then grown vertically in our standard growth conditions (22ºC, 16 hours light/8h dark, 60% humidity). No significant differences were found when comparing the root length between treatments or root cell morphology in propidium iodide stained roots in any of the lines included in this experiment (*herk2*, *at2g23200*, *cvy1*, *anx1*, *herk1*, *fer-5*, *anx2*, *the1-4*, *anj* and *eru*; data not shown). Similarly, primary root growth and cell morphology in response to the actin filament destabilising drug LatB were studied. In a pilot experiment, plants were germinated and grown vertically on plates with half-strength MS, 1% agar for 10 days under our standard growth conditions, and subsequently transferred to plates containing 50 nM LatB and to control plates. Interestingly, although no significant differences were found in responsiveness to LatB in terms of root length, *herk2* roots displayed cell distortion events throughout the primary root in all plants observed in the LatB-supplemented conditions (Figure A1.1). Cell morphology defects observed in these lines suggested a possible LatB-promoted actin filament destabilisation, which could lead to a phenotype of loss-of-polarity during cell expansion. These initial results for encouraged us to pursue the characterisation of a possible new function for HERK2 further.

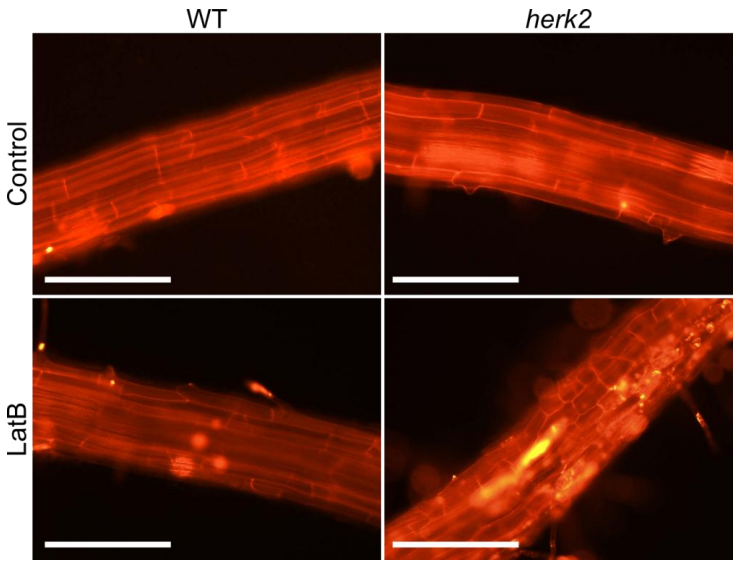

Figure A1.1 Latrunculin-B-induced cell distortion in the expansion zone of primary roots of *herk2.* Epifluorescence microscopy images of propidium iodide-stained roots were obtained for 3-5 seedlings per line. Seeds were germinated and grown vertically for 10 days under standard conditions and then transferred to either control plates or LatB-supplemented plates (50 nM LatB) and allowed to grow for four days under standard conditions. Multiple zones with distorted cells were found in *herk2* roots exposed to 50 nM LatB. Scale bars represent 100 µm.

To this end, an experiment was set up to determine the degree of susceptibility of this individual line to the actin filament destabilising drug in comparison to Col-0 wild-type (WT) plants. A range of concentrations including 0, 10, 25, 50, 75, 100, 150 and 200 nM of LatB was tested in an experiment similar to the one described above. For each condition, four day old WT and *herk2* seedlings (n = 5) grown in vertical half-strength MS were transferred to plates containing the different concentrations of LatB and grown under our standard conditions for four additional days. Root length and cell morphology were studied with the expectation of finding defects in *herk2* seedlings at concentrations of 50 nM LatB and higher. Surprisingly, both *herk2* and WT seedlings presented a similar pattern of response to the range of treatments here tested (Figure A1.2A). Root growth fluctuated around 1.0 and 1.4 cm growth for concentrations 0 nM to 150 nM, and strongly decreased to 0.4 cm at 200 nM Lat-B for both WT and *herk2* (Figure A1.2A). Only on 100 nM LatB did we detected a small but statistically significant difference between WT and *herk2* root growth (Figure A1.2A; Student's *t* tests; $0.01<p<0.05$). No qualitative differences were found regarding the effect of LatB on cell morphology between *herk2* and WT, which presented elongated cells between 0 and 150 nM (Figure A1.2B). A remarkable shape change towards isodiametric morphology was observed at 200 nM LatB for both WT and *herk2*, similar to what was observed for *herk2* at 50 nM in the pilot experiment (Figure A1.2B). Given the lack of reproducibility of the cell morphology defect observed in *herk2* roots in 50 nM LatB in our pilot experiment, the latter was replicated in the same conditions with freshly prepared stocks to rule out bioactivity loss of the LatB stock used in the second experiment as the cause of the discrepancies between experiments. Unfortunately, the phenotype observed in *herk2* insertion line in response to LatB in our pilot experiment could not be reproduced (data not shown). We could however observe a noticeable correlation between regions containing distorted and isodiametric cells and parts of the root that had undergone mishandling during the sample preparation. Cell distortion could be found in all regions in which roots had been bent when transferred to the second growth media or to the microscope slide. We concluded that mishandling was likely the cause of the previously observed differences and the reason why it could not be reproduced in a repetition of the initial experiment. In hindsight, higher concentrations of this compound would have been more useful to detect differences in our insertion lines. Analysing WT response to various concentrations of the drug at different times would have helped us determine the WT response curve and therefore the conditions in which to best test the responsiveness of the mutant lines under our conditions.

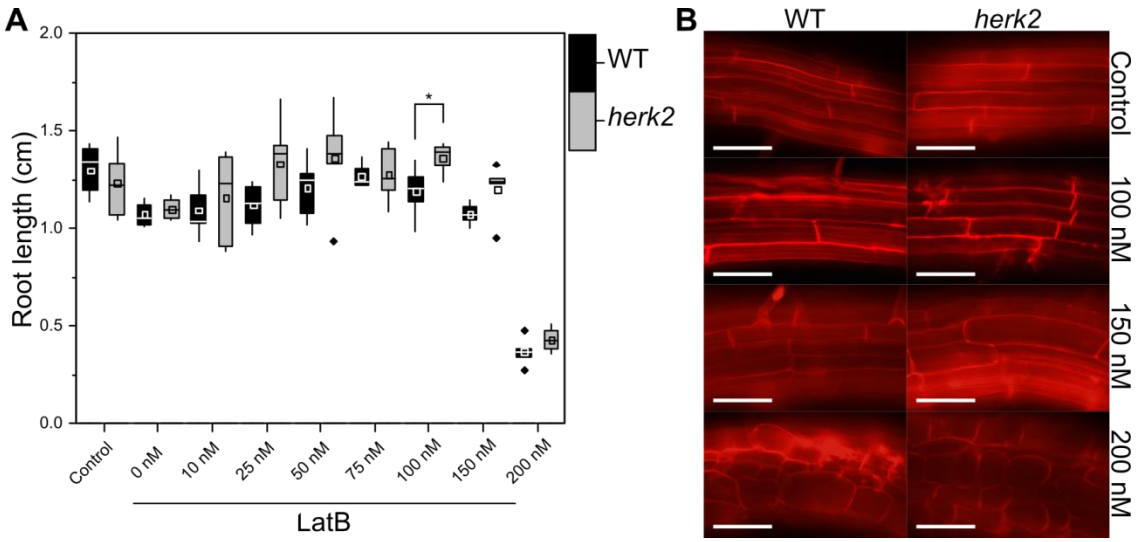

Figure A1.2 Root elongation in response to a range of concentrations of the actin destabilising drug Latrunculin-B. Seedlings were grown on MS plates for four days and were then transferred to plates containing different concentrations of LatB for another four days. **A**, quantification of root growth after four days on LatB (n = 4-5). Statistically significant differences were analysed in Student's *t* test (*, 0.01<p<0.05). **B**, fluorescence images from propidium iodide stained roots in 0, 100, 150 and 200 nM of LatB. Cell distortion phenotypes in *herk2* and WT control lines were only found when exposed to high LatB concentrations. Scale bar represents 50 µm.

A1.2.2 Petiole length (supplemental to section 3.2.2.3 from Chapter 3)

FER, HERK1, THE1 and HERK2 have been linked to cell expansion in petioles. *fer-4* single knock-out, *fer* strong knock-down lines, *herk1 the1-4* double mutant and *herk1 herk2 the1-4* triple mutant plants display a reduction in petiole cell elongation which leads to shorter petioles in the rosette leaves of these plants [74, 112, 126]. To explore the possible involvement of other CrRLK1L members in petiole growth we carried out a petiole length screen of rosette leaves from the set of single and double homozygous T-DNA insertion lines available at that time (*herk1*, *the1-4*, *herk2*, *fer-5*, *cvy1*, *eru*, *at2g23200*, *anj*, *herk2 fer-5*, *herk2 cvy1*, *herk2 eru*, *herk2 at2g23200* and *herk2 anj*). Between 25 and 30 seeds per line were sown in soil after a three day stratification period and grown in our standard conditions for 14 days, after which five healthy seedlings per line, at similar developmental stages, were chosen to continue with the experiment. Plants were analysed when the stem from their primary inflorescence reached 0.5 cm in length to standardise the developmental stage across lines and individuals. Rosette leaves were separated from the stem at the stem-petiole junction and their petiole and full leaf lengths measured (Figure A1.3).

Mean petiole lengths were consistent across lines for the first three leaves, and increased in variability in leaves five to ten (data not shown). I therefore compared

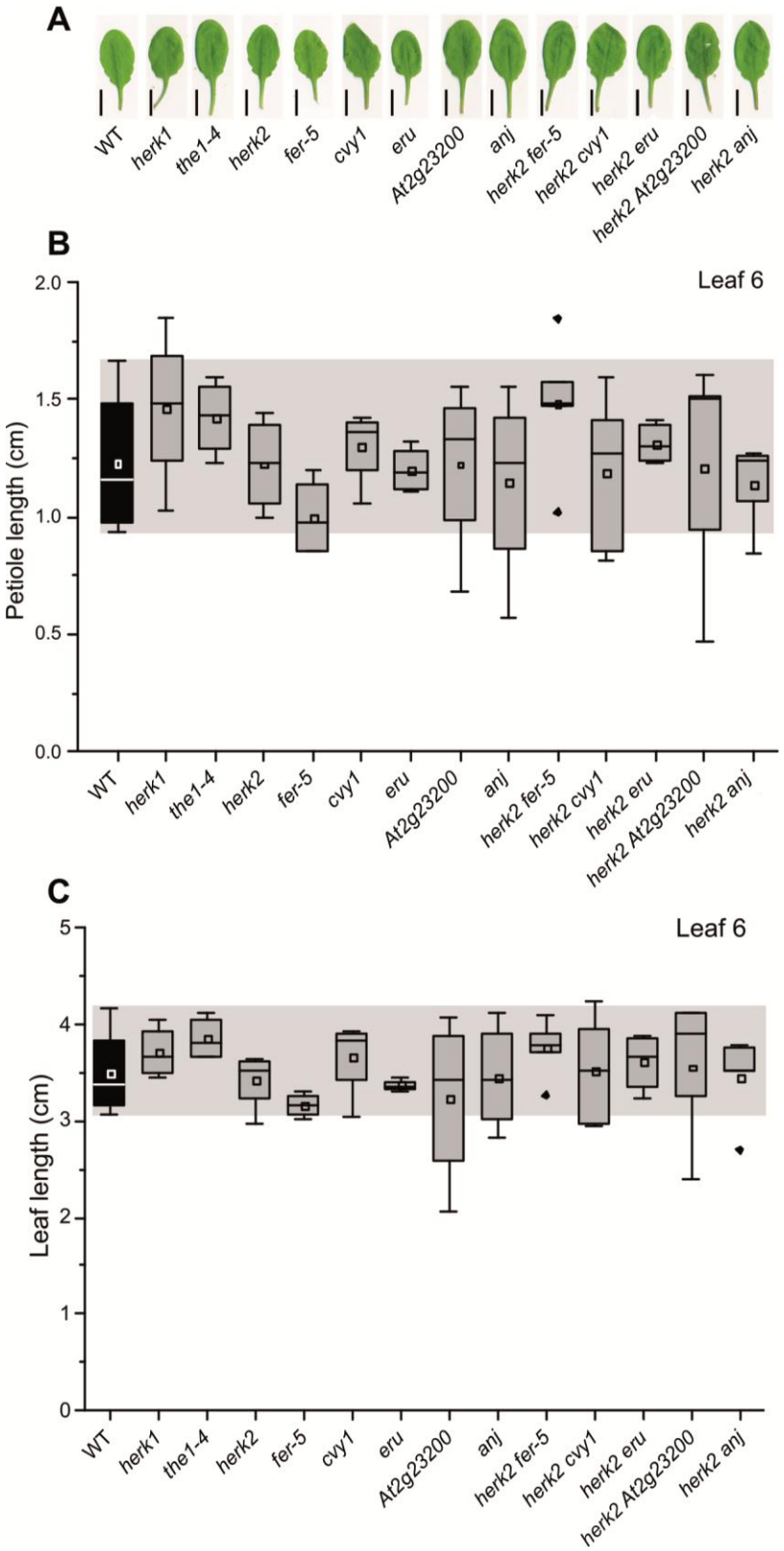

Figure A1.3 Petiole length in CrRLK1L T-DNA insertion lines. A, representative photographs of rosette leaf 6 from each line analysed. Scale bars represent 1 cm. **B**, quantification of the leaf 6 petiole length from the lines tested. **C**, quantification of the leaf 6 full leaf length. Between 8 and 10 plants were analysed per line. No statistically significant differences were found in one-way ANOVA.

petiole and whole leaf lengths for leaf 6 but found no statistically significant differences between lines (Figure A1.3B-C). The *fer-5* insertion line presented the shortest mean petioles, in agreement with what has been published for the *fer-4* knock-out and *fer* knock-down lines (Figure A1.3B; [74, 112, 126]). The difference observed between *fer-5* and WT is nevertheless not significant in this assay (Student's *t* test, p>0.05; *fer-5*; NASC ID: N655026). In *fer-5*, the T-DNA insertion is located at the end of the kinase domain and therefore expresses a truncated version of the full length FER [74]. It is thus likely that the role of FER in petiole elongation is partially rescued by the truncated transcript expressed in the *fer-5* line. This situation would agree with defects in trichomes, root hairs and root response to auxins, for instance, in which *fer-4* knock-out presents a more severe phenotype than the hypomorphic *fer-5* allele [74]. Additional CrRLK1L T-DNA insertion lines obtained at a later stage of this PhD project displayed short petiole phenotypes and are described in detail in Chapter 3 of this thesis.

A1.2.3 Root hair development (supplemental to section 3.2.2.1 from Chapter 3)

Root hairs develop through tip growth, a highly polarised cell expansion mechanism in which CrRLK1L members FER and ERU play a fundamental role [74-77]. In order to test whether additional members contribute to root hair development, we performed a series of experiments in which seeds from the available single and double homozygous insertion lines were grown vertically in control plates (half-strength MS supplemented with 1% sucrose) and plates supplemented with 125 nM of the auxin 1-naphtaleneacetic acid (NAA) under our standard growth conditions for six days. Auxins like NAA promote root hair growth in Arabidopsis seedlings and are commonly used to facilitate the identification of mutants affected in such process [250].

A total of 200 root hairs from four plants per insertion line were measured from the differentiation zone of roots in control and auxin-supplemented conditions. All lines tested presented an increase in root hair length in response to auxin except for the *eru* and *herk2 eru* lines (Figure A1.4). The previously characterised *fer-5* and *eru* along with their respective *herk2* double insertion lines (*herk2 fer-5* and *herk2 eru*) presented significant differences in root hair length compared to Col-0 wild-type (WT) in auxin-supplemented conditions (Figure A1.4; see also Chapter 3). This indicates that we were able to reproduce the *fer* auxin reduced sensitivity phenotype described in the literature [74]. Our results also suggest that *eru* defects in root hair formation (linked to Ca^{2+} and NH_4^+ transport balance into the vacuole) cannot be rescued by an exogenous source of auxins [75-76]. We found no statistically significant differences in root hair elongation in the remaining lines when compared to WT in control or auxin-

supplemented conditions (Figure A1.4). This doesn't exclude the possibility of severe defects in root hair formation in these lines under growth conditions that differ in temperature or media composition from the ones used in the experiments here presented. Alternatively, performing a more detailed screen in which root hair collapse and burst are examined could also inform the role of CrRLK1L receptors in root hair development. Results regarding the *fer-5* and *eru* lines were explained in detail in the main text of this thesis (Chapter 3).

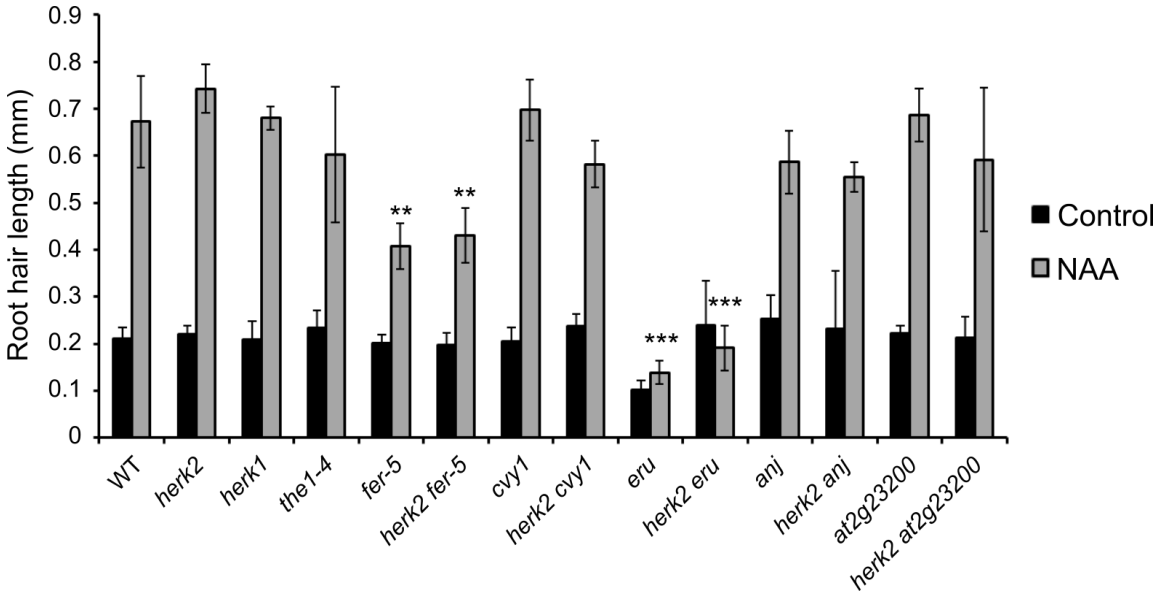

Figure A1.4 Root hair length in CrRLK1L insertion lines. Seeds were germinated and grown in vertical half-strength MS in control or NAA-supplemented conditions for 6 days. 50 root hairs were measured from four seedlings per line (n = 4). Significant differences between lines tested with one-way ANOVA followed by Tukey's significant difference test and statistically significant differences with WT were represented by **, $p<0.01$ or ***, $p<0.001$ (Tukey's tests).

A1.2.4 Effect on root development of auxins, osmotic stress and medium pH

Common elements in the CrRLK1L signalling pathway in different developmental processes include H^+-ATPases, auxin signalling related elements like RAC/ROP GTPases and plasma membrane NADPH oxidases, which modulate apoplastic pH and ROS gradients formation, respectively [136]. Plants with loss-of-function mutations in CrRLK1Ls like FER are impaired in such responses and display growth defects when exposed to changes in medium pH or exogenous sources of auxins [74, 79, 97]. In order to unravel possible new functions of different CrRLK1Ls in such responses we carried out the following set of pilot experiments in which root growth from confirmed insertion lines was studied in vertical growth assays when exposed to different conditions: auxins (125 nM NAA), osmotic stress (100 mM NaCl) and variation in

medium pH (pH 4.0 and 7.0). Seeds from all plants were grown in control conditions (vertical half-strength MS, pH 5.7, 1% sucrose) and in plates supplemented with the corresponding compound under our standard growth conditions. Primary root length was measured from all plants six days after germination (between 8-10 plants per line; except in osmotic stress conditions in which germination of most lines was delayed or arrested).The overall result of this set of experiments reflected the expected general trends in response to the conditions applied; root growth was reduced in response to auxins, osmotic stress and low pH, while root growth was promoted in high pH medium conditions (Figure A1.5). In this preliminary experiment, bacterial contamination affected WT growth in control conditions, as reflected by the reduction in mean root length in comparison with the mean root length in the test lines (Figure A1.5A). This prevented us from concluding whether certain differences obtained in the control conditions are relevant.

Growth under high (pH 7.0) and low pH (pH 4.0) conditions resulted in a general trend of root growth promotion and reduction, respectively, compared to control conditions (pH 5.8; Figure A1.5C and D). Two lines displayed a significant difference when compared to WT: *herk2 fer-5* in high pH and *herk2 eru* in low pH, with a moderate reduction in mean root length (Figure A1.5C and D). Whereas the latter still remains unconfirmed, we repeated the experiment to confirm the possible *herk2 fer-5* phenotype in root elongation in high pH by repeating the pilot experiment with the each of the double and single homozygous lines involved (*herk2 fer-5*, *herk2*, and *fer-5*) with a higher number of biological replicates (n = 25-30). A small but statistically significant reduction in root length was observed in *herk2 fer-5* seedlings in comparison with WT in both control and high pH conditions (Figure A1.6A). No differences were found for *fer-5* seedlings whereas *herk2* seedlings presented a small but statistically significant increase in root length under control conditions (Figure A1.6A). These preliminary results suggest an interaction between the CrRLK1L genes HERK2 and FER in controlling root elongation. They nevertheless require replication and testing under different conditions (i.e. multiple pH levels, at earlier and later time points) and controlling for germination times, as germination delays could also explain the small differences obtained in root lengths.

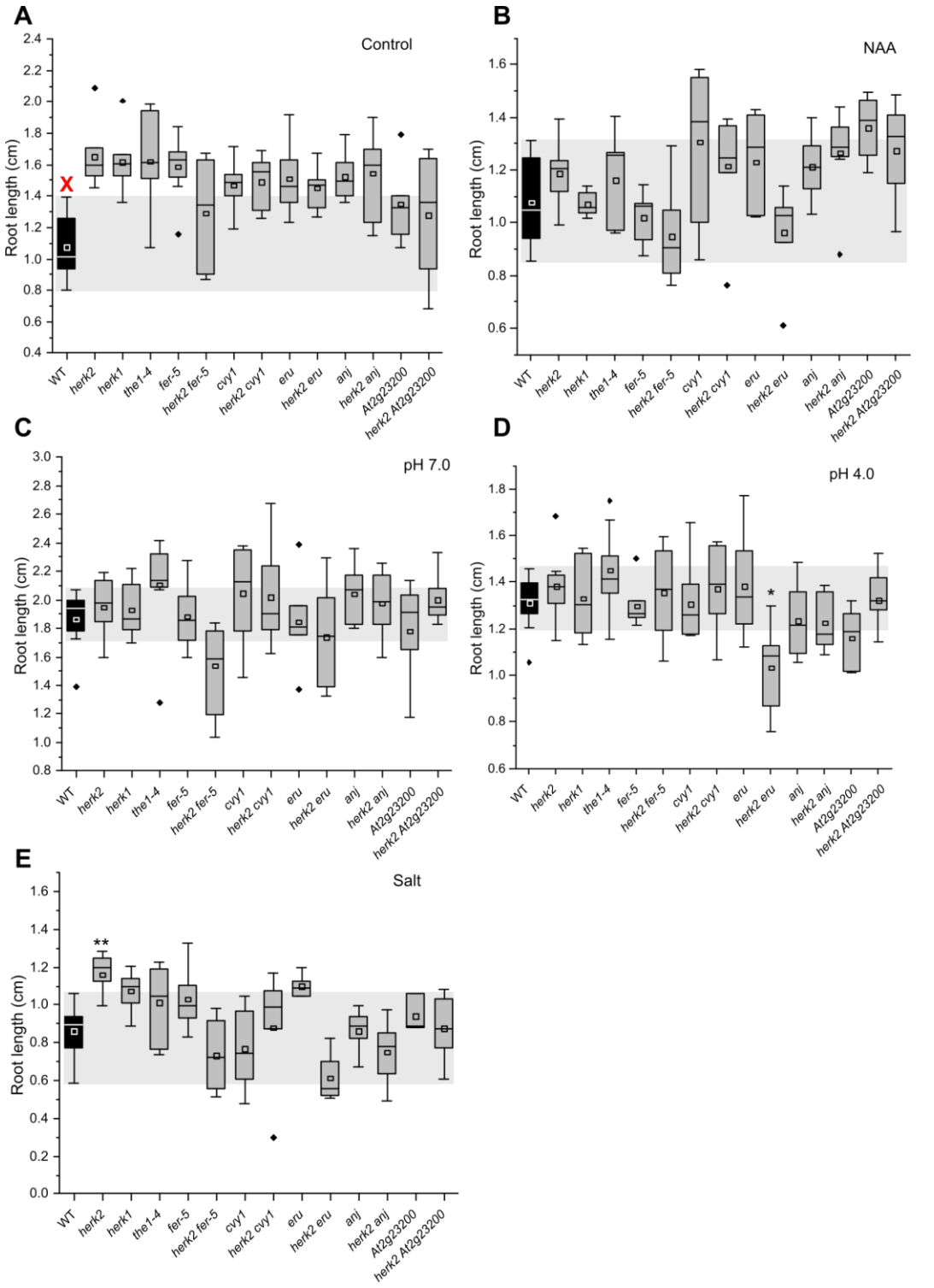

Figure A1.5 Root length of CrRLK1L insertion lines in auxin supplemented, osmotic stress, high pH and low pH conditions. Primary root length was measured from 6 day old seedlings germinated and grown in vertical half-strength MS plates with the corresponding control or modified conditions (A to E panels: control, 125 nM NAA, pH 7.0, pH 4.0 and 100 mM NaCl). Root length was measured from 8-10 seedlings per line and condition except for the salt-supplemented condition (n = 3-5). Significant differences between lines tested with one-way ANOVA followed by Tukey's significant difference test and statistically significant differences with WT were represented by *, $p<0.05$; **, $p<0.01$ or ***, $p<0.001$ (Tukey's tests). Red cross, growth affected by contaminations.

Exogenous auxin supplementation resulted in considerable root growth inhibition in most lines tested except for *at2g23200* and *herk2 at2g23200* which could suggest a reduced auxin sensitivity phenotype in the uncharacterised *at2g23200* line (Figure A1.5B). To obtain further support for this hypothesis we repeated the experiment for the lines involved (*at2g23200*, *herk2*, *herk2 at2g23200*) with a higher number of biological replicates (n = 25-30). Results obtained in this experiment contradict the previously obtained differences, with *herk2 at2g23200* line responding in a similar manner to the auxin treatment as the WT control and *herk2* line (Figure A1.6B). Surprisingly, the *at2g23200* mutant line displayed a reduction in root length when compared to WT in both control and auxin-supplemented conditions, contradicting the results obtained in the pilot experiment (Figure A1.6B). Given the two-to-three fold increase in biological replicates alongside the absence of contamination in the second experiment, we concluded that there was not enough evidence to support the initial hypothesis for the uncharacterised *at2g23200* line.

Osmotic stress strongly affected seed germination, reducing the number of biological replicates (seeds did not germinate or presented different degrees of germination delay), preventing us from confidently concluding that differences observed in root length between insertion lines and WT were significant or caused by their variable germination delays (Figure A1.5E). These experiments should therefore be repeated in optimal conditions, using seeds of similar age, obtained and stored under the same conditions as would be necessary to avoid differences explained by variable degrees of seed dormancy and viability.

A1.2.5 Abscisic acid effect on germination (supplemental to section 3.2.3.1 from Chapter 3)

CrRLK1L receptors modulate several plant hormone pathways including ABA and ethylene [136]. The CrRLK1L-ABA link has been identified for its best characterised member, FER [97-98]. The signalling module FER-GEF-ROPGTPase directs ABI2 phosphatase activation via physical interaction with FER-activated ROPGTPases [97]. Enhanced activity of ABI2, a core ABA negative signalling element, drives ABA signalling suppression [97]. This explains the response of *fer* knock-out lines to ABA, which includes hypersensitivity in germination assays, stomatal closure and ROS accumulation in guard cells, and enhanced root growth inhibition in the presence of exogenous ABA [97]. Therefore, whether additional CrRLK1Ls are involved in ABA signalling was tested. Germination assays were chosen as a rapid method to screen multiple lines for alterations in ABA response and were performed with three ABA

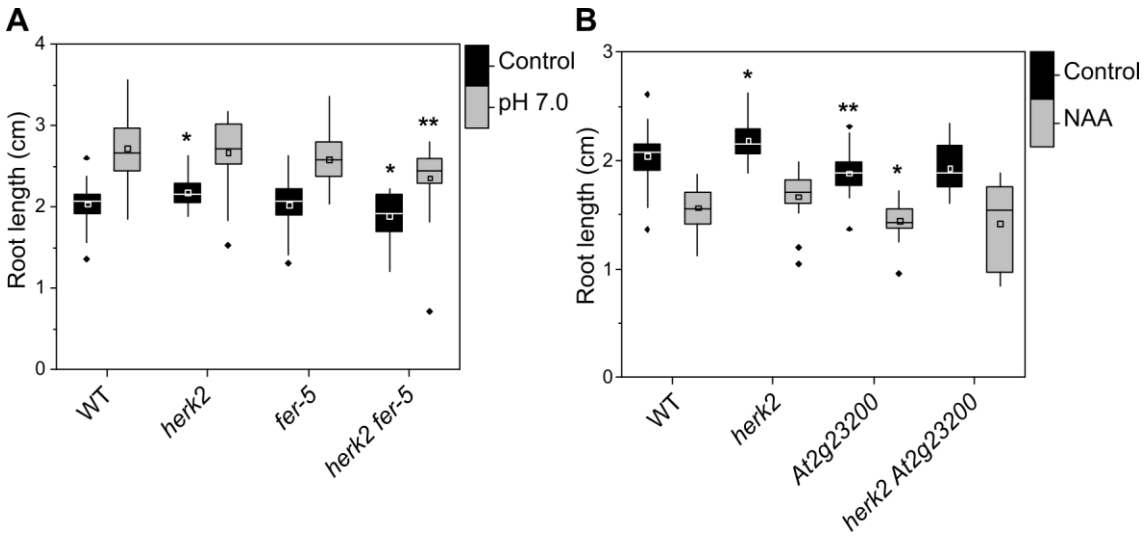

Figure A1.6 Effect of high pH and auxins on root development. Seeds from selected insertion lines were germinated and grown in vertical half-strength MS plates at high pH (pH 7.0; **A**) or supplemented with auxins (125 nM of NAA; **B**) for 6 days. Between 30 and 50 seedlings were analysed for each genotype and condition. Statistically significant differences with WT were analysed in Student's *t* tests (*, p<0.05; **. p<0.01).

concentrations (0, 1 and 2 µm). Between 40 and 60 seeds per line were sown onto half-strength MS plates supplemented with the corresponding concentration of ABA, then stratified at 4ºC for four days. Plates were transferred to our standard growth conditions, with germination stage and seedling establishment recorded on day three. The lines screened in this preliminary assay were *fer-5, herk2*, *herk2 fer-5*, *herk2 cvy1*, *herk2 at2g23200*, *herk2 anj*, *herk2 herk1*, *herk2 the1-4* and *herk2 eru*, with the intention of targeting lines in which defects are most likely to appear, that is double homozygous T-DNA insertion lines.

After three days, seeds from all lines tested germinated and presented expanded green cotyledons on control plates (Figure A1.7A). Seeds exposed to 1 µM ABA displayed a delay in germination, with lines *herk2 fer-5* and *herk2 the1-4* presenting a significantly higher proportion of seeds without cotyledon emergence (Figure A1.7B). This trend was most remarkable in the *herk2 the1-4* sample in which more than 75% of the roots had not emerged in either ABA-supplemented condition (Figure A1.7B-C). These preliminary results supported a germination delay in the presence of ABA in the double insertion line *herk2 the1-4*. Characterisation of the involvement in ABA responsiveness of the CrRLK1Ls HERK2, THE1 and HERK1 was pursued further, exploring i) the possible functional redundancy of the two CrRLK1Ls in this particular developmental window in response to ABA, as well as ii) their involvement in root elongation and desiccation (see Chapter 3).

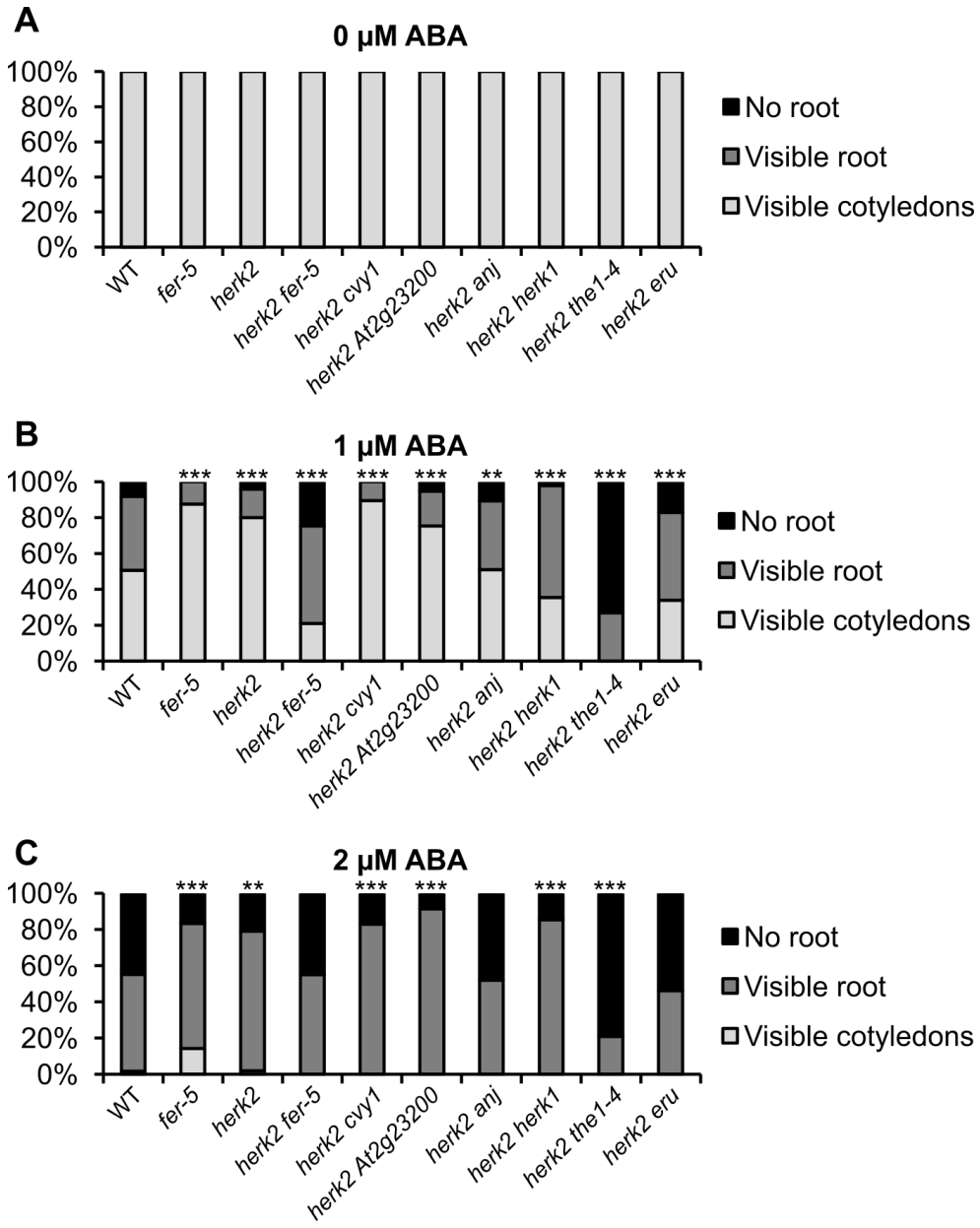

Figure A1.7 Response to ABA in germination assays. Seeds from several CrRLK1L insertion lines were sown in MS plates containing 0, 1 and 2 µM ABA, stratified for three days and incubated in our standard growth conditions for three days. These graphs summarise the percentage of germination (n = 40-60) at three different levels: seeds in which the root was not visible outside of the seed coat (no root), those in which the root had emerged (visible root) and those in which the cotyledons had also emerged (visible cotyledons); in control conditions (**A**), 1 µM ABA (**B**) and 2 µM ABA (**C**). ** $p<0.01$; *** $p<0.001$ (χ-square tests).

Annexe Table 1 ***A. thaliana* lines**

Table AT1 List of confirmed Arabidopsis lines used in this thesis. Also listed are sources, references and Nottingham Arabidopsis Stock Centre (NASC) identifiers where available.

Line (Genotype x *Construct*)	**Origin**	**Reference / NASC ID**
Col-0	NASC	N1092
fer-5	NASC	[74] N655026
fer-4	A. Cheung	[74] N69044
herk1	NASC	[126] N657488
herk2	NASC	[126] N663563
the1-4	NASC	[126] N829966
cvy1	NASC	[81] N660329
cap1/eru	NASC	[75] N666567
anx1	NASC	[65] N659315
anx2	NASC	[65] N656997
anj	NASC	N654842
at2g23200	NASC	N685400
herk2 fer-5	This study	N/A
herk2 cvy1	This study	N/A
herk2 the1-4	This study	N/A
herk2 cap1/eru	This study	N/A
herk2 anj	This study	N/A
herk2 at2g23200	This study	N/A
herk1 herk2	This study	N/A
herk1 the1-4	This study	[126]
herk1 herk2 the1-4	This study	[126]
herk1 anj	This study	N/A
herk1 cvy1	This study	N/A
lre-5	R. Palanivelu	[71] N66102
lre-7	R. Palanivelu	[193] N66104
herk1 anj lre-5	This study	N/A
ralfl4	NASC	N516969
ralfl9	NASC	N509527
ralfl14	NASC	N867840
ralfl19	NASC	N625065
ralfl24	NASC	N851932
ralfl25	NASC	N669797
ralfl31	NASC	N553792

ralfl24 ralfl31	This study	N/A
ralfl4(-/-) ralfl19(+/-)	This study	N/A
ralfl4(+/-) ralfl19(-/-)	This study	N/A
Col-0 x *pHERK1::GUS*	This study	N/A
Col-0 x *pANJ::GUS*	This study	N/A
Col-0 x *pHERK1::HERK1*	This study	N/A
Col-0 x *pANJ::ANJ-GFP*	This study	N/A
Col-0 x *pLRE::LRE-Citrine*	This study	N/A
Col-0 x *pMYB98::NTA-GFP*	This study	N/A
Col-0 x *pFER::FER-GFP*	This study	N/A
herk1 anj x *pHERK1::HERK1*	This study	N/A
herk1 anj x *pANJ::ANJ-GFP*	This study	N/A
herk1 anj x *pLRE::LRE-Citrine*	This study	N/A
herk1 anj x *pMYB98::NTA-GFP*	This study	N/A
herk1 anj x *pFER::FER-GFP*	This study	N/A
lre-5 x *pHERK1::HERK1*	This study	N/A
lre-5 x *pANJ::ANJ-GFP*	This study	N/A
lre-5 x *pLRE::LRE-Citrine*	This study	N/A
lre-5 x *pMYB98::NTA-GFP*	This study	N/A
lre-5 x *pFER::FER-GFP*	This study	N/A
Col-0 x *pLAT52::TdTomato*	M. Bayer (unpublished)	N/A
Col-0 x *pLAT52::amiRALF11/12/13*	This study	N/A
Col-0 x *pLAT52::amiRALF8/9/15*	This study	N/A
Col-0 x *pNTA::amiRALF14*	This study	N/A
Col-0 x *pRALFL4::RALFL4-GFP*	This study	N/A
Col-0 x *pRALFL19::RALFL19-GFP*	This study	N/A
Col-0 x *pRALFL4::GUS*	This study	N/A
Col-0 x *pRALFL19::GUS*	This study	N/A

Annexe Table 2 **Oligonucleotides**

Table AT2 List of oligonucleotides used for genotyping, cloning PCR or RT-PCR. Listed are oligonugleotide identifiers, nucleotide sequences (5'-3') and purpose descriptions.

Primer ID	Sequence 5'-3'	Purpose
MPK026	ACAAGGTCTGGCGGAGTTTA	CVY1 genotyping fw
MPK027	GCATCACCACACCAAAAGAGT	CVY1 genotyping rv
MPK028	AAGCAAAACCAGAGGATTTTCA	HERK2 genotyping fw
MPK029	CTGATTTGCTTCGCCTTTTC	HERK2 genotyping rv
MPK030	ATGGAGACGAACCCAATGCC	AT2G21480 genotyping fw
MPK031	ACCGGCTGATGACATTCTCA	AT2G21480 genotyping rv
MPK032	TCTTCCTCAATCCAGTCTTCACA	AT2G23200 genotyping fw
MPK033	TGACTTCAGTTCCTTTGTTGGTG	AT2G23200 genotyping rv
MPK034	TCTGGTAAAGAGAATCTACGGCA	ANX1 genotyping fw
MPK035	GTCCAAACCCCGAGCCATC	ANX1 genotyping rv
MPK036	GTTGCTCGCGGTAGTCTTCT	HERK1 genotyping fw
MPK037	CTGTCCTGAATTCCGCAAGC	HERK1 genotyping rv
MPK040	TCATCGAGAAGAATGTTGGTGGA	AT4G39110 genotyping fw
MPK041	CCCTCGACGATGGAACCAAA	AT4G39110 genotyping rv
MPK042	CTGCTAGACGTGCTTGGACT	AT5G24010 genotyping fw
MPK043	CAGAACGATCAGACTCCGCA	AT5G24010 genotyping rv
MPK044	CGAAATCTGAGACTTTAGCAACCC	ANX2 genotyping fw
MPK045	TCAGAACAAGGGCTCAACGA	ANX2 genotyping rv
MPK046	GTCACTCACCACCCATTAGTCT	AT5G38990 genotyping fw
MPK047	TACGGCACTTGAGGAATCCC	AT5G38990 genotyping rv
MPK048	AGGGAGGATTTGACGACGTT	AT5G39000 genotyping fw
MPK049	AGGTTTTGCTCAGGGTGATCC	AT5G39000 genotyping rv
MPK050	CGGTCCATTCGCCATGTACT	THE genotyping fw
MPK051	GGGAGGATCAGGTTCTAAGAGC	THE genotyping rv
MPK052	CTCCTCTGTAGCAAAACCAGGA	ANJEA genotyping & RT-PCR fw
MPK053	CTCACGTTTACTCCCTCGGG	ANJEA genotyping & RT-PCR rv
MPK055	AATACTCATCCGCCTCGACG	CAP1/ERU genotyping rv
MPK056	ACTTATCCAGACGGTGGAGC	CAP1/ERU genotyping fw
OTH077	AAGCCAGTTTTAGAGTACGAAGA	LRE genotyping fw
OTH078	TCAAGTCAACACTAACAAAGCAAAAAC AGCGG	LRE genotyping rv
MPK038	CATTGACGCGATTCATGTTT	FER genotyping & RT-PCR fw
MPK039	GAGTATTTCAGACGGCAGCA	FER genotyping & RT-PCR rv

OTH053	GCGGAACCAGTGGAGAGTCG	RALFL11 genotyping fw
OTH054	GCTAGCATATGTGGCCTAATAGC	RALFL11 genotyping rv
OTH055	ACAGGATGCACAGTTTCGATCCA	RALFL13 genotyping fw
OTH056	AAACACCTTGCATATACGAGTGT	RALFL13 genotyping rv
OTH057	TGTAGGTTAATTAATCGATATAGACGGT	RALFL12 genotyping fw
OTH058	ACACATAAAACACCTTGCATATACGC	RALFL12 genotyping rv
OTH059	TGGCCAAGGTTGCATTGGAGA	RALFL19 genotyping fw
OTH060	CGGAGAGTCTGGGCAAAGCA	RALFL19 genotyping rv
OTH061	AAGCAGAGCCAGAAATAACTTGT	RALFL4 genotyping fw
OTH062	AGATGGAAGTAAGGAGAGGCAA	RALFL4 genotyping rv
OTH063	TTGCAGGTGTTAGGGTGGGC	RALFL9 genotyping fw
OTH064	CGACATCCGTTCAAATTCCGACA	RALFL9 genotyping rv
OTH065	TCGCCGTTATTATCTCAGTGGT	RALFL14 genotyping fw
OTH066	TGAGAGAGTATCATTTCGAAGGCT	RALFL14 genotyping rv
OTH067	TGGTGGAGCATTAGGACGCA	RALFL25 genotyping fw
OTH068	GCTCGAGTCCTCTGCTTTGGA	RALFL25 genotyping rv
OTH069	CCTCTTGGTTTTGGATTCTACGT	RALFL26 genotyping fw
OTH070	ACCCATTAACCCTACCATGAAGT	RALFL26 genotyping rv
OTH071	CAACGAAAGCCTGGCCCATT	RALFL34 genotyping fw
OTH072	ACCAATCCACCCCTCACGAC	RALFL34 genotyping rv
OTH073	TGTCGTTTGTGTCTCTAGCGCA	RALFL31 genotyping fw
OTH074	GGGAATTGACTGTTTATGTTTTGGC	RALFL31 genotyping rv
OTH075	AAGAAGAACATGTGGGTCAAAGCCT	RALFL24 genotyping fw
OTH076	CTCCTCTCCTTCTTCCTCTCCGATT	RALFL24 genotyping rv
GEN005	ATTTTGCCGATTTCGGAAC	SALK LB genotyping primer
GEN029	GTGGATTGATGTGATATCTCC	GABI LB genotyping primer
GEN035	AACGTCCGCAATGTGTTATTAAGTTGTC	WISC LB genotyping primer
MPK098	TAGGTACCTAGAATGTTTTTCTCAAGTTTTCTTCC	pHERK1 fw
MPK103	TAAGGATCCTCTTCCTTCAGATTTCACCAGTTGTG	HERK1 rv
MPK110	TTAGGTACCTTGTGGAATCATGAAATCGTAGTGT	pANJ fw
MPK113	TAGGATCCACGTCCCTCAGATTTGATCAGCTGCG	ANJ rv
MPK096	TAGGTACCCGAGTTGTAAAAGGCCTGGC	pFER fw
MPK101	TAAGGATCCACGTCCCTTTGGATTCAT	FER rv

	GA	
CLN084	AGAAACGTGAGATCTGCAAACATATTGCTTGACGA	HERK1-KD fw
CLN085	AGATCTCACGTTTCTGTGAATGACCGGTTTCGAGT	HERK1-KD rv
CLN082	AGAAACGTCAGATCCGCCAACATATTGCTTGA	ANJ-KD fw
CLN083	GGATCTGACGTTTCTGTGAATCACGGGTTTCG	ANJ-KD rv
CLN078	CACCTAGAATGTTTTTCTCAAGTTTTCTTCC	pHERK1 pENTR/D-TOPO fw
CLN079	AACCTGGAAATGGAACAGATC	pHERK1 pENTR/D-TOPO rv
CLN080	CACCTTGTGGAATCATGAAATCGTAGT	pANJ pENTR/D-TOPO fw
CLN081	TTCACAAAACCTGGAAATTTTAAATAATT	pANJ pENTR/D-TOPO rv
CLN045	CACCATGGGTATTGAAAAGTTTGAAACTTTCATC	HERK1 pENTR/D-TOPO fw
CLN046	TCTTCCTTCAGATTTCACCAGTTGTG	HERK1 pENTR/D-TOPO rv
CLN047	CACCATGGGTGGTGAAAAGTTTGGATTTTTGATTTGG	ANJ pENTR/D-TOPO fw
CLN048	ACGTCCCTCAGATTTGATCAGCTGCG	ANJ pENTR/D-TOPO rv
CLN049	CACCATGAAGATCACAGAGGGACG	FER pENTR/D-TOPO fw
CLN050	ACGTCCCTTTGGATTCATGA	FER pENTR/D-TOPO rv
MPK159	GGATATTGATCTTAGCACTCTTGTGG	HERK1exJM Y2H fw
MPK144	AACCCGAGATTACTCTTACTGCT	HERK1exJM Y2H rv
MPK160	GCTTGATCTGAGCTCTTATTTATCCA	ANJexJM Y2H fw
MPK148	CCACCAACATTCTTCTTAGTGGTTG	ANJexJM Y2H rv
CLN056	GATATCGGATGGTGTGTTTGAATCA	LRE(23-138) Y2H fw
CLN057	CCGGCGTTTAGGTTATGTGAATAGAG	LRE(23-138) Y2H rv
OTH031	GATCATATTCTATGTTATTCCGATCTCTCTTTTGTATTCC	amiRALFL11/12/13 Primer I
OTH032	GATCGGAATAACATAGAATATGATCAAAGAGAATCAATGA	amiRALFL11/12/13 Primer II
OTH033	GATCAGAATAACATACAATATGTTCACAGGTCGTGATATG	amiRALFL11/12/13 Primer III
OTH034	GAACATATTGTATGTTATTCTGATCTACATATATATTCCT	amiRALFL11/12/13 Primer IV
OTH035	GATTGCAATCGTAGTACGATCGGTCTCTCTTTTGTATTCC	amiRALFL4/19 Primer I
OTH036	GACCGATCGTACTACGATTGCAATCAA	amiRALFL4/19 Primer II

	AGAGAATCAATGA	
OTH037	GACCAATCGTACTACCATTGCATTCAC AGGTCGTGATATG	amiRALFL4/19 Primer III
OTH038	GAATGCAATGGTAGTACGATTGGTCTA CATATATATTCCT	amiRALFL4/19 Primer IV
OTH039	GATTAGGGTGGGCTTAGTCACAATCTC TCTTTTGTATTCC	amiRALFL8/9/15 Primer I
OTH040	GATTGTGACTAAGCCCACCCTAATCAA AGAGAATCAATGA	amiRALFL8/9/15 Primer II
OTH041	GATTATGACTAAGCCGACCCTATTCAC AGGTCGTGATATG	amiRALFL8/9/15 Primer III
OTH042	GAATAGGGTCGGCTTAGTCATAATCTA CATATATATTCCT	amiRALFL8/9/15 Primer IV
OTH043	GATTGTCACATTTTACCGGACAATCTC TCTTTTGTATTCC	amiRALFL18 Primer I
OTH044	GATTGTCCGGTAAAATGTGACAATCAA AGAGAATCAATGA	amiRALFL18 Primer II
OTH045	GATTATCCGGTAAAAAGTGACATTCAC AGGTCGTGATATG	amiRALFL18 Primer III
OTH046	GAATGTCACTTTTTACCGGATAATCTA CATATATATTCCT	amiRALFL18 Primer IV
OTH047	GATAATGTGAATGGACATCACACTCTC TCTTTTGTATTCC	amiRALFL14 Primer I
OTH048	GAGTGTGATGTCCATTCACATTATCAA AGAGAATCAATGA	amiRALFL14 Primer II
OTH049	GAGTATGATGTCCATACACATTTTCAC AGGTCGTGATATG	amiRALFL14 Primer III
OTH050	GAAAATGTGTATGGACATCATACTCTA CATATATATTCCT	amiRALFL14 Primer IV
CLN090	CACCTTAGTCCGACATCTTACACTGTT	pRALFL4 pENTR/D-TOPO fw
CLN091	TAGGTACCTTAGTCCGACATCTTACAC TGTT	pRALFL4 fw
CLN092	AATGAGTTATTATTGCTCTTTTGTTTAG G	pRALFL4 rv
CLN093	TAAGGATCCTTAGCGAGCGTACCTATA GC	RALFL4 rv
CLN096	CACCTGTCATTACGGAGTCTTCCC	pRALFL19 pENTR/D-TOPO fw
CLN097	TAGGTACCTGTCATTACGGAGTCTTCC C	pRALFL19 fw
CLN098	TTGGTTTTCTTTGTTTTGTTTTGCT	pRALFL19 rv

CLN099	TAAGGATCCTTAAGAAGTTTGCCTGTAGCAATG	RALFL19 rv
CLN102	ATACTGCAGGAGTATTATGGCATTGGGAAAACT	rbcSterm fw
CLN103	ATACTGCAGATTGATGCATGTTGTCAATCAATTG	rbcSterm rv
GEN011	GCGGATAACAATTTCACACAGGAAACAG	HA-LRE fw
CLN073	TAGCGGCCGCTCAAGTCAACACTAACAAAGCA	HA-LRE rv
CLN035	TATTGTACAGTGAGCAAGGGCGAGGAG	GFP fw
CLN036	ATTTGTACATTACTTATAAAGCTCGTCCATGCCG	GFP-disruptedBsrGI rv
CLN044	ACAACTTTATGGATGGTGCAG	pNTA Fw
CLN051	TAGGATCCGAGTGAAGGAAATGAGAGGTG	pNTA rv
CLN054	TAGGTACCTTGAGGAATGATCGATTCTGG	pLAT52 fw
CLN055	TATGTACAGGAATTTTTTTTTTTGGTGTGTGTAC	pLAT52 rv